UNIVERSIDADE D
COIMBRA

Fábio Manuel Santos Rodrigues

Development of Catalysts and Sustainable Catalytic Processes for Transformation of Olefins into High value Products

Tese no âmbito do doutoramento em Química, ramo de especialização em Catálise e Sustentabilidade orientada pela Professora Doutora Maria Miguéns Pereira, co-orientada pela Professora Doutora Marta Piñeiro Gómez e apresentada ao Departamento de Química da Faculdade de Ciências e Tecnologia da Universidade de Coimbra

Outubro de 2020

Universidade de Coimbra

Departamento de Química - Faculdade de Ciências e Tecnologia

Development of Catalysts and Sustainable Catalytic Processes for Transformation of Olefins into High Value Products

Fábio Manuel Santos Rodrigues

Tese de doutoramento em Química, ramo de especialização em Catálise e Sustentabilidade, orientada pela Professora Doutora Maria Miguéns Pereira, co-orientada pela Professora Doutora Marta Piñeiro Gómez e apresentada ao Departamento de Química da Faculdade de Ciências e Tecnologia da Universidade de Coimbra

Coimbra, 2020

“Se eu vi mais longe, foi por estar sobre ombros de gigantes”

Isaac Newton (1676)

Agradecimentos

É com grande alegria e realização pessoal que vejo uma das etapas mais exigentes da minha vida chegar ao fim. Vários sentimentos passam pela minha pessoa ao escrever estas palavras, se por um lado existe o orgulho por outro, existe a humildade e gratidão para com todos os que, de alguma forma, estiveram comigo e contribuíram para a realização desta tese. Todo este percurso só foi possível com a contribuição direta e indireta de muitas pessoas e apesar de eu não me expressar da melhor forma por palavras, não posso deixar de vos agradecer.

Em primeiro lugar, agradeço à Professora Doutora Mariette Pereira pela sua disponibilidade, contribuição científica e orientação ao longo do meu percurso académico e pelos ensinamentos que me trouxeram até aqui. O meu muito obrigado.

À minha co-orientadora Professora Doutora Marta Piñeiro agradeço a contribuição e orientação científica, o apoio, o otimismo e boa disposição com que encarou os desafios que foram surgindo.

Durante a realização dos trabalhos apresentados nesta tese tive o privilégio de colaborar com outros grupos de investigação e por isso fui conhecendo muitas pessoas que contribuíram para o meu sucesso. Gostaria de agradecer ao Professor Matthias Beller, por me ter recebido no seu grupo de investigação no "LIKAT institut" com todo o carinho e humildade, numa fase inicial do meu doutoramento. Ao Professor Luís Figueiredo e Professora Sónia Carabineiro agradeço a colaboração no que diz respeito aos materiais de carbono. À Professora Luísa Martins e Professor Armando Pombeiro agradeço toda a colaboração e hospitalidade, durante o tempo que passei em Lisboa que contribuiu bastante para a minha formação.

Tenho também de agradecer ao Departamento de Química e a todos os seus funcionários. Um agradecimento especial à Doutora Sílvia Gramacho pela contribuição nas análises de GC-MS e pela sua boa disposição contagiante. Ao Professor Doutor Rui Brito e ao Pedro Cruz do serviço de Ressonância Magnética Nuclear do Centro de Química de Coimbra (CCC-NMR) agradeço a colaboração na obtenção dos espetros de RMN.

Agradeço o apoio financeiro da Fundação para a Ciência e Tecnologia (FCT) através da cedência da bolsa de doutoramento do Programa Doutoral CATSUS - Catálise e

Sustentabilidade (PD/BD/114340/2016). Agradeço também ao Professor Armando Pombeiro pela coordenação deste programa doutoral que em muito contribuiu para a desenvolvimento da área da catálise em Portugal.

A todos os colegas do Grupo de Catálise e Química Fina que partilharam comigo os dias menos felizes, os dias de trabalho árduo, mas também os dias de conquistas e convívio com experiências que ficam fora desta tese. Ana Almeida, Carlos Monteiro, César Henriques, Gilberto Aquino, Mário Calvete, Rui Carrilho, Sara Pinto, Liliana Damas, Lucas Dias, Carolina Vinagreiro, Vanessa Tomé, Giusi Piccirillo, Andreia Gonzalez, Rafael Aroso, Diana Gomes, obrigado pelo companheirismo ao longo destes anos, pelo convívio diário e por toda a solidariedade. Gostaria de dar uma palavra especial aos amigos que ganhei nesta aventura, Lili, Vanessa, Giusi, Andreia e Rafael. O que não nos mata, torna-nos mais fortes, e no nosso caso criou uma ligação que levo para a vida obrigado pela partilha que vai para além do trabalho.

Aos amigos de sempre, para sempre, Diogo, Jaime, Ricardo, Rita, Telmo, Diana, Sara, Melodia, Vânia, Andreia, Teresa. Obrigado pela partilha e companheirismo que sempre nutrimos e que de certa forma, ajudou a moldar o homem que sou hoje.

À minha família, em especial aos meus pais Licínio e Maria e ao meu irmão Hervê foram vocês que me ajudaram a chegar aqui, apesar de não saberem nada de reações químicas, sabem todo o meu percurso de vida, sem a vossa dedicação e ajuda nada disto seria possível. Devo tudo aquilo que alcancei a vocês. Obrigado pelo amor e por compreenderem as minhas ausências mais prolongadas. À minha segunda família Fernando, Teresa, Dona Júlia, Marta, Alexandre e Laurinha agradeço todo o carinho, por me terem acolhido na vossa família e ajudarem em tudo que podem, obrigado.

Por último, e como os últimos são sempre os primeiros, agradeço à minha Mulher Patrícia, o apoio N°1, por todo o amor, compreensão e generosidade. Sem ti não teria conseguido chegar aqui, esta tese é também tua.

Table of Contents

Abstract i

Resumo iii

Abbreviations and Symbols v

Nomenclature viii

Chapter 1 Introduction 1

1.1 Catalysis for sustainability 1

1.2 Hydroformylation as central reaction in sustainable catalytic processes 3

1.2.1 General aspects 3

1.2.2 Immobilized catalysts for hydroformylation reactions 6

1.3 Sequential reactions involving hydroformylation 12

1.3.1 Sequential hydroformylation/reduction 14

1.3.2 Sequential hydroformylation/reductive amination (Hydroaminomethylation) 19

1.3.3 Sequential hydroformylation/acetalization 27

1.4 Main goals 34

1.5 References 35

Chapter 2 Dual Catalytic System for Sequential Hydroformylation/Hydrogenation of Hindered Olefins 47

2.1 Introduction 47

2.2 Monophosphite synthesis 48

2.3 Sequential hydroformylation/hydrogenation of olefins to alcohols 52

2.3.1 Catalytic system optimization 52

2.3.2 Reaction Scope 58

2.4 Conclusion 65

2.5 References 66

Chapter 3 Immobilization of Rh/Phosphine catalyst onto nanomaterials 69

3.1 Introduction 69

3.2 Nanomaterials functionalization 71

3.2.1 MWCNT@NH_2 synthesis 71

3.2.2 MNP@NH_2 synthesis 72

3.3 Hybrid nanocatalyst synthesis 76

3.4 Catalytic evaluation 81

3.5 Conclusion 86

3.6 References 87

Chapter 4 Sequential Hydroformylation/Acetalization of Olefins using a Rh/Fe Bimetallic Catalytic System 89

4.1 Introduction 89

4.2 Catalyst synthesis 91

4.2.1 Homogeneous type catalysts 91

4.2.2 Heterogeneous type catalysts 95

4.3 Sequential hydroformylation/acetalization of olefins 105

4.3.1 Catalytic homogeneous studies 105

4.3.2 Catalytic heterogeneous studies 112

4.4 Conclusion 116

4.5 References 117

Chapter 5 Experimental 121

5.1 General Information 121

5.1.1 Solvents and Chemicals 121

5.1.2 Instrumentation and Methodologies 123

5.2 Experimental of Chapter 2 128

5.2.1 Ligand synthesis 128

5.2.2 General procedure for the hydroformylation/reduction of olefins 130

5.2.3 Characterization of the isolated alcohols 131

5.3 Experimental of Chapter 3 134
5.3.1 Synthesis and functionalization of the nanomaterials 134
5.3.2 Synthesis of PPh_3 functionalized nanomaterials 136
5.3.3 Synthesis of the hybrid nanocatalysts 137
5.3.4 General procedure for the hydroformylation of styrene 138
5.4 Experimental of Chapter 4 138
5.4.1 Homogeneous catalysts synthesis 138
5.4.2 Heterogeneous catalysts synthesis 140
5.4.3 General procedures for the hydroformylation/acetalization of olefins 143
5.4.4 Reaction scope 144
5.5 References 147

Abstract

The studies described in this PhD thesis are focused on the development of sequential sustainable catalytic processes centered on the hydroformylation reaction, for transformation of olefins into value-added products, such as alcohols, amines and acetals. Additionally, seeking higher sustainability, iron hybrid nanomaterials were synthesized and evaluated as reusable heterogeneous catalysts for hydroformylation and sequential hydroformylation/acetalization reactions.

The thesis is divided into five chapters.

Chapter 1 provides a critical review of recent literature focused on the main topics of the thesis, regarding sequential reactions centered on hydroformylation and the most relevant methodologies for immobilization of hydroformylation catalysts.

Chapter 2 describes the synthesis of racemic BINOL using sustainable methodologies and two BINOL-derived monophosphites. Furthermore, the development of an active and selective dual catalytic system based on the combination of Rh/*tris*-helical-BINOL phosphites with Ru-based Shvo's-complex to promote the sequential hydroformylation/hydrogenation reaction of highly substituted olefins is described. The process optimization was performed using 2,3-dimethylbut-2-ene as model substrate, leading to formation of 3,4-dimethylpentan-1-ol in 90% yield and 99% chemoselectivity (40 bar CO/H_2 (1:3), 120 °C). This innovative catalytic system was further expanded to a variety of aromatic and aliphatic substituted olefins, to obtain the corresponding alcohols in up to 94% yield.

In Chapter 3 a synthetic methodology to prepare hybrid nanocatalysts using catalytic hydroaminomethylation of vinyl phosphines as a synthetic tool was developed. Using this strategy, Rh/phosphine functionalized carbon nanotubes and iron oxide magnetic nanoparticles were prepared and fully characterized. The resulting hybrid nanocatalysts were evaluated in rhodium-catalyzed hydroformylation of styrene, where the iron oxide magnetic nanoparticle-based catalyst demonstrated higher activity and selectivity for branched aldehydes. Furthermore, they were easily recovered by simple magnetic separation and reused in three consecutive runs without significant loss of activity and selectivity.

Chapter 4 describes the development of a sustainable selective hydroformylation/acetalization sequential process for transformation of olefins into the corresponding ethyl acetals, using ethanol as green reagent and solvent. This sequential reaction was first optimized under homogeneous conditions, through the use of a bimetallic catalytic system, based on Rh(I)/phosphorus ligands and [$FeBr_2\{\kappa^3$-$HC(pz)_3\}$] (pz = pyrazol-1-yl). In addition, the studies of the immobilization of Rh(I)/*N*-xantphos onto MNP@Cl through nucleophilic substitution and a Fe(II)-allyl-*C*-scorpionate complex onto MNP@NH_2 through hydroaminomethylation reaction are presented. The heterogeneous catalysts, MNP@*N*-xantphos/Rh(I) and MNP@NH-$(CH_2)_4$-O-$CH_2C(pz)_3FeBr_2$ were fully characterized and then applied in catalytic hydroformylation/acetalization sequential process, leading to full conversions and high selectivity (up to 93%). Furthermore, these catalysts were recovered by simple magnetic separation and reused in four consecutive runs, without substantial loss of activity neither selectivity. This study represents the first report of the combination of Rh(I)/phosphorus and Fe(II)/*C*-scorpionate catalysts, both in homogenous and heterogeneous conditions.

In Chapter 5, the techniques, instrumentation and experimental procedures are described, as well as the characterization of all the materials and products.

Keywords: Catalysis; Hybrid materials; Olefins, Small molecules activation; Tandem reactions

Resumo

Os estudos descritos nesta tese de doutoramento estão focados no desenvolvimento de processos catalíticos sequenciais sustentáveis tendo a hidroformilação como reação central, para transformação de olefinas em produtos de elevado valor acrescentado, como álcoois, aminas e acetais. Adicionalmente, em busca de uma maior sustentabilidade, nanomateriais híbridos de ferro foram sintetizados e avaliados como catalisadores heterogéneos reutilizáveis para reações de hidroformilação e hidroformilação/acetalização sequencial.

A tese encontra-se dividida em cinco capítulos.

O Capítulo 1 apresenta uma revisão crítica da literatura recente focada nos principais tópicos da tese, no que diz respeito às reações sequenciais centradas na hidroformilação e as metodologias mais relevantes para a imobilização de catalisadores de hidroformilação.

No Capítulo 2 descreve-se a síntese de BINOL racémico através de metodologias sustentáveis e de dois monofosfitos derivados de BINOL. Aqui são também apresentados os estudos do desenvolvimento de um sistema catalítico dual ativo e seletivo, baseado na combinação de ródio/fosfito tris-helicoidal derivado de BINOL com o complexo de ruténio Shvo, para promover a reação sequencial de hidroformilação/hidrogenação de olefinas polissubstituídas. A otimização do processo foi efetuada usando 2,3-dimetilbut-2-eno como substrato modelo, que conduziu à formação de 3,4-dimetilpentan-1-ol com 90% de rendimento e 99% de quimiosseletividade (40 bar CO/H_2 (1:3), 120 °C). Este sistema catalítico inovador foi aplicado a uma variedade de olefinas aromáticas e alifáticas substituídas, tendo-se obtido os álcoois correspondentes com rendimentos até 94%.

No Capítulo 3, apresentam-se os estudos de desenvolvimento de uma metodologia sintética inovadora para preparar nanocatalisadores híbridos usando a hidroaminometilação catalítica de vinil-fosfinas como ferramenta sintética. Usando esta estratégia, foram preparados nanotubos de carbono funcionalizados com Rh/fosfina e nanopartículas magnéticas de óxido de ferro, e apresenta-se a sua completa caracterização. Os nanocatalisadores híbridos foram avaliados na hidroformilação de estireno catalisada por ródio, onde o catalisador imobilizado em nanopartículas

magnéticas de óxido de ferro demonstrou maior atividade e seletividade para o aldeído ramificado. Adicionalmente, os catalisadores foram recuperados por simples separação magnética e reutilizados em três ciclos consecutivos sem perda significativa nem de atividade nem de seletividade.

No Capítulo 4 descreve-se o desenvolvimento de um processo sustentável sequencial de hidroformilação/acetalização, seletivo para a transformação de olefinas nos acetais correspondentes, usando etanol como reagente verde e solvente. Esta reação sequencial foi otimizada em condições homogéneas, através do uso de um sistema catalítico bimetálico, baseado em Rh(I)/fósforo e [$FeBr_2\{\kappa^3$-$HC(pz)_3\}$] (pz = pirazol-1-il). Neste capítulo, encontra-se ainda descrita a preparação de novos catalisadores heterogéneos, a partir da imobilização de Rh(I)/*N*-xantphos em MNP@Cl através de uma reação de substituição nucleofílica e de um complexo Fe-(II)-alil-C-escorpionato imobilizado em MNP@NH_2, através de um processo inovador de hidroaminometilação. Os catalisadores heterogéneos, MNP@*N*-xantphos/Rh(I) e MNP@NH-$(CH_2)_4$O-$CH_2C(pz)_3FeBr_2$ foram completamente caracterizados e aplicados em reações sequencias de hidroformilação/acetalização, tendo-se obtido conversões completas, elevada seletividade e rendimentos (até 93 %). Os catalisadores foram recuperados por simples separação magnética e reutilizados em quatro ciclos consecutivos, sem perda substancial de atividade nem de seletividade. Este estudo representa um exemplo pioneiro da combinação de catalisadores Rh(I)/fósforo e Fe(II)/C-escorpionato, tanto em condições homogéneas como heterogéneas.

No Capítulo 5, encontram-se descritas as técnicas, instrumentação e procedimentos seguidos, assim como a completa caracterização de todos os materiais e produtos sintetizados.

Palavras Chave: Catálise; Materiais híbridos; Olefinas; Ativação de moléculas pequenas; Reações tandem.

Abbreviations and Symbols

[α]	specific rotation
δ	chemical shift
λ	wavelength
^{1}H-NMR	proton nuclear magnetic resonance spectroscopy
^{13}C-NMR	carbon 13 nuclear magnetic resonance spectroscopy
^{31}P-NMR	phosphorous 31 nuclear magnetic resonance spectroscopy
acac	acetylacetonate
APTES	(3-aminopropyl)triethoxysilane
ax	axial
BINOL	1,1'-Bi-2-naphthol
CATSUS	Catalysis and Sustainability PhD program
CPTES	(3-Chloropropyl)triethoxysilane
d	doublet
dd	doublet of doublets
dt	doublet of triplets
dq	doublet of quartets
DEAD	diethyl azodicarboxylate
DMAP	2-dimethylaminopyridine
DME	1,2-dimethoxyethane
DMF	*N,N*-dimethylformamide
EI	Electronic ionization
ESI	Electrospray ionization
eq	equatorial
FID	Flame ionization detector
FT-IR	Fourier-transform infrared spectroscopy
GC	Gas chromatography
GC-MS	Gas chromatography - mass spectrometry
GC-FID	Gas chromatography - flame ionization detector

h	hours
HRMS	High-resolution mass spectrometry
ICP-OES	Inductively coupled plasma - optical emission spectrometry
Igepal CO-520	polyoxyethylene (5) nonylphenylether (branched)
IR	Infrared spectroscopy
IUPAC	International Union of Pure and Applied Chemistry
J	coupling constant
L	ligand
m	multiplet
$[M]^+$	molecular ion
MNP	magnetic nanoparticles
m/z	mass/charge relation
MWCNT	Multiwalled carbon nanotubes
min	minutes
MS	Mass spectrometry
N-xantphos	4,6-Bis(diphenylphosphino)phenoxazine
NMR	Nuclear magnetic resonance spectrometry
ppm	parts per million
q	quartet
rpm	rotations per minute
p	pentet
pz	pyrazol-1-yl
s	singlet
t	triplet
TEM	Transmission electron microscopy
TEOS	Tetraethoxysilane
TG	Thermogravimetry
THF	Tetrahydrofuran
TLC	Thin-layer chromatography
TMS	Tetramethylsilane

Xantphos	4,5-Bis(Difenilfosfino)-9,9-Dimetilxanteno
XPS	X-ray photoelectron spectroscopy

Nomenclature

In this thesis, the IUPAC recommendations of 1993 were followed to number and name all compounds.[i,ii] The numbering and nomenclature of one of each family of compounds synthesized are presented below.

The adopted nomenclature of BINOL derivatives and *tris*-binaphthyl monophosphites was based on the aforementioned regulations (Figure II)

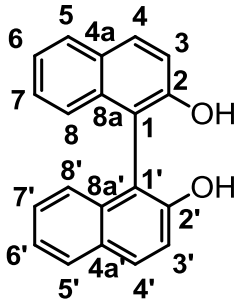

Figure I Nomenclature for 1,1'-Bi-2-naphthol molecule.

C-scorpionate ligands are based on the pyrazole molecule and numbered as presented in Figure II.

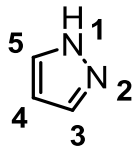

Figure II Nomenclature for 1H-Pyrazole molecule.

Concerning terpene's nomenclature, the trivial names were used instead of IUPAC nomenclature, for simplicity and historical reasons, as presented in Figure III.

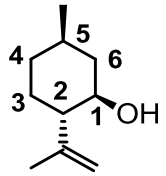

IUPAC name: (*1R,2S,5R*)-5-methyl-2-(prop-1-en-2-yl)cyclohexan-1-ol

Trivial name: (-)-isopulegol

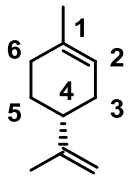

IUPAC name: (*R*)-4-Isopropenyl-1-methylcyclohex-1-ene

Trivial name: (+)-limonene

Figure III

References

[i] A. D. McNaught, A. Wilkinson, *IUPAC Compendium of Chemical Terminology - Gold Book.* Blackwell Scientific Publications: Oxford, **2014**.

[ii] A. C. Fernandes, B. Herold, H. Maia, A. P. Rauter, J. A. R. Rodrigues, *Guia IUPAC para a Nomenclatura de Compostos Orgânicos*, Lidel, Lisboa, **2002**.

Chapter 1

Introduction

1.1 Catalysis for sustainability

The recognition of the importance to develop less polluting chemical processes goes back to the end of the twentieth century when P. Anastas introduced a new philosophy called *Green Chemistry*.[1-3] He defined *Green Chemistry* as the "design of chemical products and processes to reduce or eliminate the generation of hazardous substances" [2]. This concept was centered on 12 principles, which are presented in Figure 1.1.

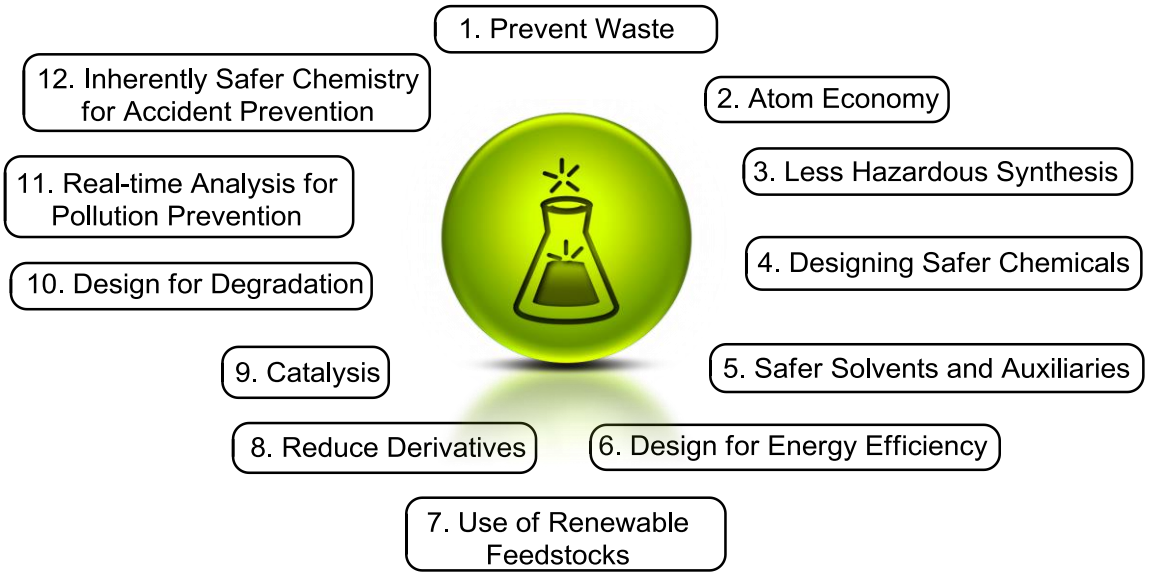

Figure 1.1 The twelve principles of Green Chemistry.

The relevance of implementing these principles has progressively been more recognized by both academy and industry.[1,4-7] It is now accepted that Chemistry can only play a central role in the development of our society if its ultimate goal is guided by sustainability values.[8-10] In this context, the term 'sustainable chemistry' has been introduced more recently, aiming to transfer the *Green Chemistry* philosophy towards environmental, cultural, economic, and social concerns, Figure 1.2.

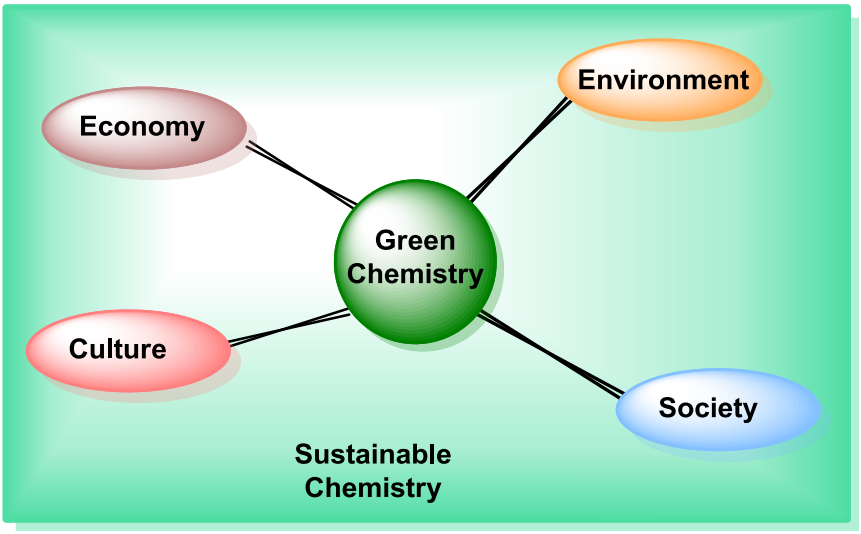

Figure 1.2 Green Chemistry and Sustainability

Pursuing the main goal of the *Catalysis and Sustainability Inter-university PhD Programme*,[11] the motivation of this thesis was centered on the development of sustainable chemical synthetic processes for the preparation of added-value products. To meet the sustainable development objectives of the doctoral program, the studies were conducted by following some of the Green Chemistry principles, namely **Principles 1** and **8 – Prevent waste and Reduce derivatives** (by the implementation of sequential reactions), **Principle 2 – Atom Economy** (hydroformylation and hydrogenation as 100% atom economy reaction), **Principle 5 – Benign solvents and auxiliaries** (use of 2-methyl-THF and ethanol as solvents), **Principles 6 and 9 – Energy efficiency and Catalysis** (application of catalytic processes to increase selectivity and decrease global process energetics) and **Principle 7 – Use of renewable feedstock** (use of nature abundant terpenes as substrates and ethanol as a renewable harmless reagent), Figure 1.3.

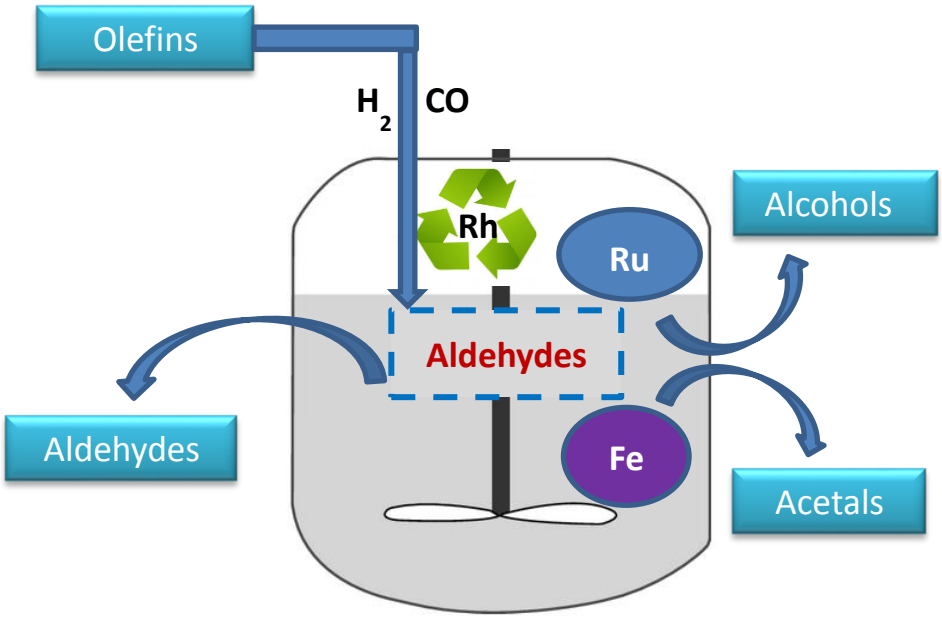

Figure 1.3 Hydroformylation as central reaction for the development of sustainable processes.

To achieve these goals, in our studies, catalytic hydroformylation was selected as a relevant 100% atom economical process, and its use as a central reaction to prepare fine chemicals, using sequential processes that transform olefins into amines, alcohols and acetals, in only one step, without isolating the aldehyde intermediates.[12-17] These sequential processes prevent the consumption of solvents and purification materials (silica, alumina), leading to more sustainable processes.[18-21] Bearing in mind that the most active and selective hydroformylation catalysts are based on rhodium complexes which, in addition to being toxic, are extremely expensive, we have designed strategies to carry out their recovery and reuse.[22-26] Among these strategies, we highlight the immobilization of rhodium complexes onto solid supports. In addition, we also sought to develop new inexpensive and environmentally friendly iron-scorpionate catalysts,[27-31] to promote sequential acetalization reactions.

1.2 Hydroformylation as central reaction in sustainable catalytic processes

1.2.1 General aspects

The hydroformylation reaction is the *syn* addition of a hydrogen atom and a formyl group to a C-C double bond, which allows the one-pot preparation of aldehydes directly

from olefins, (Scheme 1.1). This reaction requires the use of catalysts, which are generally based on transition-metal complexes.[32-35]

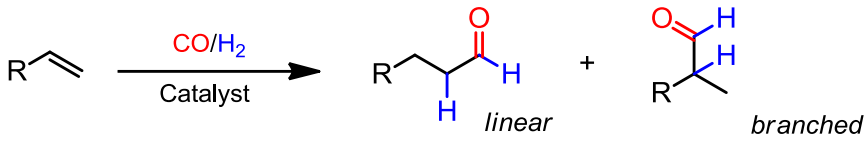

Scheme 1.1 Hydroformylation of a terminal olefin.

Since its discovery by Otto Roelen in 1938,[36,37] catalytic hydroformylation has been widely studied both for academic and industrial purposes. Its relevance was early recognized, being extensively applied for the mass production of important synthetic aldehydes whose derivatives have been applied in polymer and surfactant industries. [35,38-41] Nowadays, more than 10 million tons of products are obtained by hydroformylation every year.[42]

One of the most important aspects that require optimization in hydroformylation reactions is selectivity since the reaction occurs in the presence of metal complexes that, under reducing conditions, can give reduced and isomerized products, decreasing the yield for the desired product (Scheme1.2).

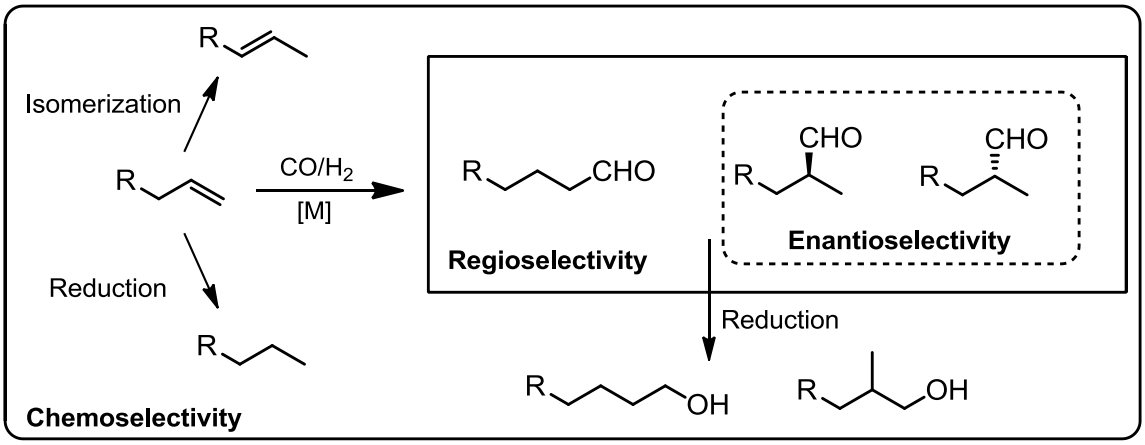

Scheme 1.2 Selectivity in the hydroformylation reactions.

The need to control selectivity led to the development of catalysts with different properties through the synthesis of new complexes bearing suitable ligands capable to modulate their electronic, acid-base and steric features. Several transition metals have

been tested as catalysts but the activity of the metal complexes for catalytic hydroformylation follows the order:[39,43]

$$Rh \gg Co > Ir > Ru > Pt > Pd > Fe$$

Rhodium-based catalysts are the most commonly used since they often lead to highest activity and selectivity. Over the year, in order to increase the activity and selectivity, several kinds of phosphorus ligands have been developed being considered the "holy grail" of catalysis.[44-52] Some of the most widely applied catalysts are rhodium complexes coordinated with monodentate triphenylphosphine,[53,54] (Wilkinson catalyst – Nobel prize) and the bidentate xantphos that, due to its large bite angle gives high selectivity towards linear aldehydes.[44,55-57] In the 1980's, van Leeuwen had discovered a peculiar effect of bulky aryl monophosphites,[58-60] whose rhodium complexes led to very high rates, chemo- and regioselectivities, also in the hydroformylation of disubstituted olefins, allowing the possibility of using milder reaction conditions, (Scheme 1.3). In addition, a great variety of chiral phosphites ligands, have been developed, which resulted in highly enantioselective rhodium catalysts.[61-68] The latter are out of the scope of this thesis.

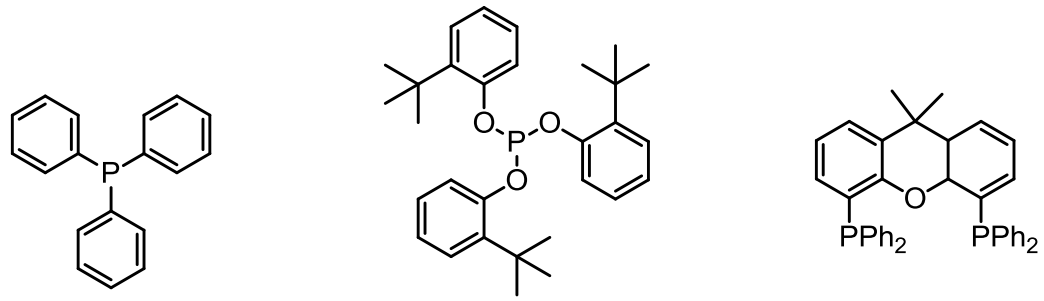

Triphenylphosphine | **Tris(O-*tert*-butylphenyl) phosphite** | **Xantphos**

Scheme 1.3 Relevant phosphorus ligands for hydroformylation.

In the last years, the global requirement for more sustainable and greener processes has boosted the development of more active and selective catalysts, ligands and processes looking for Rh reutilization and/or substitution by other metal catalysts. Some advances in the implementation of less or non-toxic catalysts have been made, such as iron catalysts. However, only a few examples are shown to be effective and with limited

applications, so rhodium is still considered the metal of choice for chemoselective hydroformylation reactions.[69,70] The use of hydroformylation in sequential processes also contributes to increase the sustainability of the overall process and if the catalysts are immobilized onto solid supports, the toxicity and overall cost issues of the process will be significantly lowered. This is also one of the main goals of this work and recent results presented in the literature describing the use of heterogeneous Rh catalysts in hydroformylation reactions are presented in the following section.

1.2.2 Immobilized catalysts for hydroformylation reactions

The immobilization of metal catalysts onto solid supports is a topic of great scientific interest since the high activity and selectivity typical of homogenous catalysts are combined with the advantage of reutilization, characteristic of the heterogeneous catalysts. In general, metal complexes can be immobilized through different strategies, which include covalent coordination, electrostatic interactions, adsorption or encapsulation.[22-26]

In order to achieve reusable hydroformylation catalysts, the previous strategies have been widely used to promote the immobilization of rhodium complexes onto several supports. For instance, rhodium complexes can be covalently supported using functionalized ligands (Scheme 1.4A),[71-74] rhodium nanoparticles can be dispersed in solid materials (Scheme 1.4B),[23,75-78] single rhodium atoms can be deposited in solid supports with or without the addition of ligands (Scheme 1.4C)[72,75,79,80] and ionic rhodium complexes can be immobilized into a supported ionic liquid phase (SILP), through a coating of the solid support with an ionic liquid layer (Scheme 1.4D).[81-84] In addition, the development of biphasic processes based on organic/fluorinated solvent,[85-87] organic/water,[88-92] and organic/ionic liquid[93-96] can also allow catalyst recovery, leading to reusable hydroformylation systems (Scheme 1.4E).

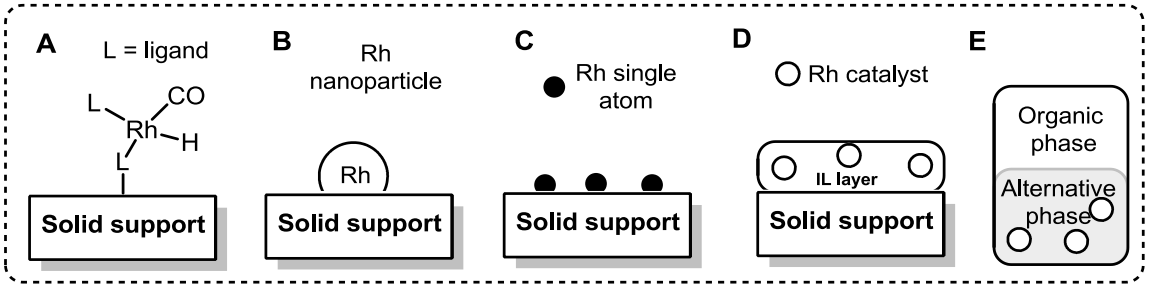

Scheme 1.4 Strategies for preparation of reusable Rh-based catalysts.

Due to the importance of these heterogeneous systems, the relevant achievements in this field were recently reviewed.[23-25,75,97] Therefore, considering the high interest of the topic and the main goal of this thesis, the state of the art regarding the immobilization of Rh-based catalysts for hydroformylation, since 2018, is presented in Table 1.1.

Table 1.1. State of the art of hydroformylation with Rh-immobilized catalysts.

Entry	Catalyst	Substrate	Selectivity l:b [%]	Reutilization cycles
1	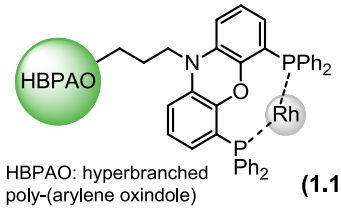 HBPAO: hyperbranched poly-(arylene oxindole) **(1.1)** Smet[74]	Oct-1-ene	94:6	5
2	Rh/**1.2** 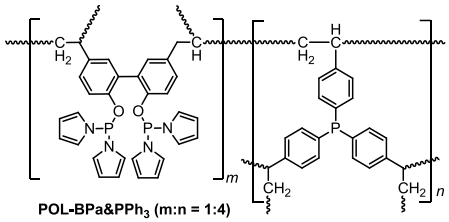 Xie[98]	Hex-1-ene	Up to 99:1	10
3	Rh/**1.3** 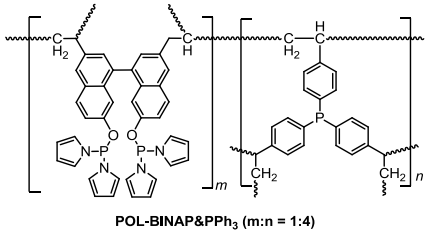 Jia[99]	Diphenylacetil-ene	-	10

Table 1.1. State of the art of hydroformylation with Rh-immobilized catalysts (cont.).

Entry	Catalyst	Substrate	Selectivity *l:b* [%]	Reutilization cycles
4	Rh_2O_3@S-1-II (**1.4**) 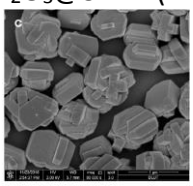 Zhang[100]	Dec-1-ene	Up to 87:13	7
5	Rh/MgSNTs (**1.5**) 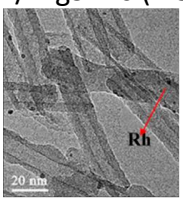 Huang[101]	Vinyl acetate	9:91	4 with gradual leaching
6	Rh/Li-TNT (**1.6**) 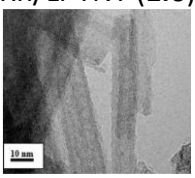 Huang[102]	Vinyl acetate	-	Not tested
7	Rh catalyst (**1.7**) 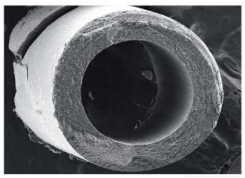 Haumann[103]	But-1-ene	up to 99:1	Not tested
8	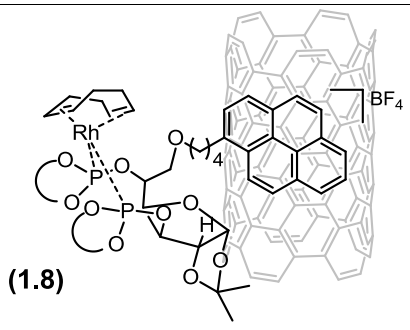 Godard[104]	Norbornene	*ee* up to 71%	Conversion decreases after 80 minutes due to leaching

Table 1.1. State of the art of hydroformylation with Rh-immobilized catalysts (cont.).

Entry	Catalyst	Substrate	Selectivity *l:b* [%]	Reutilization cycles
9	Rh/$(PPh_3)n@SiO_2$ (**1.9**) 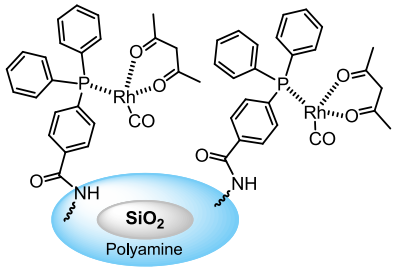 Rosenberg[105]	oct-1-ene	62:38	Loss of activity and selectivity over reutilizations
10	Rh(I)-TPPTS@MCM-41 (**1.10**) 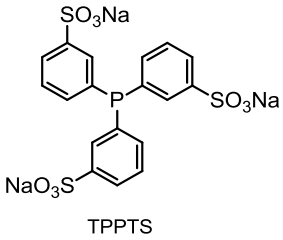 TPPTS Meijboom[106]	oct-1-ene	90:10 to 80:20	Loss of activity and selectivity after the 5th run

Smet[74] described the immobilized *N*-xantphos on hyperbranched poly-(arylene oxindole) supports (**1.1**), *via* a one-step post functionalization (Scheme 1.5). This immobilized catalyst was evaluated in the Rh(I)-catalyzed hydroformylation of oct-1-ene under mild conditions (4.8 bar; 75 °C; 20 min) and microwave irradiation. The authors obtained 95% conversion and 94:6 *l/b* (linear/branched) aldehyde selectivity (Table 1.1, Entry 1), where the high activity was attributed to the dendritic nature of the support. Furthermore, the immobilized rhodium catalyst was recovered, without significant loss of activity along five cycles. This catalyst was also active in the aminocarbonylation reaction of bromobenzene using propylamine as nucleophile.

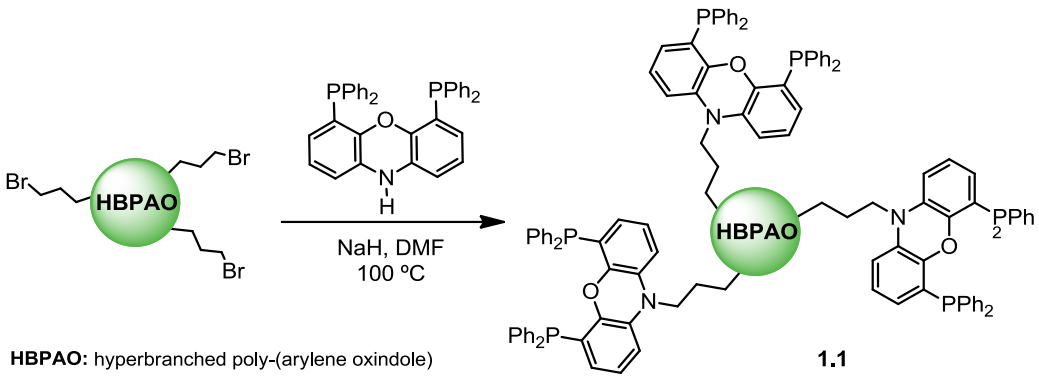

Scheme 1.5 Immobilization of *N*-Xantphos onto a functionalized hyperbranched polymer.

Xie[98] promoted the synthesis of a porous organic polymer *via* copolymerization of divinyl-functionalized phosphoramidite and *tris*-(4-vinylphenyl)phosphine (**1.2**). After [Rh(CO_2)(acac)] encapsulation, the solid was evaluated in catalytic hydroformylation of hex-1-ene (P = 20 bar T = 90 °C; 5 h) leading to full conversion and selectivity for linear aldehyde up to 99% was obtained. It should be mentioned that no loss of activity neither selectivity was observed after 10 reutilization cycles, (Table 1.1, Entry 2). Using the same strategy Xie's group developed other Rh-based catalyst supported on organic polymer for the hydroformylation of alkynes.[99] The heterogeneous Rh/**1.3** was evaluated in the hydroformylation of diphenylacetylene at a temperature of 70 °C, 10 bar of *syngas* pressure, over 20 h and full conversion was observed. The desired aldehydes were obtained with 90% selectivity with the *cis* isomer being the most abundant (60% *E/Z*). It is noteworthy that the catalyst was reused 10 times without significant loss in activity and selectivity (Table 1.1, Entry 3).

Zhang[100] reported the preparation of a set of Rh oxide catalysts encapsulated into microporous zeolites. The new materials were applied in the hydroformylation of terminal olefins and performed well, obtaining over 95% olefin conversion and usually over 95% aldehyde selectivity. Catalyst **1.4** converted 99% of dec-1-ene to aldehydes with 94% aldehyde selectivity and 87% linear isomer using 80 °C, and 50 bar of *syngas* pressure over 12 h. The catalyst was recycled over 7 cycles without significant loss of activity and selectivity (Table 1.1, Entry 4).

Huang reported the preparation of two heterogeneous catalytic systems for the Rh-catalyzed hydroformylation of vinyl acetate. In one approach Rh(0) was immobilized onto silicate nanotubes *via* impregnation-calcination method, (Scheme 1.6).[101] The

heterogeneous catalyst **1.5** was evaluated using 110 °C of temperature, 60 bar of *syn* gas over 8 h obtaining 97 % vinyl acetate conversion with 68% selectivity for aldehydes (91% of the branched isomer). The catalyst was reused four times and a significant Rh leaching was observed along with a consequent loss of activity over the cycles (Table 1.1, Entry 5)

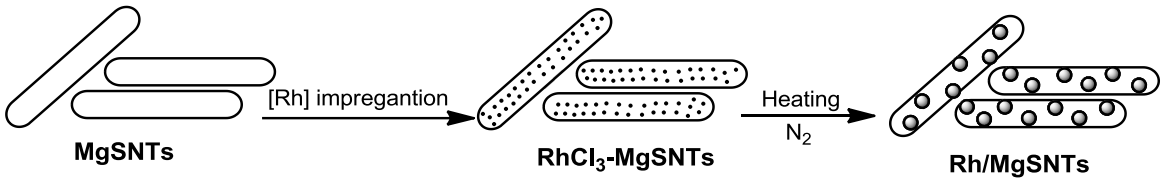

Scheme 1.6 Preparation of the heterogeneous catalyst **1.5** through Rh impregnation followed by calcination (MgSNTs: Magnesium silicate nanotubes).

Similarly, in another study, Rh was immobilized into TiO_2 nanotube (TNT) using alkali or alkali-earth cations as additives (Li, Na, K, Mg, Ca, Sr).[102] The obtained catalysts were evaluated in the hydroformylation of vinyl acetate. The utilization of Rh/Li-TNT (**1.6**) as catalyst led to full conversion and 81% aldehyde selectivity after 1 h of reaction, temperature and CO/H_2 pressure were not reported, (Table 1.1, Entry 6). Additionally, the author states that Rh/TNTs modified with alkali or alkali-earth cations improved the reaction selectivity for the aldehyde product, this fact, may be attributed to the presence of the ions that conduced to an improvement of the CO adsorption.

Haumann[103] described the preparation of MWCNT/SILP (supported ionic liquid phase) based composites (**1.7**) and their application as heterogeneous catalysts for hydroformylation of but-1-ene under mild reaction conditions (P= 10 bar T= 100 °C) and high conversions with 100% regioselectivity for linear aldehydes were obtained. Nevertheless, 20% of isomerization towards but-1-ene isomers were observed, (Table 1.1, Entry 7).

Godard[104] prepared a set of new chiral Rh/1,3-diphosphite furanose based ligands immobilized onto multiwalled carbon nanotubes (MWCNTs) and graphene oxide (GO) by π-π stacking and carbon beads through encapsulation(**1.8**). These catalysts were evaluated in the asymmetric hydroformylation of norbornene under continuous flow conditions (T = 20 °C; Substrate = 0.75 M, Substrate flow = 0.33 mL/min, CO/H_2 flow = 44.4 mL/min) obtaining up to 71% of *ee*. The catalyst immobilized onto carbon beads was

revealed to be more stable although, after 120 minutes the conversion decreases from 35% to 28% due to catalyst leaching, *ee* remains constant. (Table 1.1, Entry 8)

Rosenberg[105] described the immobilization of $Rh/(PPh_3)_n$ complexes (**1.9**) onto silica polyamine composite (SPC) and evaluated them in the hydroformylation of oct-1-ene. The author observed high activity and selectivity for aldehydes in the first run (99% conversion, 94% aldehydes, Table 1.1, Entry 9, but after the second run great loss of selectivity for aldehydes was observed (62%) and after the fifth run the conversion collapse to 22% due to catalyst leaching despite the regioselectivity was constant (62:38 *l/b* after the second run).

Meijboom[106] described the preparation of Rh(I)-complexes using triphenylphosphine and trisodium salt (TPPTS) as ligand, anchored on MCM-41 and SBA-15 mesoporous silica materials (**1.10**). The influence of the solid support structure in the hydroformylation of oct-1-ene was studied. The results suggest that the hexagonal pore structure of the MCM-41 support enhanced the activity of immobilized catalysts for the hydroformylation of oct-1-en. These heterogenized catalysts gave *n*-nonanal regioselectivity in the range of 80–90% that is comparable to the homogeneous counterparts 70–96% (Table 1.1, Entry 10). In addition, the catalysts were reused over five runs without loss of activity or selectivity under optimized reaction conditions (T = 100 °C; P = 40 bar; 10 h).

1.3 Sequential reactions involving hydroformylation

Sequential reactions under hydroformylation conditions take advantage of the reactivity of the carbonyl group to obtain new synthons with high functionalization through one-step processes. As previously mentioned, the first reaction step starts from an olefin to give an aldehyde with one more carbon through hydroformylation reaction, and a subsequent second reaction step occurs leading to the one-pot formation of a different compound.[12,17,107-109] Several examples of sequential reactions that may occur under hydroformylation conditions have been reported in the literature, namely hydroformylation/hydrogenation,[13,110-112] hydroformylation/acetalization,[113-115] hydroaminomethylation,[15,16,116,117] hydroformylation/Wittig olefination,[118-120] hydroformylation/cyclization,[121-123] hydroformylation/aldol condensation,[124-126]

hydroformylation/elimination,[127-129] hydroformylation/Fischer indole synthesis,[130-132] among others.[12,133-135] Herein we highlight the hydroformylation/hydrogenation, hydroaminomethylation and hydroformylation/acetalization sequences since these reactions constitute the main goals of this thesis, (Scheme 1.7 A-C).

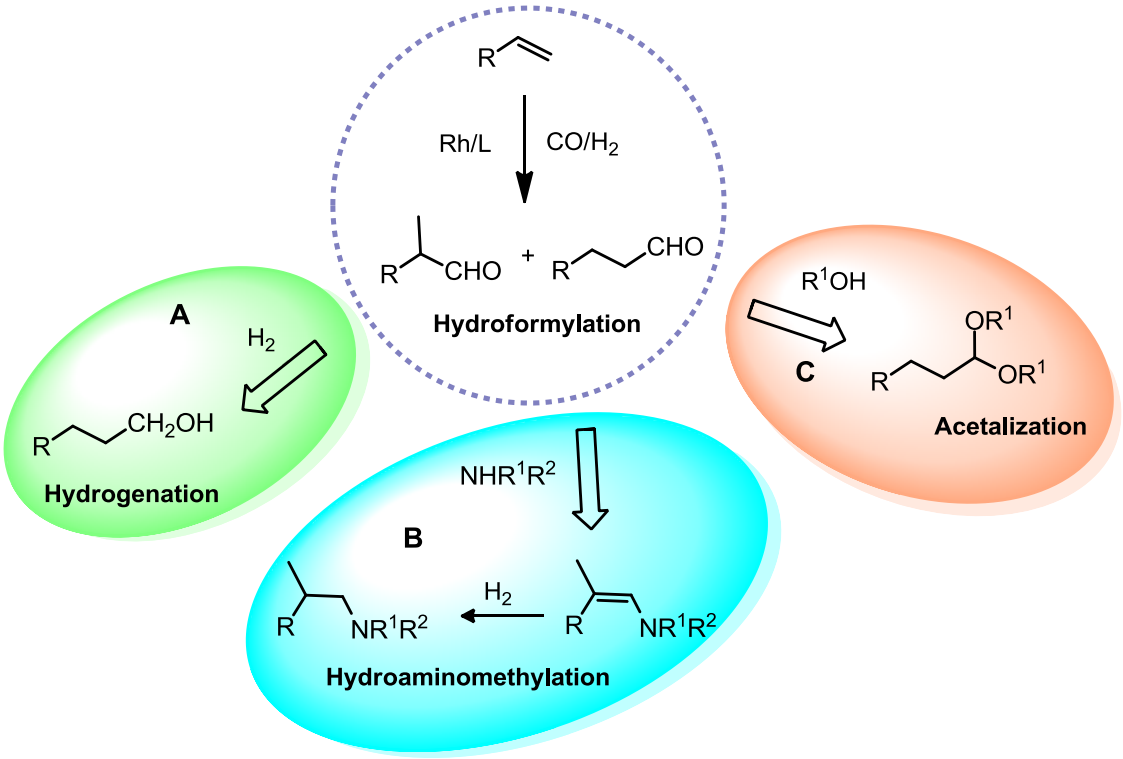

Scheme 1.7 Selected examples of sequential processes using hydroformylation as central reaction.

It should be highlighted that isomerization/hydroformylation sequential reaction is also a relevant sequential transformation, isomerization occurs before hydroformylation leading to the formation of alkene isomers and consequently to aldehyde isomers as we observed in the studies presented in Chapter 2. This sequential process is important, mainly for the production of linear aldehydes using internal olefins as substrates. Generically the isomerization/hydroformylation can be defined as a 1,2-addition of hydrogen and a formyl group that occurs in a different position from the original double bond. The shift of the double bond to internal positions of an alkyl chain may also occur and be interesting to obtain substituted aldehydes. The review from Börner in 2014, describes some of the main developments in this field.[136] Since then, some studies of the

isomerization prior to hydroformylation demonstrate to be relevant in this sequential process to enable the control of the overall regioselectivity.[137-139]

1.3.1 Sequential hydroformylation/reduction

Hydroformylation/reduction consists in the preparation of alcohols directly from olefins through the sequential reduction of aldehydes produced *via* a hydroformylation reaction (Scheme 1.7A) There are three main approaches for the preparation of alcohols *via* hydroformylation: i) one-pot hydroformylation followed by hydrogenation, using a single catalyst process; ii) one-pot hydroformylation followed by hydrogenation using two different catalysts iii) a multi-step sequence, where catalytic hydroformylation is followed by reduction with stoichiometric reagents, (Scheme1.8).

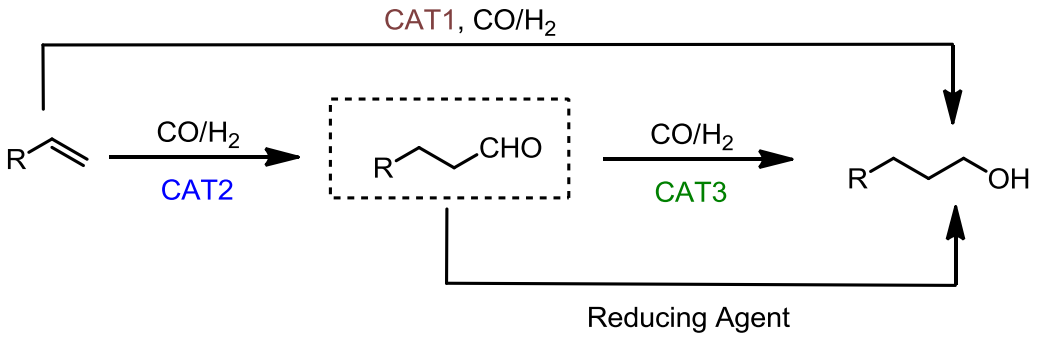

Scheme 1.8 Different catalytic approaches for hydroformylation/reduction of olefins.

The achievements in this field have been reviewed by several authors[12,14,35,108] and the last review was published in 2015.[13] Therefore, the publications of the last five years, regarding this topic, are presented in Table 1.2.

Table 1.2. State of the art for the past 5 years in sequential hydroformylation/reduction reactions.

Entry	Catalyst	Substrate and Conditions[a]	Conversion (selectivity)[b] [%]
1	$Co_2(CO)_8$/**1.14** 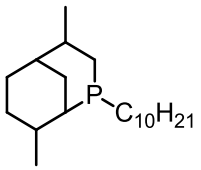 Alper[111]	Dec-1-ene I: T = 110 °C, P = 41 bar (CO/H_2,),NaOAc 22 h II: T = 0 °C, $NaBH_4$, MeOH, 1 h	100 (99) 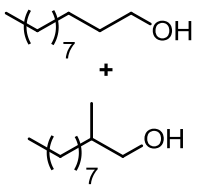
2	10 wt% Au/Co_3O_4 (**1.15**) 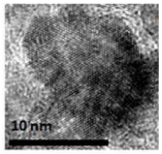 Wang[140]	Dicyclopentadiene T = 150 °C, P = 60 bar, PPh_3, 10 h	90 (98) 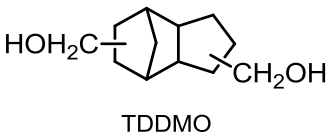 TDDMO
3	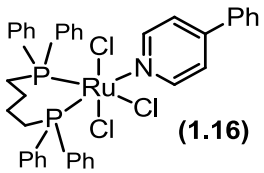 **(1.16)** Batista[114]	Dec-1-ene T = 160 °C, P = 90 bar (CO/H_2), 24 h	99 (23) 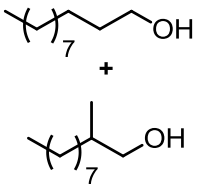
4	$[Rh(CO)_2acac]$/**1.17** 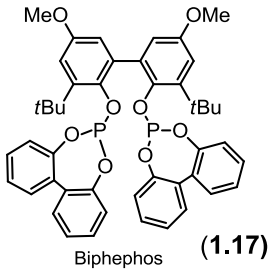 (**1.17**) $[Ru_3(CO)_{12}]$/**1.18** 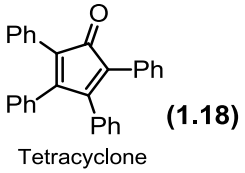 **(1.18)** Tetracyclone Vorholt[110]	Methyl 10-undecenoate T = 150 °C, P = 40 bar (CO/H_2), 1 h	98 (84) 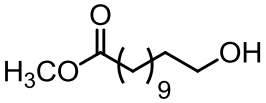

a) Optimized conditions for the selected example, b) Selectivity for alcohol products.

Table 1.2. State of the art for the past 5 years in sequential hydroformylation/reduction reactions (cont.).

Entry	Catalyst	Substrate and Conditions[a]	Conversion (selectivity)[b] [%]
5	Co_3O_4 (**1.19**) 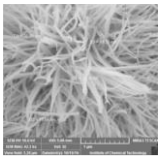 Bhanage[141]	Oct-1-ene T = 150 °C, P = 55 bar (CO/H_2, 1:2), 12 h	92 (94) 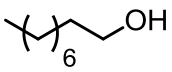
6	5% Au/Cs-Co3O4 (**1.20**) Meijboom[112]	Oct-1-ene T = 140 °C, P = 40 bar (CO/H_2, 1:2), 16 h	92 (95) 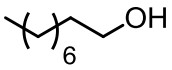
7	$[Ir(COD)Cl]_2$/**1.21** 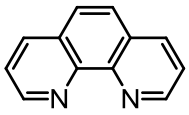 1,10-phenanthroline (**1.21**) Xia[142]	Oct-1-ene T = 120 °C, P = 30 bar (CO), Formic acid, 16 h	94 (56) 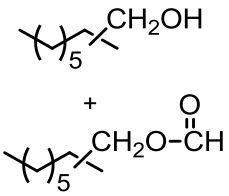

a) Optimized conditions for the selected example, b) Selectivity for amine products.

Alper[111] reported the cobalt-catalyzed hydroformylation of alkenes in the presence of a range of cyclic phosphine ligands (Scheme 1.9), followed by stoichiometric $NaBH_4$ reduction of aldehydes to the respective alcohols. The effect of reaction conditions such as the presence of additives, solvents, *syngas* pressure, and nature of the alkenes were described.

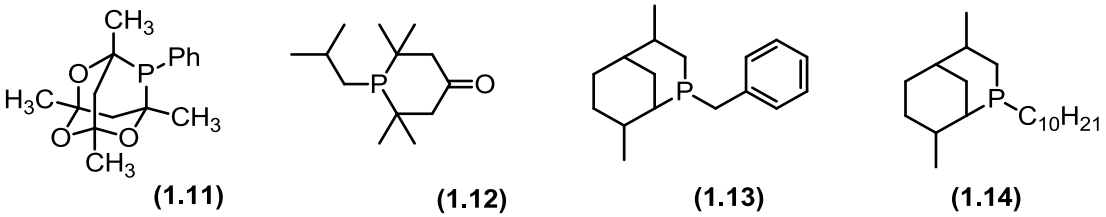

(1.11) **(1.12)** **(1.13)** **(1.14)**

Scheme 1.9 Selected phosphine ligands used by Alper.[111]

The best result for the hydroformylation of dec-1-ene was achieved using **1.14** in the presence of $Co_2(CO)_8$ at 110 °C, 41 bar (CO/H_2, 1:2) for 22 h. After this period the

aldehydes obtained, *via* hydroformylation, were sequentially reduced to the respective alcohols through the addition of $NaBH_4$ and MeOH, at 0 °C, for 1 h. With these optimized conditions, dec-1-ene was fully converted to alcohols with 99% selectivity. (Table 1.2, Entry 1)

Wang[140] prepared a set of Co_3O_4 supported gold nanoparticles (Au/Co_3O_4, **1.15**) and evaluated their activity for the "*one-pot*" hydroformylation/reduction of dicyclopentadiene (DCPD) to tricyclodecanedimethylol (TDDMO) (Scheme 1.10). The synthesis of TDDMO was accomplished using 10 *wt*% Au/Co_3O_4 and PPh_3 as an additive, at a temperature of 140-150 °C and CO/H_2 pressure of 60 to 90 bar. The authors obtained over 90% alcohol selectivity after 10 h (Table 1.2, Entry 2).

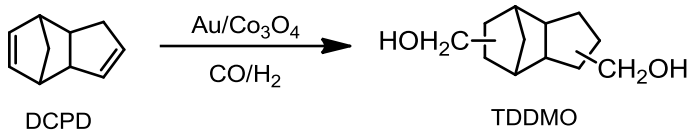

Scheme 1.10 Synthesis of TDDMO from DCPD *via* one-pot hydroformylation/reduction

Batista[114] reported a single catalytic process using *mer*-[$RuCl_3$(dppb)(4-Phpy)[143] (**1.16**) to catalyze the hydroformylation-hydrogenation of dec-1-ene. In this reaction, the Ru complex is able to catalyze both hydroformylation and hydrogenation steps, without the use of any additional catalyst or additive. Under optimized conditions, T = 160 °C, P = 90 bar (CO/H_2), full conversion of dec-1-ene and 23% selectivity for undecanol was achieved in 24 h. (Table 1.2, Entry 3).

Aiming the valorization of castor oil, a sequential hydroformylation/hydrogenation was developed by Vorholt.[110] In this system, [$Rh(CO)_2$acac]/**1.17** complex was applied as hydroformylation catalyst and [$Ru_3(CO)_{12}$]/**1.18** was used in the hydrogenation step. The best result was obtained with methyl-10-undecenoate, at 150 °C and 40 bar CO/H_2 pressure, along 1 h. Under these reaction conditions, the authors obtained 98% conversion and 84% selectivity for the desired hydroxylated linear product. Additionally, the authors reported the reutilization of the catalyst by applying a method for selective product crystallization. The separation of the product from the reaction media allowed the reutilization of the catalyst along two additional runs without significant loss of activity (Table 1.2 Entry 4).

Bhanage[141] developed a synthetic strategy for *n*-nonanol, using fine fibrous cobalt oxide (Co_3O_4, **1.19**) as nanocatalyst to promote the hydroformylation/hydrogenation of oct-1-ene, under phosphine-free conditions. The author reports the effect of several reaction conditions, including syngas pressure, catalyst/substrate ratio, solvent and temperature and the best performance of the fibrous Co_3O_4 catalyst was achieved at temperature of 150 °C, pressure of CO/H_2 of 55 bar (1:2), in THF, for 12 h. Under these reaction conditions, a 92% conversion with 94% selectivity for nonan-1-ol were obtained. Moreover, the Co_3O_4 nanocatalyst was recovered and recycled up to two cycles without significant loss of activity and selectivity. After the second reutilization both conversion and selectivity decreased from 89 to 60% and 90 to 55%, respectively (Table 1.2, entry 5).

Another heterogeneous cobalt catalyst for the hydroformylation/hydrogenation of alkenes was developed by Meijboom.[112] In this study 5% *wt* Au/Cs-Co_3O_4 (**1.20**) was prepared and evaluated in the direct synthesis of alcohols, starting from linear olefins. When oct-1-ene (8 mmol) was introduced in the autoclave at temperature of 140 °C, 40 bar of CO/H_2, (1:2), in THF, and 40 mg of catalyst, for 16 h, 92% conversion and 95% selectivity for nonan-1-ol were obtained, (Table 1.2, entry 6). Once again, the use of tetrahydrofuran as solvent resulted in the best catalytic activity when compared with the other solvents (toluene, heptane, hexane, ethanol). The authors proposed that THF a crucial role in the stabilization of the active species on the catalyst surface. Additionally, the catalyst was reused up to four consecutive cycles without significant loss in activity.

Xia[142] reported an 1,10-phenanthroline (**1.21**) modified iridium complex as an active catalyst in the hydroformylation reaction and formic acid (FA) as hydrogen source. This feature enabled the application of such system to promote the sequential hydroformylation/reduction of olefins, (Scheme 1.11).

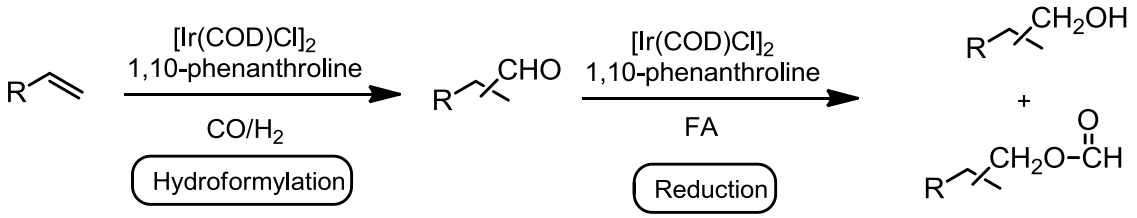

Scheme 1.11 One-pot hydroformylation/reduction of olefins with FA as hydrogen source.

The study reports the optimization of the catalytic system and its application in a large scope of olefins and 52 to 70 % yields for the desired reduced products were achieved. It should be noted that a mixture of alcohols and formate esters were obtained due to further alcohol esterification with formic acid. As example, oct-1-ene was 94% converted with 56% selectivity for the desired alcohols using $[Ir(COD)Cl]_2$/**1.21** as catalyst at T = 120 °C, 30 bar CO pressure and formic acid as hydrogen source, over 16 h (Table 1.2, Entry 7).

In sum, a diversity of active and selective homogeneous and heterogeneous catalysts based on Rh, Ru, Ir, Co and Au have been developed and optimized in recent years to promote hydroformylation/reduction processes, in order to obtain alcohols directly from olefins. However, despite the advances achieved in recent years, a great challenge remains to achieve regarding the application of this sequential process to sterically hindered substrates (such as di, tris and tetra-substituted olefins). This was one of the objectives of the work developed in this thesis and the results are presented in Chapter 2.

1.3.2- Sequential hydroformylation/reductive amination (Hydroaminomethylation)

Hydroaminomethylation (Scheme 1.7B), consists of a sequence of three reactional steps. In the first one, the olefins are converted into aldehydes through hydroformylation, which upon reaction which a primary or secondary amine, present in the reaction medium, give the respective imines or enamines through a condensation step. The last step is resultant from the hydrogenation of the enamine or imine intermediates to provide the final amine products (Scheme 1.12).

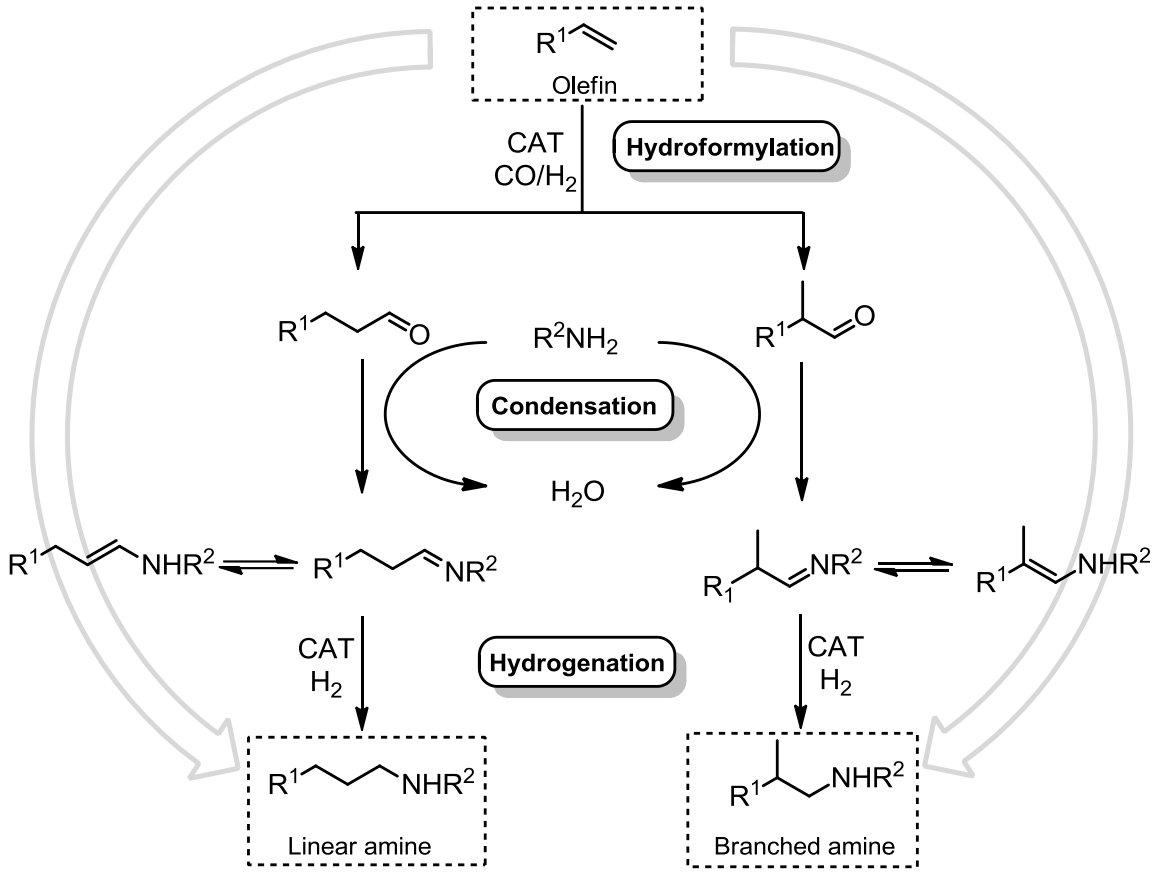

Scheme 1.12 Sequential hydroaminomethylation process.

The relevance of this sequential reaction is clearly evidenced by the large number of reports in the literature[16,116,144-147] including the recent review by Gaunt, "New Strategies for the Transition-Metal Catalyzed Synthesis of Aliphatic Amines", where some of the most relevant aspects of the hydroaminomethylation reaction for the synthesis of aliphatic amines are described.[148] The last update from state of the art regarding hydroaminomethylation of olefins was published in 2018.[15] Therefore, we present a literature review of this reaction published over the last three years (Table 1.3)

Table 1.3. State of the art for the hydroaminomethylation of olefins.

Entry	Catalyst	Substrate and Conditions[a]	Conversion (selectivity)[b] [%]
1	Hydroaminomethylation: $[Rh(octanoate)_2]_2$ Amine splitting: Shvo's catalyst 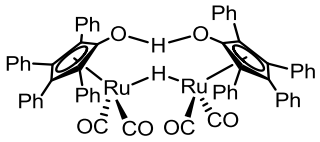 Shvo's Catalyst Vorholt[149]	Dicyclopentadiene T = 140 °C, P = 60 bar (CO/H_2), 3h T = 160 °C, NH_3, 16 h	99 (53) 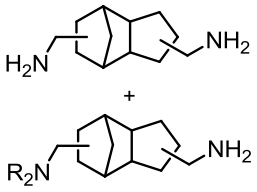
2	$[Rh(cod)Cl]_2$/sulfoxantphos 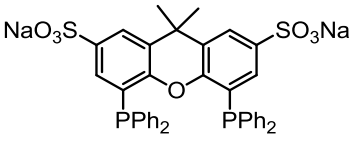 Sulfoxantphos Vorholt[117]	Oct-1-ene T = 100 °C, P = 50 bar (CO/H_2, 1:3), 6h	85 (79) 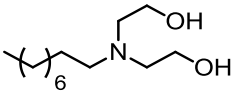
3	[Ir(COD)Cl]/**1.25** 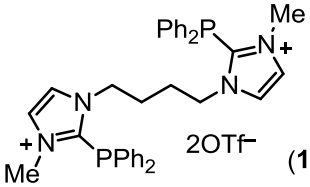 (**1.25**) Liu[150]	Hex-1-ene T = 140 °C, P = 40 bar CO, 3 mL H_2O, 22h	93(99) 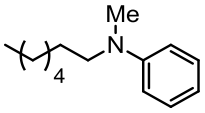
4	RAME-β-CD $[Rh(CO)_2acac]$/TPPTS 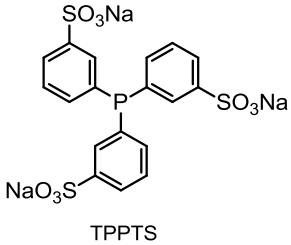 TPPTS Bhanage[151]	Eugenol T = 80 °C, P = 30 bar (CO/H_2), 8 h	92 (88) 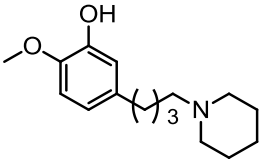

a) Optimized conditions for the selected example, b) Selectivity for amine products.

Table 1.3. State of the art for the hydroaminomethylation of olefins (cont.).

Entry	Catalyst	Substrate and Conditions[a]	Conversion (selectivity)[b] [%]
5	$[Rh(COD)(OMe)]_2$/**1.26** 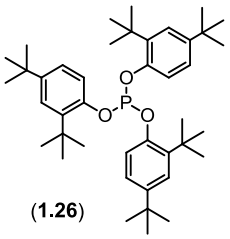 (**1.26**) Gusevskaya[152]	Limonene T = 100 °C, P = 60 bar (CO/H_2), 48 h	100 (98) 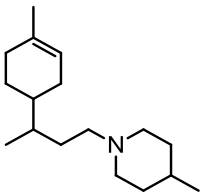
6	$[Rh(COD)_2]BF_4$/**1.27** 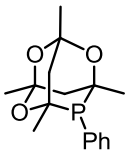 (**1.27**) Godard[153]	methyl methacrylate T = 70 °C, P = 30 bar (CO/H_2), 72 h	94 (87) 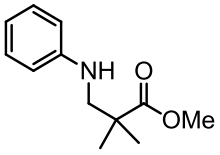
7	$[Rh(CO)_2(acac)]$/**1.28** 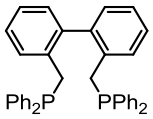 (**1.28**) 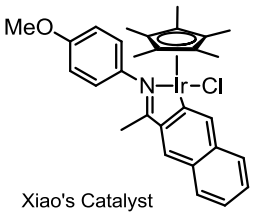 Xiao's Catalyst Hartwig[154]	Dec-1-ene T = 80 °C, P = 3.4 bar (CO/H_2), 20 h Aqueous sodium formate buffer (pH = 4.8)	78 (isolated yield) 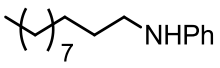
8	Ru_3CO_{12} Monflier[155]	Methyl undecenoate T = 110 °C, P = 100 bar (CO/H_2), 36 h	100 (96) 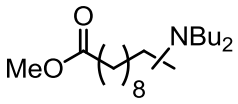
9	$[Rh(CO)_2(acac)]$/**1.29** 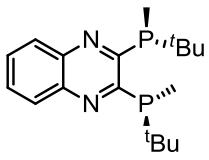 (R,R)-QuinoxP (**1.29**) Godard[156]	methyl methacrylate T = 90 °C, P = 10 bar (CO/H_2, 1:4), 16h	69 (63) 73 ee 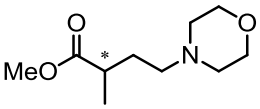

a) Optimized conditions for the selected example, b) Selectivity for amine products.

Table 1.3. State of the art for the hydroaminomethylation of olefins (cont.).

Entry	Catalyst	Substrate and Conditions[a]	Conversion (selectivity)[b] [%]
10	$[Ir(COD)Cl]_2$/**1.30** 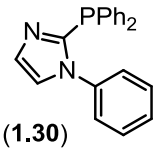 (**1.30**) Lin[157]	Oct-1-ene T = 120 °C, P = 40 bar (CO/H_2, 5:1), 7h	99 (87) 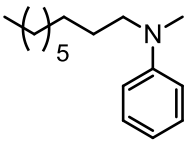
11	$[RhCl(COD)]_2$/**1.31** 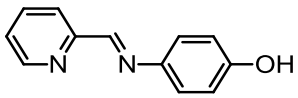 (**1.31**) Mapolie[158]	Oct-1-ene T = 85 °C, P = 30 bar (CO/H_2, 1:1), 2h	99 (89) 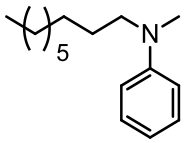

a) Optimized conditions for the selected example, b) Selectivity for amine products.

Vorholt[149] published a two-step sequential process for the preparation of primary amines, directly from olefins, using a combination of Rh/P-ligands with Ru/Shvos´s catalysts. This catalytic sequential system describes firstly the use of hydroaminomethylation catalyzed by $[Rh(octanoate)_2]_2$ without the addition of any ligand, as a synthetic tool for preparation of secondary amines (Scheme 1.13A). Then, the obtained secondary amine (**1.23**) was reacted with ammonia, using a Ru-Shvo's catalyst, to yield the desired primary amine (**1.24**), *via* amine splitting (Scheme 1.13B). Dicyclopentadiene (**1.24**) was used as model substrate and up to 29% yield for the desired diamine product and 24% yield for the primary monoamine product was obtained. The overall conversion for the hydroaminomethylation step reached 67% using 140 °C and 60 bar of *syngas*, for 3 h, (Table 1.3, Entry 1).

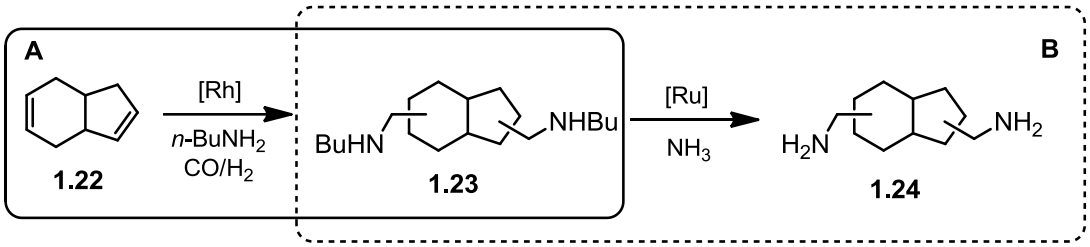

Scheme 1.13 Sequential strategy for the preparation of primary amines from dicyclopentadiene. A: hydroaminomethylation. B: Ru-catalyzed amine splitting.

The same author reported another sustainable strategy for hydroaminomethylation, under aqueous conditions, using Rh/sulfoxantphos as catalyst, oct-1-ene as substrate and diethanolamine as nucleophile, at 100 °C temperature and P(CO/H_2 1:3) = 50 bar, finding up to 85% of olefin conversion and 79% selectivity for the desired amine, after 6 h, (Table 1.3, Entry 2).[117]

Liu[150] reported the hydroaminomethylation of olefins in water, using an Ir/ionic diphosphine as catalyst for the hydroformylation step and a reverse water shift reaction (RWSC) as an alternative hydrogen source. The use of[Ir(COD)Cl]/**1.25** at RWGS conditions at 140 °C, 40 bar CO, *N*-methylaniline in water (3 mL) over 22 h led to a 93% conversion of hex-1-ene into the *N*-methylaniline derivative with 99% selectivity (Table 1.3, Entry 3). In addition, the use of water as hydrogen donor was advantageously shown to completely inhibit the production of alkanes as reduction side products.

Another relevant example of the use of the hydroaminomethylation reaction, under aqueous conditions, was described by Bhanage[151] aiming at the functionalization of natural relevant molecules (eugenol, anethole and estragole). The reactions were catalyzed by rhodium/trisulfonated triphenylphosphine complexes (TPPTS) in the presence of cyclodextrins. The addition of cyclodextrins as a mass transfer agent remarkably increased the reaction rate and the selectivity for linear amines, particularly when RAME-β-CD (RAME = randomly methylated) was used as a mass transfer agent. The evaluation of different reaction conditions is reported and the catalytic system (Rh/TPPTS/RAME-β-CD) gave the best results. Using a pressure of 30 bar (CO/H_2) at 80 °C, over 8 h, 92% of eugenol was converted to the desired piperidine derivative with 88% selectivity (Table 1.3, Entry 4). It should be noticed that this catalytic system was recycled up to five times without a significant loss in activity and selectivity.

The application of hydroaminomethylation reaction to promote the functionalization of several bio-renewable alkenes (estragole, limonene, camphene and β-pinene) using alternative renewable solvents was reported by Gusevskaya.[152] It is noteworthy that the use of *p*-cymene anisole or ethanol as alternative solvents in the hydroaminomethylation reaction of natural terpenes, catalyzed by [Rh]/**1.26**, gave similar results to the ones obtained with toluene. As selected example, limonene was converted to 98% of the respective exocyclic amine derivative, using [Rh]/**1.26** as catalyst and 4-4-methylpiperidine as nucleophile, at 100 °C and 60 bar (CO/H_2) over 48 h (Table 1.3, Entry 5).

Godard[153] successfully achieved the synthesis of β-2,2-amino esters via Rh-catalyzed hydroaminomethylation using methyl methacrylate as starting material and secondary or aromatic amines as nucleophiles. The application of $[Rh(COD)_2]BF_4$/**1.27** as catalytic system and aniline as nucleophile at 70 °C, 30 bar (CO/H_2) for 72 h, gave aniline-methyl methacrylate derivatives with 94% conversion and 87% selectivity for the linear product, (Table 1.3 Entry 6). The author also reported that the presence of molecular sieves, to avoid the presence of water is crucial to obtain the final amino ester in good yields.

Hartwig[154] reported the hydroaminomethylation of a set of α-olefins at low *syn*gas pressure (1 to 3.5 bar) and temperatures (70-80 °C) using rhodium diphosphine complexes as catalyst for the hydroformylation step followed by a transfer hydrogenation reductive amination step, catalyzed by iridium complexes and sodium formate as hydrogen source. As an illustrative example, dec-1-ene reacted with aniline in the presence of $[Rh(CO)_2acac]$/**1.28** and Xiao's catalyst at 80 °C, 3.4 bar (CO/H_2) under aqueous sodium formate buffer (pH = 4.8) for 20 h yielding 78% of the desired linear amine (Table 1.3, Entry 7).

The hydroaminomethylation of a set of unsaturated oleochemicals was published by Monflier.[155] Remarkably, the authors used $[Ru_3CO_{12}]$ as catalyst in total absence of phosphines. As selected example, we highlight the hydroaminomethylation reaction (96% amine selectivity) methyl undecenoate, using dibutylamine as nucleophile at temperature of 110 °C, pressure of 100 bar (CO/H_2) along 36 h, (Table 1.3, Entry 8). These results are of great importance for industrial purposes since the obtained amino-products can be directly used in polymers, surfactants and lubricants.

Godard[156] reported the application of asymmetric intermolecular hydroaminomethylation of alkenes using a rhodium single catalyst bearing the (R,R)-QuinoxP as ligand for the preparation of chiral γ-aminobutyric esters (Scheme 1.14). Methyl methacrylate was used as model substrate for the optimization of reaction conditions. At optimized conditions, using morpholine as amine and Rh/**1.29** as catalyst, at 90 °C and 10 bar (CO/H_2, 1:4) for 16 h, 63% yield and 73% *ee* of the desired product was obtained. (Table 1.3, Entry 9). This hydroaminomethylation of α-alkyl acrylates is an efficient tool for the regio and enantioselective synthesis of γ-amino esters. A scope of several α-alkyl-acrylates is also presented with *ee'*s up to 86%.

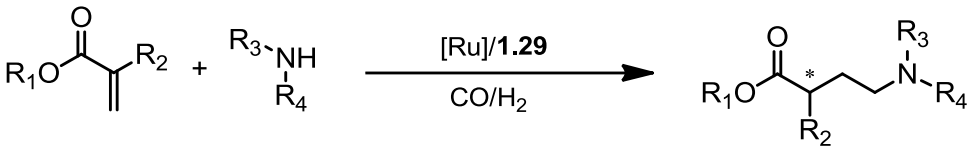

Scheme 1.14 Synthetic strategy for the preparation of chiral γ-aminobutyric esters *via* asymmetric hydroaminomethylation.

Lin[157] evaluated the electronic and steric effects of Ir(I) complexes containing different phosphine type ligands (neutral and ionic, mono- and diphosphines) for the hydroamynomethylation of olefins using oct-1-ene as model substrate. He reported the Ir(I)/mono-phosphine ligand (**1.30**) as the best catalyst for the hydroaminomethylation, at a temperature of 120 °C and pressure of 40 bar (CO/H_2, 5:1) over 7 h. Under these reaction conditions, the authors obtained 99% of olefin conversion and 87% selectivity for amines (Table 1.3 entry 10).

Mapolie[158] developed a new Rh(I)/**1.31** complex as catalysts for the hydroaminomethylation of oct-1-ene and reported their evaluation under several conditions. The catalyst showed the best performance at 85 °C, 30 bar (CO/H_2, 1:1) for 2 h. Under these reaction conditions, oct-1-ene was fully converted with 89% selectivity for the amine product (Table 1.3, Entry 11). They also reported the influence of the amine basicity in the rate of the reaction and concluded that more basic amines lead to faster reactions and consequently the yield of the desired *N*-alkylated amine increased.

Several developments regarding hydroaminomethylation have been made in the last three years mostly Rh and Ir modified catalyst were applied with success for the

transformation of several olefins using a wide range of amines. In most cases, high activity and selectivity of the catalysts were observed. These publications demonstrate the relevance of hidroaminomethylation for the synthesis of new amine bonds starting from olefins.

1.3.3 Sequential hydroformylation/acetalization

Another relevant sequential transformation for the preparation of fine chemicals based on hydroformylation as central reaction (Scheme 1.7C) is the hydroformylation/acetalization, which is also one of the main goals of this thesis. This sequential process usually requires an Rh/P catalyst for the hydroformylation step and an acid to catalyze the second transformation of aldehydes into the desired acetals (Scheme 1.15).

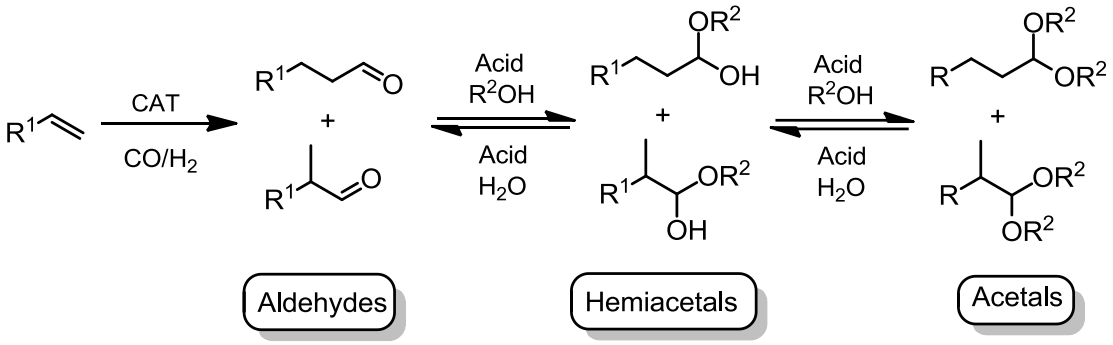

Scheme 1.15 Preparation of acetals from olefins *via* hydroformylation/acetalization

Although there are currently no review articles exclusively dedicated to hydroformylation/acetalization reaction, this sequential process has been recently reviewed in several books and review articles focused on hydroformylation as central reaction.[12,35,39,159] Therefore, herein we present a literature revision for the sequential hydroformylation/acetalization reactions, published over the last five years and the main results are summarized in Table 1.4.

Table 1.4. State of the art for hydroformylation/acetalization reaction.

Entry	Catalyst	Substrate and Conditions[a]	Conversion (selectivity)[b][%]
1	[$Rh(CO)_2(acac)$]/TPPTS 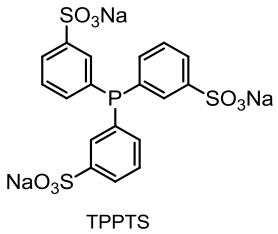 TPPTS H_2SO_4 (1M) Karakhanov[115]	Oct-1-ene T = 70 °C, P = 40 bar (CO/H_2), 5 h	99 (92) 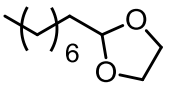
2	[$Rh(CO)_2(acac)$]/PPh_3, Amberlyst-16 Karakhanov [160]	Oct-1-ene T = 80 °C, P = 40 bar (CO/H_2), 3 h	99(97) 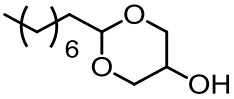
3	[$Rh(CO)_2(acac)$]/**1.32** 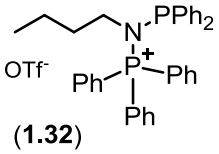 (**1.32**) Liu[161]	Oct-1-ene T = 100 °C, P = 40 bar (CO/H_2), 3 h	99(87) 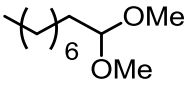
4	[$Rh(CO)_2acac$]/**1.33** 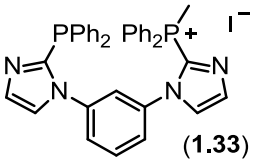 (**1.33**) Liu[162]	Styrene T = 100 °C, P = 40 bar (CO/H_2), 7 h [Bmim]BF4	99(97) 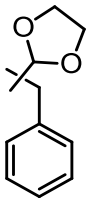
5	[$Rh(CO)_2acac$]/**1.34** 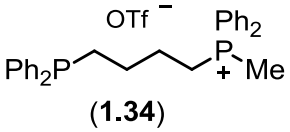 (**1.34**) Liu[163]	Oct-1-ene T = 100 °C, P = 40 bar (CO/H_2), 3 h	97(97) 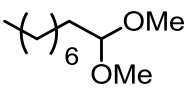
6	[$IrCl_3.3H_2O$]/**1.35** 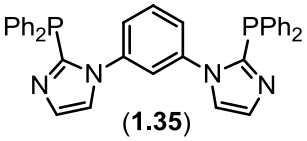 (**1.35**) Liu[164]	Hex-1-ene T = 110 °C, P = 40 bar (CO/H_2, 5:1), 8 h	97(92) 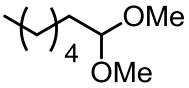

a) Optimized conditions for the selected example, b) Chemoselectivity for acetal products.

Table 1.4. State of the art for hydroformylation/acetalization reaction (cont.).

Entry	Catalyst	Substrate and Conditions[a]	Conversion (selectivity)[b][%]
7	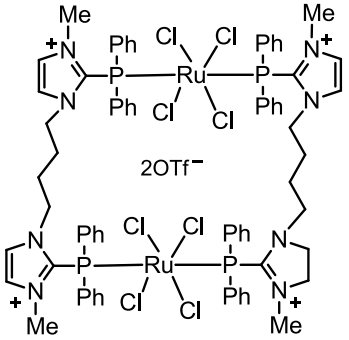 (**1.37**) Liu[113]	Oct-1-ene T = 120 °C, P = 40 bar (CO/H_2), 48 h	99(90) 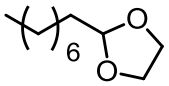
8	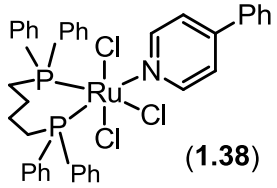 (**1.38**) mer-[$RuCl_3$(dppb)(4-Phpy)] Batista[114]	Dec-1-ene T = 160 °C, P = 100 bar ($CO/H_{2,}$), 24 h	99(52) 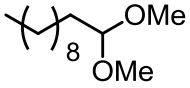

a) Optimized conditions for the selected example, b) Chemoselectivity for acetal products.

Karakhanov[115] described the sequential hydroformylation/acetalization of oct-1-ene catalyzed by [$Rh(CO)_2$(acac)]/TPPTS (TPPTS = *tris*(3-sulfonatophenyl)phosphine trisodium salt) and H_2SO_4 (1M) at 70 °C and pressure of 40 bar (CO/H_2), using polyols/water as solvent and acetalization reagents. Under these reaction conditions and using ethylene glycol as reagent, full substrate conversion of oct-1-ene was achieved with 92% for acetal formation. The use of water-soluble TPPTS as ligand facilitates the reutilization of the catalyst by the application of a biphasic system, where the catalyst remains in the aqueous phase and the products are separated in the organic phase. The Rh/TPPTS system was reused over 5 cycles without significant loss of the catalyst activity (Table 1.4, Entry 1). Recently, Karakhanov published a follow-up study on the preparation of acetals with sequential hydroformylation/acetalization where a series of olefins and polyols were tested in this water-soluble catalytic system.[165] Additionally, Karakhanov[160] also reported the application of cation-exchange resins (Amberlyst-16, Wofatit KPS 200, Nafion) to act as catalysts in the acetalization step. One of the best results described

relates to the use of oct-1-ene as substrate, glycerol as alcohol, Rh/PPh_3 as hydroformylation catalyst, amberlyst-16 as acid catalyst, at 80 °C, and pressure of 40 bar (CO/H_2). Under these reaction conditions, full substrate conversion and 97% acetal selectivity was obtained (Table 1.4, Entry 2).

Liu[161] developed a series of ionic phosphonium-based aminophosphines which encompass bifunctional moieties of a phosphine and a Lewis acidic phosphonium group (Scheme 1.16). These molecules were applied as ligands in the Rh-catalyzed hydroformylation/acetalization of olefins. When oct-1-ene is the substrate and methanol is used as solvent and reagent, at 70 °C and 40 bar CO/H_2 pressure, the $[Rh(CO)_2acac]$/**1.32** is the best catalyst, giving full conversion and 87% of acetal selectivity after 5 h, (Table 1.3, Entry 3). Complex $[Rh(CO)_2acac]$/**1.32** also exhibited good results for a wide range of olefins and different alcohols.

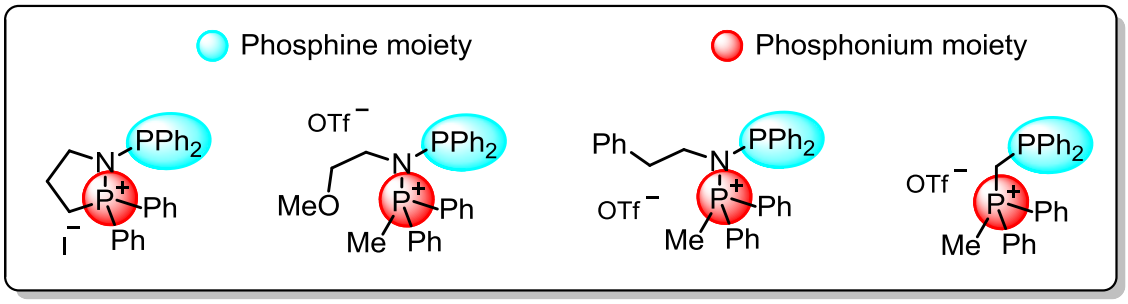

Scheme 1.16 Bifunctional ligands developed by Liu and coworkers.

Another Liu´s publication[162] reports the synthesis of a novel set of bi-functional phosphines containing also a phosphonium group as Lewis acid. The application of rhodium complexes of these ligands as catalysts for the hydroformylation/acetalization of olefins was accomplished with promising results. The application of $[Rh(CO)_2acac]$/**1.33** catalytic system to a set of olefins resulted in full conversions and generally high selectivity to acetals, over 80% in most cases (120 °C, 40 bar (CO/H_2), 7 h). Moreover, the $[Rh(CO)_2acac]$/**1.33** system could be recycled several times using a biphasic system composed by $[Bmim]BF_4$ ionic liquid. The ionic nature of the ligand keeps it on the IL phase while the products remain in the organic phase, composed by the unreacted substrate and the reaction products, aldehydes and acetals (Scheme 1.17). The authors applied this biphasic system to the hydroformylation/acetalization of styrene using ethylenoglycol as

acetalization reagent, at 100 °C and 40 bar CO/H_2 pressure, for 7 h and full conversion with 97% selectivity for acetals was reported (Table 1.4, Entry 4). The catalyst was recycled for 7 runs with a small activity loss (from 99 to 86%).

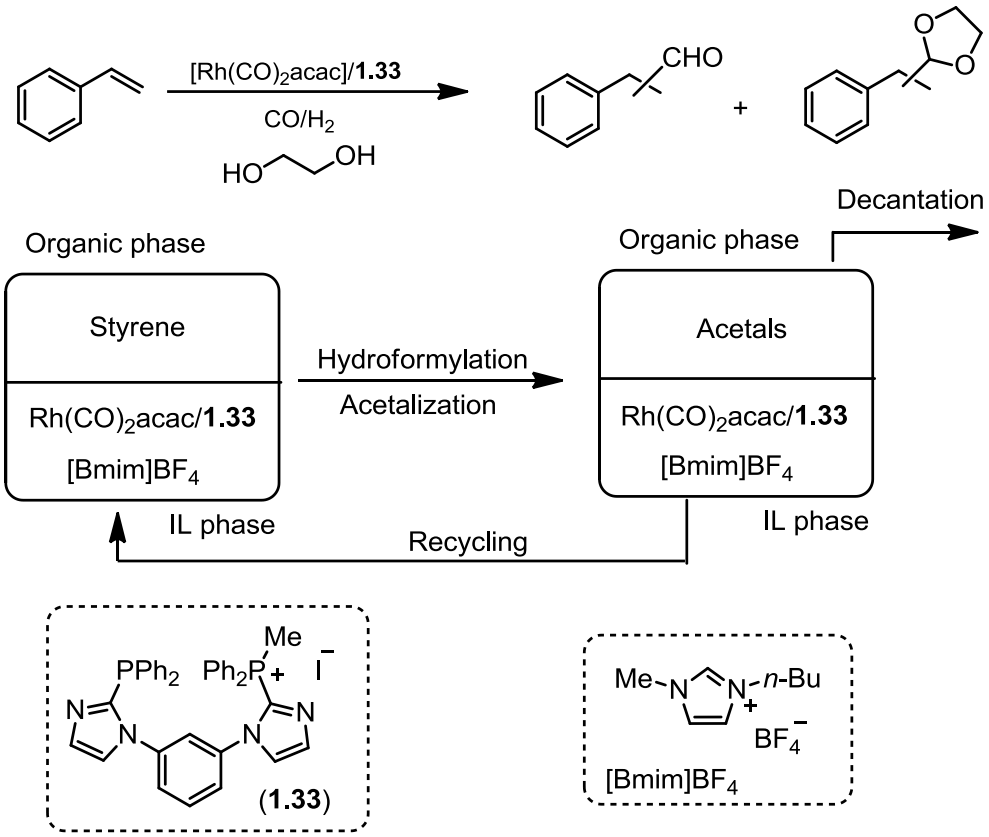

Scheme 1.17 Biphasic system for the hydroformylation/acetalization of styrene.

In 2017 Liu[163] prepared another set of phosphine-functionalized phosphonium-based ionic liquids with the same bi-functional features. The use of diphosphonium-based ionic liquid as co-solvent enabled the reutilization of the catalyst in the hydroformylation/acetalization of olefins. As an example $[Rh(CO)_2acac]$/**1.34** was evaluated as catalyst in the transformation of oct-1-ene under optimized reaction conditions (100 °C, 40 bar CO/H_2, 3 h) yielding 97% of olefin conversion and 97% of acetal selectivity, (Table 1.4, Entry 5) The catalytic system was recycled up to seven times without significant loss of activity and selectivity.

Liu pursued the studies of sequential hydroformylation/acetalization of olefins by developing an $IrCl_3.3H_2O$/electron-deficient phosphine complex.[164] The best result was achieved with hex-1-ene as substrate, $[IrCl_3.3H_2O]$/**1.35** as catalyst and methanol as

alcohol, at 110 °C and pressure of 40 bar CO/H_2 (5:1). After 8 h the authors obtained 97% conversion and 92% of acetal selectivity, (Table 1.4, Entry 6). Additionally, the catalyst based on the iridium complex of the ionic phosphine **1.36** was recovered using $[Bmim]PF_6$ and tested in the hydroformylation/acetalization of hex-1-ene, (Scheme 1.18). This catalytic system gave promising results and the catalyst was recycled 6 times with a constant small decrease in activity after the third cycle to the sixth (from 88 to 77% acetal yield).

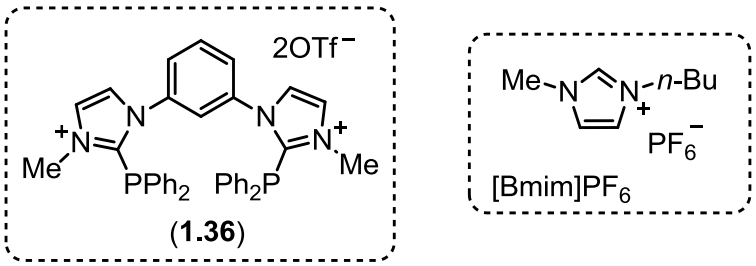

Scheme 1.18 Structure of the ionic phosphine **1.36** and the ionic liquid $[Bmim]PF_6$

Liu also reported a Ru(III)-catalyzed three-step tandem hydroformylation/acetalization/hydrogenolysis to produce alcohol derivatives from olefins but using aldehydes and acetals as intermediary species (Scheme 1.19).[113] Despite the main goal of this study be the preparation of alcohols from olefins, it should be noted that, under specific reaction conditions, complex **1.37** is able to selectively prepare acetals. Using oct-1-ene as substrate and ethylene glycol as solvent, at 120 °C and 40 bar (CO/H_2,) pressure, over 48 h, **1.37** was able to convert 99% of the olefin onto 90% selectivity for the product acetal, (Table 1.4, Entry 7)

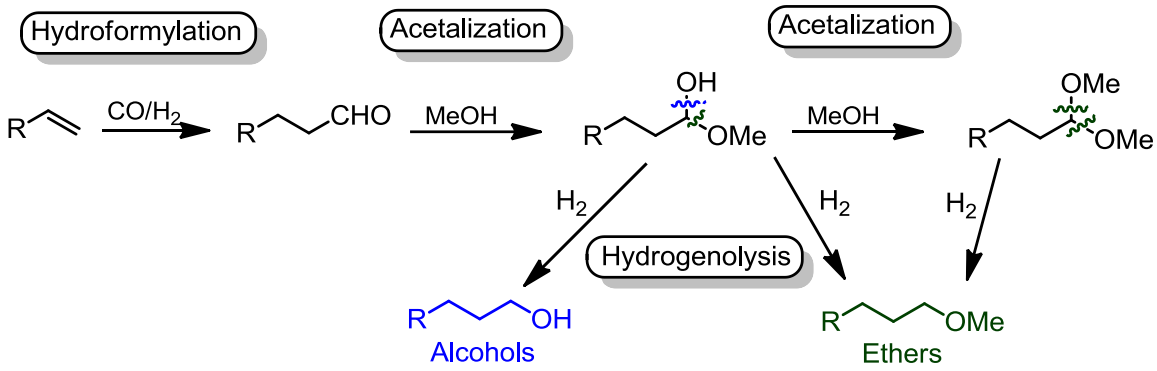

Scheme 1.19 Tandem hydroformylation/acetalization/hydrogenolysis to produce alcohol derivatives from olefins catalyzed by **1.37** catalyst.

The utilization of a set of Ru-based catalysts in the preparation of acetals from olefins was also reported by Batista[114] and *mer*-[$RuCl_3$(dppb)(4-Phpy)] complex (**1.38**) revealed to be the catalyst with the best performance. As an example, the hydroformylation/acetalization of dec-1-ene with methanol, at 160 °C and 100 bar of CO/H_2, over 24 h, lead to 99% substrate consumption and 52% acetal selectivity (Table 1.4, Entry 8).

In recent years, several ligands have been synthesized and applied in metal-catalyzed hydroformylation/acetalization reactions. We consider that Liu greatly contributed with the development of a set of bifunctional ligands. Phosphines containing also a phosphonium group that can act as catalyst in the acetalization step. Usually, the reported catalytic systems revealed high activity and selectivity towards the desired acetals. Considering the enormous relevance of sequential hydroformylation/acetalization reactions, it was also the main goal of the present work the development of heterogeneous catalysts for the valorization of olefins.

1.4 Main goals

The overall objectives of the studies described in this thesis are focused on the development of sustainable catalytic processes, able to promote the direct transformation of olefins into added-value products, namely, aldehydes, alcohols and acetals. In order to increase the sustainability of the processes, innovative methodologies were intended to immobilize homogeneous catalysts on solid supports (MNPs and MWCNTs), with the purpose of their recovery and reuse.

Thus, as specific objectives, it was intended to develop active and selective hydroformylation systems using rhodium catalysts, and also to develop sequential hydroformylation/reduction and hydroformylation/acetalization processes using Rh/Ru and Rh/Fe bimetallic catalysts, respectively, to obtain the corresponding alcohols and acetals (Scheme 1.20).

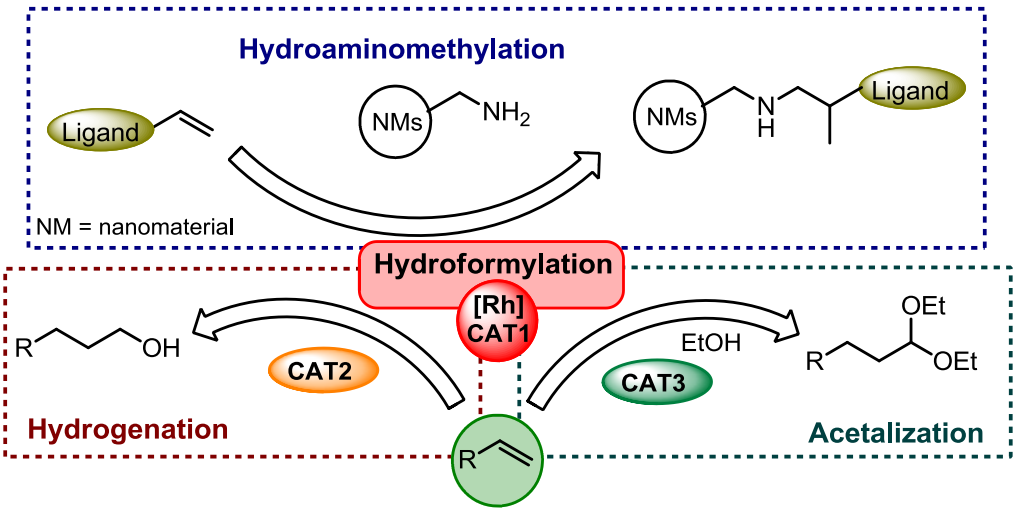

Scheme 1.20 Thesis graphical abstract

1.5 References

[1] P. Marion, B. Bernela, A. Piccirilli, B. Estrine, N. Patouillard, J. Guilbot, F. Jérôme, *Green Chem.* "Sustainable chemistry: how to produce better and more from less?" **2017**, *19*, 4973-4989.

[2] P. Anastas, N. Eghbali, *Chem. Soc. Rev.* "Green chemistry: principles and practice" **2010**, *39*, 301-312.

[3] P. T. Anastas, J. C. Warner, *Green Chemistry: Theory and Practice*, Oxford University Press, New York, **1998**.

[4] P. J. Dunn, *Chem. Soc. Rev.* "The importance of green chemistry in process research and development" **2012**, *41*, 1452-1461.

[5] R. A. Sheldon, *ACS Sustain. Chem. Eng* "Metrics of Green Chemistry and Sustainability: Past, Present, and Future" **2017**, *6*, 32-48.

[6] R. A. Sheldon, *Green Chem.* "The E factor 25 years on: the rise of green chemistry and sustainability" **2017**, *19*, 18-43.

[7] H. C. Erythropel, J. B. Zimmerman, T. M. de Winter, L. Petitjean, F. Melnikov, C. H. Lam, A. W. Lounsbury, K. E. Mellor, N. Z. Janković, Q. Tu, L. N. Pincus, M. M. Falinski, W. Shi, P. Coish, D. L. Plata, P. T. Anastas, *Green Chem.* "The Green ChemisTREE: 20 years after taking root with the 12 principles" **2018**, *20*, 1929-1961.

[8] B. A. de Marco, B. S. Rechelo, E. G. Totoli, A. C. Kogawa, H. R. N. Salgado, *Saudi Pharm J* "Evolution of green chemistry and its multidimensional impacts: A review" **2019**, *27*, 1-8.

[9] L. Marcelino, J. Sjöström, C. A. Marques, *Sustainability* "Socio-Problematization of Green Chemistry: Enriching Systems Thinking and Social Sustainability by Education" **2019**, *11*, 7123.

[10] P. Tundo, E. Griguol, *Chem. Int.* "Green Chemistry for Sustainable Development" **2018**, *40*, 18-24.

[11] "http://catsus.tecnico.ulisboa.pt/" **10/10/2020**.

[12] B. P. Bondžić, *J. Mol. Catal. A: Chem.* "Rh catalyzed multicomponent tandem and one-pot reactions under hydroformylation conditions" **2015**, *408*, 310-334.

[13] G. M. Torres, R. Frauenlob, R. Franke, A. Börner, *Catal. Sci. Technol.* "Production of alcohols via hydroformylation" **2015**, *5*, 34-54.

[14] E. V. Gusevskaya, J. Jiménez-Pinto, A. Börner, *ChemCatChem* "Hydroformylation in the Realm of Scents" **2014**, *6*, 382-411.

[15] P. Kalck, M. Urrutigoity, *Chem. Rev.* "Tandem Hydroaminomethylation Reaction to Synthesize Amines from Alkenes" **2018**, *118*, 3833-3861.

[16] C. Chen, X.-Q. Dong, X. Zhang, *Org. Chem. Front.* "Recent progress in rhodium-catalyzed hydroaminomethylation" **2016**, *3*, 1359-1370.

[17] P. Kalck, M. Urrutigoity, *Rhodium Catalysis* "Tandem Rhodium Carbonylation Reactions" **2018**, *61*, 69-98.

[18] T. L. Lohr, T. J. Marks, *Nat. Chem.* "Orthogonal tandem catalysis" **2015**, *7*, 477-482.

[19] D. E. Fogg, E. N. dos Santos, *Coord. Chem. Rev.* "Tandem catalysis: a taxonomy and illustrative review" **2004**, *248*, 2365-2379.

[20] L. F. Tietze, *Chem. Rev.* "Domino Reactions in Organic Synthesis" **1996**, *96*, 115-136.

[21] A. Galván, F. J. Fañanás, F. Rodríguez, *Eur. J. Inorg. Chem.* "Multicomponent and Multicatalytic Reactions - A Synthetic Strategy Inspired by Nature" **2016**, *2016*, 1306-1313.
[22] A. Kirschning, *Top. Curr. Chem.* "Immobilized Catalysts" **2004**, *242*, 1-42.
[23] M. J. Jacinto, P. K. Kiyohara, S. H. Masunaga, R. F. Jardim, L. M. Rossi, *Appl. Catal. A, Gen.* "Recoverable rhodium nanoparticles: Synthesis, characterization and catalytic performance in hydrogenation reactions" **2008**, *338*, 52-57.
[24] Â. C. B. Neves, M. J. F. Calvete, T. M. V. D. Pinho e Melo, M. M. Pereira, *Eur. J. Org. Chem.* "Immobilized Catalysts for Hydroformylation Reactions: A Versatile Tool for Aldehyde Synthesis" **2012**, *2012*, 6309-6320.
[25] C. Li, W. Wang, L. Yan, Y. Ding, *Front. Chem. Sci. Eng.* "A mini review on strategies for heterogenization of rhodium-based hydroformylation catalysts" **2017**, *12*, 113-123.
[26] M. Benaglia, A. Puglisi, *Catalyst Immobilization*, Wiley-VCH, Weinheim, **2020**.
[27] J. M. Munoz-Molina, T. R. Belderrain, P. J. Perez, *Dalton Trans* "Group 11 *tris*(pyrazolyl)methane complexes: structural features and catalytic applications" **2019**, *48*, 10772-10781.
[28] L. M. D. R. S. Martins, *Coord. Chem. Rev.* "C-scorpionate complexes: Ever young catalytic tools" **2019**, *396*, 89-102.
[29] L. M. D. R. S. Martins, A. J. L. Pombeiro, *Eur. J. Inorg. Chem.* "Water-Soluble C-Scorpionate Complexes - Catalytic and Biological Applications" **2016**, *2016*, 2236-2252.
[30] B. G. Rocha, T. C. Mac Leod, M. F. Guedes da Silva, K. V. Luzyanin, L. M. Martins, A. J. Pombeiro, *Dalton Trans* "NiII, CuII and ZnII complexes with a sterically hindered scorpionate ligand (TpmsPh) and catalytic application in the diasteroselective nitroaldol (Henry) reaction" **2014**, *43*, 15192-15200.
[31] T. F. S. Silva, E. C. B. A. Alegria, L. M. D. R. S. Martins, A. J. L. Pombeiro, *Adv. Synth. Catal.* "Half-Sandwich Scorpionate Vanadium, Iron and Copper Complexes: Synthesis and Application in the Catalytic Peroxidative Oxidation of Cyclohexane under Mild Conditions" **2008**, *350*, 706-716.
[32] C. Claver, *Rhodium Catalysis*, Springer, **2018**.
[33] U. Gellrich, T. Koslowski, *WIREs Comput. Mol. Sci.* "Rh chemistry through the eyes of theory" **2016**, *6*, 311-320.
[34] P. W. N. M. van Leeuwen, *Homogeneous Catalysis*, Springer, Amsterdam, **2004**.
[35] R. Franke, D. Selent, A. Borner, *Chem. Rev.* "Applied hydroformylation" **2012**, *112*, 5675-5732.
[36] O. Roelen*, Vol. DE849548*, **1938**.
[37] G. D. Frey, *J. Organomet. Chem.* "75 Years of oxo synthesis – The success story of a discovery at the OXEA Site Ruhrchemie" **2014**, *754*, 5-7.
[38] E. Billig, A. G. Abatjoglou, D. R. Bryant, R. E. Murray, J. M. Mather, US4599206A, **1986**.
[39] A. Börner, R. Franke., *Hydroformylation: Fundamentals, Processes, and Applications in Organic Synthesis*, Wiley-VCH, Weinheim, **2016**.
[40] P. W. N. M. van Leeuwen, C. Claver, *Rhodium Catalyzed Hydroformylation*, Kluwer Academic Publishers, New York, **2002**.

[41] B. R. Tudor, M. Ashley, *Platinum Met. Rev.* "Enhancement of Industrial Hydroformylation Processes by the Adoption of Rhodium-Based Catalyst: Part II" **2007**, *51*, 164-171.
[42] L. Wu, Q. Liu, R. Jackstell, M. Beller, *Angew. Chem. Int. Ed. Engl.* "Carbonylations of alkenes with CO surrogates" **2014**, *53*, 6310-6320.
[43] F. P. Pruchnik, *Organometallic Chemistry of the Transition Elements*, Plenum Press, New York, **1990**.
[44] P. W. N. M. van Leeuwen, P. C. J. Kamer, *Catal. Sci. Technol.* "Featuring Xantphos" **2018**, *8*, 26-113.
[45] T. Scherpf, C. Schwarz, L. T. Scharf, J. A. Zur, A. Helbig, V. H. Gessner, *Angew. Chem. Int. Ed. Engl.* "Ylide-Functionalized Phosphines: Strong Donor Ligands for Homogeneous Catalysis" **2018**, *57*, 12859-12864.
[46] P. C. J. Kamer, P. W. N. M. van Leeuwen, *Phosphorus(III) Ligands in Homogeneous Catalysis: Design and Synthesis*, John Wiley & Sons, Ltd, Chichester, **2012**.
[47] E. I. Musina, A. S. Balueva, A. A. Karasik, *Phosphines: preparation, reactivity and applications, Vol. 48*, RSC, **2019**.
[48] P. A. Aguirre, C. A. Lagos, S. A. Moya, C. Zuniga, C. Vera-Oyarce, E. Sola, G. Peris, J. C. Bayon, *Dalton Trans* "Methoxycarbonylation of olefins catalyzed by palladium complexes bearing P,N-donor ligands" **2007**, 5419-5426.
[49] M. Diéguez, M. M. Pereira, A. M. Masdeu-Bultó, C. Claver, J. C. Bayón, *J. Mol. Catal. A: Chem.* "Rhodium-diphosphine catalysts for the hydroformylation of styrene: the influence of the excess of ligand and the chelate ring size on the reaction selectivity" **1999**, *143*, 111-122.
[50] J. C. Bayón, C. Claver, A. M. Masdeu-Bultó, *Coord. Chem. Rev.* "Homogeneous catalysis with transition metal complexes containing sulfur ligands" **1999**, *193-195*, 73-145.
[51] A. Peixoto, A. Abreu, A. Almeida, A. Neves, P. Abreu, M. Moreno, J. Bayon, A. Pais, M. Pereira, *Current Organic Synthesis* "BINOL-Based Ditopic Diphosphite Ligands – Synthesis, Evaluation and Regioselectivity Optimization of Catalytic Hydroformylation by 2^3 Factorial Design" **2014**, *11*, 301-309.
[52] R. M. B. Carrilho, A. C. B. Neves, M. A. O. Lourenço, A. R. Abreu, M. T. S. Rosado, P. E. Abreu, M. E. S. Eusébio, L. Kollár, J. C. Bayón, M. M. Pereira, *J. Organomet. Chem.* "Rhodium/tris-binaphthyl chiral monophosphite complexes: Efficient catalysts for the hydroformylation of disubstituted aryl olefins" **2012**, *698*, 28-34.
[53] J. A. Osborn, G. Wilkinson, J. J. Mrowca, *Inorg. Synth.* "Tris(triphenylphosphine)halorhodium(I)" **1967**, *10*, 67-71.
[54] J. A. Osborn, F. H. Jardine, J. F. Young, G. Wilkinson, *J. Chem. Soc. A* "The preparation and properties of tris(triphenylphosphine)halogenorhodium(I) and some reactions thereof including catalytic homogeneous hydrogenation of olefins and acetylenes and their derivatives" **1966**.
[55] C. A. Tolman, *Chem. Rev.* "Steric effects of phosphorus ligands in organometallic chemistry and homogeneous catalysis" **1977**, *77*, 313-348.
[56] P. C. Kamer, P. W. van Leeuwen, J. N. Reek, *Acc. Chem. Res.* "Wide bite angle diphosphines: xantphos ligands in transition metal complexes and catalysis" **2001**, *34*, 895-904.
[57] M. Kranenburg, Y. E. M. van der Burgt, P. C. J. Kamer, P. W. N. M. van Leeuwen, K. Goubitz, J. Fraanje, *Organometallics* "New Diphosphine Ligands Based on

Heterocyclic Aromatics Inducing Very High Regioselectivity in Rhodium-Catalyzed Hydroformylation: Effect of the Bite Angle" **1995**, *14*, 3081-3089.

[58] T. Jongsma, G. Challa, P. W. N. M. van Leeuwen, *J. Organomet. Chem.* "A mechanistic study of rhodium tri(o-t-butylphenyl)phosphite complexes as hydroformylation catalysts" **1991**, *421*, 121-128.

[59] A. van Rooy, E. N. Orij, P. C. J. Kamer, P. W. N. M. van Leeuwen, *Organometallics* "Hydroformylation with a Rhodium/Bulky Phosphite Modified Catalyst. A Comparison of the Catalyst Behavior for Oct-1-ene, Cyclohexene, and Styrene" **1995**, *14*, 34-43.

[60] P. W. N. M. van Leeuwen, C. F. Roobeek, *J. Organomet. Chem.* "Hydroformylation of less reactive olefins with modified rhodium catalysts" **1983**, *258*, 343-350.

[61] M. Diéguez, O. Pàmies, C. Claver, *Tetrahedron: Asymmetry* "Recent advances in Rh-catalyzed asymmetric hydroformylation using phosphite ligands" **2004**, *15*, 2113-2122.

[62] M. Diéguez, O. Pàmies, A. Ruiz, C. Claver, *New J. Chem.* "Asymmetric hydroformylation of styrene catalyzed by carbohydrate diphosphite-Rh(I) complexes" **2002**, *26*, 827-833.

[63] A. T. Axtell, J. Klosin, G. T. Whiteker, C. J. Cobley, M. E. Fox, M. Jackson, K. A. Abboud, *Organometallics* "Bridging Group Effects in Chelating Bis(2,5-diphenylphospholane) Ligands for Rhodium-Catalyzed Asymmetric Hydroformylation" **2009**, *28*, 2993-2999.

[64] T. P. Clark, C. R. Landis, S. L. Freed, J. Klosin, K. A. Abboud, *J. Am. Chem. Soc.* "Highly active, regioselective, and enantioselective hydroformylation with Rh catalysts ligated by Bis-3,4-diazaphospholanes" **2005**, *127*, 5040-5042.

[65] R. Tanaka, K. Nakano, K. Nozaki, *J. Org. Chem.* "Synthesis of alpha-heteroarylpropanoic acid via asymmetric hydroformylation catalyzed by Rh(I)-(R,S)-BINAPHOS and the subsequent oxidation" **2007**, *72*, 8671-8676.

[66] P. A. Evans, E. A. Clizbe, M. J. Lawler, S. Oliver, *Chem. Sci.* "Enantioselective rhodium-catalyzed allylic alkylation of acyclic α-alkoxy substituted ketones using a chiral monodentate phosphite ligand" **2012**, *3,* 1835-1838.

[67] M. J. Bravo, R. M. Ceder, A. Grabulosa, G. Muller, M. Rocamora, J. C. Bayón, D. Peral, *Organometallics* "Metal Complexes Containing Enantiopure Bis(diamidophosphite) Ligands in Asymmetric Allylic Substitution and Hydroformylation Reactions" **2015**, *34*, 3799-3808.

[68] Z. Freixa, J. Carles Bayón, *J. Chem. Soc., Dalton Trans.* "Rhodium catalyzed asymmetric hydroformylation of vinylarenes with a diphosphite ligand forming a large chelating ring" **2001**, 2067-2068.

[69] J. Pospech, I. Fleischer, R. Franke, S. Buchholz, M. Beller, *Angew. Chem. Int. Ed. Engl.* "Alternative metals for homogeneous catalyzed hydroformylation reactions" **2013**, *52*, 2852-2872.

[70] R. M. Bullock, *Catalysis without Precious Metals*, WILEY-VCH, Weinheim, **2010**.

[71] Á. Molnár, A. Papp, *Coord. Chem. Rev.* "Catalyst recycling—A survey of recent progress and current status" **2017**, *349*, 1-65.

[72] P. Serp, J. L. Figueiredo, *Carbon Materials for Catalysis*, Wiley, Hoboken, **2008**.

[73] B. M. L. Dioos, I. F. J. Vankelecom, P. A. Jacobs, *Adv. Synth. Catal.* "Aspects of Immobilisation of Catalysts on Polymeric Supports" **2006**, *348*, 1413-1446.

[74] T. Verheyen, N. Santillo, D. Marinelli, E. Petricci, W. M. De Borggraeve, L. Vaccaro, M. Smet, *ACS Appl. Polym. Mater.* "An Effective and Reusable Hyperbranched Polymer Immobilized Rhodium Catalyst for the Hydroformylation of Olefins" **2019**, *1*, 1496-1504.

[75] L. Luo, H. Li, Y. Peng, C. Feng, J. Zeng, *ChemNanoMat* "Rh-Based Nanocatalysts for Heterogeneous Reactions" **2018**, *4*, 451-466.

[76] D. Ruiz, P. Mäki-Arvela, A. Aho, R. Chimentão, C. Claver, C. Godard, J. L. G. Fierro, D. Y. Murzin, *Mol. Catal.* "Immobilized chiral rhodium nanoparticles stabilized by chiral P-ligands as efficient catalysts for the enantioselective hydrogenation of 1-phenyl-1,2-propanedione" **2019**, *477,* 110551.

[77] A. L. Tarasov, V. I. Isaeva, I. P. Beletskaya, L. M. Kustov, *Russ. J. Org. Chem.* "Conversion of carbon dioxide to propionaldehyde over cobalt and rhodium nanoparticles supported on MIL-53 (Al) metal–organic framework" **2017**, *52*, 1728-1732.

[78] D. Sharma, V. Ganesh, A. Sakthivel, *Appl. Catal. A, Gen.* "Rhodium incorporated monometallic cobalt hydrotalcite-type materials: Preparation and its applications for the hydroformylation of alkenes" **2018**, *555*, 155-160.

[79] J. Amsler, B. B. Sarma, G. Agostini, G. Prieto, P. N. Plessow, F. Studt, *J. Am. Chem. Soc.* "Prospects of Heterogeneous Hydroformylation with Supported Single Atom Catalysts" **2020**, *142*, 5087-5096.

[80] Z. Ren, Y. Liu, Y. Lyu, X. Song, C. Zheng, S. Feng, Z. Jiang, Y. Ding, *J. Catal.* "Single-atom Rh based bipyridine framework porous organic polymer: A high active and superb stable catalyst for heterogeneous methanol carbonylation" **2019**, *369*, 249-256.

[81] J. M. Marinkovic, A. Riisager, R. Franke, P. Wasserscheid, M. Haumann, *Ind. Eng. Chem. Res.* "Fifteen Years of Supported Ionic Liquid Phase-Catalyzed Hydroformylation: Material and Process Developments" **2018**, *58*, 2409-2420.

[82] P. Kaur, H. K. Chopra, *ChemistrySelect* "Exploring the Potential of Supported Ionic Liquids as Building Block Systems in Catalysis" **2020**, *5*, 12057-12086.

[83] M. Rufete-Beneite, M. C. Román-Martínez, *Catalysts* "Unraveling Toluene Conversion during the Liquid Phase Hydrogenation of Cyclohexene (in Toluene) with Rh Hybrid Catalysts" **2019**, *9,* 973.

[84] A. Weiß, M. Giese, M. Lijewski, R. Franke, P. Wasserscheid, M. Haumann, *Catal. Sci. Technol.* "Modification of nitrogen doped carbon for SILP catalyzed hydroformylation of ethylene" **2017**, *7*, 5562-5571.

[85] D. F. Foster, D. J. Adams, D. Gudmunsen, A. M. Stuart, E. G. Hope, D. J. Cole-Hamilton, *Chem. Commun.* "Hydroformylation in fluorous solvents" **2002**, 722-723.

[86] I. T. Horvath, J. Rabai, *Science* "Facile catalyst separation without water: fluorous biphase hydroformylation of olefins" **1994**, *266*, 72-75.

[87] D. F. Foster, D. Gudmunsen, D. J. Adams, A. M. Stuart, E. G. Hope, D. J. Cole-Hamilton, G. P. Schwarz, P. Pogorzelec, *Tetrahedron* "Hydroformylation in perfluorinated solvents; improved selectivity, catalyst retention and product separation" **2002**, *58*, 3901-3910.

[88] N. Pinault, *Coord. Chem. Rev.* "Homogeneous catalysts based on water-soluble phosphines" **2003**, *241*, 1-25.

[89] N. Herrmann, J. Bianga, T. Gaide, M. Drewing, D. Vogt, T. Seidensticker, *Green Chem.* "Aqueous biphasic hydroformylation of methyl oleate: a green solvent-only strategy for homogeneous catalyst recycling" **2019**, *21*, 6738-6745.
[90] A. Scrivanti, V. Beghetto, M. M. Alam, S. Paganelli, P. Canton, M. Bertoldini, E. Amadio, *Inorg. Chim. Acta* "Biphase hydroformylation catalyzed by rhodium in combination with a water-soluble pyridyl-triazole ligand" **2017**, *455*, 613-617.
[91] D. Peral, D. Herrera, J. Real, T. Flor, J. C. Bayón, *Catal. Sci. Technol.* "Strong π-acceptor sulfonated phosphines in biphasic rhodium-catalyzed hydroformylation of polar alkenes" **2016**, *6*, 800-808.
[92] I. T. Horváth, *Green Chem.* "Solvents from nature" **2008**, *10*, 1024–1028.
[93] M. Haumann, A. Riisager, *Chem. Rev.* "Hydroformylation in room temperature ionic liquids (RTILs): catalyst and process developments" **2008**, *108*, 1474-1497.
[94] T. Welton, *Coord. Chem. Rev.* "Ionic liquids in catalysis" **2004**, *248*, 2459-2477.
[95] C. P. Mehnert, R. A. Cook, N. C. Dispenziere, M. Afeworki, *J. Am. Chem. Soc.* "Supported ionic liquid catalysis--a new concept for homogeneous hydroformylation catalysis" **2002**, *124*, 12932-12933.
[96] R. L. Vekariya, *J. Mol. Liq.* "A review of ionic liquids: Applications towards catalytic organic transformations" **2017**, *227*, 44-60.
[97] S. Hanf, L. Alvarado Rupflin, R. Gläser, S. Schunk, *Catalysts* "Current State of the Art of the Solid Rh-Based Catalyzed Hydroformylation of Short-Chain Olefins" **2020**, *10,* 510.
[98] X. Jia, Z. Liang, J. Chen, J. Lv, K. Zhang, M. Gao, L. Zong, C. Xie, *Org. Lett.* "Porous Organic Polymer Supported Rhodium as a Reusable Heterogeneous Catalyst for Hydroformylation of Olefins" **2019**, *21*, 2147-2150.
[99] Z. Liang, J. Chen, X. Chen, K. Zhang, J. Lv, H. Zhao, G. Zhang, C. Xie, L. Zong, X. Jia, *Chem Commun (Camb)* "Porous organic polymer supported rhodium as a heterogeneous catalyst for hydroformylation of alkynes to alpha,beta-unsaturated aldehydes" **2019**, *55*, 13721-13724.
[100] C. Liu, J. Zhang, H. Liu, J. Qiu, X. Zhang, *Ind. Eng. Chem. Res.* "Heterogeneous Ligand-Free Rhodium Oxide Catalyst Embedded within Zeolitic Microchannel to Enhance Regioselectivity in Hydroformylation" **2019**, *58*, 21285-21295.
[101] P. Su, Y. Chen, X. Liu, H. Chuai, H. Liu, B. Zhu, S. Zhang, W. Huang, *Catalysts* "Preparation and Characterization of Rh/MgSNTs Catalyst for Hydroformylation of Vinyl Acetate: The Rh(0) was Obtained by Calcination" **2019**, *9*, 215.
[102] H. Chuai, P. Su, H. Liu, B. Zhu, S. Zhang, W. Huang, *Catalysts* "Alkali and Alkaline Earth Cation-Decorated TiO_2 Nanotube-Supported Rh Catalysts for Vinyl Acetate Hydroformylation" **2019**, *9*, 194.
[103] P. Wolf, M. Logemann, M. Schörner, L. Keller, M. Haumann, M. Wessling, *RSC Adv.* "Multi-walled carbon nanotube-based composite materials as catalyst support for water–gas shift and hydroformylation reactions" **2019**, *9*, 27732-27742.
[104] A. Cunillera, C. Blanco, A. Gual, J. M. Marinkovic, E. J. Garcia-Suarez, A. Riisager, C. Claver, A. Ruiz, C. Godard, *ChemCatChem* "Highly Efficient Rh-catalysts Immobilised by π-π Stacking for the Asymmetric Hydroformylation of Norbornene under Continuous Flow Conditions" **2019**, *11*, 2195-2205.
[105] D. Gorbunov, D. Safronova, Y. Kardasheva, A. Maximov, E. Rosenberg, E. Karakhanov, *ACS Appl Mater Interfaces* "New Heterogeneous Rh-Containing

Catalysts Immobilized on a Hybrid Organic-Inorganic Surface for Hydroformylation of Unsaturated Compounds" **2018**, *10*, 26566-26575.

[106] E. Vunain, P. Ncube, K. Jalama, R. Meijboom, *J. Porous Mater.* "Confinement effect of rhodium(I) complex species on mesoporous MCM-41 and SBA-15: effect of pore size on the hydroformylation of 1-octene" **2017**, *25*, 303-320.

[107] A. Behr, A. J. Vorholt, K. A. Ostrowski, T. Seidensticker, *Green Chem.* "Towards resource efficient chemistry: tandem reactions with renewables" **2014**, *16*, 982-1006.

[108] P. Eilbracht, L. Barfacker, C. Buss, C. Hollmann, B. E. Kitsos-Rzychon, C. L. Kranemann, T. Rische, R. Roggenbuck, A. Schmidt, *Chem. Rev.* "Tandem Reaction Sequences under Hydroformylation Conditions: New Synthetic Applications of Transition Metal Catalysis" **1999**, *99*, 3329-3366.

[109] M. Beller, *Top Organometal Chem.* "Synthetic Applications of Tandem Reaction Sequences Involving Hydroformylation" **2006**, *18*, 65-95.

[110] M. R. L. Furst, V. Korkmaz, T. Gaide, T. Seidensticker, A. Behr, A. J. Vorholt, *ChemCatChem* "Tandem Reductive Hydroformylation of Castor Oil Derived Substrates and Catalyst Recycling by Selective Product Crystallization" **2017**, *9*, 4319-4323.

[111] G. Achonduh, Q. Yang, H. Alper, *Tetrahedron* "From alkenes to alcohols by cobalt-catalyzed hydroformylation–reduction" **2015**, *71*, 1241-1246.

[112] C. O. Oseghale, B. M. Mogudi, C. A. Akinnawo, R. Meijboom, *Appl. Catal. A, Gen.* "In-Situ generation of surface-active HCo(CO)y like intermediate from gold supported on ion-promoted Co3O4 for induced hydroformylation-hydrogenation of alkenes to alcohols" **2020**, *602,* 117735.

[113] P. Wang, D.-L. Wang, H. Liu, X.-L. Zhao, Y. Lu, Y. Liu, *Organometallics* "Production of Alcohols from Olefins via One-Pot Tandem Hydroformylation–Acetalization–Hydrogenolysis over Bifunctional Catalyst Merging RuIII–P Complex and RuIII Lewis Acid" **2017**, *36*, 2404-2411.

[114] C. Rodrigues, F. G. Delolo, J. Norinder, A. Börner, A. L. Bogado, A. A. Batista, *J. Mol. Catal. A: Chem.* "Hydroformylation-hydrogenation and hydroformylation-acetalization reactions catalyzed by ruthenium complexes" **2017**, *426*, 586-592.

[115] D. N. Gorbunov, S. V. Egazaryants, Y. S. Kardasheva, A. L. Maksimov, E. A. Karakhanov, *Russ. Chem. Bull.* "Synthesis of cyclic acetals by hydroformylation of oct-1-ene in the presence of polyols" **2015**, *64*, 943-947.

[116] T. Vanbésien, J. Le Nôtre, E. Monflier, F. Hapiot, *Eur. J. Lipid Sci. Technol.* "Hydroaminomethylation of oleochemicals: A comprehensive overview" **2018**, *120*.

[117] T. A. Faßbach, F. O. Sommer, A. J. Vorholt, *Adv. Synth. Catal.* "Hydroaminomethylation in Aqueous Solvent Systems - An Efficient Pathway to Highly Functionalized Amines" **2018**, *360*, 1473-1482.

[118] Q. Ruan, L. Zhou, B. Breit, *Catal. Commun.* "New phosphorus self-assembling ligands for the tandem hydroformylation–Wittig olefination reaction of homoallylic alcohols — A key step for stereoselective pyran synthesis" **2014**, *53*, 87-90.

[119] G. W. Wong, C. R. Landis, *Angew. Chem. Int. Ed. Engl.* "Iterative asymmetric hydroformylation/Wittig olefination sequence" **2013**, *52*, 1564-1567.

[120] A. Farwick, G. Helmchen, *Adv. Synth. Catal.* "Stereoselective Synthesis of β-Proline Derivatives from Allylamines via Domino Hydroformylation/Wittig Olefination and Aza-Michael Addition" **2010**, *352*, 1023-1032.
[121] K. Ma, B. S. Martin, X. Yin, M. Dai, *Nat. Prod. Rep.* "Natural product syntheses via carbonylative cyclizations" **2019**, *36*, 174-219.
[122] J. C. Tsai, Y. H. Lin, G. T. Chen, Y. K. Gao, Y. C. Tseng, C. L. Kao, W. H. Chiou, *Chem. Asian J.* "Rhodium-Catalyzed Domino Hydroformylation/Double-Cyclization Reaction of Arylacetylenecarboxamides: Diastereoselectivity Studies and Application in the Synthesis of 1-Azabicyclo[x.y.0]alkanes" **2018**, *13*, 3190-3197.
[123] C. G. Vieira, M. C. de Freitas, E. N. dos Santos, E. V. Gusevskaya, *ChemCatChem* "Synthesis of Fragrance Ingredients by Tandem Hydroformylation-Cyclization of Limonene Catalyzed by Rhodium Complexes and Pyridinium p-Toluenesulphonate" **2012**, *4*, 795-801.
[124] Y.-Q. Li, Q. Zhou, D.-L. Wang, P. Wang, Y. Lu, Y. Liu, *Mol. Catal.* "Co-catalysis for one-pot tandem hydroformylation-aldol condensation-hydrogenation with involvement of phosphino-phosphonium based bi-functional ligand and aniline" **2017**, *439*, 25-30.
[125] L. Kollár, P. Pongrácz, *J. Organomet. Chem.* "Tandem hydroformylation/aldol condensation reactions: Synthesis of unsaturated ketones from olefins" **2018**, *866*, 184-188.
[126] X. Fang, R. Jackstell, R. Franke, M. Beller, *Chemistry* "Domino-hydroformylation/aldol condensation catalysis: highly selective synthesis of alpha,beta-unsaturated aldehydes from olefins" **2014**, *20*, 13210-13216.
[127] L. Diab, U. Gellrich, B. Breit, *Chem Commun (Camb)* "Tandem decarboxylative hydroformylation-hydrogenation reaction of alpha,beta-unsaturated carboxylic acids toward aliphatic alcohols under mild conditions employing a supramolecular catalyst system" **2013**, *49*, 9737-9739.
[128] T. Smejkal, B. Breit, *Angew. Chem. Int. Ed. Engl.* "A supramolecular catalyst for the decarboxylative hydroformylation of alpha,beta-unsaturated carboxylic acids" **2008**, *47*, 3946-3949.
[129] B. Breit, A. Bruch, A. Gebert, *Synthesis* "Tandem-Directed Regioselective Hydroformylation/β-Elimination: A Practical Method for the Synthesis of Enals" **2008**, *2008*, 2169-2176.
[130] P. Kohling, A. M. Schmidt, P. Eilbracht, *Org. Lett.* "Tandem hydroformylation/Fischer indole synthesis: a novel and convenient approach to indoles from olefins" **2003**, *5*, 3213-3216.
[131] A. M. Schmidt, P. Eilbracht, *J. Org. Chem.* "Synthesis of pharmacologically relevant indoles with amine side chains via tandem hydroformylation/Fischer indole synthesis" **2005**, *70*, 5528-5535.
[132] P. Linnepe Nee Kohling, A. M. Schmidt, P. Eilbracht, *Org. Biomol. Chem.* "2,3-Disubstituted indoles from olefins and hydrazines via tandem hydroformylation-Fischer indole synthesis and skeletal rearrangement" **2006**, *4*, 302-313.
[133] A. R. Almeida, R. D. Dias, C. J. P. Monteiro, A. R. Abreu, P. M. P. Gois, J. C. Bayon, M. M. Pereira, *Adv. Synth. Catal.* "Rhodium-Catalysed Tandem Hydroformylation/Arylation Reaction with Boronic Acids" **2014**, *356*, 1223-1228.
[134] M. A. Subhani, K. S. Muller, F. Koc, P. Eilbracht, *Org Biomol Chem* "A new one-pot hydroformylation/Strecker synthesis as a versatile synthetic tool for

polyfunctional compounds and functionalization of dendrimers" **2009**, *7*, 4000-4008.

[135] K. Dong, X. Fang, R. Jackstell, M. Beller, *Chem. Commun. (Camb)* "A novel rhodium-catalyzed domino-hydroformylation-reaction for the synthesis of sulphonamides" **2015**, *51*, 5059-5062.

[136] M. Vilches-Herrera, L. Domke, A. Börner, *ACS Catal.* "Isomerization–Hydroformylation Tandem Reactions" **2014**, *4*, 1706-1724.

[137] Y. Yuki, K. Takahashi, Y. Tanaka, K. Nozaki, *J. Am. Chem. Soc.* "Tandem isomerization/hydroformylation/hydrogenation of internal alkenes to n-alcohols using Rh/Ru dual- or ternary-catalyst systems" **2013**, *135*, 17393-17400.

[138] A. Jörke, T. Gaide, A. Behr, A. Vorholt, A. Seidel-Morgenstern, C. Hamel, *Chem. Eng. J.* "Hydroformylation and tandem isomerization–hydroformylation of n-decenes using a rhodium-BiPhePhos catalyst: Kinetic modeling, reaction network analysis and optimal reaction control" **2017**, *313*, 382-397.

[139] L. Le Goanvic, J. Ternel, J.-L. Couturier, J.-L. Dubois, J.-F. Carpentier, *Catalysts* "Rhodium-Biphephos-Catalyzed Tandem Isomerization–Hydroformylation of Oleonitrile" **2018**, *8,* 21.

[140] Y. Ma, S. Qing, Z. Gao, X. Mamat, J. Zhang, H. Li, W. Eli, T. Wang, *Catal. Sci. Technol.* "Tandem hydroformylation and hydrogenation of dicyclopentadiene by Co3O4 supported gold nanoparticles" **2015**, *5*, 3649-3657.

[141] S. S. Bhagade, S. R. Chaurasia, B. M. Bhanage, *Catal. Today* "Reductive-hydroformylation of 1-octene to nonanol using fibrous Co 3 O 4 catalyst" **2018**, *309*, 147-152.

[142] L. Liu, H. Gao, S.-Q. Yang, X.-C. Chen, Y. Lu, Y. Liu, F. Xia, *J. Catal.* "Ir-catalyzed tandem hydroformylation-transfer hydrogenation of olefins with (trans-/cis-)formic acid as hydrogen source in presence of 1,10-phenanthroline" **2020**, *385*, 183-193.

[143] K. Wohnrath, M. P. de Araujo, L. R. Dinelli, A. A. Batista, I. de Sousa Moreira, E. E. Castellano, J. Ellena, *J. Chem. Soc., Dalton Trans.* "Electrosynthesis of binuclear ruthenium complexes from [RuCl3(dppb)(L)] precursors [L = pyridine, 4-methylpyridine or dimethyl sulfoxide; dppb = 1,4-bis(diphenylphosphino)butane]" **2000**, 3383-3386.

[144] F. Shi, X. Cui, *Catalytic Amination for N-Alkyl Amine Synthesis*, Elsevier, **2018**.

[145] M. Ahmed, A. M. Seayad, R. Jackstell, M. Beller, *J. Am. Chem. Soc.* "Amines made easily: a highly selective hydroaminomethylation of olefins" **2003**, *125*, 10311-10318.

[146] S. Hanna, J. C. Holder, J. F. Hartwig, *Angew. Chem. Int. Ed. Engl.* "A Multicatalytic Approach to the Hydroaminomethylation of alpha-Olefins" **2019**, *58*, 3368-3372.

[147] S. Raoufmoghaddam, *Org Biomol Chem* "Recent advances in catalytic C-N bond formation: a comparison of cascade hydroaminomethylation and reductive amination reactions with the corresponding hydroamidomethylation and reductive amidation reactions" **2014**, *12*, 7179-7193.

[148] A. Trowbridge, S. M. Walton, M. J. Gaunt, *Chem. Rev.* "New Strategies for the Transition-Metal Catalyzed Synthesis of Aliphatic Amines" **2020**, *120*, 2613-2692.

[149] S. Fuchs, T. Rösler, B. Grabe, A. Kampwerth, G. Meier, H. Strutz, A. Behr, A. J. Vorholt, *Appl. Catal. A, Gen.* "Synthesis of primary amines via linkage of

hydroaminomethylation of olefins and splitting of secondary amines" **2018**, *550*, 198-205.

[150] H. Liu, D. Yang, D. L. Wang, P. Wang, Y. Lu, G. Vo-Thanh, Y. Liu, *Chem. Commun. (Camb)* "An efficient and recyclable ionic diphosphine-based Ir-catalyst for hydroaminomethylation of olefins with H2O as the hydrogen source" **2018**, *54*, 7979-7982.

[151] S. A. Jagtap, S. P. Gowalkar, E. Monflier, A. Ponchel, B. M. Bhanage, *Mol. Catal.* "Rhodium catalyzed selective hydroaminomethylation of biorenewable eugenol under aqueous biphasic condition" **2018**, *452*, 108-116.

[152] A. de Oliveira Dias, M. G. P. Gutiérrez, J. A. A. Villarreal, R. L. L. Carmo, K. C. B. Oliveira, A. G. Santos, E. N. dos Santos, E. V. Gusevskaya, *Appl. Catal. A, Gen.* "Sustainable route to biomass-based amines: rhodium catalyzed hydroaminomethylation in green solvents" **2019**, *574*, 97-104.

[153] A. Cunillera, A. Ruiz, C. Godard, *Adv. Synth. Catal.* "Synthesis of β2,2-Amino Esters via Rh-Catalysed Regioselective Hydroaminomethylation" **2019**, *361*, 4201-4207.

[154] D. Kaiser, V. Tona, C. R. Goncalves, S. Shaaban, A. Oppedisano, N. Maulide, *Angew. Chem. Int. Ed. Engl.* "A General Acid-Mediated Hydroaminomethylation of Unactivated Alkenes and Alkynes" **2019**, *58*, 14639-14643.

[155] K. Cousin, F. Hapiot, E. Monflier, *Eur. J. Lipid Sci. Technol.* "Selective Ruthenium-Catalyzed Hydroaminomethylation of Unsaturated Oleochemicals" **2019**, *122*.

[156] A. Cunillera, M. D. de los Bernardos, M. Urrutigoïty, C. Claver, A. Ruiz, C. Godard, *Catal. Sci. Technol.* "Efficient synthesis of chiral γ-aminobutyric esters via direct rhodium-catalysed enantioselective hydroaminomethylation of acrylates" **2020**, *10*, 630-634.

[157] H. Liu, D. Yang, Y. Yao, Y. Xu, H. Shang, X. Lin, *Mol. Catal.* "The electronic and steric effects of neutral and ionic phosphines on Ir(I)-complex catalyzed hydroaminomethylation of olefins" **2020**, *485,* 110843.

[158] J. October, S. F. Mapolie, *Catal. Lett.* "Alkylation of Amines Via Tandem Hydroaminomethylation Using Imino-Pyridine Complexes of Rhodium as Catalyst Precursors" **2019**, *150*, 998-1010.

[159] A. J. Pardey, C. Longo, *Coord. Chem. Rev.* "Catalysis by rhodium complexes bearing pyridine ligands: Mechanistic aspects" **2010**, *254*, 254-272.

[160] D. N. Gorbunov, T. V. Shchukina, Y. S. Kardasheva, N. A. Sinikova, A. L. Maksimov, E. A. Karakhanov, *Pet. Chem.* "Cation-exchange resins in the hydroformylation–acetalization tandem reaction" **2016**, *56*, 711-716.

[161] P. Wang, H. Liu, Y.-Q. Li, X.-L. Zhao, Y. Lu, Y. Liu, *Catal. Sci. Technol.* "Phosphonium-based aminophosphines as bifunctional ligands for sequential catalysis of one-pot hydroformylation–acetalization of olefins" **2016**, *6*, 3854-3861.

[162] Y.-Q. Li, P. Wang, H. Liu, Y. Lu, X.-L. Zhao, Y. Liu, *Green Chem.* "Co-catalysis of a bi-functional ligand containing phosphine and Lewis acidic phosphonium for hydroformylation–acetalization of olefins" **2016**, *18*, 1798-1806.

[163] P. Wang, X. Chen, D.-L. Wang, Y.-Q. Li, Y. Liu, *Green Energy Environ.* "Efficient and recyclable Rh-catalytic system with involvement of phosphine-functionalized phosphonium-based ionic liquids for tandem hydroformylation–acetalization" **2017**, *2*, 419-427.

[164] H. Liu, L. Liu, W.-D. Guo, Y. Lu, X.-L. Zhao, Y. Liu, *J. Catal.* "Phosphine-ligated Ir(III)-complex as a bi-functional catalyst for one-pot tandem hydroformylation-acetalization" **2019**, *373*, 215-221.

[165] D. N. Gorbunov, M. V. Nenasheva, N. A. Sinikova, Y. S. Kardasheva, A. L. Maksimov, E. A. Karakhanov, *Russ. J. Appl. Chem.* "Tandem Hydroformylation–Acetalization Using a Water-Soluble Catalytic System: a Promising Procedure for Preparing Valuable Oxygen-Containing Compounds from Olefins and Polyols" **2018**, *91*, 990-995.

Chapter 2

Dual Catalytic System for Sequential Hydroformylation/Hydrogenation of Hindered Olefins

2.1 Introduction

The replacement of conventional processes by more sustainable synthetic methodologies, based on the Green Chemistry philosophy, is nowadays a topic of high interest. As stated in the introduction, the search for highly active and selective catalysts for the development of sequential processes is a relevant strategy to raise the sustainability of a synthetic process.[1,2] The application of such sequential catalytic synthetic strategies in the valorization of *oxo*-products obtained through hydroformylation of olefins is a pertinent example. In particular, we highlight the direct preparation of alcohols through sequential olefin hydroformylation/hydrogenation reactions, since this is one of the main goals of the present work. Although there are multiple examples of alcohol synthesis through this strategy,[3-7] its application in the valorization of multi-substituted olefins has still been a challenge.[8-12] Bearing that in mind, and taking into account the high activity and selectivity of Rh/binaphthyl-phosphite catalysts in the hydroformylation of aliphatic and aromatic olefins,[13-15] we describe in this chapter the development of a bimetallic catalytic system which combines Rh/*tris*-binaphthyl-monophosphites (**L2.1**) with Shvo's-Ru-complex.[16,17] We intend to perform the synthesis of alcohols, starting from a broad range of olefins, including the highly substituted 2,3-dimethylbutene, (Scheme 2.1).

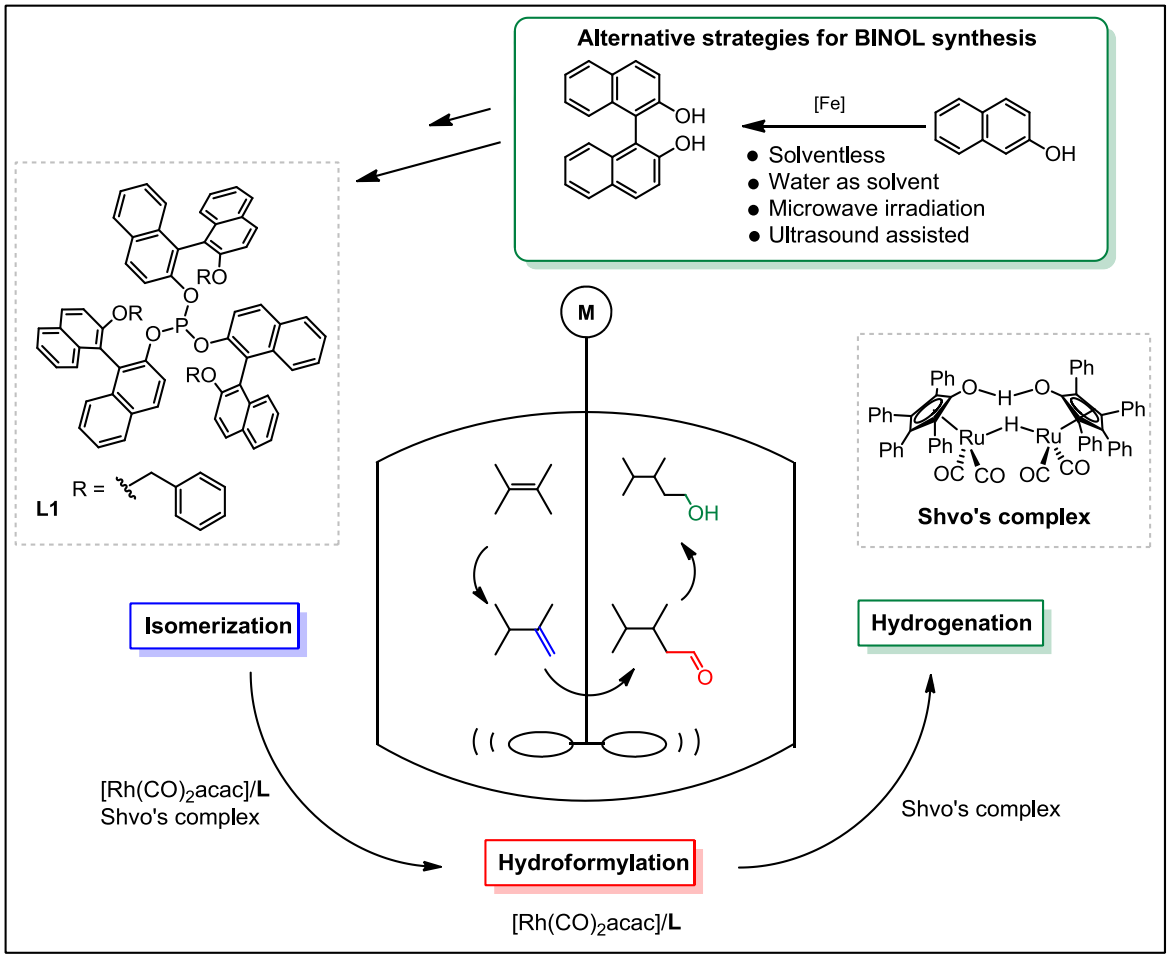

Scheme 2.1 Strategy for hydroformylation/hydrogenation of hindered olefins with [Rh]/Phosphite system and synthesis of racemic BINOL alternative methodologies.

2.2 Monophosphite synthesis

Aiming the preparation of racemic bulky *tris*-helical based BINOL monophosphites the studies started with the comparative evaluation of several alternative sustainable synthetic processes, based on the oxidative coupling of naphthol, catalyzed by Fe(III),[18-21] (Scheme 2.2), under microwave irradiation,[22] ultrasounds[23] and conventional heating.[24] After optimization, the microwave irradiation revealed to be the best approach, yielding full conversion after just 1 min of reaction.

In a typical experiment, $FeCl_3.6H_2O$ (27.0 g, 0.10 mol) and 2-naphthol (7.2 g, 0.05 mmol) were powered, mixed, and introduced in a 10 mL microwave vessel. The mixture was subjected to MW irradiation (60 W) for 1 min, at 80 °C. After cooling, full transformation into BINOL was observed by TLC, using CH_2Cl_2 as eluent. The purification

was carried out by washing the reaction crude with hot water followed by filtration in activated charcoal and recrystallization in toluene. Pure BINOL crystals were obtained in 92% isolated yield and the data obtained through characterization with ^{1}H, ^{13}C-NMR, and 2D NMR techniques are in good agreement with the literature.[25,26]

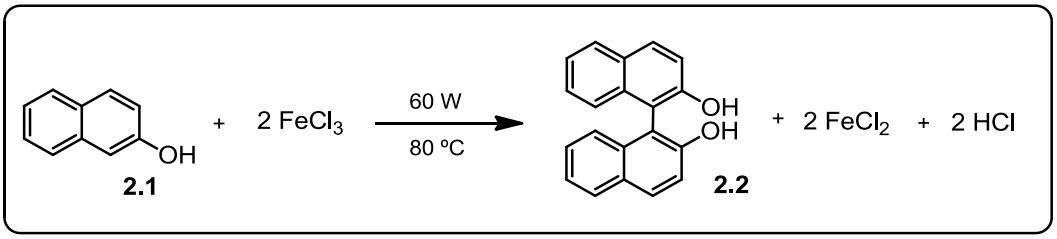

Scheme 2.2. Microwave-assisted synthesis of racemic BINOL through oxidative coupling.

Then, we pursued the studies with the preparation of bulky monophosphites for their evaluation in the sequential hydroformylation/hydrogenation of hindered olefins. As previously described by Catalysis & Fine Chemistry group,[27] the synthetic route requires a two-step procedure that includes the monoprotection of BINOL, followed by phosphorylation with PCl_3 in the presence of a base (Scheme 2.3).

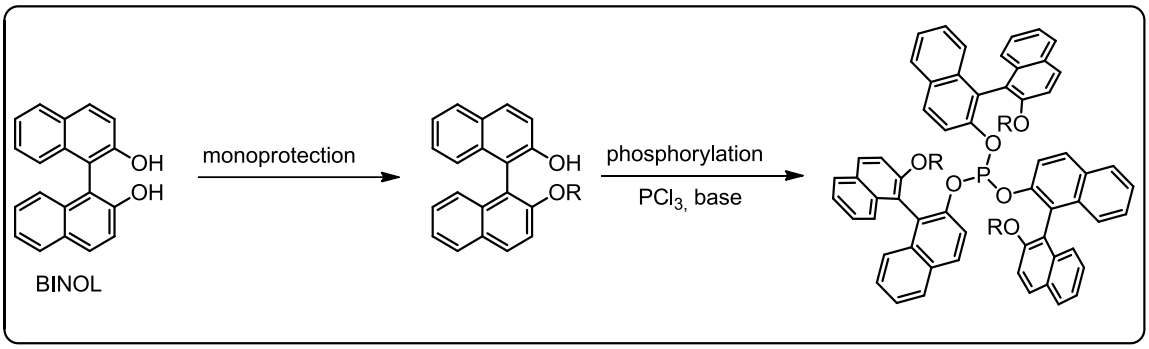

Scheme 2.3. Synthetic route for BINOL based monophosphites

The monoprotection of the previously prepared racemic BINOL (**2.2**) was performed using two different approaches: the first one, based on Mitsunobu reaction,[28] consists in the mono-etherification of BINOL with the desired alcohol, in the presence of triphenylphosphine and diethyl azodicarboxylate (DEAD).[29] (Scheme 2.4, *via* A) The second monoprotection is based on the formation of mono-ester *via* nucleophilic addition/elimination reaction of a sterically hindered acyl halide with the BINOL molecule.[30] (Scheme 2.4, *via* B)

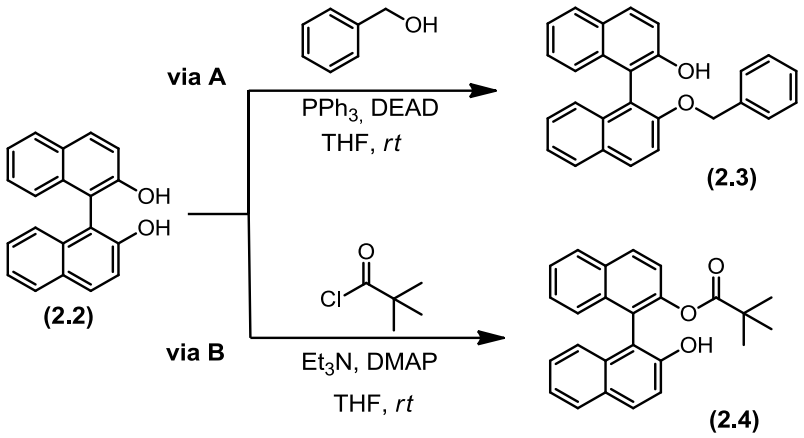

Scheme 2.4. Monoprotection of racemic BINOL with benzyl alcohol (*via* A) and pivaloyl chloride (*via* B).

In a typical procedure, diethyl azodicarboxylate (DEAD) was added dropwise, at 0 °C, to a stirring THF solution of benzyl alcohol and azeotropically dried racemic BINOL (**2.2**). Then, the reaction was kept at room temperature, under argon, for 48 h. After work-up, the crude was purified by column chromatography on silica gel, using mixtures of CH_2Cl_2 and *n*-hexane as eluents. Recrystallization from toluene/*n*-hexane yielded pure white crystals of **2.3** in 89% isolated yield (Scheme 2.4, *via* A). Then, to compare the effect of the *R*- group in the rhodium/binaphthyl monophosphite in the sequential catalytic hydroformylation/hydrogenation reactions the studies pursued with the monoprotection of BINOL (**2.2**) using a bulky pivaloyl ester group (Scheme 2.4, via B). Thus, in a standard procedure, BINOL (**2.2**), 4-dimethylaminopyridine (DMAP), and triethylamine were dissolved in dry THF. The mixture was cooled to 0 °C, and a solution of pivaloyl chloride was added dropwise. The reaction mixture was then left at room temperature for 30 h. After nearly complete disappearance of the starting material (observed by TLC), the reaction was quenched with distilled water and, after work-up, the crude product was purified by column chromatography on silica gel, using dichloromethane/*n*-hexane as eluent, providing 2'-(pivaloyloxy)-1,1'-binaphthyl-2-ol (**2.4)** in 90% isolated yield, as confirmed by NMR, see Chapter 5. Finally, aiming the preparation of binaphthyl-based monophosphite ligands to apply in the hydroformylation/hydrogenation of olefins, we proceeded with the phosphorylation of each of the previously synthesized monoprotected BINOL derivatives **2.3** and **2.4** (Scheme 2.5).

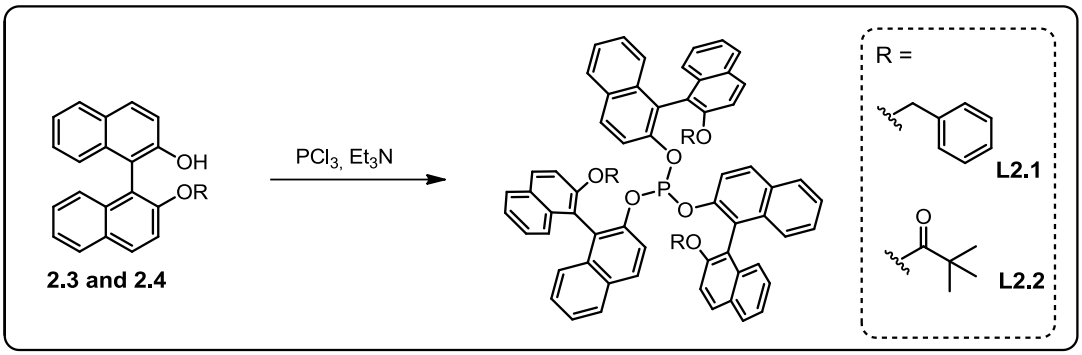

Scheme 2.5. Phosphorylation of **2.3** and **2.4** for the preparation of **L2.1** and **L2.2** phosphites.

The preparation of the monophosphite ligand **L2.1** and **L2.2** was performed according to conventional procedures described for the synthesis of tris-arylphosphites.[27,31] In a typical experiment, a dried Schlenk flask was charged with azeotropically dried **2.3** or **2.4**, dissolved in dry trimethylamine, under nitrogen atmosphere. The solution was cooled to 0 °C, and freshly distilled PCl_3 was slowly added, under magnetic stirring. The reaction progress was followed by TLC and ^{31}P-NMR. After stirring for 3 to 5 h, the solvent was evaporated under reduced pressure. Then, the residue was purified by a silica gel column chromatography, using dichloromethane/*n*-hexane (1:1) as eluent, and further recrystallized in diethyl ether/*n*-hexane, always under nitrogen atmosphere. The final products *tris*[2'-(benzyloxy)-1,1'-binaphthyl-2-yl]phosphite **L2.1** and *tris*[2'-(pivaloyloxy)-1,1'-binaphthyl-2-yl]phosphite, **L2.2**, were obtained as white solids in 73% and 70% isolated yield, respectively. The products were characterized through ^{1}H, ^{13}C, and ^{31}P-NMR spectroscopy and HRMS and all the data are presented in Chapter 5. Further, the ^{31}P-NMR *tris*[2'-(benzyloxy)-1,1'-binaphthyl-2-yl]phosphite **L2.1** is in good agreement with literature.[27] As example, the ^{31}P-NMR of the new *tris*[2'-(pivaloyloxy)-1,1'-binaphthyl-2-yl]phosphite, **L2.2** present a single signal at δ = 133.57 ppm (Figure 2.1) which corroborate its high phosphorus purity.

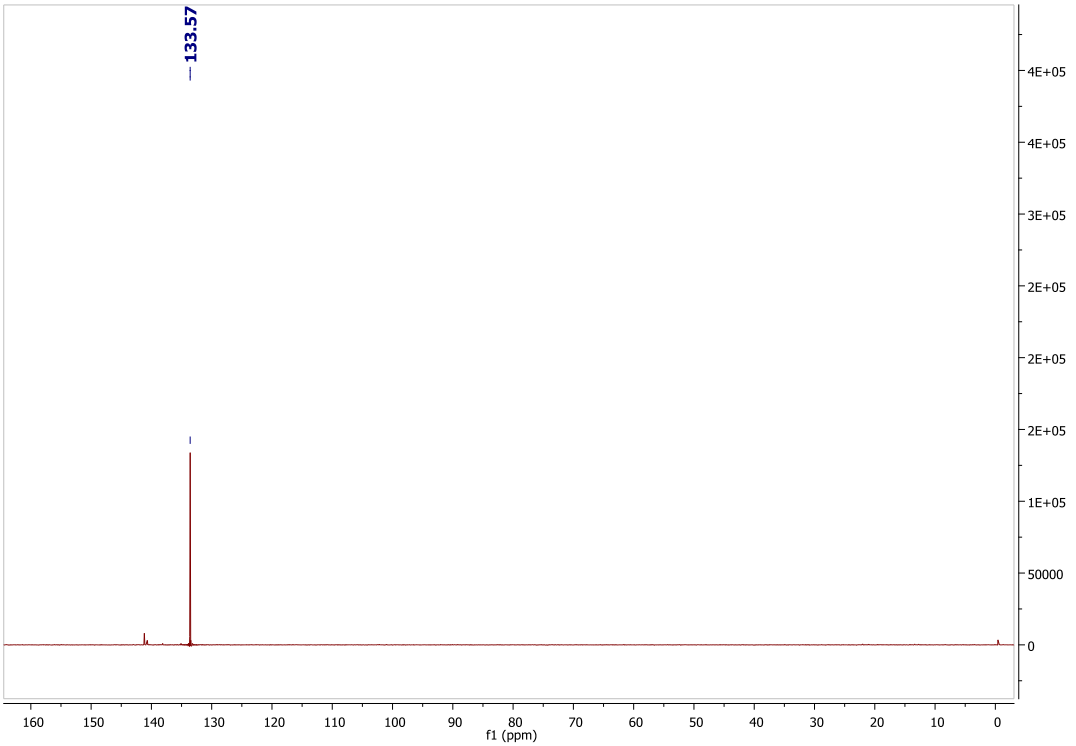

Figure 2.1 ^{31}P-NMR (162 MHz) spectrum of **L2.2** in $CDCl_3$.

The evaluation of Rh/**L2.1** and Rh/**L2.2** in the preparation of alcohols *via* sequential hydroformylation/hydrogenation reaction is described in the next section, the results were published in chemsuschem journal.[32]

2.3 Sequential hydroformylation/hydrogenation of olefins to alcohols

2.3.1 Catalytic system optimization

Pursuing the main goal of this thesis in developing catalytic systems for the sustainable valorization of highly hindered olefins, we pursued our studies with the optimization of sequential hydroformylation/hydrogenation reactions. From the several reports in this field (see Chapter 1), so far, the hydroformylation of hindered olefins remains a challenge. To overcome this issue, we hypothesized that the use of highly active and selective Rh/bulky monophosphite catalysts in the hydroformylation step could provide a promising catalytic system for implementation of the designed sequential processes. In this chapter, we describe the combination of Rh/tris-binaphthyl-based helical monophosphites (**L2.1**-**L2.3**) with Ru-Shvo's-complex,[16,17] aiming the one-pot

transformation of highly substituted olefins into alcohols with one additional carbon atom. **L2.3** was kindly provided by Dr. Rui Carrilho from the Catalysis & Fine Chemistry Laboratory of Coimbra Chemistry Centre-University of Coimbra.

Initially, we started with the optimization of the sequential process using 2,3-dimethylbut-2-ene **2.5** as selected substrate. In general, optimization reactions were started at a temperature of 120 °C under 12 bar CO and 25 bar H_2 pressure along 20 h, in the presence of 0.077 mol% of [$Rh(CO)_2$acac] and 0.154 mol% of the selected ligand **L2.1-L2.3**. Then, in selected experiments and to speed up the hydrogenation step, 0.038 mol% of the Shvo's-complex was added. These studies started with the evaluation of the effect of ligand structure on the activity and selectivity of the catalytic system. Therefore, the hydroformylation reactions were carried out using [$Rh(CO)_2$acac] as catalyst precursor in presence of structurally different *tris*-binaphthyl-based helical monophosphites **L2.1-L2.3** and previously described diphosphine Xantphos.[8,33] The results are summarized in Table 2.1.

In a blank experiment, the hydroformylation reaction of 2,3-dimethylbut-2-ene **2.5** was carried out in the absence of any phosphorus ligand and 61% of conversion with 49% of aldehyde **2.7** and only 3% of the desired alcohol **2.6** were obtained (Table 2.1, Entry 1). Then, we performed another experiment, under the same reaction conditions, but using Xantphos as phosphorus ligand and a similar conversion and aldehyde selectivity were obtained (60%; 48% respectively), but with 10% of hydrogenated product **2.8** and only 2% of the desired alcohol **2.6** (Table 2.1, Entry 2). Since the use of bulky phosphite π–acceptor Rh/ligands is known to significantly increase the activity and selectivity for aldehydes of hydroformylation reactions, we hypothesized that the results of the Rh/Xantphos catalytic system may be improved if the Rh catalytic hydroformylation was performed in the presence of bulky *tris*-binaphthyl monophosphites **L2.1-L2.3**. As expected, under these reaction conditions, the Rh/*tris*-binaphthyl monophosphites **L2.1-L2.3** gave higher conversions and selectivity for aldehydes (84%, 62%, and 82%, respectively) being the formation of the desired alcohol still negligible (<5%; Table 2.1, Entries 3-5).

Table 2.1. Hydroformylation/hydrogenation of 2,3-dimethylbut-2-ene: Catalytic system evaluation.[a]

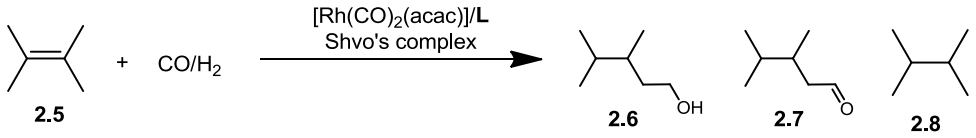

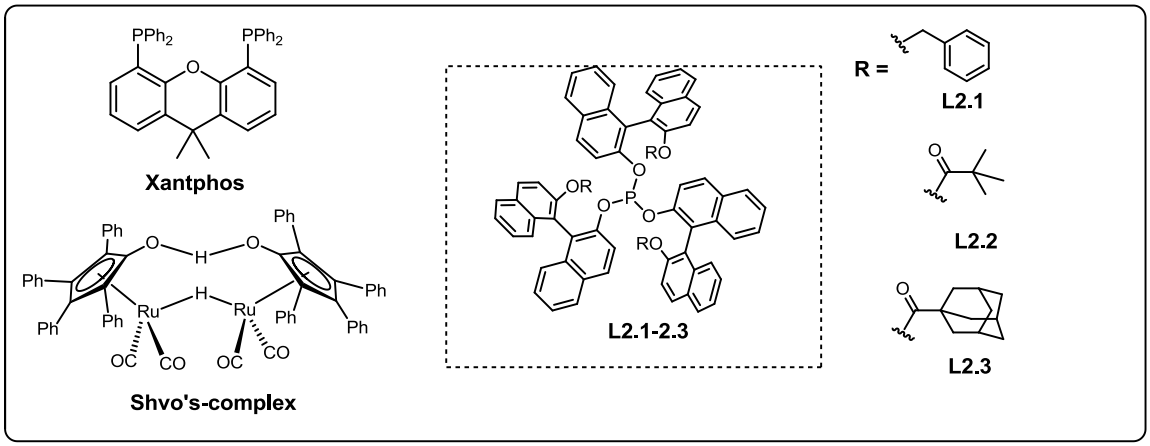

Entry	Ligand	Catalyst	Conv. (%)[b]	Yield (%)[b]		
				2.6	2.7	2.8
1	-	$[Rh(CO)_2acac]$	61	3	49	9
2	Xantphos	$[Rh(CO)_2acac]$	60	2	48	10
3	L2.1	$[Rh(CO)_2acac]$	84	4	77	3
4	L2.2	$[Rh(CO)_2acac]$	62	5	56	1
5	L2.3	$[Rh(CO)_2acac]$	82	4	75	3
6	L2.1	$[Rh(CO)_2acac]$ + Shvo's catalyst	88	46	40	2
7	-	$[Rh(CO)_2acac]$ + Shvo's catalyst	65	42	14	9
8	-	Shvo's catalyst	29	11	6	12
9	L2.1	-	0	-	-	-
10	-	-	0	-	-	-

a) Reaction conditions: 2,3-dimethylbut-2-ene **2.5** (10.0 mmol), $[Rh(CO)_2acac]$ (7.7 µmol), **L** (15.4 µmol) (Rh/**L** = 1:2), Shvo's-complex (3.8 µmol), solvent: 30 mL of toluene, CO (12 bar) and H_2 (25 bar) at 120 °C for 20 h. b) Determined by GC, using isooctane as external standard.

Then, to assess the catalytic activity of each system, we registered the gas consumption overtime for these experiments, along 20 h. As can be observed in Figure 2.2, the system Rh/**L2.1** presented a higher gas consumption rate when compared with **L2.2** and **L2.3.** This result corroborates the different conversion values obtained for the same reaction time. The lower activity observed for the catalytic system Rh/**L2.2** may be attributed to the low Rh/L ratio (1:2) and the lack of incubation period before the addition of substrate. Additionally, the bulkiness of **L2.2** may difficult the formation of the Rh/**L2.2** complex.

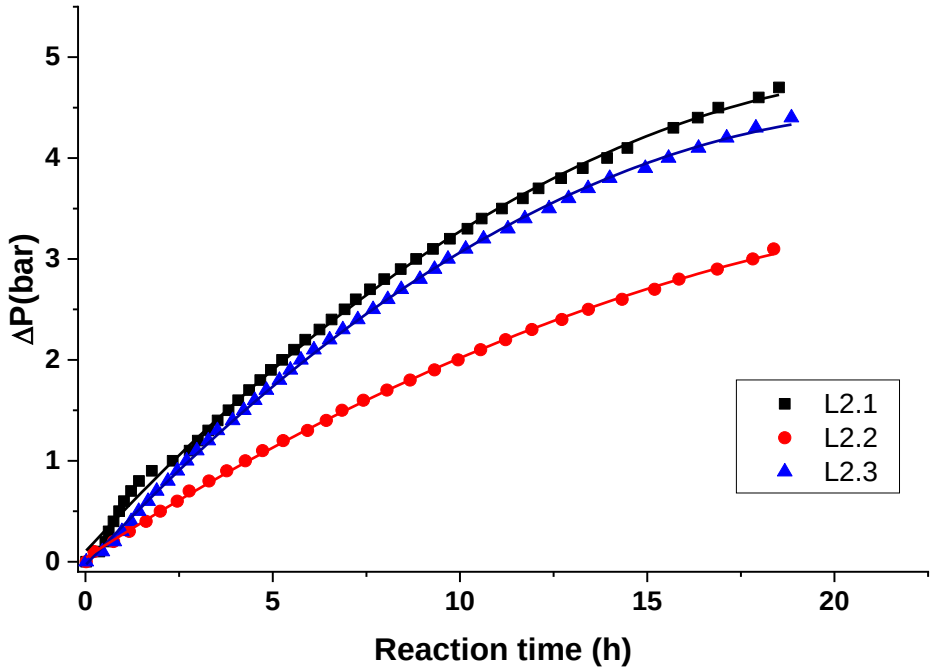

Figure 2.2 Gas consumption (bar) over time for the experiments whose results are presented in Table 2.1 (Entries 3-5) (Rh/**L** = 1:2).

Finally, aiming to improve the final hydrogenation step of the aldehyde onto the desired alcohol, Shvo's-Ru-complex[17] (Ru/S = 1300), was added to the Rh/**L2.1** system (Table 2.1, Entry 6). The application of this dual Rh-Ru catalytic system, for the same reaction time, considerably improved the alcohol selectivity (46%) and did not reduce the overall activity (Table 2.1, Entries 3 and 6). However, performing the reaction without **L2.1** (Table 2.1, Entry 7) or without the Rh/**L2.1** combination (Table 2.1, Entry 8) the conversion was significantly lower (65% and 29%). Additionally, we also performed one blank experiment in the exclusive presence of the Shvo´s-complex and 11% of alcohol **2.6** and

12% of undesired alkane **2.8** was obtained (Table 2.3, Entry 8). As expected, experiments performed in the absence of any catalyst in the presence or absence of **L1** did not give any conversion (Table 2.1, Entries 9 and 10). In sum, the best results of this optimization process, for the one-pot transform of **2.5** into the desired alcohol **2.6** was achieved with Rh/**L2.1** combined with Shvo's-Ru-complex.

Then, to improve the results of this Rh/**L2.1**-Ru-Shvo's-complex, we evaluated the effect of reaction conditions (CO/H_2 total pressure, H_2 partial pressure, temperature and substrate concentration) in more detail, and the results are presented in Table 2.2. First, we reduced the hydrogen content of syngas mixture to 1:1 CO/H_2, with 20 bar total pressure: under these reaction conditions, 71% conversion, 38% of aldehyde **2.7** and only 28% of the desired alcohol **2.6** were obtained (Table 2.2, Entry 1). This result clearly demonstrates the beneficial effect of the low CO/H_2 ratio. Therefore, we evaluated the effect of increasing H_2 partial pressure to 20, 30 and 50 bar, while keeping CO pressure constant at 10 bar. We further observed, not only an improvement in reaction conversions (75, 81 and 97%, respectively), but also a significant increase in reaction yields for the formation of desired alcohol **2.6** (44, 77 and 91%, respectively; Table 2.2, Entries 2-4). Since it is well-known that the activity of Shvo's complex is temperature-sensitive,[8,17] we decided to evaluate the activity and selectivity of the bimetallic Rh-Ru system under milder reaction conditions (80 °C and 100 °C). The total conversion was significantly lower (10% and 24%) and almost only the presence of aldehyde **2.7** was observed (Table 2.2, Entries 5 and 6), which indicates that temperatures above 100 °C are required for activation of Shvo's-Ru catalyst.

Finally, aiming to develop sustainable systems involving low solvent consumption, we also evaluated the effect of reaction concentration by reducing the amount of solvent used, from 30 mL to 20 mL and 5 mL, and the results are presented in Table 2.2 (Entries 7 and 8). From the critical analysis of these experiments, we can conclude that neither the activity nor the selectivity for the desired alcohol **2.6** were significantly affected upon the increase of concentration. These results demonstrate the potential viability of this catalytic system for industrial transposition under sustainable reaction conditions.

Table 2.2 Rhodium/phosphite/ruthenium-catalyzed hydroformylation/hydrogenation of 2,3-dimethylbut-2-ene: Optimization of reaction conditions.[a]

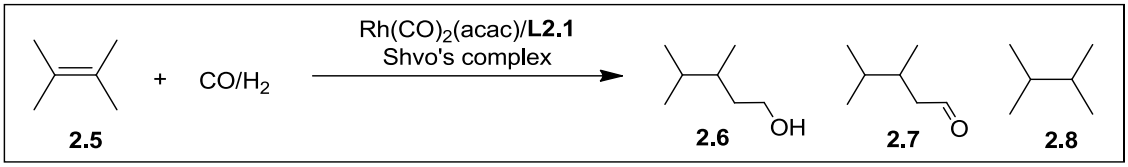

Entry	p_{H2} (bar)	p_{CO} (bar)	T (°C)	$V_{Sol.}$ (mL)	Conv. (%)[b]	Yield (%)[b]		
						2.6	2.7	2.8
1	10	10	120	30	71	28	38	4
2	20	10	120	30	75	44	31	0
3	30	10	120	30	81	77	0	4
4	50	10	120	30	97	91	0	6
5	30	10	80	30	10	0	9	1
6	30	10	100	30	24	0	24	0
7	30	10	120	20	93	90	0	3
8	30	10	120	5	90	88	0	2

a) Reaction conditions: 2,3-dimethylbut-2-ene **1** (10.0 mmol), [$Rh(CO)_2$acac] (7.7 µmol), **L2.1** (15.4 µmol), Shvo's-complex (3.8 µmol), solvent: toluene, 20 h. b) Determined by GC, using isooctane as external standard.

To give an insight about the mechanism of this sequential process and the possible involved intermediates, the reaction progress was measured by taking aliquots, at regular intervals, from the mixture along 24 h. The product yield and remaining substrate conversion curves are plotted in Figure 2.3. From its analysis, we can observe that the isomerized terminal olefin **2.9** (see Scheme 2.6) was not detected. Hence, we conclude that the constant rate k2 (hydroformylation of **2.9**) is higher than k1 (isomerization of **2.5**). We can also observe that the aldehyde hydrogenation rate (k3) is almost constant along all the processes, independently of the amount of aldehyde present.

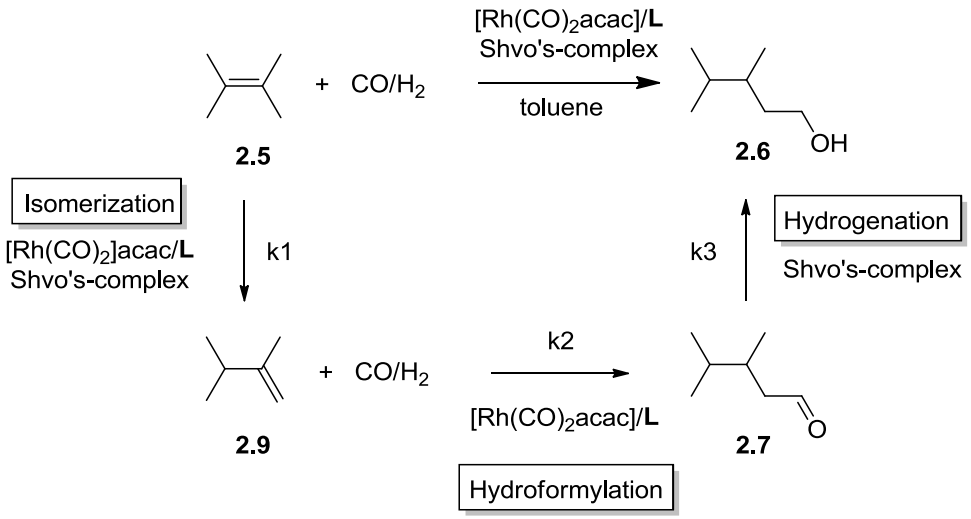

Scheme 2.6 Proposed route for the conversion of olefin to desired alcohol.

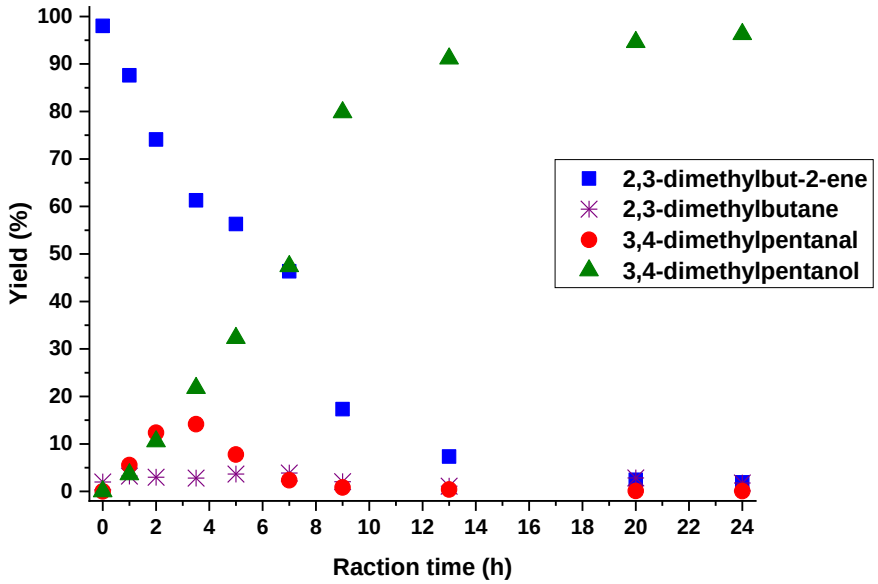

Figure 2.3 Reaction progress of hydroformylation/hydrogenation of 2,3-dimethylbut-2-ene **2.5**: Substrate and product yield *vs*. time. Reaction conditions: **2.5** (40.0 mmol), $[Rh(CO)_2acac]$ (30.8 µmol), **L2.1** (61.6 µmol), Shvo's-complex (15.2 µmol), toluene (20 mL), with 40 bar constant pressure (p_{CO} = 10 bar, p_{H2} = 30 bar), T = 120 °C. Yield determined by GC analysis, using isooctane as external standard.

2.3.2 Reaction Scope

Aiming the transposition of this sequential hydroformylation/hydrogenation catalytic process for industrial applications, the studies pursued with its evaluation to the valorization of a broad range of olefins and the results are presented in Table 2.3. Firstly,

we extended the catalytic process to other aliphatic di- and tri-substituted alkenes (**2.10**-**2.13**; Table 2.3, Entries 1-4). When a mixture of 1, 2 and 3 octene(s) **2.10** were submitted to the above optimized Rh-hydroformylation Ru-hydrogenation conditions, full conversion, chemoselectivity of 51% and 37% yield for the linear alcohol **2.10a,** was obtained**.** The high amount of alkanes obtained with under these reaction conditions (48%) can be attributed to low chemoselectivity offered by Shvo's hydrogenation catalyst for these internal linear olefins (Table 2.3, Entry 1). Next, we performed similar reactions but using the branched 3-ethylbut-2-ene (**2.11**) as substrate and similar results were obtained, except a slightly higher formation of the linear alcohol **2.11a**, in 45% yield (Table 2.3, Entry 2). Then, due to the high industrial interest in the valorization of isomeric mixtures, obtained from oil refineries, this catalytic hydroformylation/hydrogenation system was further evaluated in the mixtures of diisobutylenes (**2.12**) and quite high chemoselectivity (95%) with 99% regioselectivity for the linear alcohol **2.12a** (Table 2.3, Entry 3) was obtained. Finally, when dibutene mixture **2.13** (bearing internal olefins) was used as substrate, 68% of terminal alcohols **2.13a** were obtained, but almost without olefin reduction (3%). These results point out the lower activity of Ru-Shvo's catalysts for the hydrogenation of internal olefins.

Next, internal and terminal mono- and di-substituted aromatic olefins (**2.14**-**2.16**) were also successfully transformed into the desired alcohols. In this case, selectivity for the terminal alcohol is strongly dependent from olefin structure (Table 2.3, Entries 5-7). The terminal di-substituted alkene **2.14** was converted to the linear alcohol **2.14a** in 94% yield, almost without formation of the alkane reduction product (5%) (Table 2.3, Entry 5). However, in the case of *trans*-1,2-disubstituted (*E*)-prop-1-en-1-ylbenzene **2.15**, the branched alcohol **2.15b** was obtained as the major product (73% yield) again without formation of alkane. (Table 2.3, Entry 6). This result may be attributed to lower olefin isomerization due to the thermodynamic stabilization of the intermediate rhodium-benzyl complex. Additionally, we also used the internal di-substituted aromatic olefin **2.16** as substrate and, as expected, the desired alcohol **2.16a** was obtained with 88% yield (Table 2.5, Entry 7).

Table 2.3 Scope of rhodium–phosphite/ruthenium catalyzed hydroformylation/hydrogenation of olefins.[a]

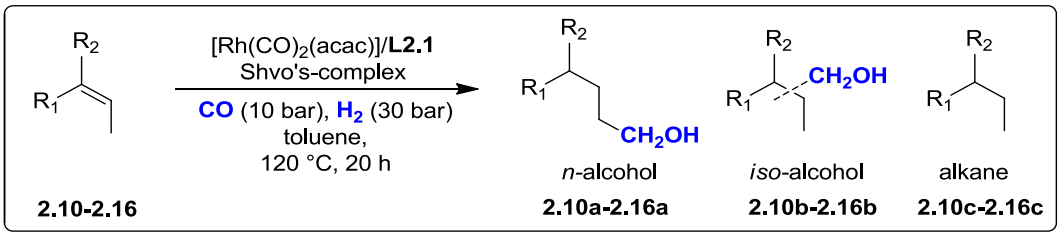

Entry	Substrate	Major product	Yield (%) Major Product [*n*/*i*]	Yield (%) Alkanes c
1	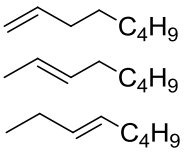 **2.10**	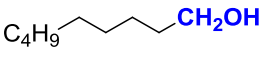 **2.10a**	37 [71/29]	48
2	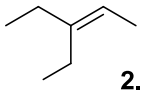 **2.11**	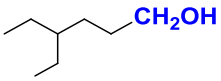 **2.11a**	45 [87/13]	48
3	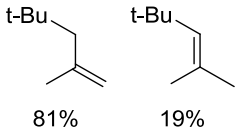 81% 19% **2.12** diisobutylene	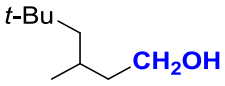 **2.12a**	95 [99/1]	5
4	Dibutene mixture[b] **2.13**	C9-n-alcohols[c] **2.13a**	68 [70/30]	3
5	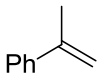 **2.14**	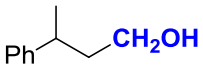 **2.14a**	94 [99/1]	5
6	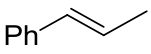 **2.15**	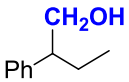 **2.15b**	73 [25/75]	2
7	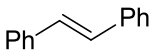 **2.16**	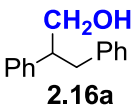 **2.16a**	88	10

a) Reaction conditions: alkene (4.0 mmol), [Rh(CO)$_2$acac] (3.1 µmol), **L2.1** (6.2 µmol), Shvo's-complex (1.5 µmol),CO (10 bar), H_2 (30 bar), solvent: toluene (2 mL), 20 h at 120 °C. Conversions were in all cases 98%. Determined by GC-MS. b) Mixture of C_8-alkene which mainly consist of 4-methylhept-2-ene (75%), 3,4-dimethylhex-2-ene (15%), oct-2-ene (9%). c) Corresponding C_9-*n*-alcohols of dibutene mixture (**2.13**).

Then, the substrate scope was extended to naturally occurring *di*- and *tri*-substituted olefins **2.17-2.19** that are of great interest in the valorization of renewable feedstock, Table 2.6. In all cases, conversions were above 99%, where we highlight the hydroformylation/hydrogenation of the internal double bonds of methyl oleate **2.17**, which led to the formation of branched *oxo* alcohols with **2.17b** as the major product in 84% NMR yield, (Table 2.4, Entry 1). It should be noted that this compound is of great relevance for industrial application.[34,35] This observation is in agreement with previous results where Rh/bulky phosphite catalytic hydroformylation of methyl oleate **2.17** also gave high regioselectivity for this aldehyde.[36] Moreover, the *tri*-substituted terpenic olefin citronellol **2.18** was also used as substrate and 80% chemoselective for alcohols with 51% regioselectivity for the linear diol **2.18a** was obtained. Once again, partial hydrogenation of the olefin was observed (19%, Table 2.4, Entry 2). Finally, as a selected example of a bioactive steroid derivative, the reaction was extended to stigmasterol **2.19,** leading to the preferential formation of terminal alcohols with 61% chemoselectivity and 43% yield of the terminal linear alcohol, **2.19a** (Table 2.4, Entry 3)

Table 2.4 Rhodium-phosphite/ruthenium catalyzed hydroformylation/hydrogenation of industrial/biological relevant substrates.[a]

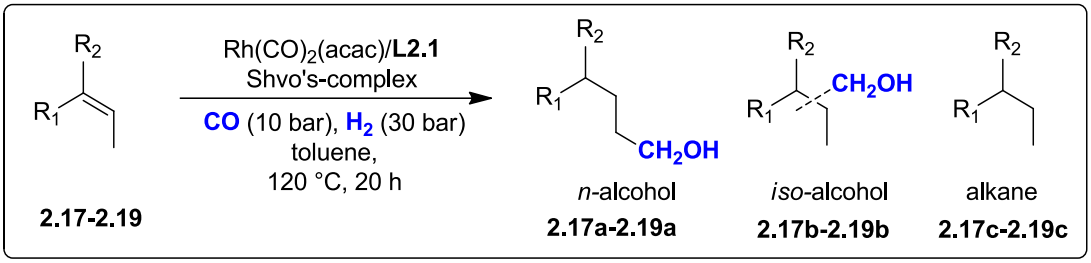

Entry	Substrate	Major product	Yield (%) Major Product [*n/i*]	Yield (%) Alkanes c
1	Methyl oleate **2.17**	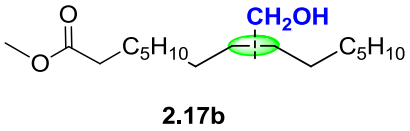 **2.17b**	84 [7/93]	9
2	Citronellol **2.18**	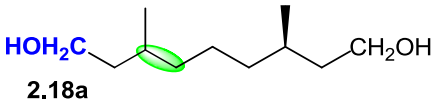 **2.18a**	51 [65/35]	19
3[b]	Stigmasterol **2.19**	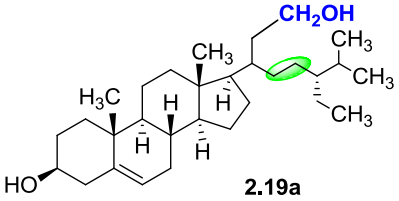 **2.19a**	43 [70/30]	38

a) Reaction conditions: alkene (10.0 mmol), [$Rh(CO)_2acac$] (7.7 µmol), **L2.1** (15.4 µmol), Shvo's-complex (3.8 µmol), CO (10 bar), H_2 (30 bar), solvent: toluene (5 mL), 20 h at 120 °C. Conversions were in all cases 99%. Determined by GC-MS. b) Reaction conditions: steroid (0.48 mmol), [$Rh(CO)_2acac$] (9.8 µmol), **L2.1** (19.6 µmol), Shvo's-complex (4.9 µmol), p(CO) = 10 bar, p(H_2) = 30 bar, solvent: toluene (3 mL), 48 h at 120 °C. Conversion determined by NMR analysis of the reaction crude. Conversions were, in all cases, 99%.

Non-available compounds to be used as GC standard have been isolated through silica gel column chromatography and characterized with ^1H, ^{13}C-NMR, and mass spectrometry and their data is described in Chapter 5. As a selected example, the ^1H and ^{13}C-NMR spectra of compound **2.14a** are presented and discussed in Figures 2.4 and 2.5, respectively**.**

The ^1H-NMR spectrum of **2.14a** shows signals in the typical aromatic region from $\delta = 7.24$ to $\delta = 7.36$ ppm, assigned to the $H_{2'}$ to $H_{6'}$ protons of the aromatic ring. Next, at $\delta = 3.55$ - 3.60 ppm, we can observe a multiplet assigned to the H_1 protons, that are under

the influence of the hydroxyl group. The multiplet signal at $\delta = 2.90$ - 2.95 ppm was assigned to the H_3 proton, and the quartet at $\delta =$ 1.89 ppm (J = 6.9 Hz) was attributed to the H_2 protons. Finally, the doublet signal at $\delta = 1.32$ ppm (J = 7.0 Hz) was assigned to the three H_4 protons of methyl group. A similar analysis can be performed in the **2.14a** ^{13}C-NMR spectrum. The highly shifted signal at $\delta = 147.0$ ppm was assigned to the substituted carbon $C_{1'}$ of the aromatic ring, the remaining signals in the aromatic region ($\delta = 126.2$, 127.0, and 128.6 ppm) were assigned to the $C_{2'}$ - $C_{6'}$ carbons. Next, the $\delta = 61.2$ ppm signal was assigned to the C_1 carbon, functionalized with the hydroxyl group. Then the signals at $\delta = 41.0$ and 36.5 ppm were assigned to the C_3 and C_2 carbons, respectively. Finally, the less shifted signal at $\delta = 22.5$ ppm was assigned to the C_4 carbon from the methyl group.

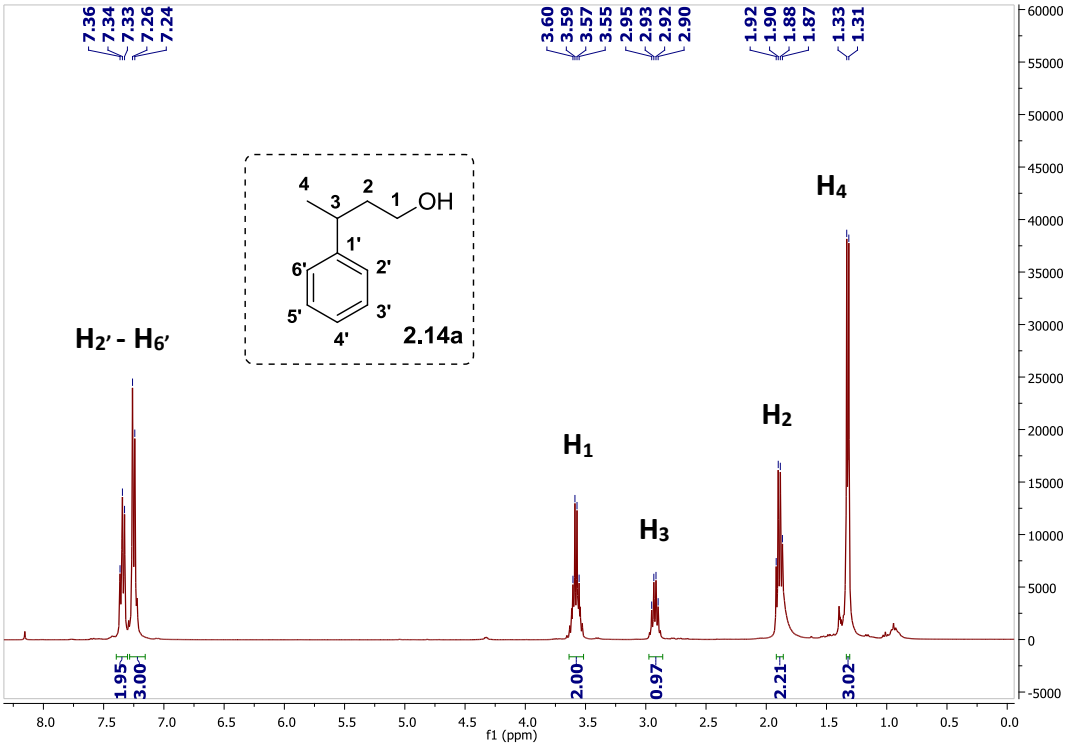

Figure 2.4 ^{1}H-NMR (400 MHz) spectrum of the compound **2.14a** in $CDCl_3$.

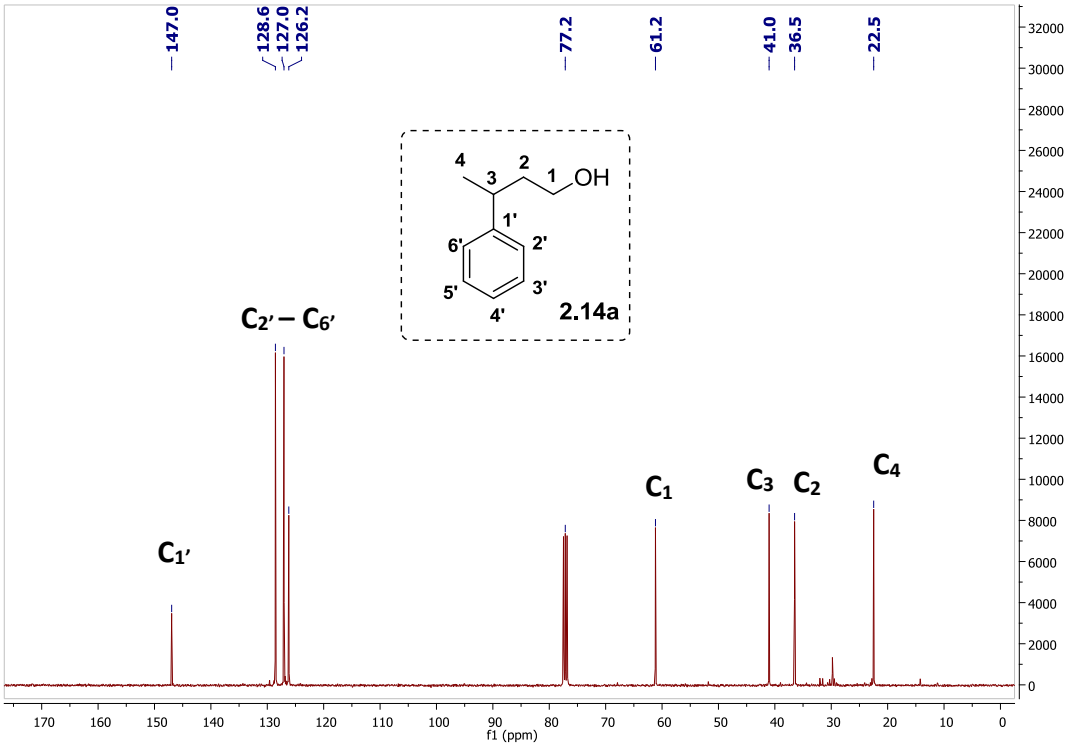

Figure 2.5 ^{13}C-NMR (100 MHz) spectrum of the compound **2.14a** in $CDCl_3$.

2.4 Conclusion

In this chapter we described the optimization of an active and selective dual catalytic system to promote tandem hydroformylation/hydrogenation reactions by combination of Rh/bulky monophosphite hydroformylation catalysts with Ru-Shvo's-hydrogenation catalyst. When compared with previously known catalysts, we can conclude that the dual system developed herein has the great advantage of being able to promote sequential hydroformylation/hydrogenation of terminal and also of less reactive internal C-C double bonds. In all cases, good substrate conversions were obtained, but in the less substituted olefins the hydrogenation of C-C double bond as side reaction led to the formation of alkane products. After optimization of reaction parameters and kinetics studies, we concluded that the partial pressure of H_2 is crucial to obtain the desired alcohols (P_{H2} = 30 bar, P_{CO} = 10 bar) and Rh/**L**/Ru/S (1:2:1:1300) at 120 °C are the best reaction conditions to sequentially transform highlysubstituted olefins onto the desired alcohols. This catalytic system was also evaluated in other potential biologically active substrates like methyl oleate, citronellol and stigmasterol and reasonable to good yields have been obtained. Therefore, we can conclude that this new dual Rh/bulky monophosphites with Ru-based Shvo's complex is active to promote tandem hydroformylation/hydrogenation catalytic reactions, being particularly useful for functionalization of highly substituted alkenes. The results presented here pave the way for more efficient preparation of value-added *oxo* alcohols from inexpensive industrial feedstock (dibutene mixture, diisobutylene) and renewable materials (methyl oleate, citrollenol).

In sum, these alternative dual Rh/Ru catalytic system allowed the one-pot transformation of a family of olefins (alkyl, aryl, internal and terminal double bonds) into the corresponding alcohols in good yields.

2.5 References

[1] A. Behr, A. J. Vorholt, K. A. Ostrowski, T. Seidensticker, *Green Chem.* "Towards resource efficient chemistry: tandem reactions with renewables" **2014**, *16*, 982-1006.

[2] L. F. Tietze, *Chem. Rev.* "Domino Reactions in Organic Synthesis" **1996**, *96*, 115-136.

[3] L. H. Slaugh, R. D. Mullineaux, *J. Organomet. Chem.* "Novel Hydroformylation catalysts" **1968**, *13*, 469-477.

[4] G. M. Torres, R. Frauenlob, R. Franke, A. Börner, *Catal. Sci. Technol.* "Production of alcohols via hydroformylation" **2015**, *5*, 34-54.

[5] B. P. Bondžić, *J. Mol. Catal. A: Chem.* "Rh catalyzed multicomponent tandem and one-pot reactions under hydroformylation conditions" **2015**, *408*, 310-334.

[6] R. Franke, D. Selent, A. Borner, *Chem. Rev.* "Applied hydroformylation" **2012**, *112*, 5675-5732.

[7] L. H. Slaugh, R. D. Mullineaux, *US patent* "Hydroformylation of olefins" **1966**, 3239569 A.

[8] K. Takahashi, M. Yamashita, K. Nozaki, *J. Am. Chem. Soc.* "Tandem hydroformylation/hydrogenation of alkenes to normal alcohols using Rh/Ru dual catalyst or Ru single component catalyst" **2012**, *134*, 18746-18757.

[9] L. Wu, I. Fleischer, R. Jackstell, I. Profir, R. Franke, M. Beller, *J. Am. Chem. Soc.* "Ruthenium-catalyzed hydroformylation/reduction of olefins to alcohols: extending the scope to internal alkenes" **2013**, *135*, 14306-14312.

[10] Y. Yuki, K. Takahashi, Y. Tanaka, K. Nozaki, *J. Am. Chem. Soc.* "Tandem isomerization/hydroformylation/hydrogenation of internal alkenes to n-alcohols using Rh/Ru dual- or ternary-catalyst systems" **2013**, *135*, 17393-17400.

[11] E. V. Gusevskaya, J. Jiménez-Pinto, A. Börner, *ChemCatChem* "Hydroformylation in the Realm of Scents" **2014**, *6*, 382-411.

[12] K. Takahashi, M. Yamashita, T. Ichihara, K. Nakano, K. Nozaki, *Angew. Chem.* "High-Yielding Tandem Hydroformylation/Hydrogenation of a Terminal Olefin to Produce a Linear Alcohol Using a Rh/Ru Dual Catalyst System" **2010**, *122*, 4590-4592.

[13] R. M. B. Carrilho, A. C. B. Neves, M. A. O. Lourenço, A. R. Abreu, M. T. S. Rosado, P. E. Abreu, M. E. S. Eusébio, L. Kollár, J. C. Bayón, M. M. Pereira, *J. Organomet. Chem.* "Rhodium/tris-binaphthyl chiral monophosphite complexes: Efficient catalysts for the hydroformylation of disubstituted aryl olefins" **2012**, *698*, 28-34.

[14] G. N. Costa, R. M. B. Carrilho, L. D. Dias, J. C. Viana, G. L. B. Aquino, M. Pineiro, M. M. Pereira, *J. Mol. Catal. A: Chem.* "Highly efficient Rh(I)/tris-binaphthyl monophosphite catalysts for hydroformylation of sterically hindered alkyl olefins" **2016**, *416*, 73-80.

[15] A. R. Almeida, R. M. B. Carrilho, A. F. Peixoto, A. R. Abreu, A. Silva, M. M. Pereira, *Tetrahedron* "Sequential reactions from catalytic hydroformylation toward the synthesis of amino compounds" **2017**, *73*, 2389-2395.

[16] Y. Shvo, D. Czarkie, Y. Rahamim, D. F. Chodosh, *J. Am. Chem. Soc.* "A new group of ruthenium complexes: structure and catalysis" **1986**, *108*, 7400-7402.

[17] B. L. Conley, M. K. Pennington-Boggio, E. Boz, T. J. Williams, *Chem. Rev.* "Discovery, applications, and catalytic mechanisms of Shvo's catalyst" **2010**, *110*, 2294-2312.
[18] N. V. Tkachenko, K. P. Bryliakov, *Mini-Reviews in Organic Chemistry* "Transition Metal Catalyzed Aerobic Asymmetric Coupling of 2-Naphthols" **2019**, *16*, 392-398.
[19] P. Loxq, E. Manoury, R. Poli, E. Deydier, A. Labande, *Coord. Chem. Rev.* "Synthesis of axially chiral biaryl compounds by asymmetric catalytic reactions with transition metals" **2016**, *308*, 131-190.
[20] H. Wang, *Chirality* "Recent advances in asymmetric oxidative coupling of 2-naphthol and its derivatives" **2010**, *22*, 827-837.
[21] F. Jia, Z. Li, *Org. Chem. Front.* "Iron-catalyzed/mediated oxidative transformation of C–H bonds" **2014**, *1*, 194-214.
[22] S.-J. Ji, J. Lu, X. Zhu, J. Yang, J.-P. Lang, L. Wu, *Synth. Commun.* "Microwave-Assisted Efficient Oxidative Coupling of 2-Naphthols in the Solid State" **2006**, *32*, 3069-3074.
[23] S. B. Patil, P. R. Singh, M. P. Surpur, S. D. Samant, *Ultrason. Sonochem.* "Ultrasound-promoted synthesis of 1-amidoalkyl-2-naphthols via a three-component condensation of 2-naphthol, ureas/amides, and aldehydes, catalyzed by sulfamic acid under ambient conditions" **2007**, *14*, 515-518.
[24] H. Egami, T. Katsuki, *J. Am. Chem. Soc.* "Iron-catalyzed asymmetric aerobic oxidation: oxidative coupling of 2-naphthols" **2009**, *131*, 6082-6083.
[25] K. W. Eckenroad, L. E. Thompson, T. G. Strein, D. Rovnyak, *Magn. Reson. Chem.* "Proton NMR assignments for R,S-1,1'-binaphthol (BN) and R,S-1,1'-binaphthyl-2,2'-diyl hydrogen phosphate (BNDHP) interacting with bile salt micelles" **2007**, *45*, 72-75.
[26] K. K. W. Mak, *J. Chem. Educ.* "Synthesis and Resolution of the Atropisomeric 1,1'-Bi-2-naphthol: An Experiment in Organic Synthesis and 2-D NMR Spectroscopy" **2004**, *81*, 1636-1640.
[27] R. M. B. Carrilho, A. R. Abreu, G. Petöcz, J. C. Bayón, M. J. S. M. Moreno, L. Kollár, M. M. Pereira, *Chem. Lett.* "New Binaphthyl-based C_3-symmetric Chiral Hemilabile Monophosphite Ligands: Synthesis and Characterization of Their Platinum Complexes" **2009**, *38*, 844-845.
[28] O. Mitsunobu, *Synthesis* "The Use of Diethyl Azodicarboxylate and Triphenylphosphine in Synthesis and Transformation of Natural Products" **1981**, *1981*, 1-28.
[29] M. Takahashi, K. Ogasawara, *Tetrahedron: Asymmetry* "An expedient route to some monoalkyl ethers of enantiomerically pure bi-β-naphthol" **1997**, *8*, 3125-3130.
[30] M. T. Reetz, H. Guo, J. A. Ma, R. Goddard, R. J. Mynott, *J. Am. Chem. Soc.* "Helical triskelion monophosphites as ligands in asymmetric catalysis" **2009**, *131*, 4136-4142.
[31] P. W. N. M. van Leeuwen, C. F. Roobeek, *J. Organomet. Chem.* "Hydroformylation of less reactive olefins with modified rhodium catalysts" **1983**, *258*, 343-350.
[32] F. M. S. Rodrigues, P. K. Kucmierczyk, M. Pineiro, R. Jackstell, R. Franke, M. M. Pereira, M. Beller, *ChemSusChem* "Dual Rh-Ru Catalysts for Reductive Hydroformylation of Olefins to Alcohols" **2018**, *11*, 2310-2314.
[33] P. W. N. M. van Leeuwen, P. C. J. Kamer, *Catal. Sci. Technol.* "Featuring Xantphos" **2018**, *8*, 26-113.

[34] F. Ma, M. A. Hanna, *Bioresour. Technol.* "Biodiesel production: a review" **1999**, *70*, 1-15.

[35] X. Yin, H. Ma, Q. You, Z. Wang, J. Chang, *Applied Energy* "Comparison of four different enhancing methods for preparing biodiesel through transesterification of sunflower oil" **2012**, *91*, 320-325.

[36] L. Damas, G. Costa, J. Ruas, R. Carrilho, A. Abreu, G. Aquino, M. Calvete, M. Pineiro, M. Pereira, *Current Microwave Chemistry* "Microwave Assisted Reactions of Natural Oils: Transesterification and Hydroformylation/Isomerization as Tools for High Value Compounds" **2015**, *2*, 53-60.

Chapter 3

Immobilization of Rh/Phosphine catalyst onto nanomaterials

3.1 Introduction

The use of homogeneous catalysts is well established and developed side-by-side with the design of ligands and their metal complexes.[1-4] Homogeneous catalysts exhibit some important aspects that make their use very convenient, their well defined molecular structure and the direct fine-tuning of their structure lead to significant improvements in activity and selectivity outcomes.[5] However, concerns about the sustainability in industrial chemical processes, namely catalyst handling, separation and recycling, which often result in undesired products and environment transition metal contaminations, led researchers to develop innovative phosphorus ligand-based hybrid materials to support them. Among the several supports that can be used for the heterogenization of homogeneous catalysts,[6-9] we highlight the use of carbon-based nanomaterials,[10-12] and magnetic nanoparticles,[13-16] due to their simplicity in functionalization and potential reusability. The most relevant industrial application of a homogeneous catalyst is still the rhodium/phosphorus catalyzed hydroformylation reaction.[2,4,17-19] However, the imperative need to find methods for rhodium recovery due to its price led scientists to direct their efforts towards the search for immobilized rhodium catalysts. In this context, we can find some approaches to promote the immobilization of Rh/phosphorus ligands onto solid supports for hydroformylation in the literature.[20-22] Nevertheless, in our perspective, the best strategy to ensure the preparation of immobilized catalysts is the

use of a covalent binding methodology which is known to avoid metal leaching. Some of the best results achieved so far arise from the parallel development of synthetic strategies for carbon nanomaterials[10-12,23,24] and magnetic nanoparticles functionalization,[7,13,25-28] with the appropriate phosphine derivatization.[20,29-31] Still, we consider that the development of more sustainable approaches for the synthesis of hybrid phosphorus-based nanomaterials remains a great challenge. To that respect, and to the best of our knowledge, the use of the high atom economy hydroaminomethylation reaction[32,33] to covalently link vinyl-triphenylphosphine onto carbon nanotubes and silica-coated iron oxide magnetic nanoparticles has never been reported (Scheme 3.1). We consider that this efficient sequential strategy may pave the way for the preparation of formyl substituted ligands, through hydroformylation reaction, allowing the straightforward *in situ* preparation of hybrid materials.

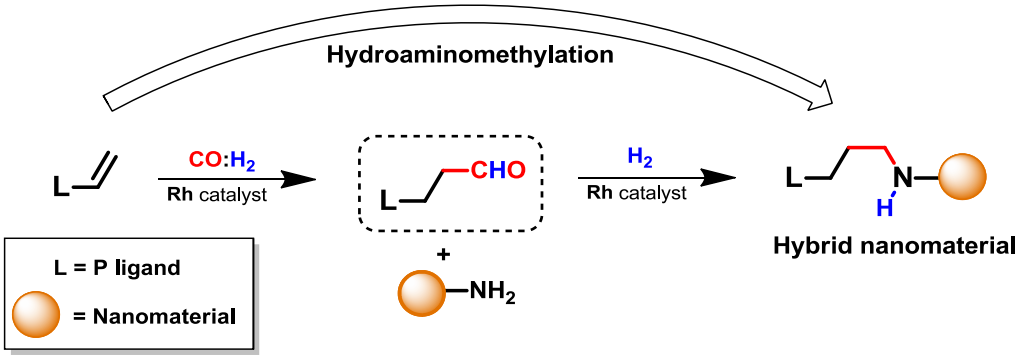

Scheme 3.1 Synthesis of immobilized P-ligands through hydroaminomethylation strategy.

In this chapter, we describe our studies regarding the synthesis and functionalization of multiwalled carbon nanotubes (MWCNT) and iron magnetic nanoparticles (MNP). The amine-functionalized nanomaterials were further used as supports for the immobilization of a triphenylphosphine vinyl derivative through hydroaminomethylation, followed by $[Rh(CO)_2(acac)]$ complexation. The catalytic activity and reutilization stability of both hybrid nanomaterials were evaluated in the hydroformylation of styrene. We also describe the full characterization of the new phosphorus/carbon nanotubes and magnetic nanoparticles materials by standard techniques (XPS, IR, TEM, TG, ICP-OES).

3.2 Nanomaterials functionalization

Pursuing our main goal regarding the synthesis and evaluation of the potential best support for the immobilization of Rh(I)/Phosphine type catalysts, the studies were initiated with the synthesis and functionalization of multiwalled carbon nanotubes (**MWCNT**) and iron magnetic nanoparticles (**MNP**).

3.2.1 MWCNT@NH_2 synthesis

The synthesis of **MWCNT@NH_2** was performed in two steps (Scheme 3.2), following the procedures adapted from the literature.[23,34,35]

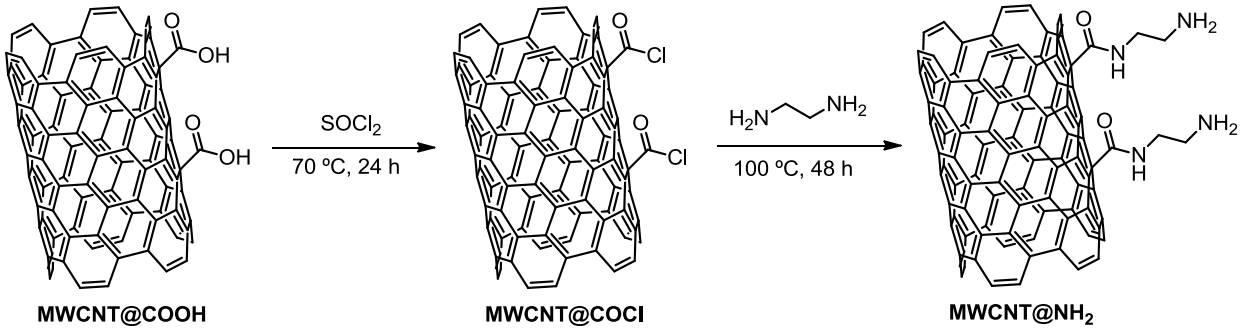

Scheme 3.2 Synthetic route for MWCNT@NH_2.

The commercially available oxidized multiwalled carbon nanotubes containing carboxylic groups (**MWCNT@COOH**) with 3.86 COOH *Wt%*, an average diameter of 8 nm, length of 10-30 mm, and purity higher than 98% were purchased from NANOCYL (NC3101 series). An amount of **MWCNT@COOH** (1.2 g) was transformed into the corresponding acyl chloride derivative by treatment with an excess of thionyl chloride at 70 °C, for 24 h, under nitrogen atmosphere. The resulting solid **MWCNT@COCl** was carefully washed with dry THF (1 L), until neutral pH was obtained, and dried under vacuum for 12 h. Then, the obtained solid was dispersed in excess of freshly distilled ethylenediamine and kept at 100 °C for 48 h. The obtained aminated material **MWCNT@NH_2** was then carefully washed with ethanol (750 mL) and THF (250 mL) and finally dried under vacuum. All functionalized carbon materials were characterized by X-ray photoelectron spectroscopy (XPS), and the results are presented in Table 3.1.

Table 3.1 XPS analysis of the carbon nanotube materials

Sample	XPS At(%)					
	C1s	N1s	O1s	Cl2p[(a)]	P2p	Rh
MWCNT@COOH	95.45	0.19	4.38	-	-	-
MWCNT@COCl	93.61	0.18	5.49	0.72	-	-
MWCNT@NH_2	95.0	2.0	3.0	-	-	-

[(a)]2p1; 2p3

The commercial **MWCNT@COOH** analysis shows the expected atomic percentage of oxygen (4.38 At%) and the XPS of **MWCNT@COCl** material indicates the presence of 0.72 At% of atomic chlorine. The **MWCNT@NH_2** sample revealed the presence of 95.0 At(%) of carbon, 2.0 At(%) of nitrogen, and 3.0 At(%) of oxygen, which is indicative of the presence of 0.82 mmol of NH_2 groups per gram of functionalized material. To calculate the molar amount of NH_2 groups, we considered the atomic contribution of each one of the atomic components of the sample and converted the At% to the molar amount per gram of material.

3.2.2 MNP@NH_2 synthesis

Following your studies on the nanomaterials functionalization, **MNP@NH_2** was obtained through the preparation of magnetite followed by their coating with silica and further amine functionalization (Scheme 3.3), following the methods reported earlier.[36,37]

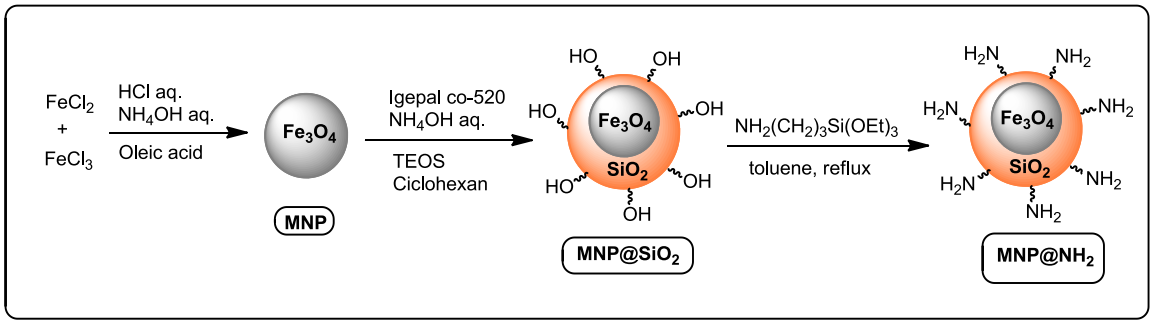

Scheme 3.3 Synthetic route for the synthesis of functionalized iron core-shell magnetic nanoparticles MNP@NH_2.

The magnetic cores were obtained by co-precipitation of Fe^{2+}/Fe^{3+} ions under alkaline reaction conditions, followed by stabilization with oleic acid. So, a mixture of an aqueous solution of $FeCl_3$ and an HCl solution of $FeCl_2$ was added to aqueous NH_3 (1 M) and stirred for 30 min. This dispersion was then washed with acetone and re-dissolved in distilled water. Oleic acid dissolved in acetone was then, added dropwise to this dispersion, under vigorous mechanical stirring along 30 min. The obtained stabilized **MNP** were magnetically recovered and dispersed in cyclohexane. To remove the non-stabilized particles, the final solution was centrifuged. Finally, a stock solution containing 72 mg of **MNP**/mL of cyclohexane was obtained.

To attain a uniform silica coating on the iron oxide surfaces, the previously obtained **MNP** were reacted with tetraethyl orthosilicate (TEOS) under alkaline reaction conditions, after which the obtained precipitate was washed, dried and calcined at 500 °C for 2 h. This process is called reverse microemulsion method and is depicted in scheme 3.4.[38]

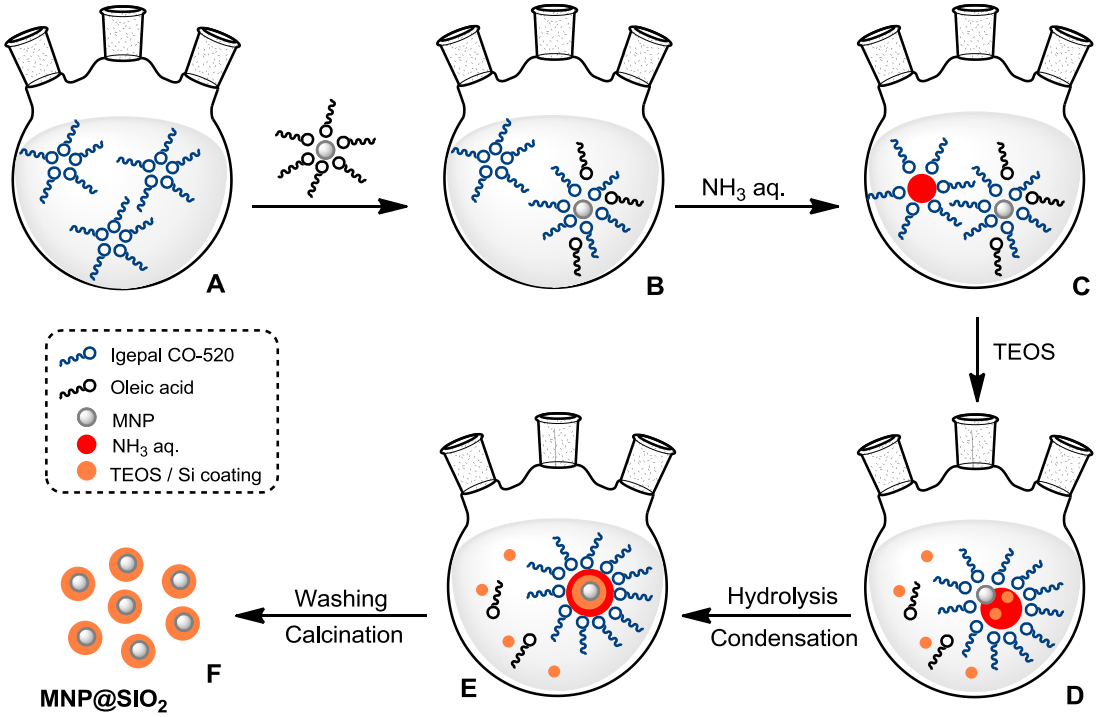

Scheme 3.4 Reverse microemulsion method for the preparation of **MNP@SIO$_2$**.

First, surfactant Igepal CO-520 was dispersed in cyclohexane to prepare the microemulsion **A**, then, the previously prepared **MNPs** stabilized with oleic acid were added to the dispersion, promoting ligand exchange between the oleic acid and the Igepal

CO-520, **B**. After this, an aqueous solution of ammonium hydroxide (29% V/V) was added to the microemulsion, filling the interior of the remaining micelles, **C**. Then, tetraethyl orthosilicate (TEOS), was slowly added dropwise and the reaction occurred along 16 h under slow mechanical stirring (300 rpm). In this step, the hydrolysis of TEOS occurs in the oil/water interface promoting the ligand exchange in the **MNP** and their transfer to the water phase, **D**. The growth of the silica coating around the **MNP** occurs through a condensation reaction of the hydrolyzed TEOS, **E**. After stirring (300 rpm) for 16 h at room temperature, the obtained nanoparticles were precipitated with methanol, recovered by centrifugation (7000 rpm, 30 min) and washed with ethanol (three times) Finally, the desired solid material was dried for 24 h, at room temperature, and calcined at 500 °C for 2 h, **F**. Silica coated nanoparticles (**MNP@SiO_2**) were obtained and analyzed by transmission electron microscopy (TEM) Figure 3.1B.

TEM analysis shows the formation of small magnetite nanoparticles (≈ 5.5 nm, Figure 3.1A, with corresponding size distribution histogram depicted in Figure 3.1C). Subsequent coating with silica afforded **MNP@SiO_2**magnetic nanoparticles, with sizes of ≈ 44.5 nm (Figure 3.1B, with size distribution presented in Figure 3.1D).

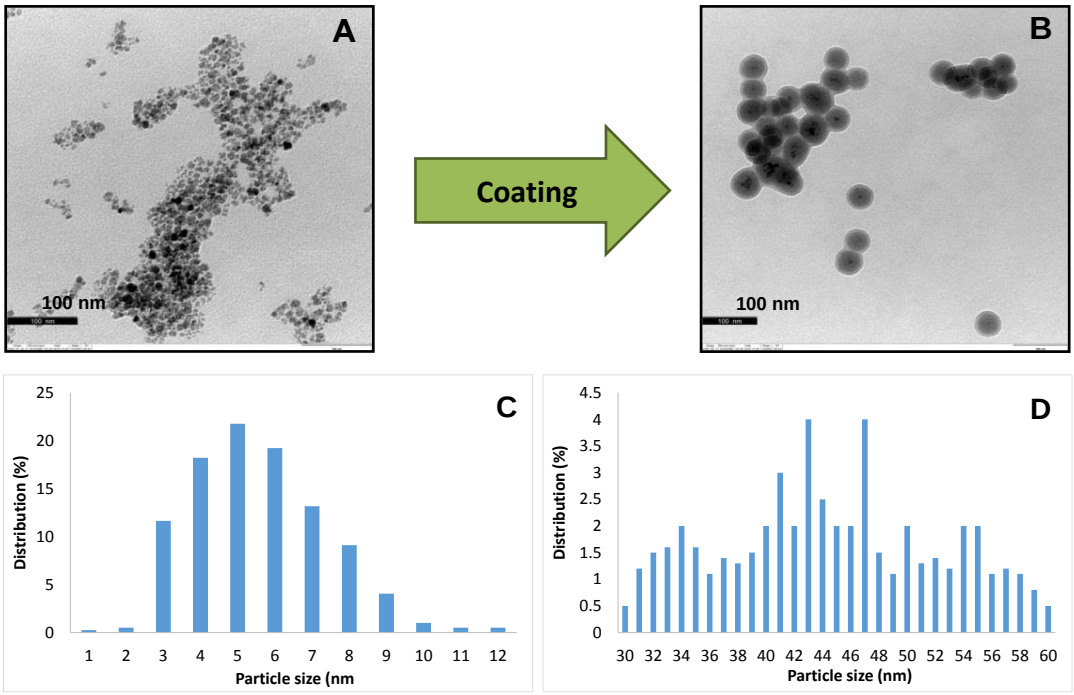

Figure 3.1 TEM images: A) Fe_3O_4 (≈ 5.5 nm), B) **MNP@SiO_2** (≈ 44.5 nm) and corresponding size distribution histograms, C and D, respectively)

The amino-functionalized material was then prepared by reaction of **MNP@SiO$_2$** with 3-aminopropyltriethoxysilane (APTES), in dry toluene, for 2 h; after this period, the particles were washed, centrifuged and dried, providing the desired aminopropyl magnetic nanoparticles **MNP@NH$_2$**. The characterization of the material **MNP@NH$_2$** was performed by comparison of the FTIR spectra with the initial **MNP@SiO$_2$** and TG analysis. The FTIR spectrum of **MNP@SiO$_2$** (Figure 3.2) shows a narrow band at 3740 cm^{-1} attributed to the presence of -OH silanol groups on the particle surface. The FTIR spectrum of the **MNP@NH$_2$** material displays the -OH silanol peak previously observed (3740 cm^{-1}) and additional bands at 3371; 3309 and 1597 cm^{-1} (attributed to antisymmetric, symmetric elongation, and deformation of the NH_2 group, respectively); 2931-2865 and 1450 cm^{-1} (elongation and deformation of the CH_2 group, respectively) and 1410 cm^{-1} (characteristic of the deformation of the Si-CH_2 bond).[28,39]

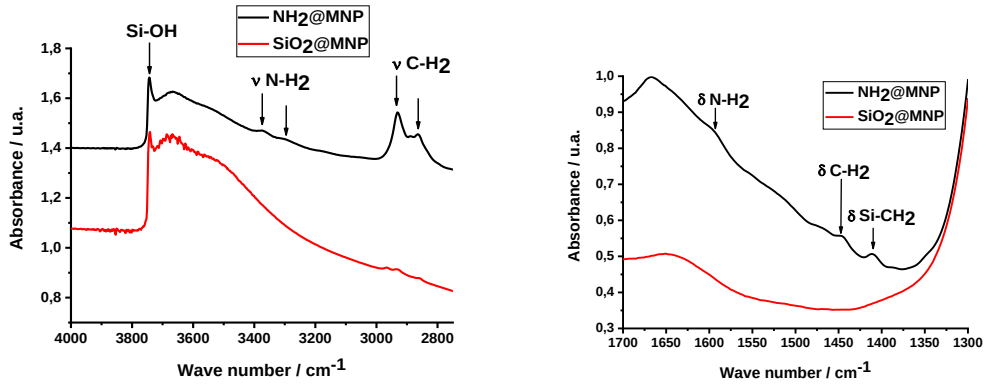

Figure 3.2 FTIR spectral regions of interest of **SiO$_2$@MNP** and **MNP@NH$_2$**.

In addition, **MNP@NH$_2$** was analyzed by thermogravimetry, and a mass loss of 3.8% in the temperature range 200 °C - 600 °C was observed, which indicates that the material contains 0.65 mmol of propylamine groups/g of **MNP@NH$_2$** material (Figure 3.3). The observed mass loss below 200 °C is attributed to the desorption of water and residual organic solvents.

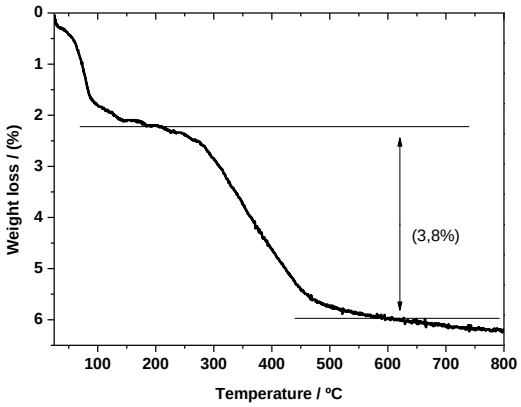

Figure 3.3 TG curve of the **MNP@NH$_2$** sample.

3.3 Hybrid nanocatalyst synthesis

The amine-functionalized nanomaterials were used as support for the immobilization of triphenylphosphine vinyl derivative through hydroaminomethylation followed by [Rh(CO)$_2$(acac)] complexation.

MWCNT@PPh$_3$ and MNP@PPh$_3$synthesis

The synthesis of hybrid phosphine-functionalized nanomaterials (**MWCNT@PPh$_3$** and **MNP@PPh$_3$**) was performed *via* hydroaminomethylation reaction. First, we evaluated the hydroformylation of the 4-(diphenylphosphino)styrene using [Rh(CO)$_2$(acac)] as catalyst precursor under 65 °C and 30 bar of syngas for 20 h and full conversion was obtained, with 95% selectivity for the branched isomer **3.2** (Scheme 3.5).

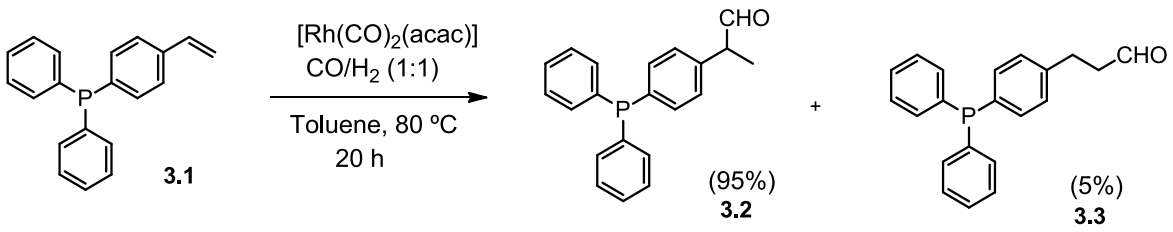

3.1 **3.2** **3.3**

Scheme 3.5 Hidroformylation of **3.1.**

This experiment's reaction crude was analyzed by NMR spectroscopy (Figure 3.4-3.6). ^{1}H-NMR spectrum, (Figure 3.4) presents signals at δ = 9.7 ppm, assigned to the formyl proton (H_1), in the range from δ = 7.61 to 7.10 ppm, attributed to the aromatic protons, a multiplet signal at δ = 3.58 to 3.53, which was assigned to the H_2 proton, and a doublet at δ = 1.37 ppm to the H_3 protons. The ^{13}C-NMR spectrum (Figure 3.5), corroborates this assignment, following the same pattern, δ = 200.9 ppm the aldehyde carbon (C_1), from δ = 138.4 to 128.5 ppm the signals from aromatic carbons, the δ = 52.9 and 14.6 ppm signal were attributed to the C_2 and C_3 carbons, respectively.

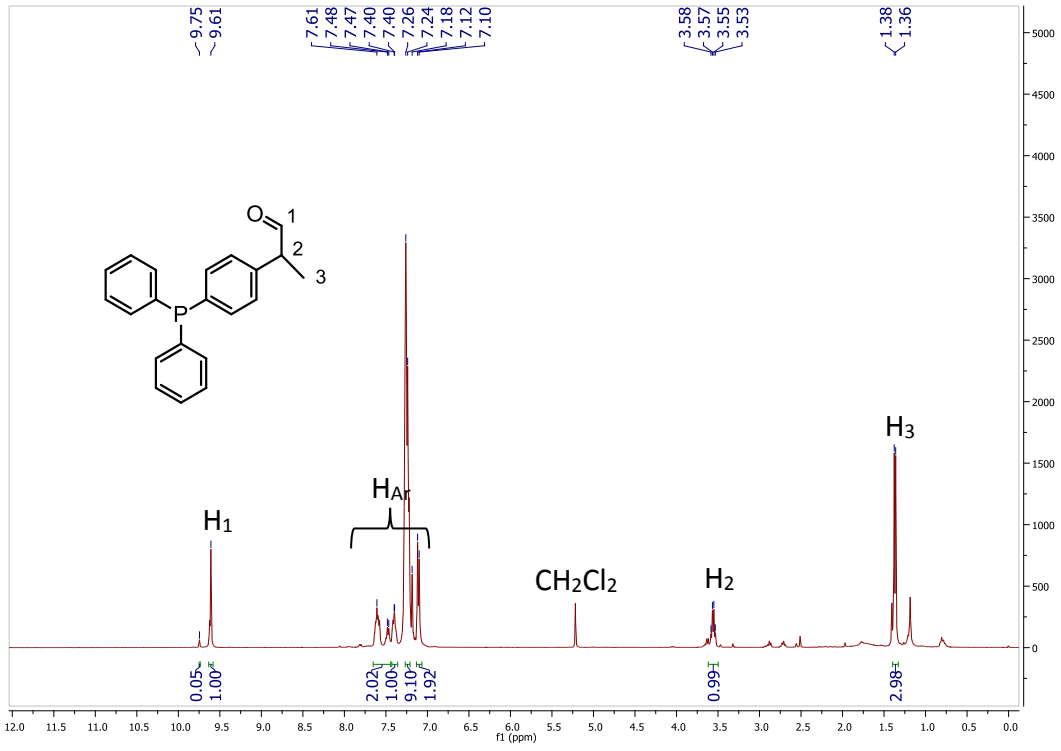

Figure 3.4 ^{1}H-NMR (400 MHz) spectrum of the **3.1** hydroformylation crude in $CDCl_3$.

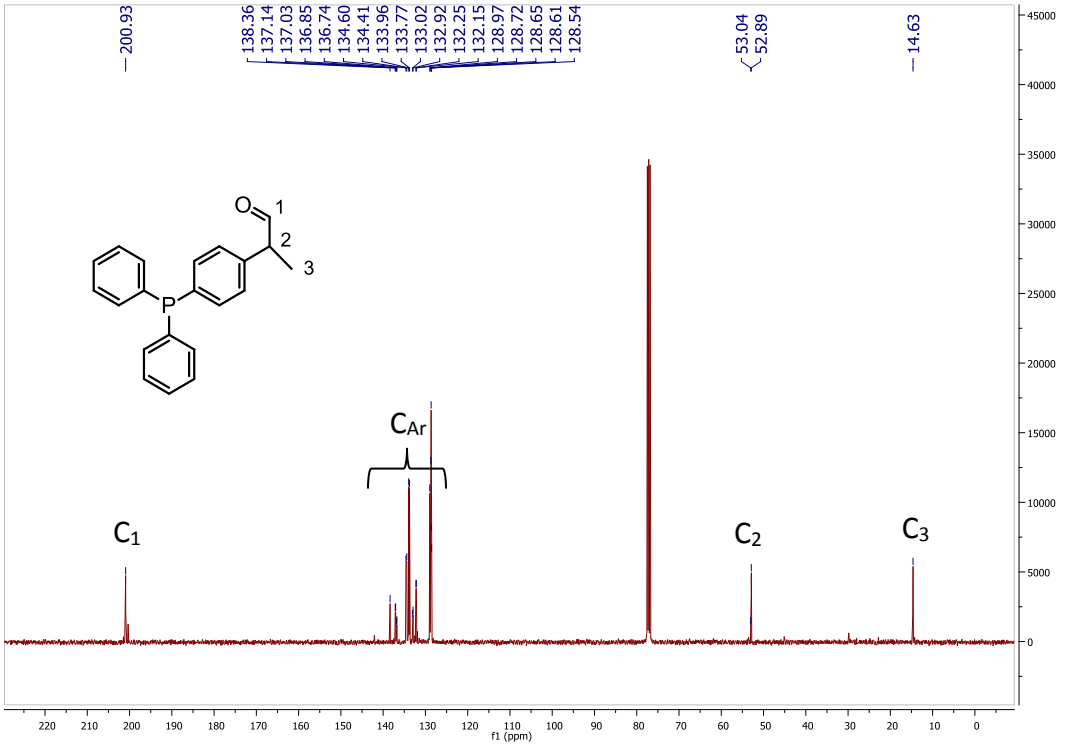

Figure 3.5 ^{13}C-NMR (100 MHz) spectrum of the **3.1** hydroformylation crude in $CDCl_3$.

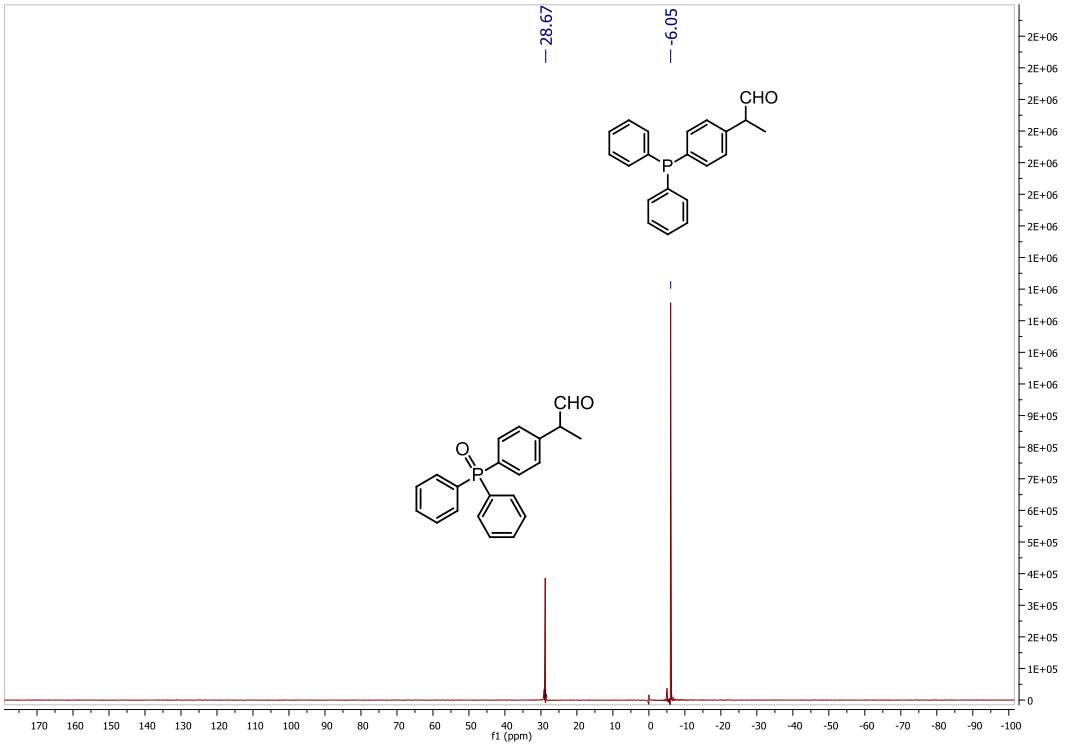

Figure 3.6 ^{31}P-NMR (162 MHz) spectrum of the **3.1** hydroformylation crude in $CDCl_3$ using phosphoric acid as reference.

Additionally, the ^{31}P-NMR spectrum, presented in Figure 3.6, shows 2 signals, one at δ = 6.0 ppm, attributed to the compound **3.2** and another at δ = 28.7 ppm attributed to the product of the oxidation of **3.2**.[40]

With this information, we proceeded the studies with the hydroformylation of **3.1** in the presence of the aminated nanomaterials, to promote the immobilization of the vinyl phosphine derivative *via* hydroaminomethylation (Scheme 3.6).

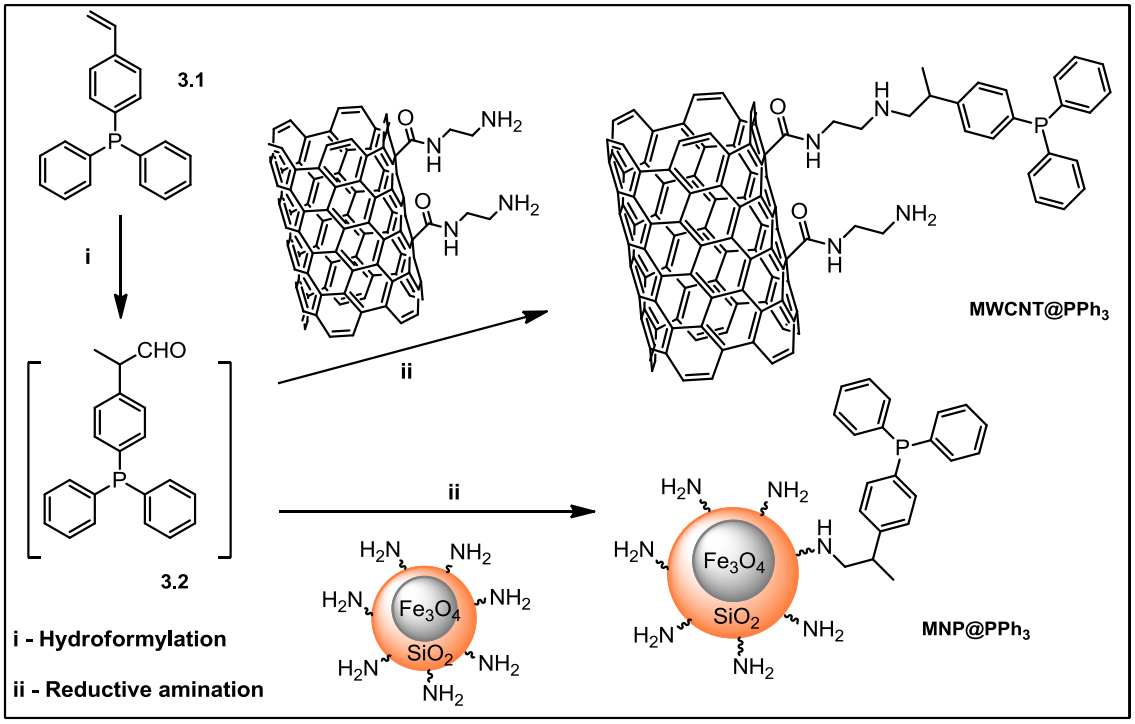

Scheme 3.6 Diphenyl(4-vinylphenyl)phosphine one-pot covalent immobilization on the amine-functionalized materials *via* hydroaminomethylation.

Diphenyl(4-vinylphenyl)phosphine, [$Rh(CO)_2(acac)$] and the selected aminated material [**MWCNT@NH$_2$** (0.82 mmol NH_2/g material) or **MNP@NH$_2$** (0.65 mmol NH_2/g material)] were introduced in a stainless steel high-pressure reactor, under inert atmosphere. After adding freshly dried toluene solvent *via* cannula, the reactor was pressurized with 30 bar (CO/H_2, 1:1), and kept at 65 °C, for 48 h, with vigorous magnetic stirring and constant pressure. The reactor was then cooled to room temperature, degassed, and finally charged with H_2 (P = 30 bar), at 65 °C, for an additional 4 h (Scheme 3.6), after which it was cooled to room temperature and depressurized.

To remove the unreacted diphenyl(4-vinylphenyl) phosphine and residual Rh complex, the **MWCNT@PPh$_3$** material was isolated using several centrifugation/toluene

washing cycles, under inert atmosphere. After drying under vacuum, the desired **MWCNT@PPh$_3$** was characterized by XPS, which showed the presence of 0.3 At% of atomic phosphorus (0.23 mmol of PPh_3/g material) (Table 3.2, entry 3). Regarding **MNP@PPh$_3$**, this material was easily isolated from the reaction medium by simple application of an external magnet. After solvent decantation, the solid was washed several times with toluene and dried. The solid **MNP@PPh$_3$** was then analyzed by XPS, showing 0.7 At% of phosphorus, with no rhodium detection (Table 3.2, Entry 4). However, to avoid some inherent XPS limitations,[41] we further used ICP-OES as a more quantifying characterization tool, displaying a value of 0.13 mmol PPh_3/g material, which was then used in further calculations. It should be mentioned that the ICP analysis also corroborated the presence of only vestigial amounts of rhodium (4×10^{-3} mmol Rh/g material).

Table 3.2 XPS analysis the new hybrid materials.

Entry	Sample	XPS At(%)					
		C1s	N1s	O1s	Si2p	P2p	Rh
1	**MWCNT@NH$_2$**	95.0	2.0	3.0	-	-	-
2	**MNP@NH$_2$**	22.4	3.5	52.9	21.2	-	-
3	**MWCNT@PPh$_3$**	94.9	1.7	3.1	-	0.3	-
4	**MNP@PPh$_3$**	32.6	2.7	44.3	19.7	0.7	-
5	**MWCNT@PPh$_3$-[Rh] (CAT3.1)**	91.0	2.0	6.6	-	0.2	0.2

[Rh(CO)$_2$(acac)] complexation

To prepare the desired Rh/phosphine hybrid catalysts (**CAT3.1** and **CAT3.2**), each of the previously described phosphine functionalized materials **MWCNT@PPh$_3$** (0.23 mmol P/g material) or **MNP@PPh$_3$** (0.13 mmol P/g material) and [Rh(CO)$_2$(acac)] were weighed into a Schlenk tube, under inert atmosphere, and then toluene was added (Scheme 3.7). The complexation reaction was performed, along 15 h, at room temperature, under N_2 atmosphere. The **CAT3.1** and **CAT3.2** materials were isolated, respectively, by centrifugation or external magnetic separation, as described above. After drying, **CAT3.1**

and **CAT3.2** were characterized by XPS and ICP-OES analysis, respectively, displaying values of 0.16 mmol Rh/g material (**CAT3.1**, Table 3.2, Entry 5) and 0.11 mmol Rh/g material (**CAT3.2**).

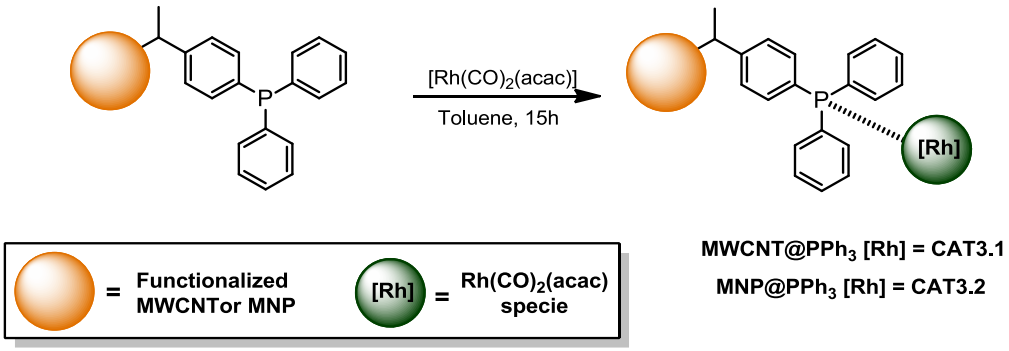

Scheme 3.7 Complexation of $[Rh(CO)_2(acac)]$ onto the phosphine functionalized nanomaterials thought complexation.

3.4 Catalytic evaluation

The catalytic activity and stability of previously prepared hybrid nanocatalysts (**CAT3.1** and **CAT3.2)** were evaluated in the hydroformylation of styrene.

Hydroformylation of styrene

Using styrene as a model substrate, the catalysts **CAT3.1** and **CAT3.2** were evaluated in the hydroformylation reaction at a constant pressure of 30 bar (CO, H_2 1:1), and temperature of 80 °C, for 17 h (Scheme 3.8).

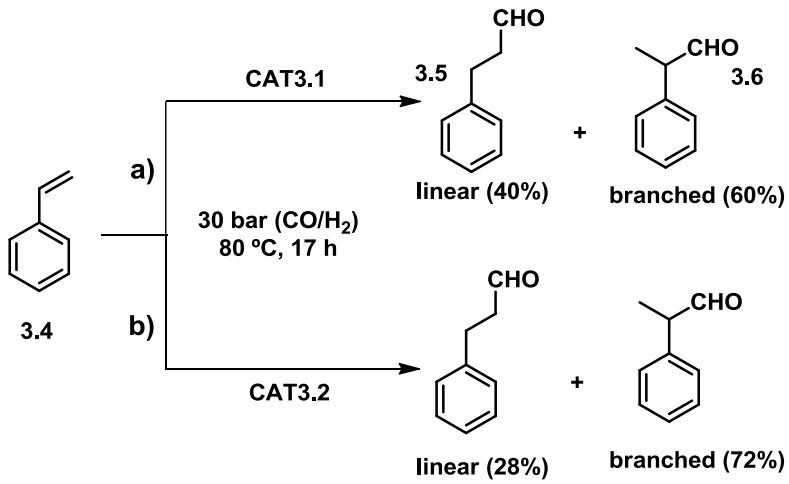

Scheme 3.8 Hydroformylation of styrene. Reaction conditions: a) styrene: rhodium = 500:1; b) styrene: rhodium = 300:1.

In a typical reaction, **CAT3.1** (80 mg, 0.16 mmol Rh/g material) was introduced in the autoclave. After degassing, the toluene and styrene were added *via* cannula, charged with 30 bar of *syngas,* and the reactor was maintained at 80 °C for 17 h. The reactor was then cooled to room temperature, depressurized, and opened in a glove box under inert atmosphere. The hybrid catalyst **CAT3.1** was separated from the reaction crude by centrifugation and washed several times with toluene, while a sample of the reaction mixture was analyzed by GC-MS, displaying 99% conversion with regioselectivity of 60% for the branched aldehyde (Table 3.3). In addition, the hydroformylation of styrene was also performed using **CAT3.2** (200 mg, 0.11 mmol Rh/g material), under similar reaction conditions as above. In this case, **CAT3.2** was separated from the reaction mixture by the application of an external magnet and a sample of the crude mixture was then analyzed by GC-MS, showing 87% conversion with regioselectivity of 72% for the branched aldehyde (Table 3.3).

Table 3.3 Hydroformylation of styrene catalyzed by **CAT3.1** and **CAT3.2**.

Catalyst	Conversion (%)	branched aldehyde (%)	linear aldehyde (%)
CAT3.1	99	60	40
CAT3.2	87	72	28

a) 80 °C, 30 bar (CO/H_2)

The highest regioselectivity for the branched aldehyde obtained using **CAT3.2** suggests that the immobilized [$RhH(PPh_3)(CO)_n$] is the catalytically active species while, when **CAT3.1** is used, both immobilized [$RhH(PPh_3)(CO)_n$] and homogeneous [$RhH(CO)_4$] catalytically active species may be involved.[2]

Reutilization tests

We have also evaluated the stability/reusability of these Rh-phosphorus immobilized catalysts. Thus, the hydroformylation of styrene was performed using the general procedure described above in the presence of the same amount of **MWCNT@PPh_3-[Rh]** (**CAT3.1**). After 17 h, the reaction was stopped and catalyst **CAT3.1** was removed by centrifugation/toluene washing and once again, almost full conversion (98%) and similar regioselectivity (60% for branched aldehyde) was obtained (Table 3.4, entry 1). Then, **CAT3.1** was dried under vacuum and used as catalyst for a second cycle under the same reaction conditions. After this run, the conversion was similar (97%), but the regioselectivity dropped to 54% for the branched aldehyde (Table 3.4, entry 2). This low selectivity for the branched aldehyde may be attributed to the involvement of [$RhH(CO)_4$] active species without any coordinated phosphine,[2] which was corroborated by a blank experiment, where the hydroformylation of styrene, catalyzed by [$Rh(CO)_2(acac)$], gave 99% conversion with 47% regioselectivity for the branched aldehyde (Table 3.4, entry 3). This result led us to evaluate the possibility of the occurrence of rhodium leaching, which could be active in homogeneous reaction conditions. So, we added the same amount of styrene to the supernatant liquid, collected after the first cycle, and subjected the mixture to the reaction conditions described above. Surprisingly, we obtained similar regioselectivity for the branched aldehyde (59%), despite slightly lower activity (76%) (Table 3.4, entry 4).

Table 3.4 Reutilization tests using **CAT3.1** for the hydroformylation of styrene.[a]

Entry		Conversion (%)	branched aldehyde(%)	linear aldehyde (%)
1	**1st cycle**	98	60	40
2	**2nd cycle**	97	54	46
3	**[Rh(CO)$_2$(acac)]**	99	47	53
4	**supernatant 1st cycle**	76	59	41

a) 80 °C, 30 bar (CO/H_2)

This result points out that the carbon nanotubes are able to immobilize rhodium and phosphorus ligands both *via* hydroaminomethylation covalent linkage and by adsorption. In each cycle, the adsorbed Rh/P reagents can be leached and thus, competitive homogenous catalytic reactions occur. So, another reaction was carried out, in which the same amount of [Rh(acac)(CO)$_2$] and PPh_3 (0.024 mmol) was incubated with pristine MWCNTs (100 mg) for 15 h. Then, the solid was extensively washed using the same procedure described above. The material was evaluated as catalyst in the hydroformylation of styrene, under the reaction conditions described in Table 3.4, displaying 99% conversion with 52% regioselectivity for branched aldehyde. Furthermore, to the supernatant of this reaction, the same amount of styrene was added and, after 17 h under the same hydroformylation conditions, again, 99% conversion was obtained with 53% regioselectivity for branched aldehyde. These results demonstrate that the immobilization of Rh/P *via* hydroaminomethylation of vinyl phosphines occurred by covalent linkage and competitive adsorption, which could further lead to Rh/P leaching (Table 3.5).

Table 3.5 Pristine MWCNTs/Rh/PPh_3 catalytic system for hydroformylation of styrene.[a]

	Conversion (%)	Branched aldehyde (%)	Linear aldehyde (%)
MWCNTs/Rh/PPh_3	99	52	48
supernatant	99	53	47

a) 80 °C, 30 bar (CO/H_2)

Furthermore, we performed reutilization tests for the magnetic hybrid catalyst **MNP@PPh$_3$-[Rh]** (**CAT3.2**) where, after the first cycle, 87% conversion and 72% regioselectivity for branched aldehyde was obtained (Table 3.6, Entry 1). In this case, **CAT3.2** was removed from the reaction medium with an external magnetic bar and immediately reused. The second cycle was repeated under the same reaction conditions, reaching 80% of conversion and 67% regioselectivity for branched aldehyde (Table 3.6, entry 2). The catalyst **CAT3.2** was then used in a third cycle, where similar conversion (75%) and regioselectivity for branched aldehyde (69%) were obtained (Table 3.6, entry 3).

Table 3.6 Reutilization tests of **CAT3.2** for styrene hydroformylation.[a]

Entry		Conversion (%)	branched aldehyde(%)	linear aldehyde (%)
1	**1st cycle**	87	72	28
2	**2nd cycle**	80	67	33
3	**3rd cycle**	75	69	31
4	**supernatant 1st cycle**	-	-	-

a) 80 °C, 30 bar (CO/H_2)

To evaluate the possibility of catalyst Rh/P leaching, the same amount of styrene was added to the supernatant liquid, collected after the first cycle, and subjected the reaction mixture to the same hydroformylation reaction conditions. After 17 h, no conversion of styrene was detected (Table 3.6, Entry 4). Furthermore, ICP-OES analysis of **CAT3.2**, after three cycles, showed values of 0.11 mmol Rh/g material, demonstrating that no leaching occurred. These results clearly show that aminated iron oxide magnetic nanoparticles are excellent supports to covalently immobilize vinyl phosphines *via* hydroaminomethylation strategy. This new hybrid Rh/phosphine nanomaterial is a highly active, selective, and easily reusable catalyst for hydroformylation of styrene.

3.5 Conclusion

This chapter describes the application of catalytic hydroaminomethylation as a versatile tool to promote the covalent immobilization of vinyl-phosphorus derivatives onto amino-functionalized materials, namely amine-carbon nanotubes or iron oxide magnetic nanoparticles. The new hybrid phosphorus materials were fully characterized by TEM, XPS, TG and FTIR spectroscopy (CAT3.1 = 0.23 mmol PPh_3/g, CAT3.2 = 0.13 mmol PPh_3/g). These results open the way to promote the immobilization of a variety of vinyl functionalized ligands and their metal complexes.

We conclude that the direct immobilization of phosphines *via* adsorption processes onto multiwalled carbon nanotubes is a strategy to avoid since it easily leads to catalyst leaching. So, we highlight that the development of appropriately functionalized materials (e.g. silica, carbon, metal nanoparticles) is crucial to attain leaching-free covalently anchored ligands/catalysts. These studies undoubtedly demonstrate that aminated iron oxide magnetic nanoparticles are excellent supports to promote the covalent linkage of vinyl ligands, particularly vinyl-P-ligands to prepare stable and easily reusable Rh-based catalysts for hydroformylation reactions. The evaluation of magnetic nanoparticle-based CAT3.2 in styrene hydroformylation (30 bar *syngas*, 80 °C), led us to conclude that it is an active catalytic system with easy reuse of the catalyst after 3 reaction cycles.

This new synthetic methodology, performed through hydroaminomethylation, may contribute to the preparation of stable immobilized organometallic catalysts for multiple applications and as demonstrated also in Chapter 4 in the immobilization of allyl functionalized *C*-scorpionate onto amine-functionalized magnetic nanoparticles.

3.6 References

[1] M. M. Pereira, M. J. Calvete, R. M. Carrilho, A. R. Abreu, *Chem. Soc. Rev.* "Synthesis of binaphthyl based phosphine and phosphite ligands" **2013**, *42*, 6990-7027.

[2] P. C. J. Kamer, P. W. N. M. van Leeuwen, *Phosphorus(III) Ligands in Homogeneous Catalysis: Design and Synthesis*, John Wiley & Sons, Ltd, Chichester, **2012**.

[3] P. W. N. M. van Leeuwen, C. Claver, *Rhodium Catalyzed Hydroformylation*, Kluwer Academic Publishers, New York, **2002**.

[4] S. S. Joshi, V. V. Ranade, *Industrial Catalytic Processes for Fine and Specialty Chemicals*, Elsevier, Amsterdam, **2016**.

[5] P. W. N. M. van Leeuwen, *Homogeneous Catalysis*, Springer, Amsterdam, **2004**.

[6] B. M. L. Dioos, I. F. J. Vankelecom, P. A. Jacobs, *Adv. Synth. Catal.* "Aspects of Immobilisation of Catalysts on Polymeric Supports" **2006**, *348*, 1413-1446.

[7] M. Benaglia, A. Puglisi, *Catalyst Immobilization*, Wiley-VCH, Weinheim, **2020**.

[8] A. Kirschning, *Top. Curr. Chem.* "Immobilized Catalysts" **2004**, *242*, 1-42.

[9] P. Munnik, P. E. de Jongh, K. P. de Jong, *Chem. Rev.* "Recent developments in the synthesis of supported catalysts" **2015**, *115*, 6687-6718.

[10] Y. Yan, J. Miao, Z. Yang, F. X. Xiao, H. B. Yang, B. Liu, Y. Yang, *Chem. Soc. Rev.* "Carbon nanotube catalysts: recent advances in synthesis, characterization and applications" **2015**, *44*, 3295-3346.

[11] P. Serp, B. Machado, *Nanostructured Carbon Materials for Catalysis*, RSC, **2015**.

[12] P. Serp, J. L. Figueiredo, *Carbon Materials for Catalysis*, Wiley, Hoboken, **2008**.

[13] S. H. Bossman, H. Wang, *Magnetic Nanomaterials*, RSC, **2017**.

[14] M. B. Gawande, P. S. Branco, R. S. Varma, *Chem. Soc. Rev.* "Nano-magnetite (Fe_3O_4) as a support for recyclable catalysts in the development of sustainable methodologies" **2013**, *42*, 3371-3393.

[15] L. M. Rossi, N. J. S. Costa, F. P. Silva, R. Wojcieszak, *Green Chem.* "Magnetic nanomaterials in catalysis: advanced catalysts for magnetic separation and beyond" **2014**, *16*, 2906-2933.

[16] Y. Zhu, L. P. Stubbs, F. Ho, R. Liu, C. P. Ship, J. A. Maguire, N. S. Hosmane, *ChemCatChem* "Magnetic Nanocomposites: A New Perspective in Catalysis" **2010**, *2*, 365-374.

[17] R. Franke, D. Selent, A. Borner, *Chem. Rev.* "Applied hydroformylation" **2012**, *112*, 5675-5732.

[18] A. Börner, R. Franke., *Hydroformylation: Fundamentals, Processes, and Applications in Organic Synthesis*, Wiley-VCH, Weinheim, **2016**.

[19] M. M. Pereira, in *Sustainable Synthesis of Pharmaceuticals*, **2018**, pp. 66-104.

[20] C. Li, W. Wang, L. Yan, Y. Ding, *Front. Chem. Sci. Eng.* "A mini review on strategies for heterogenization of rhodium-based hydroformylation catalysts" **2017**, *12*, 113-123.

[21] Â. C. B. Neves, M. J. F. Calvete, T. M. V. D. Pinho e Melo, M. M. Pereira, *Eur. J. Org. Chem.* "Immobilized Catalysts for Hydroformylation Reactions: A Versatile Tool for Aldehyde Synthesis" **2012**, *2012*, 6309-6320.

[22] Á. Molnár, A. Papp, *Coord. Chem. Rev.* "Catalyst recycling—A survey of recent progress and current status" **2017**, *349*, 1-65.

[23] C. J. P. Monteiro, S. A. C. Carabineiro, T. Lauterbach, C. Hubbert, A. S. K. Hashmi, J. L. Figueiredo, M. M. Pereira, *ChemNanoMat* "(S)-BINOL Immobilized onto

Multiwalled Carbon Nanotubes through Covalent Linkage: A New Approach for Hybrid Nanomaterials Characterization" **2015**, *1*, 178-187.

[24] M. J. F. Calvete, *Future Trends For Top Materials*, Bentham Science Publishers Ltd, Sarjah, **2016**.

[25] C. A. Henriques, A. Fernandes, L. M. Rossi, M. F. Ribeiro, M. J. F. Calvete, M. M. Pereira, *Adv. Funct. Mater.* "Biologically Inspired and Magnetically Recoverable Copper Porphyrinic Catalysts: A Greener Approach for Oxidation of Hydrocarbons with Molecular Oxygen" **2016**, *26*, 3359-3368.

[26] M. J. F. Calvete, M. Piñeiro, L. D. Dias, M. M. Pereira, *ChemCatChem* "Hydrogen Peroxide and Metalloporphyrins in Oxidation Catalysis: Old Dogs with Some New Tricks" **2018**, *10*, 3615-3635.

[27] M. M. Pereira, L. D. Dias, M. J. F. Calvete, *ACS Catal.* "Metalloporphyrins: Bioinspired Oxidation Catalysts" **2018**, *8*, 10784-10808.

[28] L. D. Dias, R. M. B. Carrilho, C. A. Henriques, M. J. F. Calvete, A. M. Masdeu-Bultó, C. Claver, L. M. Rossi, M. M. Pereira, *ChemCatChem* "Hybrid Metalloporphyrin Magnetic Nanoparticles as Catalysts for Sequential Transformation of Alkenes and CO_2 into Cyclic Carbonates" **2018**, *10*, 2792-2803.

[29] I. Wauters, W. Debrouwer, C. V. Stevens, *Beilstein. J. Org. Chem.* "Preparation of phosphines through C-P bond formation" **2014**, *10*, 1064-1096.

[30] T. Scherpf, C. Schwarz, L. T. Scharf, J. A. Zur, A. Helbig, V. H. Gessner, *Angew. Chem. Int. Ed. Engl.* "Ylide-Functionalized Phosphines: Strong Donor Ligands for Homogeneous Catalysis" **2018**, *57*, 12859-12864.

[31] E. I. Musina, A. S. Balueva, A. A. Karasik, *Phosphines: preparation, reactivity and applications, Vol. 48*, RSC, **2019**.

[32] P. Kalck, M. Urrutigoity, *Chem. Rev.* "Tandem Hydroaminomethylation Reaction to Synthesize Amines from Alkenes" **2018**, *118*, 3833-3861.

[33] C. Chen, X.-Q. Dong, X. Zhang, *Org. Chem. Front.* "Recent progress in rhodium-catalyzed hydroaminomethylation" **2016**, *3*, 1359-1370.

[34] M. F. R. Pereira, J. L. Figueiredo, J. J. M. Órfão, P. Serp, P. Kalck, Y. Kihn, *Carbon* "Catalytic activity of carbon nanotubes in the oxidative dehydrogenation of ethylbenzene" **2004**, *42*, 2807-2813.

[35] J. Shen, W. Huang, L. Wu, Y. Hu, M. Ye, *Materials Science and Engineering: A* "Study on amino-functionalized multiwalled carbon nanotubes" **2007**, *464*, 151-156.

[36] M. J. Jacinto, P. K. Kiyohara, S. H. Masunaga, R. F. Jardim, L. M. Rossi, *Appl. Catal. A, Gen.* "Recoverable rhodium nanoparticles: Synthesis, characterization and catalytic performance in hydrogenation reactions" **2008**, *338*, 52-57.

[37] L. M. Rossi, L. L. R. Vono, F. P. Silva, P. K. Kiyohara, E. L. Duarte, J. R. Matos, *Appl. Catal. A, Gen.* "A magnetically recoverable scavenger for palladium based on thiol-modified magnetite nanoparticles" **2007**, *330*, 139-144.

[38] D. K. Yi, S. S. Lee, G. C. Papaefthymiou, J. Y. Ying, *Chem. Mater.* "Nanoparticle Architectures Templated by SiO2/Fe2O3Nanocomposites" **2006**, *18*, 614-619.

[39] H. Günzler, H.-U. Gremlich, *IR Spectroscopy: An Introduction*, Wiley-VCH, New York, **2002**.

[40] O. Kühl, *Phosphorus-31 NMR Spectroscopy*, Springer, Berlin, **2008**.

[41] P. v. d. Heide, *X-Ray Photoelectron Spectroscopy: An Introduction to Principles and Practices*, Wiley-VCH, Hoboken, **2012**.

Chapter 4

Sequential Hydroformylation/Acetalization of Olefins using a Rh/Fe Bimetallic Catalytic System

4.1 Introduction

One of the ultimate goals of synthetic chemists is to mimic multi-enzymatic natural systems for the construction of complex molecules using sequential multi-catalytic systems. Among them, the hydroformylation/acetalization reaction, which allows the direct transformation of olefins into high-value oxygenated products through a sequential multicatalytic process, without isolation of aldehyde intermediates is of particular interest.[1-4] Nonetheless, these systems may have problems associated with the reduction of aldehydes to alcohols, high catalyst cost and difficulties in catalyst reutilization. Therefore, advances in selective catalytic processes using homogeneous type catalysts immobilized onto solid supports, are still amongst the main challenges for the transposition of academically developed catalysts towards sustainable industrial processes.[5] To this respect, the immobilization of Rh(I)/Xantphos derivatives demonstrates the interest in this strategy to develop highly selective heterogeneous catalysts to produce linear oxo products,[6, 7] with particular interest in the use of magnetic nanoparticles as supports, since they allow catalyst reutilization by simple use of external magnets.[8-11] In parallel, the search for new active/selective catalysts led to catalysts as *C*-scorpionate metal complexes, which have been largely applied in several reactions,[12-

[15] but, to the best of our knowledge, they were never been reported as catalysts for the sequential hydroformylation/acetalization transformation neither in homogeneous nor heterogeneous processes.

Bearing this in mind, in this chapter we describe the immobilization of *N*-Xantphos onto MNP@Cl and the immobilization of a new allyl functionalized *C*-scorpionate iron(II) complex onto MNP@NH_2, through hydroaminomethylation reaction, along with their full characterization by standard spectroscopic methods, transmission electron microscopy (TEM), thermogravimetry (TG), and inductively coupled plasma optical emission spectrometry (ICP-OES). The bimetallic catalytic system Rh(I)/P-ligand type catalysts and [$FeBr_2\{\kappa^3$-$HC(pz)_3\}$] were evaluated in homogeneous phase transformation of different types of substituted olefins into the corresponding acetals. Finally, the immobilized catalysts (MNP@*N*-Xantphos/Rh(I) and MNP@NH-$(CH_2)_4O$-$CH_2C(pz)_3FeBr_2$ were further applied in the sequential hydroformylation/acetalization reaction of oct-1-ene using ethanol simultaneously as green solvent and reagent. Reutilization studies of both catalysts are also described, Scheme 4.1.

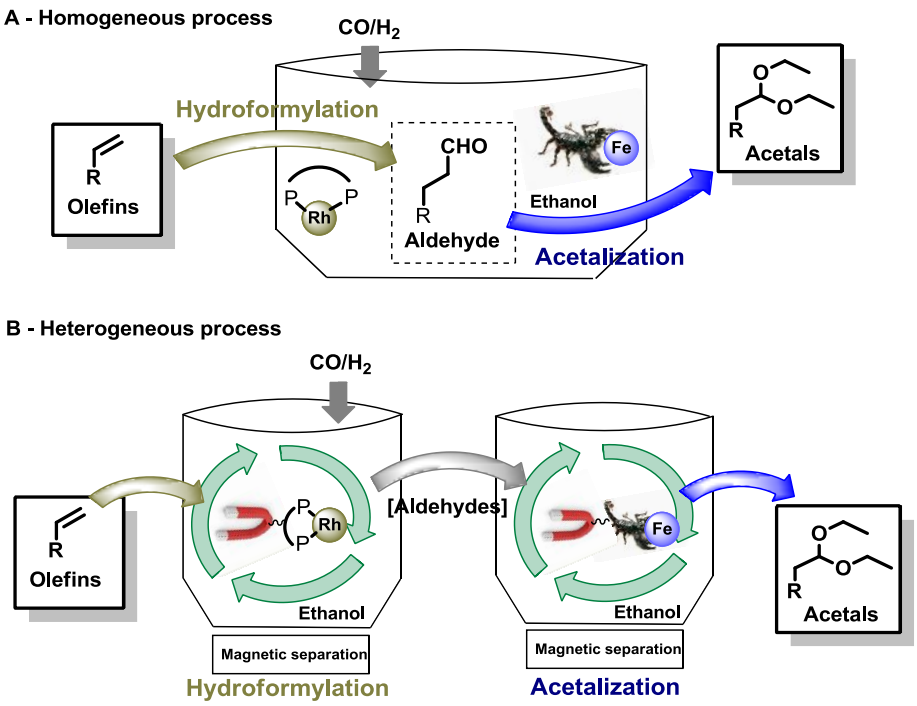

Scheme 4.1 Synthetic approaches for the hydroformylation/acetalization of olefins (A Homogeneous process, B – Heterogeneous process).

4.2 Catalyst synthesis

Pursuing our main goal regarding the development of sustainable catalysts, the studies described in Chapter 4 were initiated with the catalyst synthesis. First, we prepared the homogeneous complexes Fe/*C*-scorpionate-type catalyst to be used as Lewis acid in the acetalization reaction and Rh/P-ligand complexes for the hydroformylation reaction. Then, Rh/*N*-Xantphos and a functionalized Fe/*C*-scorpionate catalyst were immobilized onto iron magnetic nanoparticles.

4.2.1 Homogeneous type catalysts

Iron(II)-*C*-scorpionate catalyst **(CAT4.1)** was synthesized by slight modifications of previously described methods, (Scheme 4.2).[16, 17] Tris(pyrazolyl)methane ($HC(pz)_3$, pz = pyrazolyl) (**4.2**) was prepared by reacting 1*H*-pyrazole (**4.1**) with chloroform in the presence of tetra-*n*-butylammonium bromide (TBABr) and sodium carbonate, using water as solvent, for 3 days, yielding 65% of the desired product **4.2**. Then, an ethanolic solution of $HC(pz)_3$ was added dropwise to another ethanolic solution of iron(II) bromide, under inert atmosphere, at room temperature, which upon stirring for 2 hours, provided pure purple powder of $[FeBr_2\{HC(pz)_3\}]$ (**CAT4.1**) in 91% yield. **CAT4.1** was characterized through ^1H, ^{13}C-NMR spectroscopy and HRMS.

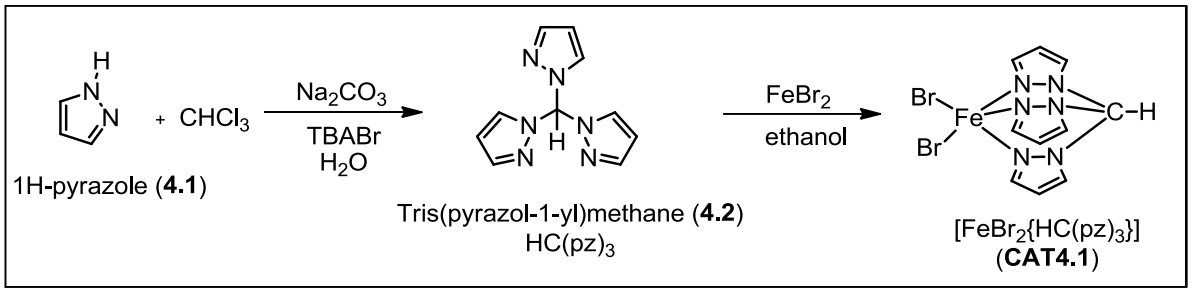

Scheme 4.2. Synthetic route for **CAT4.1**.

The ^1H-NMR spectrum of **CAT4.1**, recorded in D_2O, is presented in Figure 4.1. It shows one singlet signal at δ = 9.22 ppm assigned to sp^3 $\underline{H}C(pz)_3$ ligand and three broad singlets at δ = 8.56, 7.83 and 7.09 attributed to the three protons at the pyrazole ring. Figure 4.2 shows the ^{13}C-NMR spectrum of the same compound, where we can observe the presence

of the signals at δ = 159.8, 143.1, 114.6 ppm, assigned to the aromatic pyrazole carbons. Additionally, we can observe the signal at δ = 74.2 ppm, assigned to the H<u>C</u>(pz)$_3$ carbon. These assignments were corroborated with the acquisition of the HSQC spectrum of the compound, displaying all $^1J_{CH}$ couplings, Figure 4.3. The complex was also analyzed through electron spray ionization (ESI) high resolution mass spectrometry (HRMS), showing a peak at m/z = 348,9489 (Fig 4.4), found for a theoretical value of m/z = 348,9494 for $C_{10}H_{10}BrFeN_6^+$ [M-Br]$^+$.

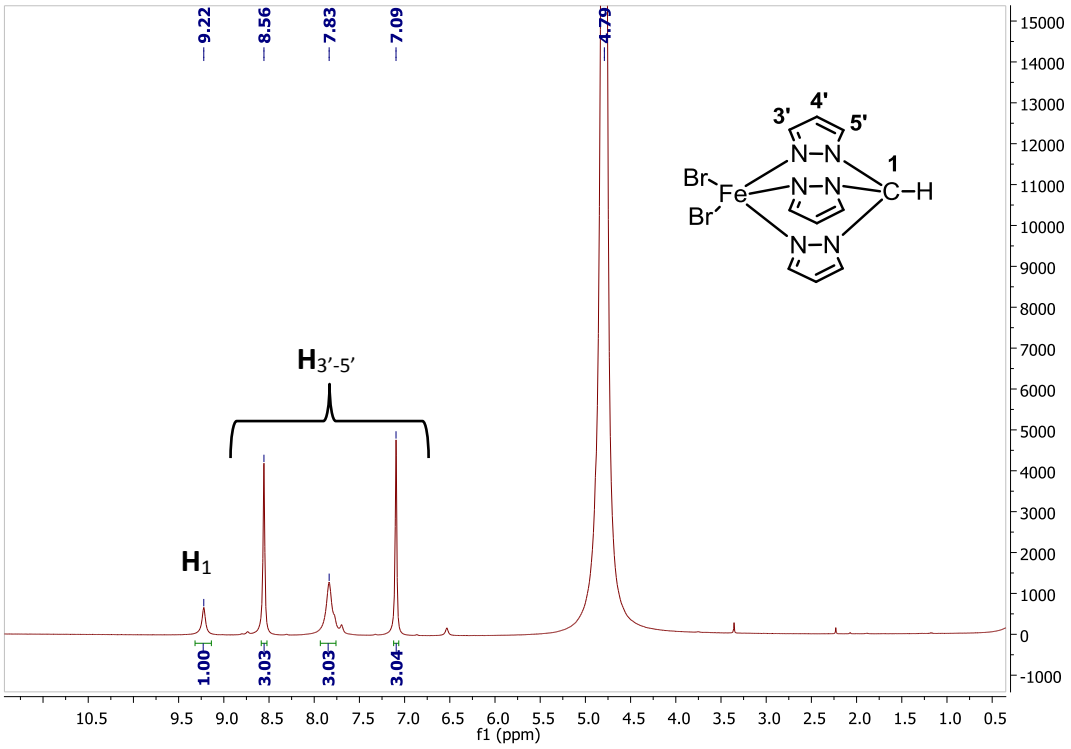

Figure 4.1 ^{1}H-NMR (400 MHz) spectrum of **CAT4.1** in D_2O.

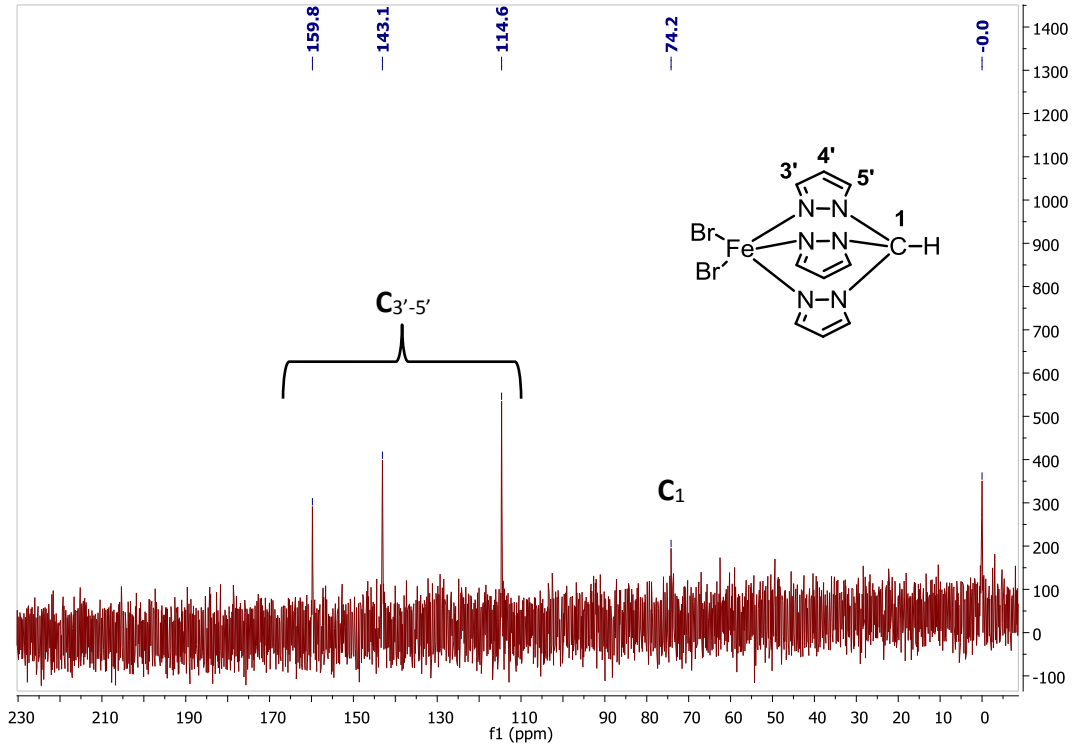

Figure 4.2 ^{13}C-NMR (100 MHz) spectrum of **CAT4.1** in D_2O.

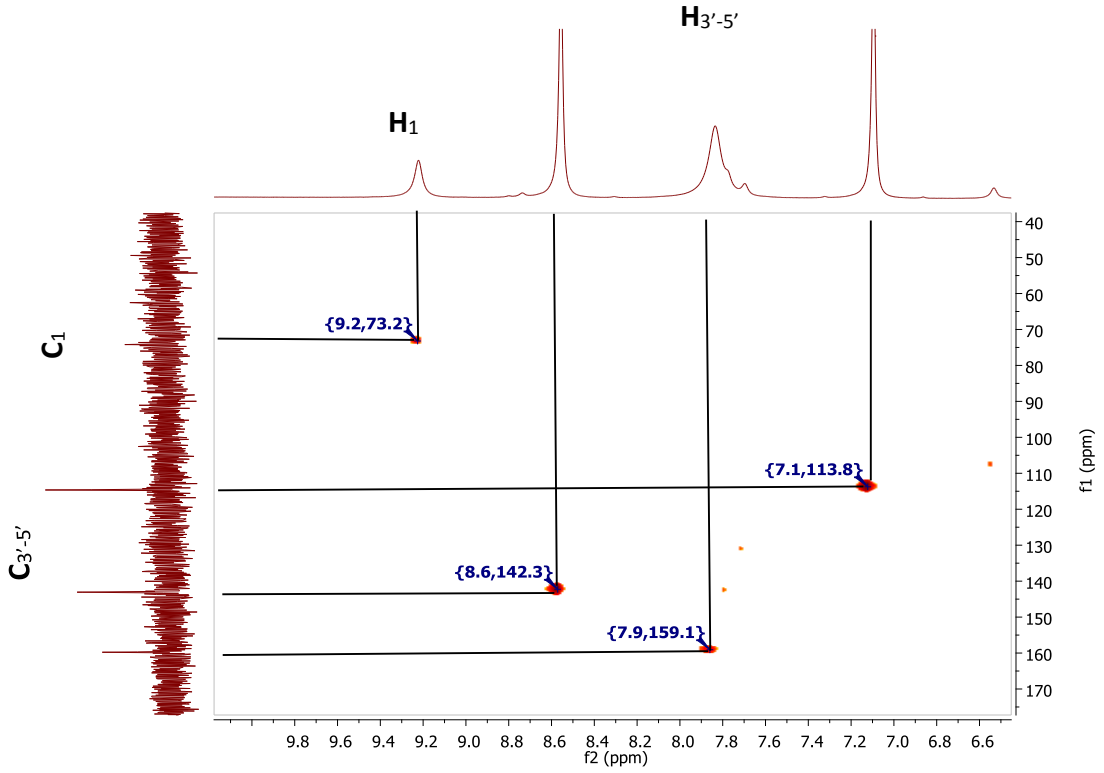

Figure 4.3 HSQC spectrum of **CAT4.1** in D_2O.

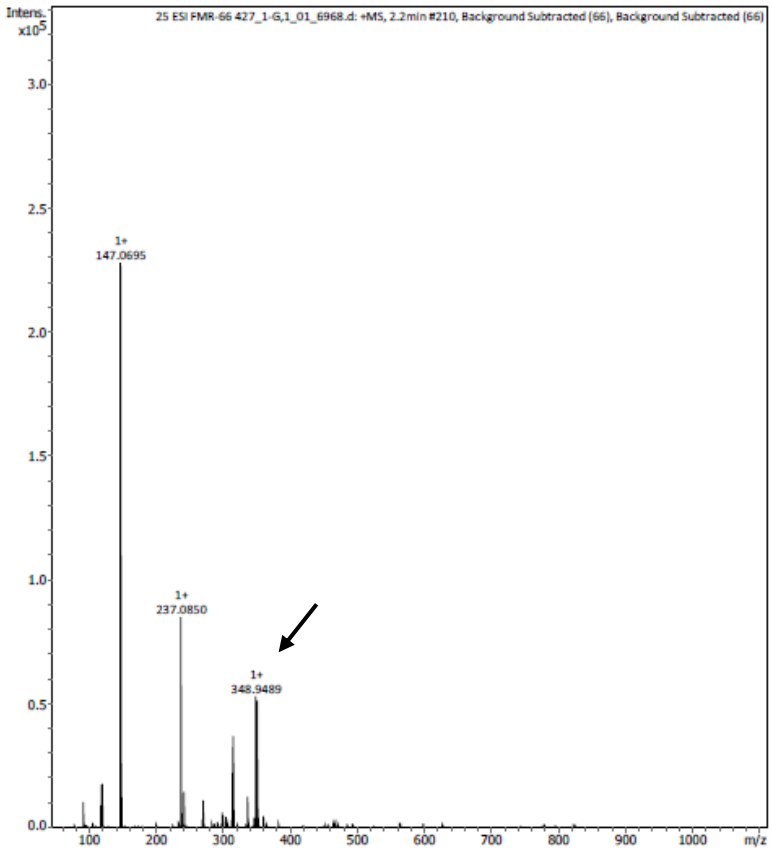

Figure 4.4 HRMS spectrum of **CAT4.1**.

The hydroformylation rhodium/phosphorus catalysts **CAT4.2, CAT4.3** and **CAT4.4** were prepared *in situ*, by mixing, in the autoclave, the selected phosphorous ligands **L4.1** = Xantphos, **L4.2** = triphenylphosphine, (both commercially available) and **L4.3** = tris[2'-(benzyloxy)-1,1'-binaphthyl-2-yl] phosphite, whose synthesis is described in Chapter 2, with the pre-catalyst $[Rh(CO)_2(acac)]$, at 80 °C and 30 bar H_2/CO (1:1), for 2 hours, using ethanol as solvent (Scheme 4.3).

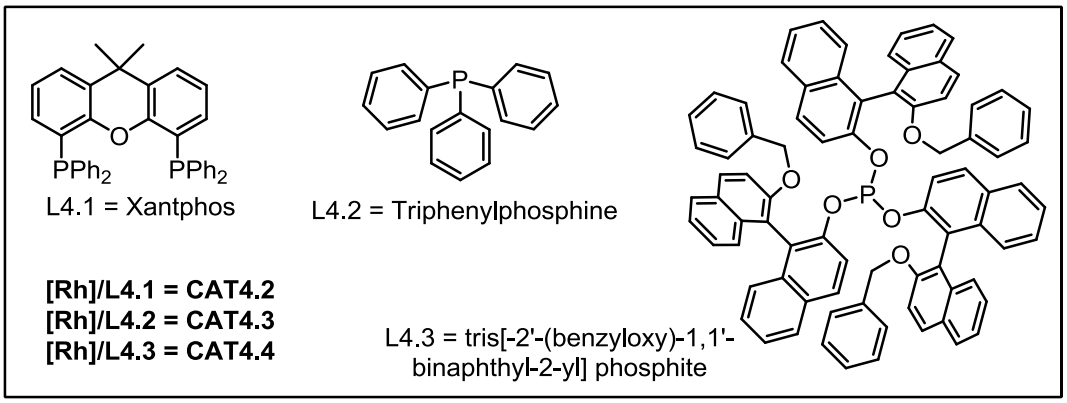

Scheme 4.3 Phosphorus type ligands used in Rh-P hydroformylation reactions.

4.2.2 Heterogeneous type catalysts

The heterogeneous catalysts **CAT4.5** and **CAT4.6** (Figure 4.5) were prepared through the previously described silica-coating and amine functionalization of magnetic iron nanoparticles (Chapter 3), followed by covalent grafting of the suitable functionalized homogeneous ligands.

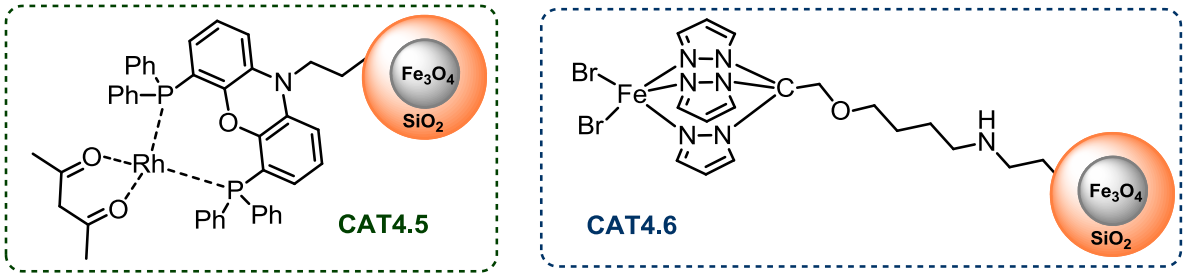

Figure 4.5 Heterogeneous catalysts for hydroformylation/acetalization of olefins.

Synthesis and functionalization of magnetic nanoparticles

Magnetic nanoparticles were obtained through sequential preparation of magnetite, followed by silica coating and further functionalization with amine or chloro containing chains (Scheme 4.4).

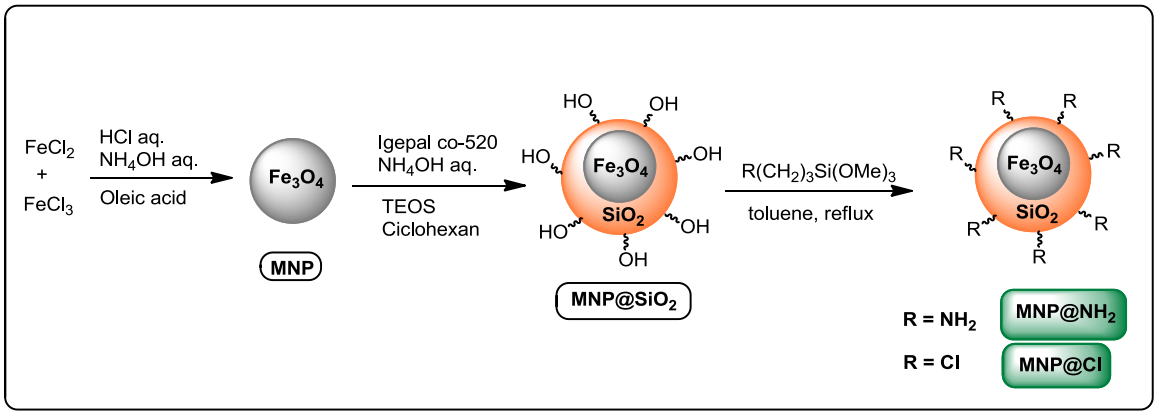

Scheme 4.4 Synthetic route for the synthesis of functionalized iron core-shell magnetic nanoparticles (MNP@Cl and MNP@NH_2).

MNPs were obtained by co-precipitation method using Fe^{2+}/Fe^{3+} ions under alkaline reaction conditions, followed by stabilization with oleic acid addition as described in Chapter 3.[18] This dispersion was then washed with acetone, re-dissolved in cyclohexane

and kept as stock dispersion of magnetite. Transmission electronic microscopy (TEM) analysis of MNP (Figure 4.6) shows the formation of magnetite nanoparticles (≈ 7 nm).

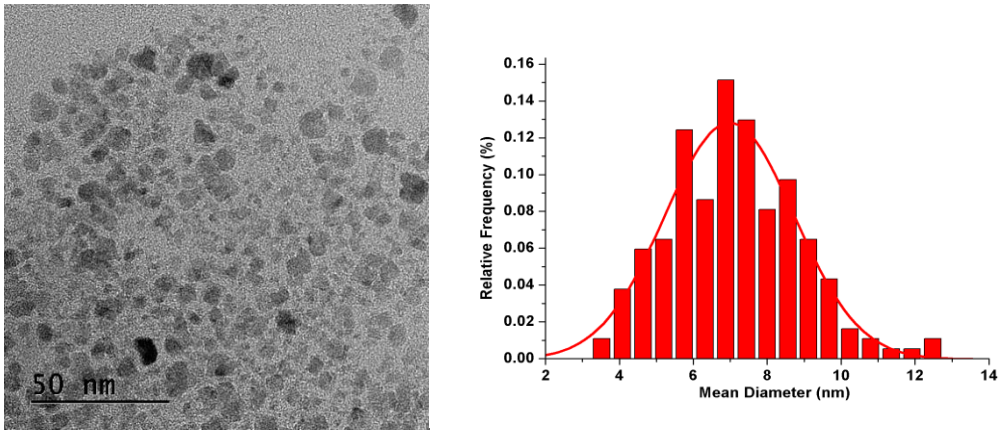

Figure 4.6 TEM image of MNP and their corresponding size distribution histogram (≈ 7 nm).

Then, MNP@SiO_2 were prepared according to a previously reported method.[19] To obtain uniform silica coating on the magnetite surfaces, the previously obtained MNP was reacted with tetraethyl orthosilicate (TEOS) under alkaline reaction conditions. MNP@SiO_2 were obtained with approximately 23 nm size, as shown in the TEM analysis (Figure 4.7).

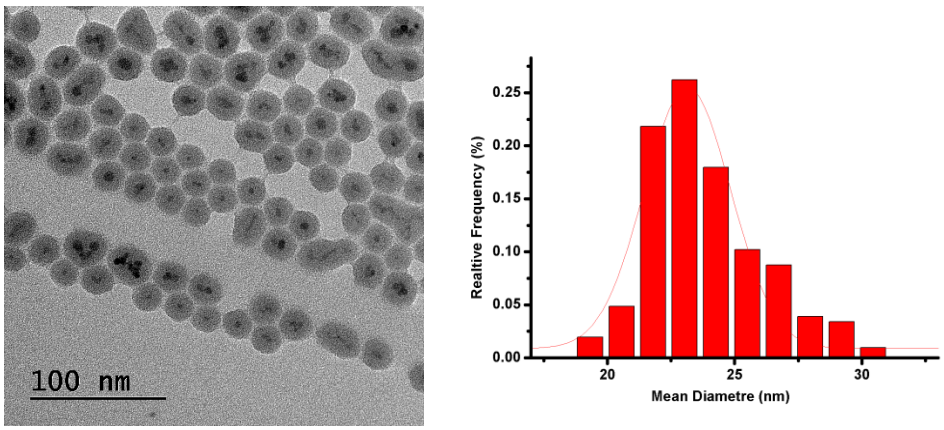

Figure 4.7 TEM image of MNP@SiO_2 and their corresponding size distribution histogram (≈ 23 nm).

Additionally, a sample of the obtained material was analyzed by thermogravimetry (Figure 4.8). MNP@SiO_2 thermogram shows a weight loss in the temperature range of 50 °C-150 °C, which was attributed to the loss of adsorbed water and organic solvents.

Another 1.5% weight loss occurred between 200 and 800 °C attributed to the decomposition of silanol groups present in MNP@SiO_2.

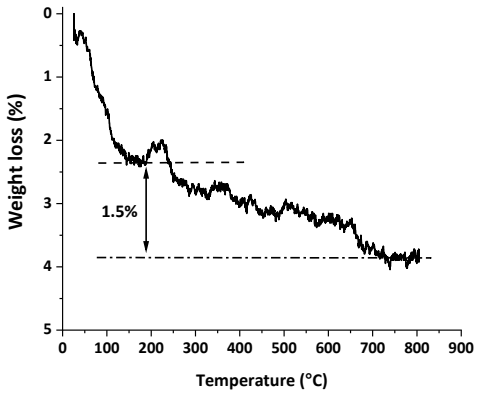

Figure 4.8 TG curve of MNP@SiO_2.

Next, chloro-functionalized MNPs were prepared by reaction of MNP@SiO_2 with (3-chloropropyl)triethoxysilane (CPTES). The resulting material was magnetically collected and washed with ethyl acetate and acetonitrile. Finally, the resulting solid was dried under vacuum, for 24 hours. The MNP@Cl were characterized by thermogravimetry analysis, (Figure 4.9).

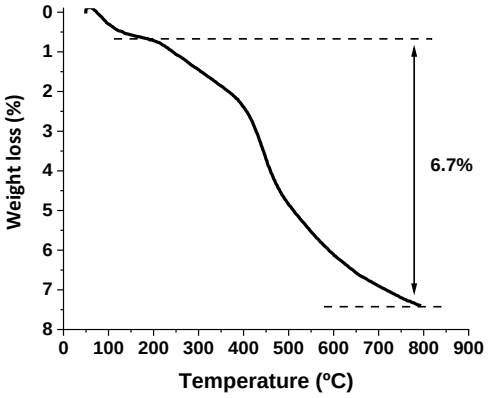

Figure 4.9 TG curve of MNP@Cl.

To quantify the 3-chloropropyl functionalization, we used the method for the quantification of the functional groups presented in the material described in Chapter 3. The thermogram of MNP@Cl presents a weight loss of 6.7% between 200 °C and 800 °C, 5.1% weight loss is attributed to 3-chrolopropyl groups thermal decomposition, corresponding to 0.66 mmol of chloropropyl groups/g of MNP@Cl material.

Then, using a similar approach as above described, amino-functionalized MNPs were prepared by reaction of MNP@SiO_2 with 3-aminopropyltriethoxysilane (APTES). The particles were washed, centrifuged and dried under vacuum, providing the desired aminopropyl functionalized magnetic nanoparticles MNP@NH_2. The characterization of the aminated material was performed by comparison of Fourier-transform infrared spectroscopy (FTIR) spectra with the initial MNP@SiO_2 spectra and thermogravimetric (TG) analysis, to quantify the organic matter present in the MNP surface, (Figure 4.10).

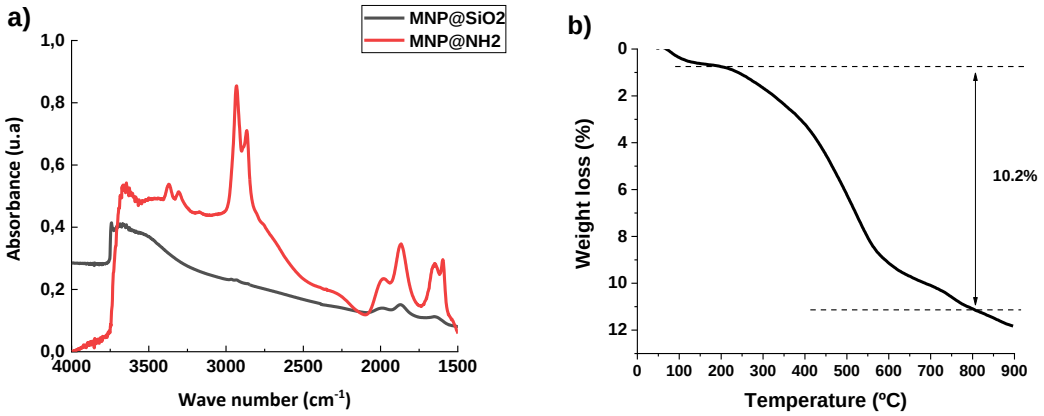

Figure 4.10 a) Comparative infrared spectra of MNP@NH_2 and MNP@SiO_2 b) TG curve of MNP@NH_2.

The FTIR spectra of MNP@NH_2 (red) and the MNP@SiO_2 (black) are presented in Figure 4.10a. The FTIR spectra show the typical-OH silanol peak (3740 cm^{-1}) and additional bands at 3371; 3309 and 1597 cm^{-1} (attributed to antisymmetric, symmetric elongation, and deformation of the NH_2 group, respectively); 2931-2865 and 1450 cm^{-1} (elongation and deformation of the CH_2 group, respectively) and 1410 cm^{-1} (characteristic of the deformation of the Si-CH_2 bond).[20] Additionally, MNP@NH_2 were also analyzed by thermogravimetry (Figure 4.10b). A weight loss between 50 °C and 200 °C, attributed to the loss of adsorbed water and solvents was observed. Another weight loss (10.2%) in the temperature range 200 °C - 800 °C was also detected, being attributed to the decomposition of silanol and 3-aminopropyl groups. The amount of 3-aminopropyl groups was calculated, as previously, by subtracting the contribution of the silanol groups decomposition (1.5%) to the TG value (10.2%). We obtained 8.7% weight loss, which indicates that the material has 1.48 mmol of propylamine groups/g of MNP@NH_2 material.

Rh/*N*-Xantphos catalyst immobilization

Aiming the reutilization of the Rh catalyst, we pursued this study with the covalent immobilization of Rh-Xantphos type catalyst. *N*-Xantphos (**4.3**) was selected as a functionalized analog of the Xantphos ligand, used as model in the homogeneous catalytic studies. So, *N*-Xantphos was reacted with sodium hydride in dry DME, at 80 °C, under inert atmosphere, for 2 hours. After that period, the previously prepared MNP@Cl was added, and the mixture was kept, under stirring, for 12 hours. Then, the obtained solid was washed with DME (3x) to remove the unreacted *N*-Xantphos. Finally, $[Rh(CO)_2(acac)]$ and fresh DME were added and the mixture was stirred for further 6 hours. After solvent removal, the solid was again washed with DME (3x), to remove the unreacted rhodium salt, and dried under vacuum. All reactions and manipulations were performed under inert atmosphere (Scheme 4.5).

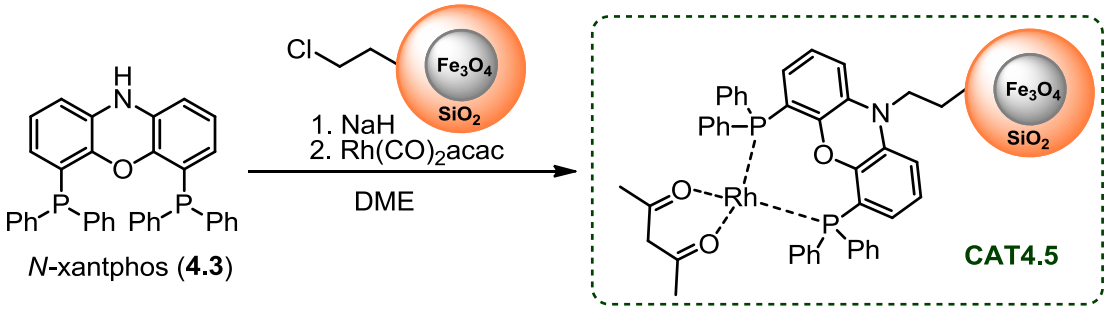

Scheme 4.5 Preparation of Rh-immobilized catalyst **CAT4.5**.

The resulting material was analyzed by thermogravimetry (Figure 4.10), and inductively coupled plasma optical emission spectrometry (ICP-OES) analysis.

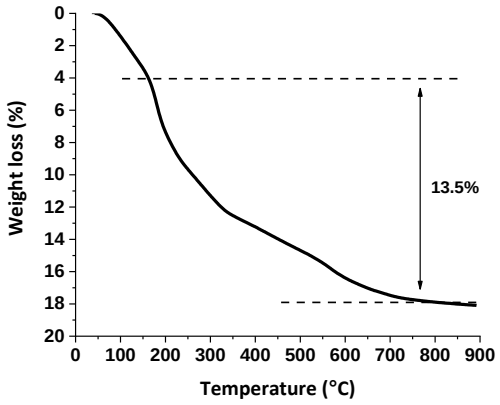

Figure 4.11 TG curve of **CAT4.5**

The thermogram of **CAT4.5** (Figure 4.11), presents a weight loss of 13.5% between 200 °C and 800 °C. The 6.8% weight loss is attributed to *N*-Xantphos ligand degradation, corresponding to approximately 0.12 mmol of organic matter for each gram of solid material, calculated as described before. Additionally, ICP-OES analysis corroborated the presence of Rh, in 0.061 mmol Rh per gram of solid material, suggesting that only 50% of the immobilized *N*-Xantphos ligand is complexed with Rh metal.

Fe-*C*-scorpionate catalyst immobilization

In order to promote the covalent immobilization of the Fe(II)/*C*-scorpionate type ligands onto aminated nanoparticles (MNP@NH_2), we used the hydroaminomethylation strategy, previously described in Chapter 3. The synthesis started with the linkage of an allyl group onto $HC(pz)_3$ ligand **4.2**, followed by complexation with $FeBr_2$ (Scheme 4.6).

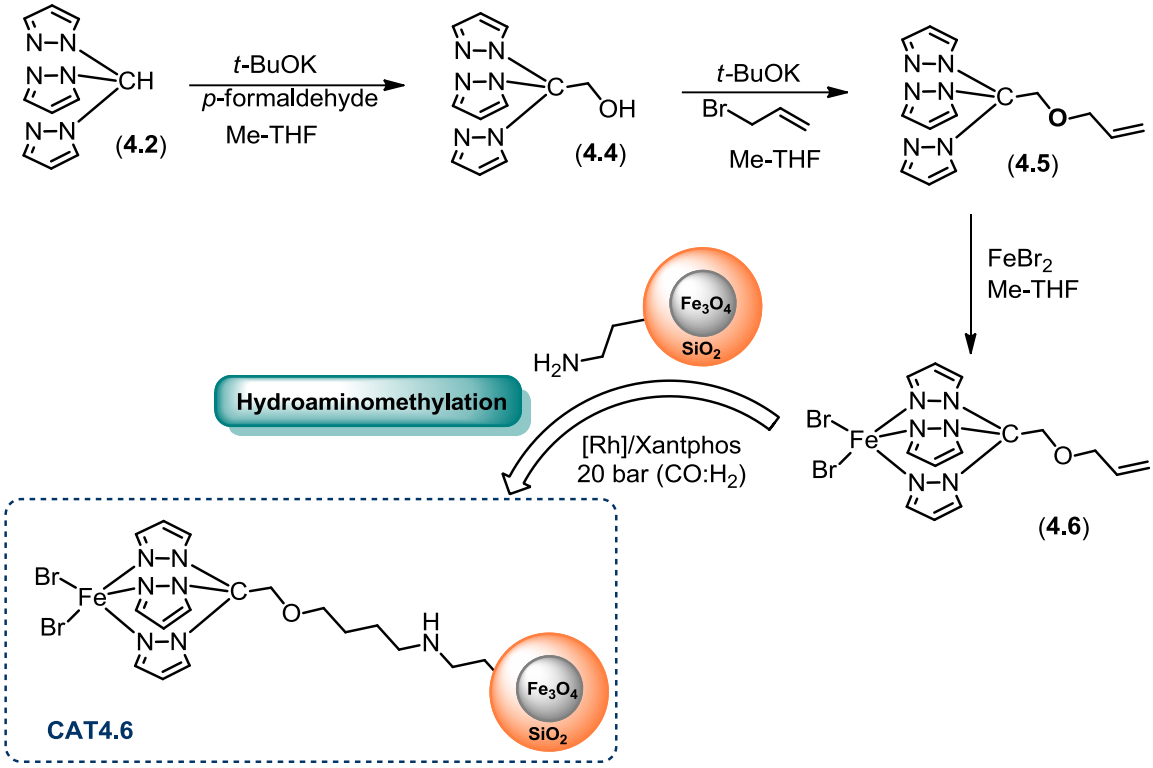

Scheme 4.6 Preparation of [$FeBr_2${$HC(pz)_3$}]-immobilized catalyst **CAT4.6** *via* hydroaminomethylation reaction.

First, ligand **4.2** reacted with *p*-formaldehyde under basic conditions to obtain *tris*-2,2,2-(1-pyrazoyl)ethanol ($HOCH_2C(pz)_3$, **4.4**).[16] After purification, this compound was mixed with allyl bromide, under basic conditions, using Me-THF as a green solvent.[21] After 12 hours, quantitative amounts of *tris*-2,2,2-(1-pyrazoyl)ethoxyallyl (**4.5**) were obtained. The compound was characterized through ^1H, ^{13}C-NMR spectrometry and HRMS (Figures 4.12-4.14).

The ^1H-NMR spectrum (Figure 4.12) shows three signals (δ = 7.65, 7.42 and 6.33 ppm) assigned to the three pyrazole protons ($H_{3'}$-$H_{5'}$). The multiplet signals at δ = 5.84-5.74 ppm and δ = 5.23-5.18 were assigned to $H_{2'}$ and $H_{3'}$ protons from the vinyl group, respectively. The singlet signal at δ = 5.09 ppm was assigned to the two H_1 protons. Finally, the doublet at δ = 3.98 ppm was assigned to the $H_{1'}$ proton. The ^{13}C-NMR spectrum is presented in Figure 4.13. We observed the presence of signals at δ = 141.3, 130.9 and 106.5 ppm, assigned to the pyrazole carbons ($C_{3''}$-$C_{5''}$). We can also observe two signals at δ = 133.7 ppm and δ = 118.0 ppm assigned to vinyl group carbons ($C_{2'}$, $C_{3'}$). The carbon C_2 was assigned to the δ = 89.9 ppm signal. Finally, the signals δ = 73.2 and δ = 73.21 ppm were assigned to C_1 and $C_{1'}$ carbons.

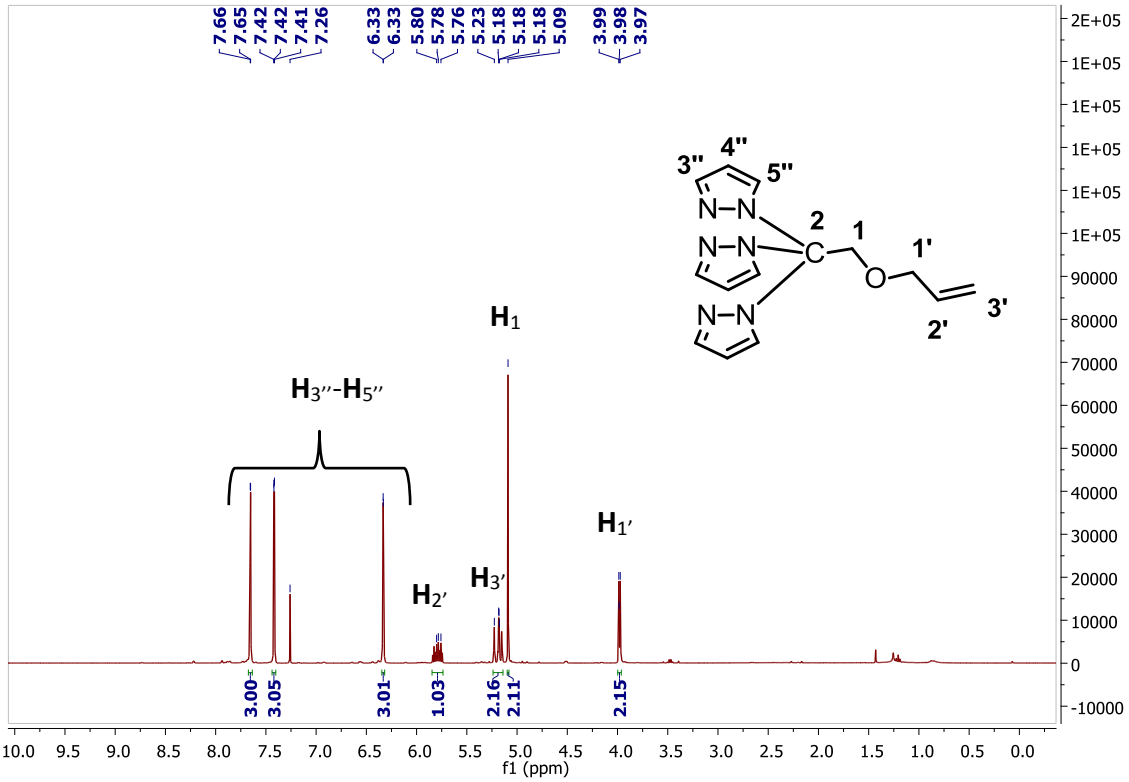

Figure 4.12 ^{1}H-NMR (400 MHz) spectrum of compound (**4.5**) using $CDCl_3$ as solvent.

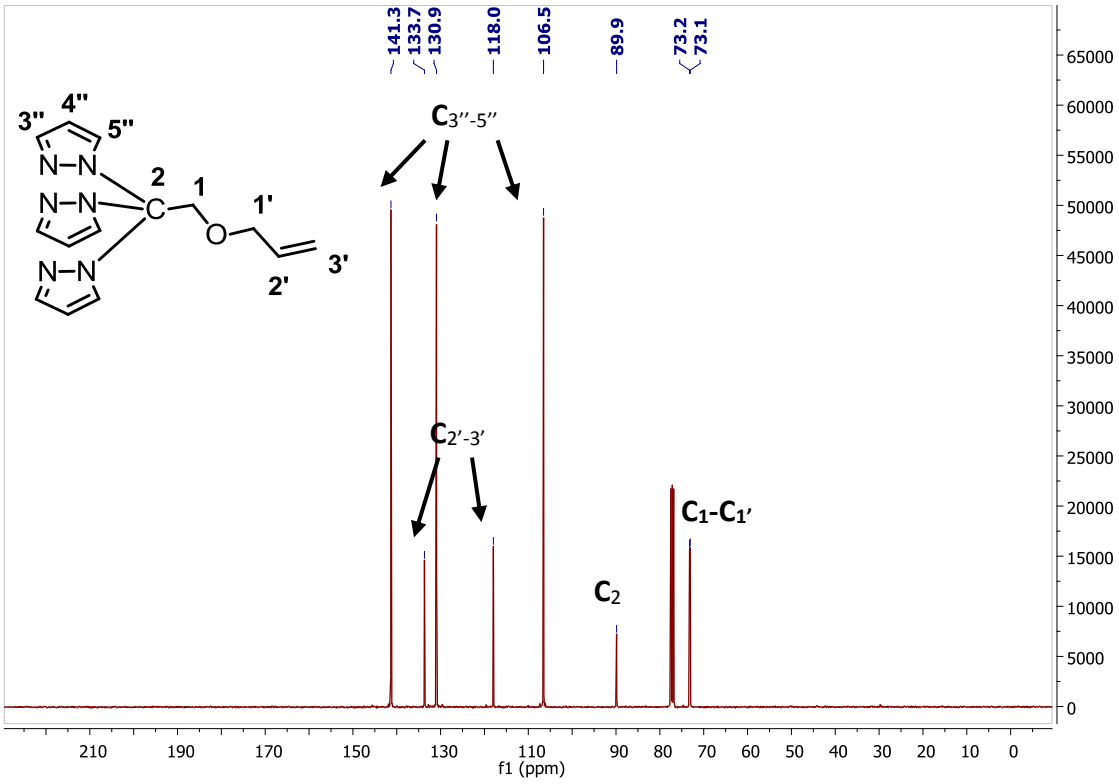

Figure 4.13 ^{13}C-NMR (100 MHz) spectrum of compound (**4.5**) using $CDCl_3$ as solvent.

The compound **4.5** was also analyzed through HRMS-ESI and for the theoretical *m/z* of $C_{13}H_{16}N_6NaO^+$ $[M+Na]^+$: 307.1279 a peak with m/z = 307.1278 was found (Figure 4.14).

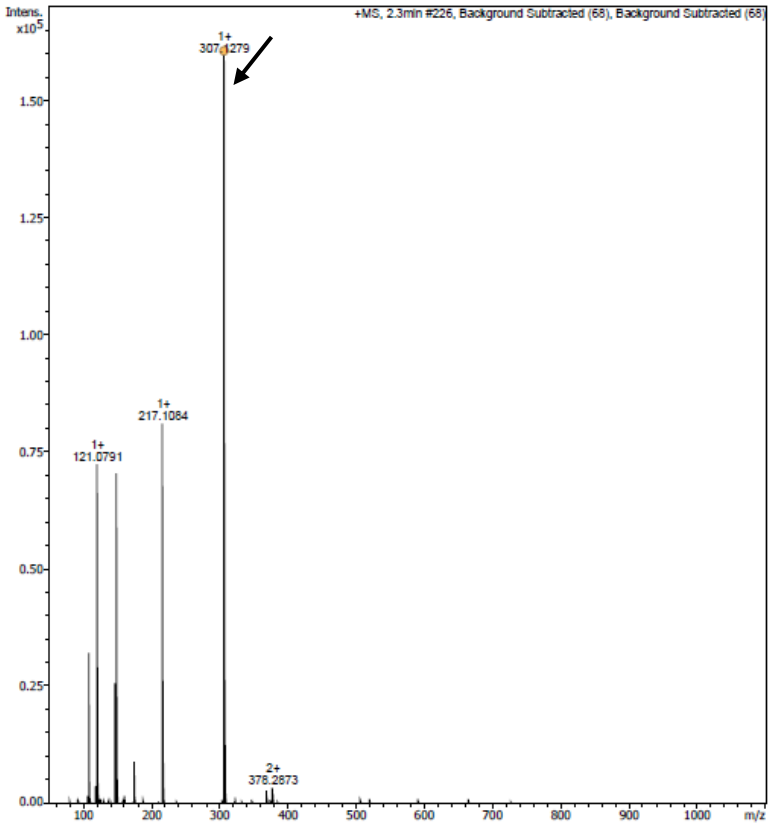

Figure 4.14 HRMS-ESI spectrum of compound (**4.5**).

Then, the complexation with iron (II) bromide was performed accordingly to the above-described method for **CAT4.1**, yielding 95% of $[FeBr_2\{allyl\text{-}HC(pz)_3\}]$ (**4.6**). HRMS analysis all confirmed the obtention of this complex (Chapter 5). Finally, complex **4.6**, $[Rh(CO)_2(acac)]$, Xantphos, the aminated magnetic nanoparticles (MNP@NH_2 containing 1.48 mmol NH_2/g material) and anisole as green solvent, were introduced in a stainless-steel high-pressure autoclave, under inert atmosphere. The reactor was then pressurized with 30 bar (CO/H_2, 1:1), and kept at 65 °C, for 48 hours, with vigorous magnetic stirring at constant pressure. The reactor was then charged with H_2 (P = 30 bar), at 65 °C, for 4 additional hours, after which, it was cooled to room temperature and depressurized. To remove non-immobilized catalyst and residual Rh complex, the obtained **CAT4.6** material was isolated from the reaction medium by the simple application of an external magnet as observed in Figure 4.15.

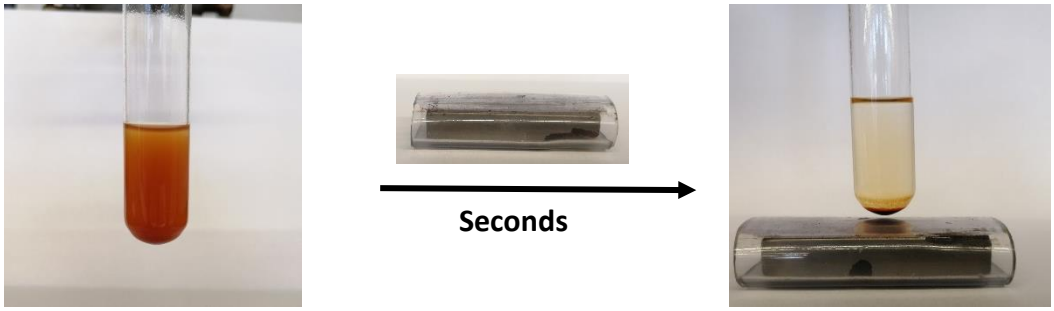

Figure 4.15 Magnetic separation of **CAT4.6** from the reaction medium.

After solvent decantation, the solid was washed several times with anisole, CH_3CN and CH_2Cl_2, and dried under vacuum. The resulting material was analyzed by thermogravimetry and ICP-OES. Thermogravimetric analysis of **CAT4.6** (Figure 4.16) revealed a weight loss of 14% in the range of 200 °C and 800 °C, which was attributed to the degradation of organic material. Once again, the amount immobilized organic material was calculated by subtracting the amount of organic matter present in MNP@NH_2 (10.2%); therefore, a 3.8% weight loss was attributed to the *C*-scorpionate type ligand, which corresponded to approximately 0.13 mmol/g of immobilized Fe/*C*-scorpionate complex in the **CAT4.6** material. Since **CAT4.6** contains iron in the core of the nanoparticle, the amount of immobilized iron complex was calculated through the difference between the molar amount of **4.6** added to the immobilization reaction (2 mmol) and the value of the iron recovered from the **CAT4.6** isolation washing process obtained by ICP-OES analysis (1.89 mmol). The obtained value was 0.12 mmol of iron per gram of material and this was the value used for all heterogeneous catalytic reactions. As expected, the ICP-OES analysis of **CAT4.6** did not show the presence of Rh.

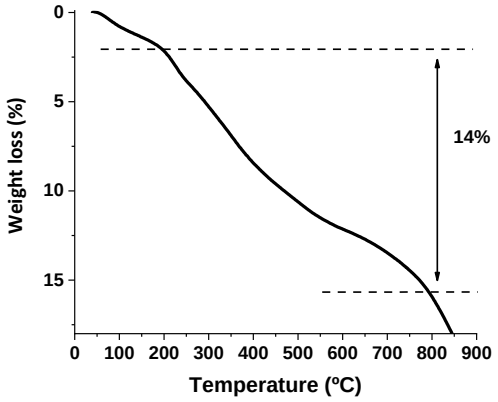

Figure 4.16 TG curve of **CAT4.6**

In sum, in this section, we described the efficient synthesis and characterization of Rh/phosphorus and Fe(II)/*C*-scorpionate catalysts and their immobilization onto iron magnetic nanoparticles. The improvements of sequential hydroformylation/acetalization of olefins using these catalysts under homogeneous and heterogeneous conditions are described in the next section.

4.3 Sequential hydroformylation/acetalization of olefins

4.3.1 Catalytic homogeneous studies

The optimization of the sequential catalytic system was performed using oct-1-ene as model substrate and ethanol as nucleophile, under 20 bar (CO/H_2, 1:1) constant pressure and temperature of 80 °C, along 24 hours, being the results presented in Table 4.1.

Initially, we evaluated the use of $[Rh(CO)_2(acac)]$ as catalyst in the sequential hydroformylation/acetalization of oct-1-ene, and near-complete olefin conversion (93%) was observed by GC after 24 hours. Nevertheless, very low chemoselectivity for aldehydes (19%) and acetals (21%) was also detected, with the main products being internal isomers (60%) (Table 4.1, Entry 1). Then, we evaluated the effect of the addition of ligand $HC(pz)_3$ (**4.2**) to the system containing $[Rh(CO)_2(acac)]$ (Rh/**4.2** =1:2.5) and again 95% conversion was obtained, but in this case with higher chemoselectivity for aldehydes (20%) and acetals (34%), and lower amount of isomeric products (46%) (Table 4.1, Entry 2). To our knowledge, this is the first example where a *C*-scorpionate-type ligand is used in rhodium-catalyzed hydroformylation/acetalization sequential processes. Additionally, the use of the bimetallic combination based on $[Rh(CO)_2(acac)]$ with $[FeBr_2\{\kappa^3\text{-}HC(pz)_3\}]$ (**CAT4.1**) provided full conversion of oct-1-ene, with higher selectivity for oxo products, including 47% acetal chemoselectivity, with concomitant isomerization decrease (36%). These results clearly evidence the beneficial effect of $[FeBr_2\{\kappa^3\text{-}HC(pz)_3\}]$ (**CAT4.1**) as a promising sustainable catalyst to enable the direct one-pot transformation of olefins toward acetals (Table 1, Entry 3).

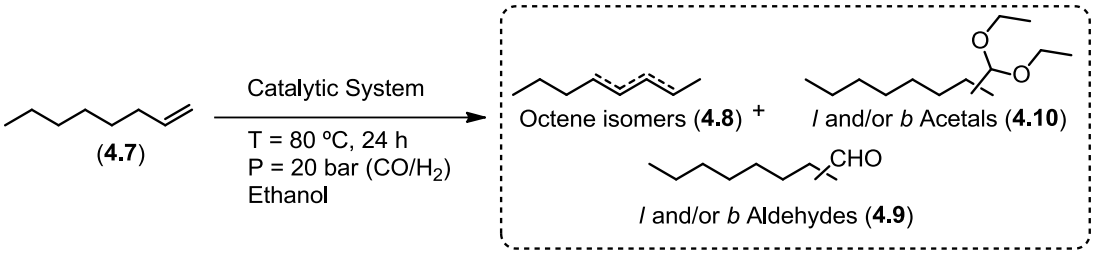

CAT4.1 = $[FeBr_2(HC(pz)_3)]$
CAT4.2 = [Rh]/xantphos
CAT4.3 = $[Rh]/PPh_3$
CAT4.4 = [Rh]/*tris*[2'-(benzyloxy)-1,1'-binaphthyl-2-yl] phosphite

Table 4.1 Optimization studies of the sequential hydroformylation/acetalization of oct-1-ene.[a]

Entry	Substrate	Catalytic system	Conv. [%][b]	Selectivity [%][b] (*l*:*b*)		
				4.8	4.9	4.10
1	Oct-1-ene	$[Rh(CO)_2(acac)]$	93	60	19 (23:77)	21 (38:62)
2	Oct-1-ene	$[Rh(CO)_2(acac)]$ $HC(pz)_3$ (**4.2**)	95	46	20 (18:82)	34 (44:56)
3	Oct-1-ene	$[Rh(CO)_2(acac)]$ **CAT4.1**	99	36	17 (27:73)	47 (61:49)
4	Oct-1-ene	**CAT4.2** **CAT4.1**	99	3	15 (80:20)	82 (93:7)
5	Oct-1-ene	**CAT4.3** **CAT4.1**	98	1	12 (24:76)	87 (66:34)
6	Oct-1-ene	**CAT4.4** **CAT4.1**	99	-	9 (32:68)	91 (69:31)
7	Oct-1-ene	**CAT4.1**	1	-	-	-
8	Nonanal	**CAT4.1**	95	-	-	100 (100:0)
9	Nonanal	$HC(pz)_3$ (**4.2**)	38	-	-	94 (100:0)[b]
10	Nonanal	$FeBr_2$	44	-	-	100 (100:0)

a) Reaction conditions: olefin 3.00 mmol, $[Rh(CO)_2(acac)]$ 0.02 mmol, P-ligand (**CAT4.2**: 0.05 mmol, **CAT4.3**: 0.10 mmol, **CAT4.4:** 0.10 mmol), **CAT4.1** (0.05 mmol) or (**4.2**) 0.05 mmol, ethanol (6 mL), 20 bar CO/H_2 (1:1) at 80 °C for 24 h. b) Determined by GC-FID analysis using isooctane as an external standard.

Next, to avoid initial isomerization and enhance the rate of aldehyde formation, we evaluated the use of the same Rh/Fe bimetallic system but using a Rh/P modified catalyst (P = Xantphos, the bulky tris[2'-(benzyloxy)-1,1'-binaphthyl-2-yl] phosphite and PPh_3; Scheme 4.3) and the results are presented in Table 4.1 (Entries 4-6). These results demonstrated that the combination of $[Rh(CO)_2(acac)]$/Xantphos (**CAT4.2**) with the *C*-scorpionate type $[FeBr_2\{\kappa^3\text{-}HC(pz)_3\}]$ (**CAT4.1**) produced the most active (99% conversion) and selective system, with 82% chemoselectivity for acetals and 93% regioselectivity for the linear isomer, as expected for phosphines with large bite angle like Xantphos (111°)[22, 23] (Table 4.1, Entry 4). Additionally, the catalytic system using triphenylphosphine as Rh/P-ligand system (**CAT4.3)**, gave 98% conversion, 87% acetal chemoselectivity but, as expected, with only 66% of regioselectivity for linear acetals (Table 4.1, Entry 5). Moreover, the combination of $[Rh(CO)_2(acac)]$/bulky phosphite (**CAT4.4)** with $[FeBr_2\{\kappa^3\text{-}HC(pz)_3\}]$ (**CAT4.1**) led to an active hydroformylation/acetalization system (99% conversion), with high chemoselectivity for acetals (91%), but lower regioselectivity for the linear isomer (69%) (Table 4.1, Entry 6). This outcome may be attributed to the concomitant hydroformylation of internal double bonds, typical of this Rh/bulky phosphite system.[24]

These results confirm the versatility of the Rh/P-ligand-Fe(II)/*C*-scorpionate bimetallic system to promote the direct transformation of olefins onto value-added acetals with chemo and regioselectivity modulated by the phosphorous ligands, always with high oxo-product selectivity. Additionally, we evaluated the activity of the Fe(II)/*C*-scorpionate catalyst (**CAT4.1**) in the hydroformylation reaction of oct-1-ene and in the direct acetalization of nonanal (Table 4.1, Entries 7-8). Regarding the exclusive use of **CAT4.1** in the hydroformylation reaction no conversion was observed (Table 4.1, Entry 7). Conversely, **CAT4.1** demonstrated to be an active Lewis acid catalyst to promote the acetalization of nonanal (95% acetal; Table 4.1, Entry 8). Furthermore, we also evaluated the catalytic effect of *C*-scorpionate ligand (**4.2**) and $FeBr_2$ in the acetalization of nonanal with ethanol and only 38% and 44% conversion was obtained, respectively (Table 4.1, entries 9 and 10)

In order to illustrate the reaction progress of the sequential hydroformylation/acetalization process using the bimetallic **CAT4.2**/**CAT4.1** system, aliquots were taken from the reactional mixture, at regular intervals, along 24 hours and

the results are plotted in Figure 4.17. From the analysis of this Figure, we observed that nearly 75% olefin conversion was achieved after just 1 hour (51% selectivity for aldehydes and 20% for acetals). As expected, after this period, the yield of aldehydes started to decrease with a concomitant increase of acetal formation. After this period, the kinetic profile of the bimetallic catalytic system shows that both, the hydroformylation (**k1**) and acetalization (**k2**) rates decrease over time, suggesting that the hydroformylation rate is dependent from olefin concentration and the acetal formation is dependent from aldehyde concentration. After 24 hours, 99% of oct-1-ene conversion was observed, 79% acetals, still 16% of non-converted aldehydes and just 4% of oct-1-ene isomers, constant along the experiment (Figure 4.17).

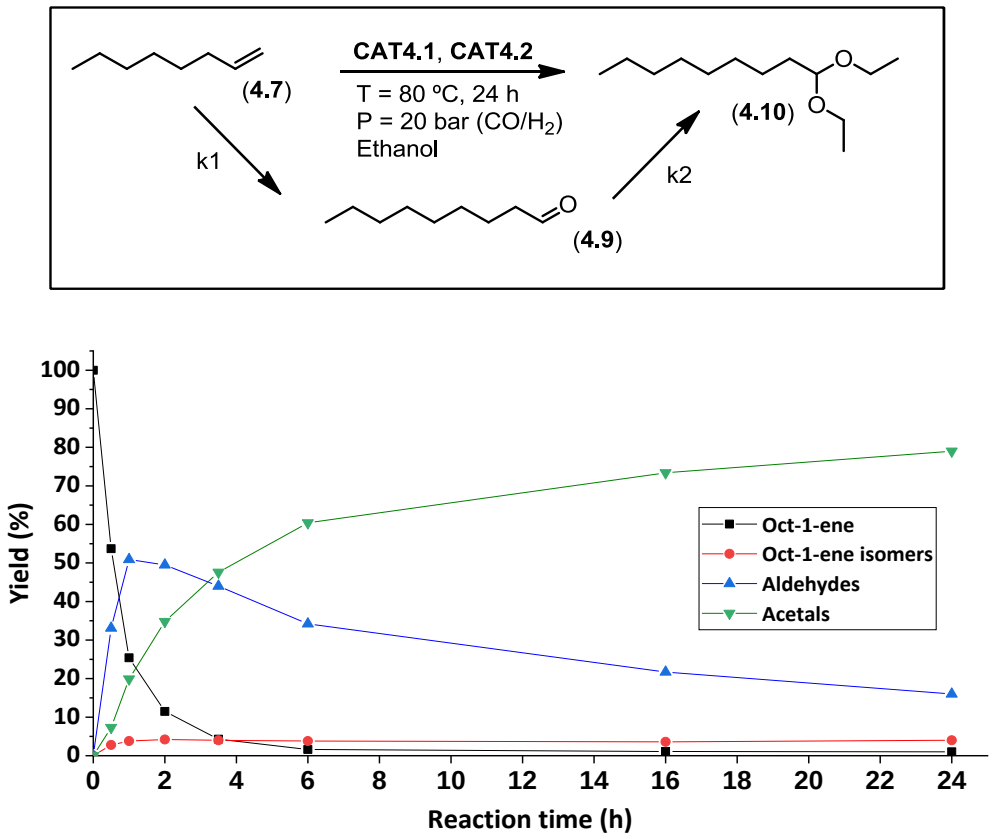

Figure 4.17 Reaction progress of hydroformylation/acetalization of oct-1-ene: Substrate and product yield *vs.* reaction time. Reaction conditions: oct-1-ene 6.00 mmol, **CAT4.2** 0.04 mmol, **CAT4.1** 0.10 mmol, ethanol 12 mL; P = 20 bar (CO/H_2); T = 80 °C. Yield determined by GC analysis of aliquots from the crude reaction using isooctane as an external standard.

Scheme 4.7 illustrates the simplified mechanisms pathways for the synthesis of acetals from terminal olefins.[25-27] As previously stated, Rh(I)/Xantphos complexes are

able to promote the regioselective formation of linear aldehydes under hydroformylation conditions. Then, the formed linear aldehydes in the presence of ethanol, when activated with a Lewis acid type catalyst (such as **CAT4.1**), promotes the direct transformation of oct-1-ene onto ethyl acetal. The first step comprises carbonyl activation by the iron catalyst, forming the intermediate **A**. Then, a nucleophilic attack by ethanol occurs yielding the hemiacetal **B**, which undergoes a consecutive nucleophilic attack of another ethanol molecule that, after dehydration releases the acetal product **C**.

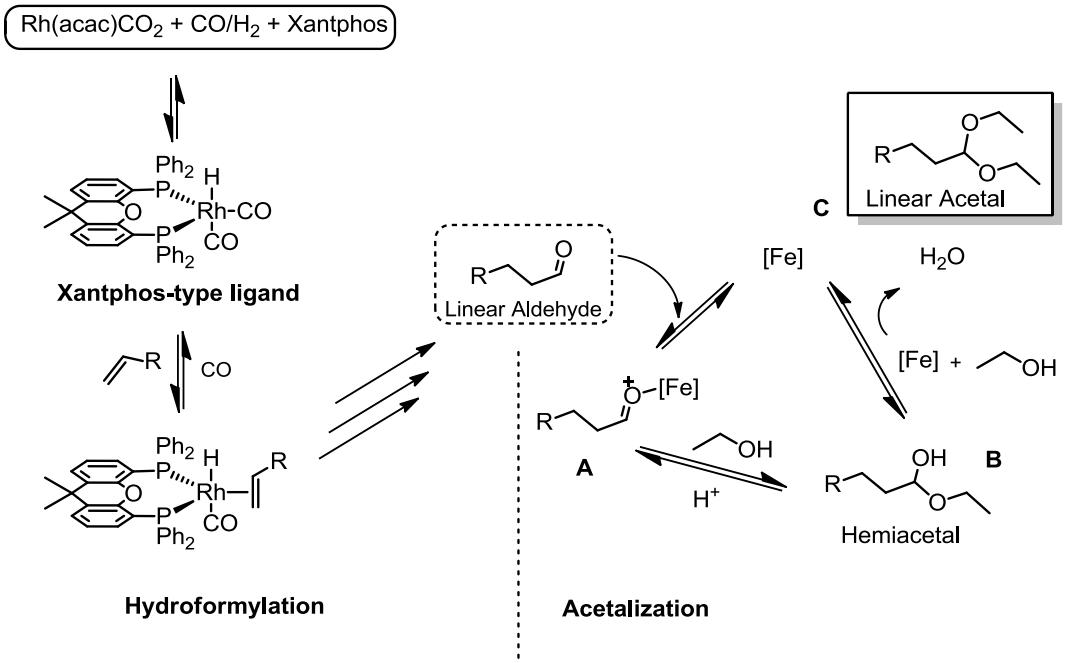

Scheme 4.7 Proposed simplified mechanisms for hydroformylation/acetalization of olefins with **CAT4.2** ([$Rh(CO)_2(acac)$]/Xantphos) and **CAT4.1** ([$FeBr_2\{\kappa^3HC(pz)_3\}$], here represented by [Fe]).

Then, the synergic effect of the combination of phosphorous based hydroformylation catalysts (**CAT4.2** or **CAT4.3)** with iron(II)-*C*-scorpionate based acetalization catalyst (**CAT4.1**) in the sequential hydroformylation/acetalization process, was further evaluated. The one-pot transformation of mono, di, and tetrasubstituted olefins into acetals, using ethanol, simultaneously as a renewable solvent and acetalization reactant, at 20 bar ($CO:H_2$) pressure and temperature of 80 °C was achieved. Since the activity and selectivity of hydroformylation reaction are strongly dependent on olefin and phosphorus ligands structure, we selected Rh/Xantphos (**CAT4.2)** to promote the hydroformylation of terminal olefins, with well-known high regioselectivity for terminal aldehydes,[28, 23] and

Rh/ tris[2'-(benzyloxy)-1,1'-binaphthyl-2-yl] phosphite (**CAT4.3**) a known catalyst for hydroformylation of highly substituted olefins.[29-31, 24] The results are presented in Table 4.2.

Table 4.2 Hydroformylation/Acetalization of several olefins using the combination of Rh/P-ligand and Fe/C-scorpionate catalysts.

Entry	Olefin	Reaction Yield [%][a]	
		Major Product (isolated yield)	Minor Products
1[b]	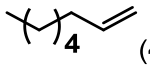 (**4.7**)	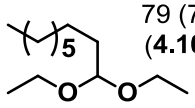 79 (70) (**4.10*l***)	Oct-1-ene isomers: 4 Aldehydes: 11 Branched Acetal: 6
2[b]	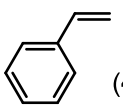 (**4.11**)	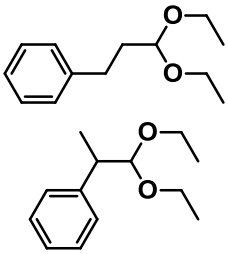 54 (41) (**4.12*l***) 36 (**4.12*b***)	Aldehydes: 10
3[c]	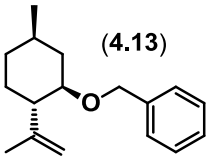 (**4.13**)	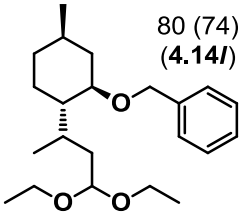 80 (74) (**4.14*l***)	Aldehydes: 20
4[c]	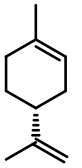 (**4.15**)	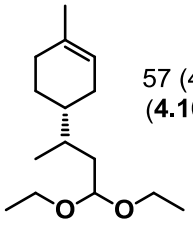 57 (40) (**4.16*l***)	Difunctionalized Acetal (isomers): 33
5[c]	 (**4.17**)	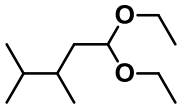 87 (76) (**4.18*l***)	Aldehyde: 13

a) Obtained by GC-MS analysis, conversions were ≥ 99% for all substrates. b) Reaction conditions: olefin 3.00 mmol, **CAT4.2** 0.02 mmol, **CAT4.1** 0.05 mmol, alcohol 6 mL, 80 °C, 20 bar CO/H_2 (1:1) for 24 h, c) Reaction conditions: olefin 1.50 mmol, **CAT4.4** 0.01 mmol, **CAT4.1** 0.05 mmol, ethanol 5 mL, 80 °C, 20 bar CO/H_2 (1:1) for 24 h.

It is worth mentioning that the bimetallic system Rh/Xantphos (**CAT4.2**) combined with [$FeBr_2\{\kappa^3$-$HC(pz)_3\}$] (**CAT4.1**) led to the direct transformation of mono-substituted oct-1-ene (**4.7**) and styrene (**4.11**) substrates into the corresponding acetals in 85% and 90% yields, and regioselectivities for linear acetals of 93% and 60%, respectively (Table 2, Entries 1 and 2). In addition, the replacement of Xantphos by the bulky tris[2'-(benzyloxy)-1,1'-binaphthyl-2-yl] phosphite (**CAT4.3**), allowed the direct transformation of di and tri-substituted olefins of terpenes ((-)-isopulegol benzyl ether derivative (**4.13**) and (+)-limonene(**4.15**)) into the corresponding acetals in 80% and 90% yields, respectively (Table 2, Entries 3-4). It should be mentioned that this is the first catalytic system that allows the formation of acetals derived from both, di and trisubstituted limonene double bonds using quite moderate reaction conditions. This result discloses the high activity of **CAT4.3** to promote the hydroformylation of highly substituted olefins when compared with Gusevskaya work, where only the terminal exocyclic limonene double bond was converted onto acetal, even using harsher reaction conditions (80 bar of CO/H_2 and 80 °C).[32] Finally, this system was able to transform even the tetrasubstituted olefin 2,3-dimethyl-2-butene (**4.17**) into the corresponding terminal acetal in 87% yield (Table 2, Entry 5), which is a relevant result for the potential valorization of the butadiene industrial mixture.[33] Major reaction products were isolated and purified and characterized by ^{1}H-NMR and mass spectrometry. (characterization data presented in Chapter 5).

These results demonstrate the versatility and potential application of these bimetallic tandem hydroformylation/acetalization catalytic systems for the direct transformation of a broad range of olefins onto high-value products. Additionally, the use of ethanol, obtained from renewable sources, both as solvent and acetalization reactant, strongly increases the sustainability of the process. Therefore, to achieve our overall goal of developing an active, selective and reusable bimetallic catalytic system we pursue the studies with the evaluation of the **CAT4.5** and **CAT4.6** (**CAT4.2** and **CAT4.1** heterogeneous counterparts) in the sequential hydroformylation/acetalization of oct-1-ene, and the results are presented in the following sections.

4.3.2 Catalytic heterogeneous studies

Before performing the sequential catalytic studies under heterogeneous conditions, the catalytic activity of **CAT4.5** in hydroformylation reaction and **CAT4.6** in acetalization were separately evaluated. In a typical experiment, heterogeneous catalysts **CAT4.5** and/or **CAT4.6** were weighed into a high-pressure autoclave, and kept with 30 bar (CO/H_2) 2 hours at 80 °C. Then, after oct-1-ene addition, the reactor was pressurized with 20 bar of CO/H_2 gas (1:1) and heated to 80 °C with magnetic stirring. After 24 hours, a sample of the reaction crude was diluted with ethanol and analyzed by gas chromatography using isooctane as an external standard. All the operations were performed under inert atmosphere.

Table 4.3 Catalytic optimization for heterogeneous hydroformylation/acetalization.[a]

Entry	Substrate	Catalyst	Conv. [%][b]	Selectivity [%][b] (*l:b*)		
				Oct-1-ene Isomers	Aldehydes	Acetals
1[c]	Oct-1-ene	**CAT4.5**	99	3	96 (98:2)	-
2[d]	Nonan-1-al	**CAT4.6**	90	-	10 (-)	90 (100:0)
3[c,d]	Oct-1-ene	**CAT4.5** **CAT4.6**	92	54	38 (75:25)	-
4[e]	Reaction crude of entry 1	**CAT4.6**	90	2	10 (98:2)	88 (99:1)

a) Reaction conditions: ethanol 6 mL, 80 °C, 20 bar CO/H_2 (1:1) for 24 h Substrate 3.00 mmol b) Obtained by GC-FID analysis. c) Substrate 3.00 mmol, **CAT4.5** 180 mg (≈ 0.02 mmol [Rh]) d) Substrate 3.00 mmol, **CAT4.6** 300 mg (≈ 0.04 mmol [Fe]) e) In absence of gas (CO/H_2).

The immobilized Rh(I)/*N*-Xantphos **CAT4.5** revealed to be very active and selective, reaching 99% conversion, 96% chemoselectivity for aldehydes and 98% regioselectivity for the linear aldehyde (Table 4.3, Entry 1). Next, we evaluated **CAT4.6** in the acetalization of nonanal using ethanol, under hydroformylation conditions, and 1,1-diethoxynonane (**4.10**) was obtained in 90% yield (Table 4.3, Entry 2). Then, the combination of **CAT4.5** and **CAT4.6** was tested, by mixing them in the autoclave and using the general procedure described above. Under these experimental conditions, we obtained 92% of conversion,

54% of oct-1-ene isomers and just 38% of aldehydes. Thus, the simultaneous use of **CAT4.5** and **CAT4.6** led to a significant loss of chemoselectivity, concomitantly with no transformation into the desired acetal (Table 4.3 Entry 3). Contrarily, when we used **CAT4.5** exclusively in the hydroformylation step and removed it from the reaction medium after 24 hours (crude contained 96% of aldehydes; Table 4.3 Entry 1), the addition of **CAT4.6** led to the formation of 87% acetals (Table 4.3, Entry 4). These results indicate that both **CAT4.5** and **CAT4.6** are active and selective for the hydroformylation/acetalization reactions, when reactions are performed in two sequential independent steps as shown in Figure 4.18.

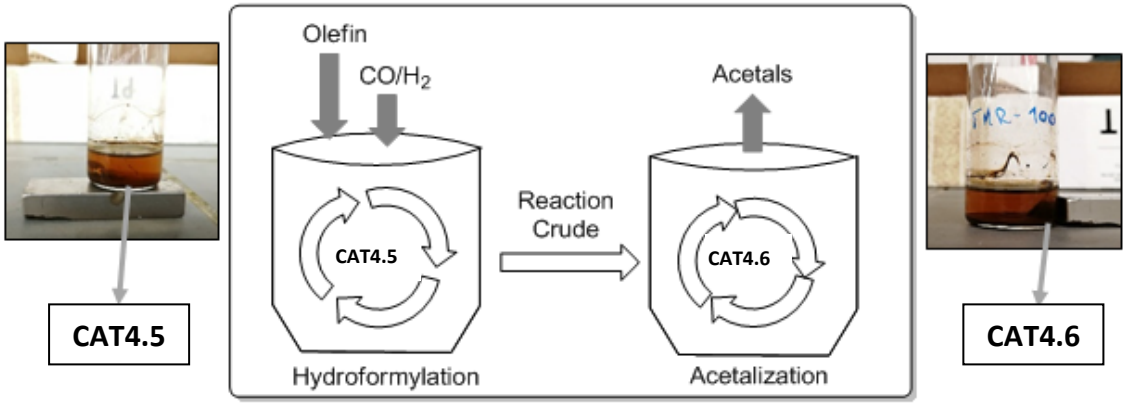

Figure 4.18 Two-step sequential system for hydroformylation/acetalization of olefins with reutilization of the catalysts through magnetic separation.

Then, pursuing our general goal of reutilization of both catalysts, we first separated **CAT4.5** from the hydroformylation crude and kept it under inert atmosphere. The reaction crude was transferred to the autoclave containing the appropriate amount of **CAT4.6** and the acetalization reaction was performed under inert atmosphere, at 80 °C. After 24 hours, the reactor was opened and the **CAT4.6** was removed with aid of an external magnet, then **CAT4.6** was kept under inert atmosphere. Both catalysts were reused in four experiments and no significant loss of activity or selectivity was observed, Figure 4.19.

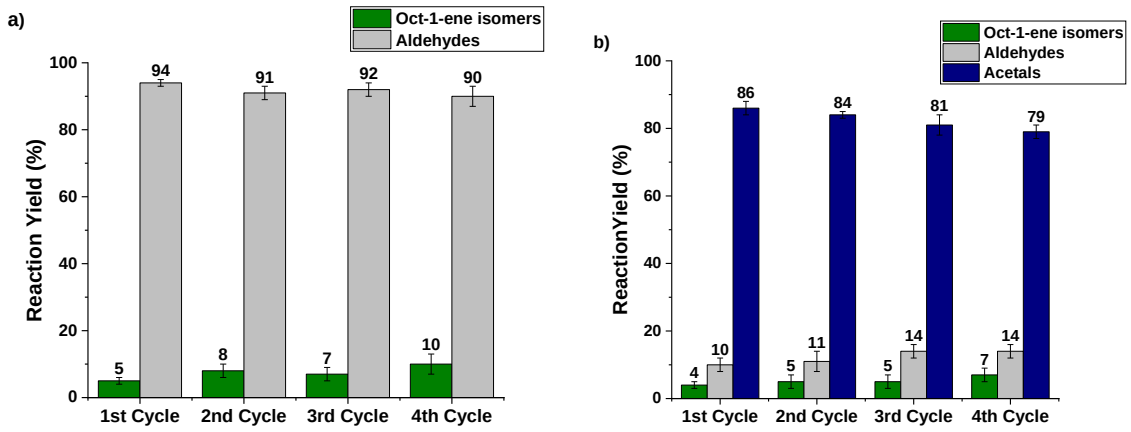

Figure 4.19 Two-step hydroformylation/acetalization of oct-1-ene, reutilization test. a) Hydroformylation step: 3 mmol oct-1-ene, **CAT4.5** 180 mg (≈ 0.02 mmol [Rh]), 6 mL ethanol at 80 °C, 20 bar ($CO:H_2$) for 24 hours. b) Reaction crude of the hydroformylation step, **CAT4.6** 300 mg (≈ 0.04 mmol [Fe]) at 80 °C for 20 hours.

Additionally, we have been able to find an alternative process for reutilization of **CAT4.1**, without the need of its immobilization onto magnetic nanoparticles. In a typical reaction, after the hydroformylation step using **CAT4.5** followed by their removal with an external magnet as described above, we added **CAT4.1** to the reaction crude. After 24 hours 93% conversion into the desired acetals was observed. Then, **CAT4.1** was recovered by precipitation from the reaction medium by lowering the temperature to 0 °C with an ice water bath (Figure 4.20).

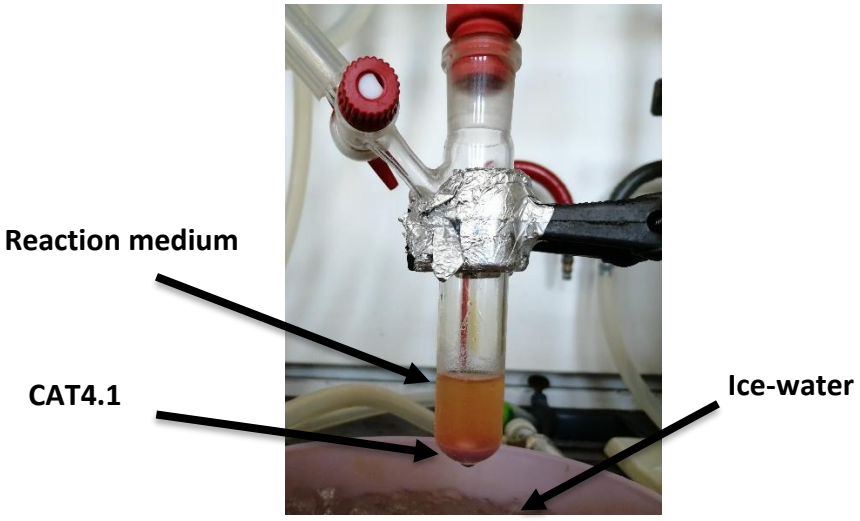

Figure 4.20 Precipitation of **CAT4.1** from the reaction medium at 0 °C (ethanol as solvent).

After decantation, the catalyst was kept under inert atmosphere. This process was repeated along four cycles and the obtained catalyst activity and selectivity were very similar to the results previously observed for approximately 90% conversion for the hydroformylation (step same **CAT4.5** catalyst) and 93 to 88 % acetal yields over the 4 cycles (Figure 4.21), against the 86 to 79% obtained with **CAT4.6**. This improvement increases the sustainability of the processes, where the non-immobilized and air-stable Fe(II)/*C*-scorpionate catalyst **CAT4.1** was recovered and reused by simple precipitation, upon temperature lowering.

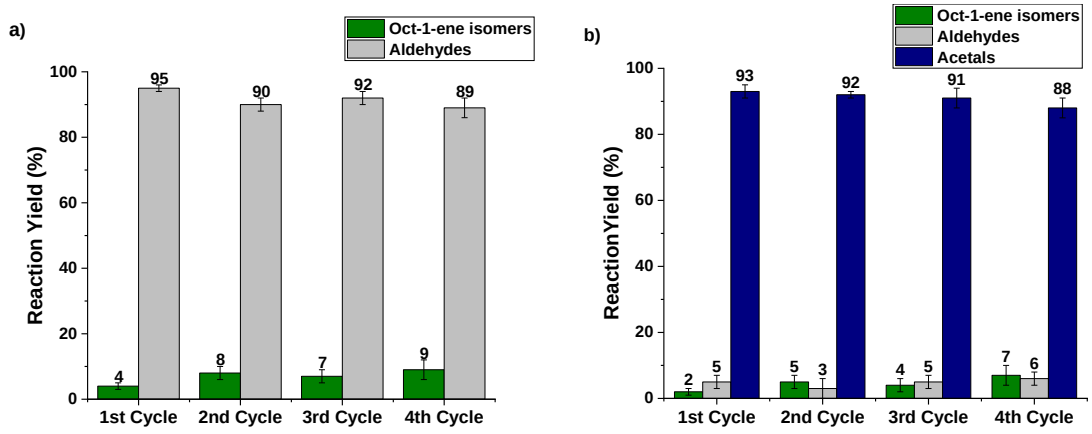

Figure 4.21. Two-step hydroformylation/acetalization of oct-1-ene, reutilization test. a) Hydroformylation step: 3 mmol oct-1-ene, **CAT4.5** 180 mg (≈ 0.02 mmol [Rh]), 6 mL ethanol at 80 °C, 20 bar ($CO:H_2$) for 24 hours. b) Reaction crude of the hydroformylation step, **CAT4.1** 18 mg (≈ 0.04 mmol [Fe]) at 80 °C for 20 hours.

4.4 Conclusion

The studies described in this chapter allowed the development of an active and selective tandem catalytic system to promote the direct transformation of olefin onto ethyl acetals using Rh(I)/P– Fe(II)/*C*-scorpionate catalysts. This study describes, for the first time, the efficient combination of Rh(I)/phosphorous catalysts with Fe(II)/*C*-scorpionates to promote the direct transformation of terminal and highly substituted olefins onto acetals. The high activity of (Rh/phosphite) allowed the preparation of limonene acetal derivatives, both at the internal and external double bonds. We also developed an efficient method to immobilize allyl functionalized *C*-scorpionates onto amine-functionalized magnetic nanoparticles through the use of hydroaminomethylation. The sequential process, using the immobilized catalysts, maintains its high activity and selectivity. Moreover, the system sustainability is largely improved by the easy magnetic separation/reutilization of Rh(I)/P and Fe(II)/*C*-scorpionate immobilized catalysts, which keep their activity/selectivity for more than four consecutive cycles. Additionally, it was found that [$FeBr_2\{\kappa^3$-$HC(pz)_3\}$] complex can be recovered from the reaction medium and reused over four cycles without loss of activity and selectivity.

In sum, this study opens the way for the preparation of multi-functionalized acetals directly from olefins using reusable Rh(I)/P and Fe(II)/*C*-scorpionate catalysts, under moderate reaction conditions.

4.5 References

[1] B. P. Bondžić, *J. Mol. Catal. A: Chem.* "Rh catalyzed multicomponent tandem and one-pot reactions under hydroformylation conditions" **2015**, *408*, 310-334.

[2] Y.-Q. Li, P. Wang, H. Liu, Y. Lu, X.-L. Zhao, Y. Liu, *Green Chem.* "Co-catalysis of a bi-functional ligand containing phosphine and Lewis acidic phosphonium for hydroformylation–acetalization of olefins" **2016**, *18*, 1798-1806.

[3] P. Kalck, M. Urrutigoity, *Rhodium Catalysis* "Tandem Rhodium Carbonylation Reactions" **2018**, *61*, 69-98.

[4] H. Liu, L. Liu, W.-D. Guo, Y. Lu, X.-L. Zhao, Y. Liu, *J. Catal.* "Phosphine-ligated Ir(III)-complex as a bi-functional catalyst for one-pot tandem hydroformylation-acetalization" **2019**, *373*, 215-221.

[5] P. Munnik, P. E. de Jongh, K. P. de Jong, *Chem. Rev.* "Recent Developments in the Synthesis of Supported Catalysts" **2015**, *115*, 6687-6718.

[6] A. J. Sandee, J. N. H. Reek, P. C. J. Kamer, P. W. N. M. van Leeuwen, *J. Am. Chem. Soc.* "A Silica-Supported, Switchable, and Recyclable Hydroformylation−Hydrogenation Catalyst" **2001**, *123*, 8468-8476.

[7] S. Ricken, P. W. Osinski, P. Eilbracht, R. Haag, *J. Mol. Catal. A: Chem.* "A new approach to dendritic supported NIXANTPHOS-based hydroformylation catalysts" **2006**, *257*, 78-88.

[8] V. Polshettiwar, R. Luque, A. Fihri, H. Zhu, M. Bouhrara, J. M. Basset, *Chem. Rev.* "Magnetically recoverable nanocatalysts" **2011**, *111*, 3036-3075.

[9] M. B. Gawande, P. S. Branco, R. S. Varma, *Chem. Soc. Rev.* "Nano-magnetite (Fe_3O_4) as a support for recyclable catalysts in the development of sustainable methodologies" **2013**, *42*, 3371-3393.

[10] M. N. Shaikh, M. Bououdina, A. A. Jimoh, M. A. Aziz, A. Helal, A. S. Hakeem, Z. H. Yamani, T.-J. Kim, *New J. Chem.* "The rhodium complex of bis(diphenylphosphinomethyl)dopamine-coated magnetic nanoparticles as an efficient and reusable catalyst for hydroformylation of olefins" **2015**, *39*, 7293-7299.

[11] J. Kudr, Y. Haddad, L. Richtera, Z. Heger, M. Cernak, V. Adam, O. Zitka, *Nanomaterials (Basel)* "Magnetic Nanoparticles: From Design and Synthesis to Real World Applications" **2017**, *7*.

[12] B. G. Rocha, T. C. Mac Leod, M. F. Guedes da Silva, K. V. Luzyanin, L. M. Martins, A. J. Pombeiro, *Dalton Trans.* "NiII, CuII and ZnII complexes with a sterically hindered scorpionate ligand (TpmsPh) and catalytic application in the diasteroselective nitroaldol (Henry) reaction" **2014**, *43*, 15192-15200.

[13] L. M. D. R. S. Martins, A. J. L. Pombeiro, *Eur. J. Inorg. Chem.* "Water-Soluble C-Scorpionate Complexes - Catalytic and Biological Applications" **2016**, *2016*, 2236-2252.

[14] L. M. D. R. S. Martins, *Coord. Chem. Rev.* "C-scorpionate complexes: Ever young catalytic tools" **2019**, *396*, 89-102.

[15] J. M. Munoz-Molina, T. R. Belderrain, P. J. Perez, *Dalton Trans.* "Group 11 tris(pyrazolyl)methane complexes: structural features and catalytic applications" **2019**, *48*, 10772-10781.

[16] D. L. Reger, T. C. Grattan, K. J. Brown, C. A. Little, J. J. S. Lamba, A. L. Rheingold, R. D. Sommer, *J. Organomet. Chem.* "Syntheses of tris(pyrazolyl)methane ligands and {[tris(pyrazolyl)methane]Mn(CO)$_3$}SO$_3$CF$_3$ complexes: comparison of ligand donor properties" **2000**, *607*, 120-128.

[17] T. F. S. Silva, E. C. B. A. Alegria, L. M. D. R. S. Martins, A. J. L. Pombeiro, *Adv. Synth. Catal.* "Half-Sandwich Scorpionate Vanadium, Iron and Copper Complexes: Synthesis and Application in the Catalytic Peroxidative Oxidation of Cyclohexane under Mild Conditions" **2008**, *350*, 706-716.

[18] L. M. Rossi, L. L. R. Vono, F. P. Silva, P. K. Kiyohara, E. L. Duarte, J. R. Matos, *Appl. Catal. A, Gen.* "A magnetically recoverable scavenger for palladium based on thiol-modified magnetite nanoparticles" **2007**, *330*, 139-144.

[19] M. J. Jacinto, P. K. Kiyohara, S. H. Masunaga, R. F. Jardim, L. M. Rossi, *Appl. Catal. A, Gen.* "Recoverable rhodium nanoparticles: Synthesis, characterization and catalytic performance in hydrogenation reactions" **2008**, *338*, 52-57.

[20] L. D. Dias, R. M. B. Carrilho, C. A. Henriques, M. J. F. Calvete, A. M. Masdeu-Bultó, C. Claver, L. M. Rossi, M. M. Pereira, *ChemCatChem* "Hybrid Metalloporphyrin Magnetic Nanoparticles as Catalysts for Sequential Transformation of Alkenes and CO_2 into Cyclic Carbonates" **2018**, *10*, 2792-2803.

[21] V. Pace, P. Hoyos, L. Castoldi, P. Dominguez de Maria, A. R. Alcantara, *ChemSusChem* "2-Methyltetrahydrofuran (2-MeTHF): a biomass-derived solvent with broad application in organic chemistry" **2012**, *5*, 1369-1379.

[22] M. Kranenburg, Y. E. M. van der Burgt, P. C. J. Kamer, P. W. N. M. van Leeuwen, K. Goubitz, J. Fraanje, *Organometallics* "New Diphosphine Ligands Based on Heterocyclic Aromatics Inducing Very High Regioselectivity in Rhodium-Catalyzed Hydroformylation: Effect of the Bite Angle" **1995**, *14*, 3081-3089.

[23] P. W. N. M. van Leeuwen, P. C. J. Kamer, *Catal. Sci. Technol.* "Featuring Xantphos" **2018**, *8*, 26-113.

[24] F. M. S. Rodrigues, P. K. Kucmierczyk, M. Pineiro, R. Jackstell, R. Franke, M. M. Pereira, M. Beller, *ChemSusChem* "Dual Rh-Ru Catalysts for Reductive Hydroformylation of Olefins to Alcohols" **2018**, *11*, 2310-2314.

[25] R. F. Heck, *Acc. Chem. Res.* "Addition reactions of transition metal compounds" **1969**, *2*, 10-16.

[26] L. A. van der Veen, M. D. K. Boele, F. R. Bregman, P. C. J. Kamer, P. W. N. M. van Leeuwen, K. Goubitz, J. Fraanje, H. Schenk, C. Bo, *J. Am. Chem. Soc.* "Electronic Effect on Rhodium Diphosphine Catalyzed Hydroformylation: The Bite Angle Effect Reconsidered" **1998**, *120*, 11616-11626.

[27] P. Kalck, M. Urrutigoïty, in *Rhodium Catalysis*, **2016**, pp. 69-98.

[28] P. C. Kamer, P. W. van Leeuwen, J. N. Reek, *Acc. Chem. Res.* "Wide bite angle diphosphines: xantphos ligands in transition metal complexes and catalysis" **2001**, *34*, 895-904.

[29] R. M. B. Carrilho, A. C. B. Neves, M. A. O. Lourenço, A. R. Abreu, M. T. S. Rosado, P. E. Abreu, M. E. S. Eusébio, L. Kollár, J. C. Bayón, M. M. Pereira, *J. Organomet. Chem.* "Rhodium/tris-binaphthyl chiral monophosphite complexes: Efficient catalysts for the hydroformylation of disubstituted aryl olefins" **2012**, *698*, 28-34.

[30] G. N. Costa, R. M. B. Carrilho, L. D. Dias, J. C. Viana, G. L. B. Aquino, M. Pineiro, M. M. Pereira, *J. Mol. Catal. A: Chem.* "Highly efficient Rh(I)/tris-binaphthyl

monophosphite catalysts for hydroformylation of sterically hindered alkyl olefins" **2016**, *416*, 73-80.

[31] A. R. Almeida, R. M. B. Carrilho, A. F. Peixoto, A. R. Abreu, A. Silva, M. M. Pereira, *Tetrahedron* "Sequential reactions from catalytic hydroformylation toward the synthesis of amino compounds" **2017**, *73*, 2389-2395.

[32] C. G. Vieira, E. N. dos Santos, E. V. Gusevskaya, *Appl. Catal. A, Gen.* "Synthesis of fragrance compounds from acyclic monoterpenes: Rhodium catalyzed hydroformylation and tandem hydroformylation/acetalization of linalool and β-citronellene" **2013**, *466*, 208-215.

[33] K. Dong, X. Fang, S. Gulak, R. Franke, A. Spannenberg, H. Neumann, R. Jackstell, M. Beller, *Nat. Commun.* "Highly active and efficient catalysts for alkoxycarbonylation of alkenes" **2017**, *8*, 14117.

Chapter 5

Experimental

This chapter contains all the information regarding materials, reagents, and solvents, as well as all the techniques and instruments used during the experimental work. It is divided into four sections: General (section 5.1), Experimental of Chapter 2 (section 5.2), Experimental of Chapter 3 (section 5.3). and Experimental of Chapter 4 (section 5.4).

5.1 General information

5.1.1 Solvents and Chemicals

All solvents and chemicals commercially obtained from Sigma-Aldrich, Merck, Strem Chemicals or FluoroChem, except when indicated. Non-commercially available ligand **L2.1** was prepared according to literature and the analytical data are in accordance with the reported literature.[1] Ligand **L2.3** was kindly provided by Doctor Rui Carrilho (University of Coimbra). Air and moisture sensitive reagents and solutions were handled under nitrogen or argon atmosphere, in a vacuum system, using *Schlenk* techniques.[2] All the glassware was dried by heating. The solvents were purified by distillation or, dried and distilled using standard procedures described below.[3,4]

Dichloromethane and chloroform

Chlorinated solvents were placed in a round-bottom flask, with anhydrous calcium chloride and pumice stone. The mixture was kept under reflux, for two hours. After

distillation, the solvent was collected and passed through a column of activated basic alumina (grade I) and stored in a flask containing activated molecular sieves (3Å). For water-sensitive experiments, dichloromethane was dried with calcium hydride, under reflux, for three hours. After distillation, the solvent was collected and stored, under nitrogen atmosphere, in a vessel containing activated molecular sieves (3Å).

Ethyl acetate

Ethyl acetate was placed in a round-bottom flask, with anhydrous calcium chloride and pumice stone. The mixture was kept under reflux, for two hours. After distillation, the solvent was collected and passed through a column of basic alumina (grade I) and stored in a flask containing activated molecular sieves (3Å).

***n*-Hexane**

n-Hexane was placed in a round-bottom flask, with anhydrous calcium chloride and pumice stone. The mixture was kept under reflux, for three hours. After distillation, the solvent was collected and passed through a column of activated basic alumina (grade I) and stored in a flask containing activated molecular sieves (3Å). For water-sensitive experiments, *n*-hexane was dried with sodium/benzophenone, under reflux, at the boiling temperature, until a strong blue color was observed. After distillation, the solvent was collected and stored, under nitrogen atmosphere, in a vessel containing activated molecular sieves (3Å).

Toluene, dimethoxyethane, tetrahydrofuran and 2-methyltetrahydrofuran

The desired solvent was placed in a round-bottom flask, with sodium flakes and benzophenone. The mixture was kept under reflux until a strong blue color was observed. After distillation, the solvent was collected and stored, under nitrogen atmosphere, in a vessel containing activated molecular sieves (3Å).

Acetone

Acetone was placed in a round-bottom flask, with anhydrous calcium chloride and pumice stone. The mixture was kept under reflux, for two hours. After distillation, the

solvent was collected and passed through a column of basic alumina (grade I) and stored in a flask containing activated molecular sieves (3Å).

Methanol, ethanol and benzyl alcohol

5.0 g of magnesium flakes and 0.5 g of iodine were placed in a two-liter round bottom flask. 50 mL of the desired alcohol was added, and the mixture was heated until the disappearance of iodine brown color. After magnesium had been totally consumed, approximately 950 mL of the corresponding alcohol was then added and the mixture was kept under reflux for 2 hours, followed by distillation from molecular sieves (3Å).

***N,N*-Dimethylformamide**

DMF was placed in a round-bottom flask equipped with a reflux condenser, with calcium hydride and the mixture was kept at 80 °C, for 6 hours. After distillation under reduced pressure, the solvent was collected and stored in a container with activated molecular sieves (3Å).

Triethylamine

Triethylamine was placed in a round-bottom flask, with sodium flakes and benzophenone. The mixture was kept under reflux until a strong blue color was observed. After distillation, the solvent was collected and stored, under nitrogen atmosphere, in a vessel containing activated molecular sieves (3Å).

5.1.2 Instrumentation and Methodologies

Water purification apparatus Milli-Q

The deionized water was obtained using a Water Purification Apparatus Milli-Q (Department of Chemistry, University of Coimbra).

Centrifuge

The centrifugation was performed using a Centromix-BLT centrifuge (Department of Chemistry, University of Coimbra).

Thin layer chromatography (TLC)

Thin layer chromatography (TLC) was performed using aluminum plates coated with silica gel 60 (Sigma-Aldrich)) with fluorescent indicator UV_{254} and UV_{366}.

Column chromatography

The reaction products were purified by column chromatography using silica gel 60 (particles of size 0.06-0.20 mm) as the stationary phase and the appropriate eluent.

Flash chromatography

The reaction products, when necessary, were purified using a flash chromatography equipment PuriFlash 420® Interchim (Department of Chemistry, University of Coimbra), equipped with a UV diode array detector and an HP-SI F0025 silica column (0.15 µm) using the appropriate eluent.

Nuclear magnetic resonance (NMR)

NMR spectra were recorded on a Bruker Avance 400 spectrometer (Department of Chemistry, University of Coimbra), using $CDCl_3$ (δ = 7.26 ppm) as deuterated solvent (unless otherwise stated). ^{1}H and ^{13}C chemical shifts, expressed in ppm, are generally relative to $CDCl_3$ (δ = 7.26 ppm) or TMS (δ = 0.00 ppm) internal standard. The data obtained are indicated in the following order: Nucleus (apparatus, solvent): chemical shift (δ, ppm) [multiplicity (*s* - singlet, *d* - doublet, *dd* - double doublet, *t* - triplet, *dt* – doublet of triplet, *q* - quartet, *dq* - doublet of quartet, *p* - pentet, *m* - multiplet and bs - broad signal), coupling constant (J, in Hertz), relative intensity (nH as the number of protons) and proton assignment (Hx).

Mass spectrometry (MS)

High-resolution mass spectrometry was carried out on a Bruker Microtof apparatus, equipped with a selective ESI detector (Unidade de Masas e Proteómica, University of Santiago de Compostela, Spain). Electron impact (EI) mass spectra were recorded on

Agilent 5975 MSD mass spectrometer (70 eV). The data are given as mass units per unit of charge (m/z).

Inductively coupled plasma optical emission spectroscopy (ICP-OES)

The percentage of Rodium, phosphorum and iron present on the hybrid materials or in solution was determined using an ICP-OES iCAP™ 7000 Series spectrometer (Department of Chemistry, University of Aveiro).

Thermogravimetry (TG)

Thermogravimetric analyses were made using a TG-DSC Perkin-Elmer STA6000 with a heating rate of 10 °C min^{-1} to a maximum temperature of 900 °C and 20 mL min^{-1} nitrogen flux (Department of Physics, University of Coimbra)

Transmission electron microscopy (TEM)

Transmission electron microscopy analyses were performed on a Philips CM 200 apparatus, at 200 kV (Institute of Chemistry, University of São Paulo, Brazil), and size distributions of the materials were calculated by a statistical size distribution by manual analysis of enlarged images using the Imagetool software (Version 3.0).

Infrared spectroscopy (IR)

The infrared spectra were obtained in a Pike Miracle spectrometer and each spectrum was obtained with a resolution of 4 cm^{-1} and 64 scans (Department of Chemistry, University of Coimbra, Portugal). The infrared spectra for the nanomaterials were obtained using a Pike Miracle spectrometer (Institute of Chemistry, University of São Paulo, Brazil) with a resolution of 4 cm^{-1} (64 scans). The samples were pressed into thin wafers (20-25 mg cm^{-2}) and heated in an IR glass cell up to 160 °C using a heating rate of 10 °C min^{-1} during 1 h, under vacuum (10 Pa) before spectra acquisition in transmission mode.

X-ray photoelectron spectroscopy (XPS)

X-ray photoelectron spectroscopy experiments were performed on a Kratos AXIS Ultra HSA, with VISION software for data acquisition and CASAXPS software for data

analysis. The analysis was carried out with a monochromatic Al Kα X-ray source (1486.7 eV), operating at 15 kV (90 W), in fixed analyzer transmission mode with a pass energy of 40 eV for regions of interest and 80 eV for survey. Data acquisition was performed with a pressure lower than 1×10^{-6} Pa, and a charge neutralization system was used. The effect of the electric charge was corrected by reference to the carbon peak (285 eV). (Faculty of Engineering, University of Porto). The molar amount of functionalization/immobilization of organic molecules was calculated by transforming the XPS atomic % (At%) into mass % (Wt%) for each element, then Wt% was converted to the correspondent molar %. Knowing the equivalents of each element present in the organic molecule we calculated the molar amount of each molecule/g of material.

Microwave system

Microwave-assisted experiments were performed in thick-walled glass vials under closed-vessel conditions, using a CEM Discover® SP Focused Microwave™ Synthesis System.

Gas chromatography (GC)

Gas chromatography was carried out using an Agilent 7820A chromatograph equipped with 30 m length and 0.32 mm inside diameter HP5 column and FID detector using nitrogen as carrier gas and isooctane as an external standard.

To quantify the reaction products a calibration curve for each one of the analytes was obtained. By variation of analyte concentration, the response factor (F) was calculated following equation 5.1.

$$\frac{Area\ X}{Area\ ES} = F(X) \times \frac{C(X)}{C(ES)}$$

Equation 5.1

The amount of each compound after the catalytic experiments was calculated by GC analysis of the reaction crudes following equation 5.2 using the known response factor (F) and concentration of external standard.

$$\frac{Area\ X \times n(ES)}{Area\ ES\ \times\ F(X)} = n(X)$$

Equation 5.2

Conversion, chemoselectivity, and regioselectivity of the catalytic experiments were calculated using equations 5.3, 5.4 and 5.5 respectively.

$$Conversion\ (\%) = \left(\frac{n(substrate\ t_0) - \ n(substrate\ in\ the\ reaction\ crude)}{n(substrate\ t_0)}\right) \times 100$$

Equation 5.3

$$Chemoselectivity\ (\%) = \left(\frac{n(all\ products\ from\ a\ functional\ group)}{n(all\ products)}\right) \times 100$$

Equation 5.4

$$Regioselectivity\ (\%) = \left(\frac{n(major\ isomer\ from\ a\ functional\ group)}{n(all\ products\ from\ that\ functional\ group)}\right) \times 100$$

Equation 5.5

Mass spectra were recorded on a GC-MS Agilent 7820A system equipped with a mass selective detector. an Agilent 7820 Gas Chromatograph system equipped with an HP5 MS column (30 m × 0.25 mm × 0.25 μm) coupled to an Agilent 5975 MSD System Technologies (70 eV) using helium as carrier gas.

The GC analyses were performed using the following conditions:

Inlet: 220 °C

Oven initial temperature: 70 °C (hold 5 min)

Ramp: 35 °C min^{-1} up to 270 °C (hold 10min)

Detector: 280 °C;

Gas flow: 1.00 mL min^{-1}.

High-pressure gas line

All the catalytic reactions that required gases (CO and H_2) were performed in a high-pressure system, belonging to the Chemistry Department at the University of Coimbra (**Figure 5.1**).

Figure 5.1 High-pressure system for catalytic reactions (Chemistry Department, University of Coimbra).

5.2 Experimental of Chapter 2

In this section, the synthetic procedures and compound characterization referring to chapter 2 is provided.

5.2.1 Ligand synthesis

Racemic 1,1'-Bi-2-naphthol synthesis (2.2)

In a typical experiment, $FeCl_3.6H_2O$ (27.0 g, 0.10 mol) and 2-naphthol (7.2 g, 0.05 mmol) were powered, mixed, and introduced in a 10 mL microwave vessel. The mixture was subjected to MW irradiation (60 W) for 1 minute, at 80 °C. After cooling, full transformation into BINOL was observed by TLC, using CH_2Cl_2 as eluent. The purification was carried out by washing the reaction crude with hot water (followed by filtration over activated charcoal, followed by recrystallization in toluene. Pure 1,1'-Bi-2-naphthol

crystals were obtained in 92% isolated yield and the data obtained through characterization with ^{1}H, ^{13}C-NNR, and 2D NMR techniques are in good agreement with the literature.[5]

***Tris*[2'-(pivaloyloxy)-1,1'-binaphthyl-2-yl]phosphite ligand synthesis (L2.2)**

The ligand **L2.2** was synthesized through acylation of BINOL with pivaloyl chloride followed by phosphorylation of the corresponding mono-ester with PCl_3, in basic medium.

A dried round-bottom flask was charged with BINOL (5.73 g, 20 mmol), 4-dimethylaminopyridine (DMAP) (25 mg, 0.2 mmol), and triethylamine (22.1 mmol, 3.1 mL) in 75 mL THF. The mixture was cooled to 0 °C and a solution of pivaloyl chloride (20 mmol, 2.46 mL) in THF (10 mL) was added dropwise. Once the addition was complete, the reaction mixture was left at room temperature for 30 h. After nearly complete disappearance of the starting material (observed by TLC), the reaction was quenched with distilled water and the mixture was extracted with ethyl acetate. The combined organic phases were washed successively with a saturated aqueous solution of $NaHCO_3$, brine, water, and then dried over Na_2SO_4. After filtration and solvent removal in vacuum, the crude product was purified by column chromatography on silica gel, using dichloromethane/*n*-hexane (3:1) as eluent, providing in 90% isolated yield (6.67 g, 18 mmol) of 2'-(pivaloyloxy)-1,1'-binaphthyl-2-ol**.**

The preparation of monophosphite ligand **L2.2** was performed, according to conventional procedures for the synthesis of *tris*-arylphosphites.[6] A dried Schlenk flask was charged with the 2'-(pivaloyloxy)-1,1'-binaphthyl-2-ol (**2.4**) (3.0 g, 8.1 mmol), which was azeotropically dried with toluene, then placed under nitrogen atmosphere and dissolved in dry triethylamine (20 mL). The solution was cooled to 0 °C and freshly distilled PCl_3 (0.25 mL, 2.7 mmol) was slowly added. The reaction progress was followed by TLC and ^{31}P-NMR. After stirring for 3-5 hours, the solvent was evaporated under reduced pressure. Then, the residue was dissolved in dichloromethane/*n*-hexane (1:1) and purified by a silica gel column chromatography, using dichloromethane/*n*-hexane (1:1) as eluent, and further purified by recrystallization in diethyl ether/*n*-hexane, always under nitrogen atmosphere. The final product *tris*[2'-(pivaloyloxy)-1,1'-binaphthyl-2-yl]phosphite, **L2.2**, with white crystalline aspect was obtained in 70% yield (2.15 g, 1.89 mmol).

2'-(pivaloyloxy)-1,1'-binaphthyl-2-ol (2.4)

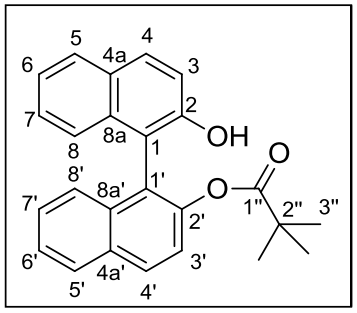

^{1}H NMR (400 MHz, $CDCl_3$) δ(ppm): 7.96 (*d*, J = 8.8 Hz, 1H), 7.87 (*d*, J = 8.2 Hz, 1H), 7.78 (*d*, J = 8.9 Hz 1H), 7.72 (*d*, J = 8.0 Hz, 1H), 7.42-7.38 (*m*, 1H), 7.28 (*d*, J = 8.8 Hz, 1H), 7.24-7.19 (*m*, 4H), 7.19-7.13 (*m*, 1H) 6.97 (*d*, J = 8.2 Hz, 1H), 6.14 (*s*, 1H, OH), 0.68 (*s*, 9H, $H_{3''}$).

^{13}C NMR (100 MHz, $CDCl_3$) δ(ppm): 177.9 ($C_{1''}$), 151.9, 148.4, 133.7, 133.6, 132.3, 130.8, 130.4, 129.1, 128.4, 128.0, 127.5, 126.8, 126.3, 125.7, 124.7,123.6, 123.1, 121.9, 118.3, 114.3, 38.8 ($C_{2''}$), 26.6 ($C_{3''}$).

***Tris*[2'-(pivaloyloxy)-1,1'-binaphthyl-2-yl]phosphite (L2.2)**

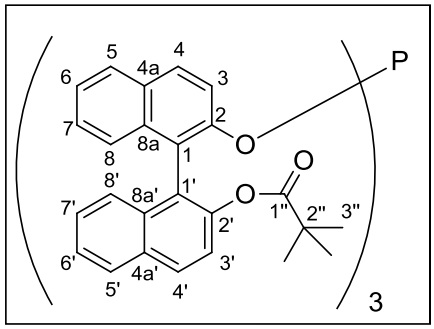

^{1}H NMR (400 MHz, $CDCl_3$) δ(ppm): 7.91(*d*, J = 8.9 Hz, 3H), 7.81 (*d*, J = 8.2 Hz, 3H), 7.72 (*d*, J = 8.1 Hz, 3H), 7.37 (*d*, J = 8.2 Hz, 3H), 7.34-7.30 (*m*, 6H), 7.20 (*d*, J = 8.2 Hz, 3H), 7.18-7.14 (*m*, 3H), 7.07-7.03 (m, 3H), 7.00 (*d*, J = 8.5 Hz, 3H), 6.78 (*d*, J = 8.4 Hz, 3H), 6.40 (*d*, J = 8.9 Hz, 3H), 0.65 (*s*, 27H).

^{13}C NMR (100 MHz, $CDCl_3$) δ(ppm): 176.5 ($C_{1''}$), 147.2, 133.6, 133.4, 131.7, 130.3, 129.5, 129.3, 128.0 127.6, 126.5, 126.4, 126.0, 125.5, 124.7, 124.5, 122.3, 121.4, 121.3, 120.3, 120.2, 38.7 ($C_{2''}$), 26.6 ($C_{3''}$).

^{31}P NMR (162 MHz, $CDCl_3$) δ(ppm): 133.6.

HRMS (ESI): m/z calcd. for $C_{75}H_{63}O_9P$ $[M+H]^+$: 1139.4288, found: 1139.4288.

5.2.2 General procedure for the hydroformylation/reduction of olefins

A 40 mL steel autoclave was charged with $[Rh(CO)_2acac]$ (1.98 mg, 7.7 µmol), tris[2'-(benzyloxy)-1,1'-binaphthyl-2-yl] phosphite ligand **L2.1** (17.8 mg, 15.4 µmol) and Shvo's-complex (4.1 mg, 3.8 µmol). The autoclave was closed, and the air was removed using a vacuum pump. Then dry toluene (5 mL) and the desired alkene (10 mmol) were added through cannula. After flushing the autoclave with 3 cycles of vacuum/synthesis gas, it was pressurized with the desired amount of H_2/CO gas and heated to the desired

temperature for 20 h, with magnetic stirring. After the reaction time, the autoclave was cooled with ice water and the pressure was released. The reaction crude was diluted with toluene and analyzed by gas chromatography, using isooctane as an external standard.

5.2.3 Characterization of the isolated alcohols

4-ethylhexan-1-ol (2.11a)

According to the general procedure for the hydroformylation/reduction of olefins **2.11a** was prepared from 3-ethylpent-2-ene **2.11** and isolated as a colorless liquid in 13% yield (195.3 mg, 1.3 mmol), through column chromatography on silica gel (eluent, pentane/ethyl acetate 6:1).

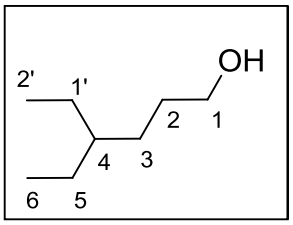

^{1}H NMR (400 MHz, $CDCl_3$) δ(ppm): 3.56 (*t*, J = 6.7 Hz, 2H, $\underline{H_1}$), 1.52-1.43 (*m*, 2H, $\underline{H_2}$), 1.27-1.09 (*m*, 7H, $\underline{H_3}$, $\underline{H_4}$, $\underline{H_5}$, $\underline{H_{1'}}$), 0.78 (*t,* J = 7.3 Hz, 6H, $\underline{H_6}$, $\underline{H_{2'}}$).

^{13}C NMR (100 MHz, $CDCl_3$) δ(ppm): 63.8 ($\underline{C_1}$), 40.4 ($\underline{C_4}$), 30.2($\underline{C_2}$), 28.9 ($\underline{C_3}$), 25.6 ($\underline{C_5}$, $\underline{C_{1'}}$), 11.1 ($\underline{C_6}$, $\underline{C_{2'}}$).

MS (EI): m/z = 129 $[M]^+$, 112, 101, 83, 70, 55.

3-phenylbutan-1-ol (2.14a)

According to the general procedure for the hydroformylation/reduction of olefins, **2.14a** was prepared from prop-1-en-2-ylbenzene **2.14** and isolated as a colorless liquid in 29% yield (435.6 mg, 2.9 mmol), through column chromatography on silica gel (eluent, hexane/ethyl acetate 5:1).

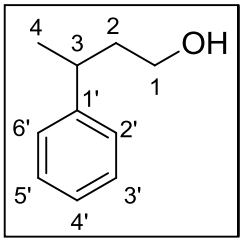

^{1}H NMR (400 MHz, $CDCl_3$) δ(ppm): 7.36-7.33 (*m*, 2H, $\underline{H_{3'}}$, $\underline{H_{5'}}$), 7.26-7.24 (*m*, 3H, $\underline{H_{2'}}$, $\underline{H_{4'}}$, $\underline{H_{6'}}$), 3.60-3.55 (*m*, 2H, $\underline{H_1}$), 2.95-2.90 (*m*, 1H, $\underline{H_3}$), 1.89 (*q*, J = 6.9, 2H, $\underline{H_2}$), 1.32 (*d,* J = 7.0 Hz, 3H, $\underline{H_4}$).

^{13}C NMR (100 MHz, $CDCl_3$) δ(ppm): 147.0 ($\underline{C_{1'}}$), 128.6 ($\underline{C_{3'}}$, $\underline{C_{5'}}$), 127.0 ($\underline{C_{2'}}$, $\underline{C_{6'}}$), 126.2 ($\underline{C_{4'}}$), 61.2 ($\underline{C_1}$), 41.0 ($\underline{C_3}$), 36.5 ($\underline{C_2}$), 22.5 ($\underline{C_4}$).

MS (EI): m/z = 150 $[M]^+$, 132, 117, 105, 91, 77, 65, 51, 39.

4-phenylbutan-1-ol (2.15a)

According to the general procedure for the hydroformylation/reduction of olefins **2.15a** was prepared from (*E*)-prop-1-en-1-ylbenzene **2.15** and isolated as a colorless liquid in 13% yield (195.3 mg, 1.3 mmol), through column chromatography on silica gel (eluent, hexane/ethyl acetate 5:1).

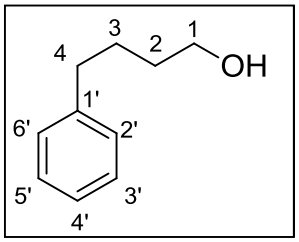

^{1}H NMR (400 MHz, $CDCl_3$) δ(ppm): 7.29-7.25 (*m*, 2H, $H_{3'}$, $H_{5'}$), 7.29-7.25 (*m*, 3H, $H_{2'}$, $H_{4'}$, $H_{6'}$), 3.63 (*t*, J = 6.4 Hz, 2H, H_1), 2.63 (*t*, J = 7.5 Hz, 2H, H_4), 1.73-1.65 (*m*, 2H, H_2/H_3), 1.62-1.55 (*m,* 2H, H_2/H_3).

^{13}C NMR (100 MHz, $CDCl_3$) δ(ppm): 142.4 ($C_{1'}$), 128.5 ($C_{3'}$, $C_{5'}$), 128.4 ($C_{2'}$, $C_{6'}$), 125.9 ($C_{4'}$), 62.9 (C_1), 35.7 (C_4), 32.4 (C_2/C_3), 27.7 (C_2/C_3).

MS (EI): m/z = 150 $[M]^+$, 132, 117, 104, 91, 77, 65, 51, 41, 31.

2-phenylbutan-1-ol (2.15ba)

According to the general procedure for the hydroformylation/reduction of olefins, **2.15ba** was prepared from (*E*)-prop-1-en-1-ylbenzene **2.15** and isolated as a colorless liquid in 24% yield (360.5 g, 2.4 mmol), through column chromatography on silica gel (eluent, hexane/ethyl acetate 5:1).

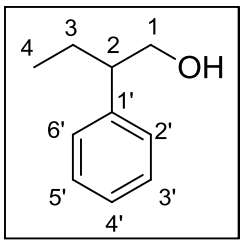

^{1}H NMR (400 MHz, $CDCl_3$) δ(ppm): 7.27-7.18 (*m*, 2H, $H_{3'}$, $H_{5'}$), 7.16-7.12 (*m*, 3H, $H_{2'}$, $H_{4'}$, $H_{6'}$), 3.70 (*dd*, J = 10.8, 5.8 Hz, 1H, H_1), 3.64 (*dd*, J = 10.8, 7.8 Hz, 1H, H_1), 2.65-2.57 (*m*, 1H, H_2), 1.73-1.63 (*m*, 1H, H_3), 1.56-1.45 (*m*, 1H, H_3), 0.76 (*t*, J = 7.4 Hz, 3H, H_4).

^{13}C NMR (100 MHz, $CDCl_3$) δ(ppm): 142.4 ($C_{1'}$), 128.7 ($C_{3'}$, $C_{5'}$), 128.2 ($C_{2'}$, $C_{6'}$), 126.8 ($C_{4'}$), 67.5 (C_1), 50.6 (C_2), 25.1 (C_3), 12.1 (C_4).

MS (EI): m/z = 150 [M]+, 119, 103, 91, 77, 65, 51, 41, 31.

2-methyl-3-phenylpropan-1-ol (2.15bb)

According to the general procedure for the hydroformylation/reduction of olefins, **2.15bb** was prepared from (*E*)-prop-1-en-1-ylbenzene **2.15** and obtained in a mixture of 50:50% with the isomeric compound **2.15ba** through column chromatography on silica gel (eluent, hexane/ethyl acetate 5:1).

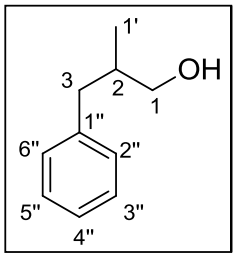

^{1}H NMR (400 MHz, $CDCl_3$) δ(ppm): 7.27-7.18 (*m*, 2H, $H_{3''}$, $H_{5''}$), 7.16-7.12 (*m*, 3H, $H_{2''}$, $H_{4''}$, $H_{6''}$), 3.73 (*dd*, J = 10.8, 6.0 Hz, 1H, H_1), 3.69 (*dd*, J = 10.8, 7.8 Hz, 1H, H_1), 2.74 (*dd*, J = 13.4, 6.2 Hz, 1H, H_3), 2.39 (*dd*, J = 13.4, 8.1 Hz, 1H, H_3) 1.95-1.87 (*m*, 1H, H_2), 0.89 (*d*, J = 6.8 Hz, 3H, $H_{1'}$).

^{13}C NMR (100 MHz, $CDCl_3$) δ(ppm): 140.8 ($C_{1''}$), 129.2 ($C_{3''}$, $C_{5''}$), 128.3 ($C_{2''}$, $C_{6''}$), 125.9 ($C_{4''}$), 67.6 (C_1), 39.8 (C_3), 37.8 (C_2), 16.5 ($C_{1'}$).

MS (EI): m/z = 150 $[M]^+$, 132, 117, 104, 91, 77, 65, 51, 39, 31.

2,3-diphenylpropan-1-ol (2.16a)

According to the general procedure for the hydroformylation/reduction of olefins, **2.16a** was prepared from (*E*)-1,2-diphenylethenedibenzene **2.16** and isolated as a colorless liquid in 83% yield (706.2 mg, 3.2 mmol), through column chromatography on silica gel (eluent, heptane/ethyl acetate 8:1).

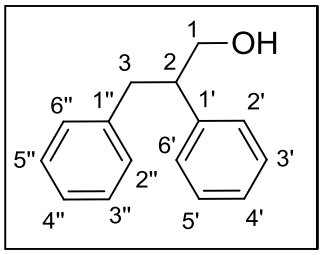

^{1}H NMR (400 MHz, $CDCl_3$) δ(ppm): 7.32-7.05 (*m*, 10H, $H_{1'}$-$H_{6'}$, $H_{1''}$-$H_{6''}$), 3.79 (*dd*, J = 12.4, 6.8 Hz, 1H, H_1), 3.77 (*dd*, J = 12.4, 7.2 Hz, 1H, H_1), 3.15-2.85 (*m*, 3H, H_2, H_3).

^{13}C NMR (100 MHz, $CDCl_3$) δ(ppm): 142.1 ($C_{1'}$), 140.1 ($C_{1''}$), 129.3 ($C_{3'}$, $C_{5'}$), 128.9 ($C_{3''}$, $C_{5''}$), 128.5 ($C_{2'}$, $C_{6'}$), 128.3 ($C_{2''}$, $C_{6''}$), 127.1 ($C_{4'}$), 126.2 ($C_{4''}$), 66.9 (C_1), 50.4 (C_2), 38.9 (C_3).

MS (EI): m/z = 212 $[M]^+$, 194, 180, 165, 141, 121, 103, 77, 51.

(3*R*)-3,7-dimethylnona-1,9-diol (2.18a)

According to the general procedure for the hydroformylation/reduction of olefins **2.24a** was prepared from citronellol **2.24** and isolated as colorless liquid in 30% (564.9 mg, 3.0 mmol) yield through column chromatography on silica gel (eluent, dichloromethane/ethyl acetate 1:1).

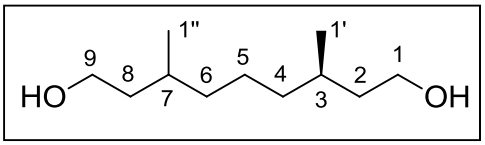

^{1}H NMR (400 MHz, $CDCl_3$) δ(ppm): 1:1 mixture of diastereoisomers: 3.69-3.58 (*m*, 4H, H_1, H_9), 2.02 (*bs*, 2H, -OH), 1.60-1.50 (*m*, 4H, H_2, H_8), 1.38-1.23 (*m,* 5H, H_4, H_5, H_6), 1.15-1.06 (*m*, 2H, H_3, H_7), 0.87 (*d*, J = 6.0 Hz, 6H, $H_{1'}$, $H_{1''}$).

^{13}C NMR (100 MHz, $CDCl_3$) δ(ppm): 1:1 mixture of diastereoisomers: 61.2 ($\underline{C_1}$, $\underline{C_9}$), 61.1 ($\underline{C_1}$, $\underline{C_9}$), 40.0 ($\underline{C_2}$, $\underline{C_8}$), 39.9 ($\underline{C_2}$, $\underline{C_8}$), 37.4 ($\underline{C_4}$, $\underline{C_6}$), 37.2 ($\underline{C_4}$, $\underline{C_6}$), 29.6 ($\underline{C_3}$, $\underline{C_7}$), 29.4 ($\underline{C_3}$, $\underline{C_7}$), 24.3 ($\underline{C_5}$), 24.2 ($\underline{C_5}$), 19.8 ($\underline{C_{1'}}$/$\underline{C_{1''}}$), 19.7 ($\underline{C_{1'}}$/$\underline{C_{1''}}$).

MS (EI): m/z = 188 $[M]^+$, 169, 151, 137, 123, 109, 95, 81, 69, 55, 41.

5.3 Experimental of Chapter 3

In this section, the synthetic procedures and compound characterization referring to chapter 3 is provided.

5.3.1 Synthesis and functionalization of the nanomaterials

Multiwalled carbon nanotubes functionalization

Oxidized multiwalled carbon nanotubes (**MWCNT@COOH**) with 3.86 COOH Wt%, an average diameter of 8 nm, length of 10-30 μm and purity higher than 98% were purchased from NANOCYL (NC3101 series).

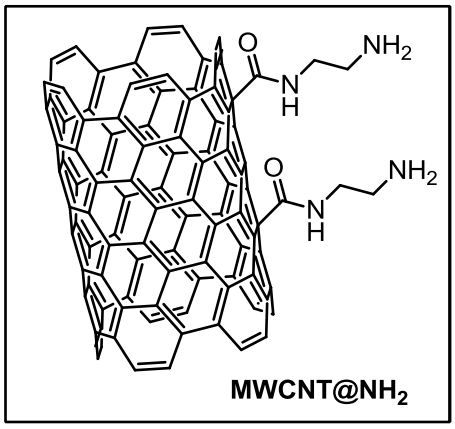

The synthesis of **MWCNT@NH_2** was performed in a two-step methodology following the procedures adapted from literature.[7] Thionylchloride (60 mL) was added to 1.2 g of **MWCNT@COOH** in a 250 mL round-bottom flask under nitrogen atmosphere. The suspension was then sonicated for 2 minutes and stirred at 70 °C for 24 hours under nitrogen atmosphere. The suspension was cooled to room temperature, filtered and washed with dry THF (ca. 1 L) until neutral pH was obtained. The filtered solid was dried under vacuum at room temperature and **MWCNT@COCl** was obtained. This material was characterized by X-ray photoelectron spectroscopy (XPS). The **MWCNT@COCl** material was then introduced in a round-bottom flask containing 70 mL of freshly distilled ethylenediamine. The solid was dispersed through sonication (2 min) and the reaction occurred at 100 °C for 48 hours, under magnetic stirring and nitrogen atmosphere. To remove the excess of ethylenediamine, the **MWCNT@NH_2** material was filtered and washed with ethanol (ca.750 mL) and THF (ca. 250 mL) after the reaction. The

MWCNT@NH_2 solid was dried and characterized by X-ray photoelectron spectroscopy (XPS). The functionalized material was obtained with 0.82 mmol of NH_2/g. To calculate the molar amount of NH_2 groups, we considered the atomic contribution of each one of the atoms presented in the sample and converted the At% of nitrogen to the molar amount of NH_2 per gram of material.

Magnetic nanoparticles functionalization

MNP@NH_2 was obtained through the preparation of magnetite followed by their coating with silica and further amine functionalization, following the methods reported earlier.[8,9]

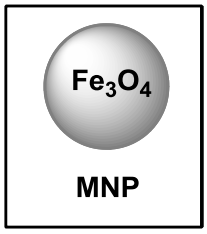

Magnetite nanoparticles (**MNP**) were prepared, according to a previously reported method.[9] A mixture of an aqueous solution of $FeCl_3$ (10 mL, 1 M) and an HCl solution (2 M) of $FeCl_2$ (2.5 mL, 2 M) was added to 250 mL of NH_4OH (1 M) under mechanical stirring (10 000 rpm) in a round-bottom flask. The **MNP** were magnetically recovered and washed with distilled water (3 × 250 mL) after 30 minutes of reaction. Then, the **MNP** were dispersed in 250 mL of distilled water. Oleic acid (2 mL, 7 mmol), in acetone (5 mL), was added dropwise to the dispersion under vigorous mechanical stirring for 30 minutes. The resulting precipitate was magnetically recovered and washed with acetone (3 × 25 mL), the resulting magnetite was then dispersed in cyclohexane (15 mL). To remove the non-stabilized particles, the final solution was centrifuged at 2000 rpm for 30 minutes and stocked under air. Finally, the solvent was evaporated and a stock solution containing 72 mg of **MNP**/mL of cyclohexane was obtained.

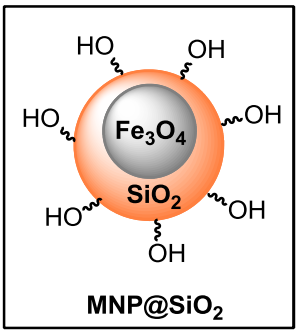

The silica coating was obtained using the reverse microemulsion method.[10] Igepal CO-520 (178.4 g), previously prepared magnetite (800 mg; 11.1 mL of stock solution in cyclohexane), and ammonium hydroxide (29%; 38 mL) were dispersed in cyclohexane (2.8 L) using ultrasounds. Then, tetraethyl orthosilicate (TEOS; 30.8 mL) was slowly added dropwise and the reaction occurred for 16 h under slow mechanical stirring (300 rpm). The solid was

precipitated with methanol (≈ 250 mL), recovered by centrifugation (7000 rpm, 30 min) and washed with ethanol (three times). Finally, the desired solid material was dried for 24 hours, at room temperature, and calcined at 500 °C for 2 hours. Silica coated nanoparticles (**MNP@SiO$_2$**) were obtained (5.40 g) and analyzed by transmission electron microscopy (TEM).

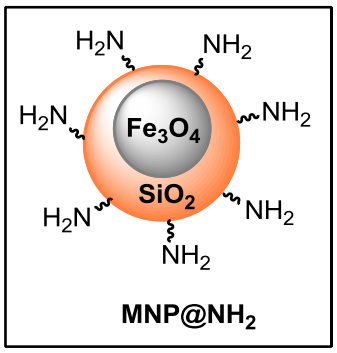

The **MNP@SiO$_2$** material (1 g), 3-aminopropyltriethoxysilane (APTES; 0.5 mL) and dry toluene (50 mL) were introduced in a round-bottom flask at reflux temperature for 2 hours. Then, the amine-functionalized solid (**MNP@NH$_2$**) was purified by washing with toluene and separated by centrifugation, the resulting material was finally dried at 100 °C for 20 hours and characterized by thermal analysis (TG) and infrared spectroscopy (FTIR)

5.3.2 Synthesis of PPh$_3$ functionalized nanomaterials

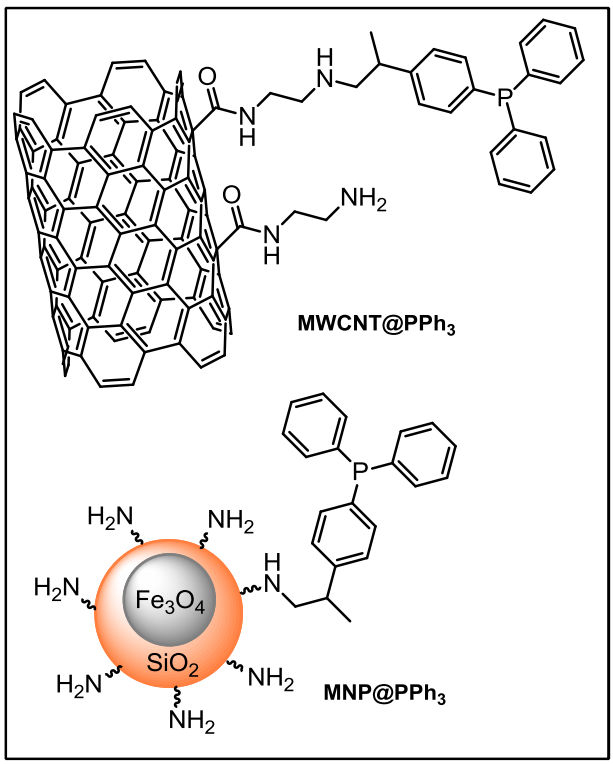

The synthesis of hybrid phosphine-functionalized nanomaterials (**MWCNT@PPh$_3$** and **MNP@PPh$_3$**) was performed *via* hydroaminomethylation reaction.

In a typical experiment diphenyl(4-vinylphenyl)phosphine (1.1 mmol), [Rh(CO)$_2$acac] (0.021 mmol) and the selected aminated material (**MWCNT@NH$_2$** (1.0 g); or **MNP@NH$_2$** (1.0 g) were weighed to a stainless steel high-pressure reactor, under inert atmosphere. After the addition of freshly dried toluene (14 mL) *via* cannula, the reactor was pressurized with 30 bar (CO/H$_2$, 1:1) at constant pressure and kept at 65 ºC for 48 hours with vigorous magnetic stirring. After this period the reactor was cooled to room temperature, degassed, and finally

charged with H_2 (P = 30 bar) at 65 °C for additional 4 hours. After this period the reactor was cooled until room temperature and depressurized and opened in a glovebox, under inert atmosphere. The **PPh_3@MWCNT** material was isolated *via* centrifugation in a falcon tube closed under inert atmosphere (10 min, 6000 rpm). Then, to remove the unreacted diphenyl(4-vinylphenyl)phosphine and residual Rh complex, the material was washed with toluene (3 times) and isolated *via* centrifugation. After drying, under vacuum, overnight, the desired **MWCNT@PPh_3** was isolated and characterized by X-ray photoelectron spectroscopy (XPS). **MNP@PPh_3** material was easily isolated from the reaction medium by application of an external magnetic field. After removal of the supernatant, the remaining solid was washed with toluene (20 mL, 3 times) and dried under vacuum at room temperature for 24 hours, the solid was then analyzed by X-ray photoelectron spectroscopy (XPS) and inductively coupled plasma atomic emission spectroscopy (ICP-OES), see Chapter 3, Table 3.2.

5.3.3 Synthesis of the hybrid nanocatalysts

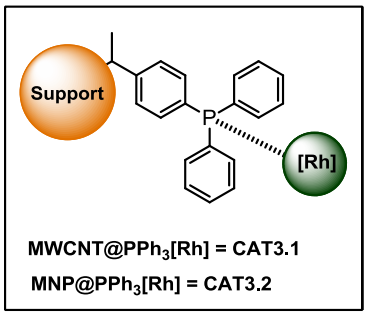

To prepare the desired Rh/phosphine hybrid catalysts (**CAT3.1** and **CAT3.2**), each one of the previously described phosphine functionalized materials **MWCNT@PPh_3** (0.23 mmol P/g material) or **MNP@PPh_3** (0.13 mmol P/g material) (500 mg) and [$Rh(CO)_2(acac)$] (0.128 mmol) were weighed to a Schlenck tube, under inert atmosphere, and toluene (15 mL) was added. The complexation reaction was kept for 15 hours under vigorous magnetic stirring, under N_2 atmosphere. The materials were isolated by centrifugation (**CAT3.1**) or external magnetic separation (**CAT3.2**) and washed five times. After drying, **CAT3.1** and **CAT3.2** were characterized by X-ray photoelectron spectroscopy (XPS) and inductively coupled plasma atomic emission spectroscopy (ICP-OES), respectively, displaying values of 0.16 mmol Rh/g material (**CAT3.1**) and 0.11 mmol Rh/g material (**CAT3.2**).

5.3.4 General procedure for the hydroformylation of styrene

Previously prepared hybrid nanocatalysts (**CAT3.1** and **CAT3.2)** were evaluated in the hydroformylation of styrene. The hybrid material **CNT@PPh$_3$-Rh** (**CAT3.1**; 80 mg) or **MNP@PPh$_3$-Rh** (**CAT3.2**; 200 mg) were weighed to a stainless-steel high-pressure reactor under inert atmosphere. After closing the reactor, styrene (6.5 mmol) and the solvent (dry toluene, 10 mL) were added *via* cannula, under vacuum. The reactor was then purged 3x with syngas and finally charged with 30 bar of an even mixture of CO and H_2 and maintained at 80 °C for 17 hours, under magnetic stirring. After that period the reactor was cooled to room temperature and depressurized. For **CAT3.1**, the reactor was opened under inert atmosphere and the hybrid material was separated from the reaction crude by centrifugation (10 min, 6000 rpm) and washed 3x with freshly dry toluene. For **CAT3.2**, the reactor was opened under inert atmosphere and the hybrid material was separated from the reaction crude by the application of an external magnet. In both cases, a sample of the crude mixture was analyzed by GC-MS.

5.4 Experimental of Chapter 4

In this section, the synthetic procedures and compound characterization referring to chapter 4 is provided.

5.4.1 Homogeneous catalysts synthesis

Preparation of CAT4.1

Tris(1-pyrazoyl)methane (4.2)

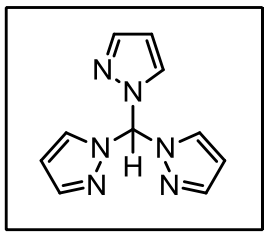

Distilled water (74 mL) was added to a 500 mL round bottom flask containing a mixture of pyrazole (5.0 g, 74 mmol) and tetra-n-butylammonium bromide (1.2 g, 3.75 mmol). With vigorous stirring, sodium carbonate (46.75 g, 450 mmol) was added gradually to the reaction mixture; constant stirring increases the efficiency of the reaction. After cooling to near room temperature (25 °C), chloroform (37 mL) was added and the flask was equipped with a reflux condenser. This mixture was

heated at gentle reflux (62 °C) for 3 days over which time it became a pale-yellow emulsion. The mixture was cooled to r.t. and filtered through a Büchner funnel to remove the excess of base. Diethyl ether (125 mL) and distilled water (75 mL) were added to the filtrate. The organic layer was removed, and the aqueous layer was washed again with diethyl ether (3×100 mL). The combined organic layers were then washed with saturated brine solution (100 mL). The organic layer was treated with activated charcoal and dried over sodium sulfate. The mixture was filtered, and the solvent was removed by rotary evaporation. The resulting pale-yellow solid was recrystallized using diethyl ether as solvent and the crystals were filtered and dried under vacuum. Tris(1-pyrazoyl)methane was obtained as white crystals with 65% yield (12.6 g).

$FeBr_2$ and 4.2 complexation

To an ethanoic (10 mL) solution of $FeBr_2$ (251 mg, 1.63 mmol), an equimolar amount of **4.2** (360 mg, 1.68 mmol) in ethanol (10 mL) was slowly added under inert atmosphere of argon, the formation of a violet precipitate is instantaneous. After stirring for 2 hours, the solid was separated by filtration under inert atmosphere and dried under vacuum. The previously obtained powder was recrystallized in ethanol through solvent evaporation and crystals were obtained. Finally, the purple crystals were washed with cold ethanol and dried under vacuum. After crystallization of the **CAT4.1** amorphous powder through slow ethanol evaporation pure purple crystals of **CAT4.1** were obtained (637 mg, 91%). The crystals were then analyzed with X-ray crystallography and the data is in good agreement with those previously described in the literature.[11]

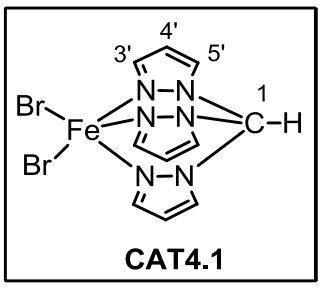

CAT4.1

^{1}H NMR (400 MHz, D_2O) δ(ppm): 9.22 (bs, 1H, $\underline{H_1}$), 8.56 (bs, 3H, $\underline{H_{3'}}$), 7.83 (bs, 3H, $\underline{H_{5'}}$), 7.09 (bs 3H, $\underline{H_{4'}}$).

^{13}C NMR (100 MHz, D_2O) δ(ppm): 159.8 ($\underline{C_{3'}}$), 143.1 ($\underline{C_{5'}}$), 114.6 ($\underline{C_{4'}}$), 74.2 ($\underline{C_1}$).

HRMS (ESI): m/z = calcd for $C_{10}H_{10}BrFeN_6^+$ $[M\text{-}Br]^+$: 348.9494; found: 348.9489.

***In situ* preparation of CAT4.2**

Xantphos (0.05 mmol) and [$Rh(CO)_2acac$] (0.02 mmol) were weighed to a stainless-steel high-pressure reactor under inert atmosphere. The reactor was then purged 3x with syngas and charged with 30 bar of CO/H_2 (1:1) and maintained at 80 °C for 2 hours under magnetic stirring using ethanol as solvent (3 mL).

***In situ* preparation of CAT4.3**

Triphenylphosphine (0.10 mmol) and [$Rh(CO)_2acac$] (0.02 mmol) were weighed to a stainless-steel high-pressure reactor under inert atmosphere. The reactor was then purged 3x with syngas and charged with 30 bar of CO/H_2 (1:1) and maintained at 80 °C for 2 hours, under magnetic stirring, using ethanol as solvent (3 mL).

***In situ* preparation of CAT4.4**

Tris[2'-(benzyloxy)-1,1'-binaphthyl-2-yl] phosphite (0.10 mmol) and [$Rh(CO)_2acac$] (0.02 mmol) were weighed to a stainless-steel high-pressure reactor under inert atmosphere. The reactor was then purged 3x with syngas and charged with 30 bar of CO/H_2 (1:1) and maintained at 80 °C for 2 hours, under magnetic stirring, using ethanol as solvent (3 mL).

5.4.2 Heterogeneous catalysts synthesis

The synthesis and functionalization of the magnetic nanoparticles used in chapter 4 were performed using the same procedures as presented in section 5.3.

Magnetic nanoparticles functionalization

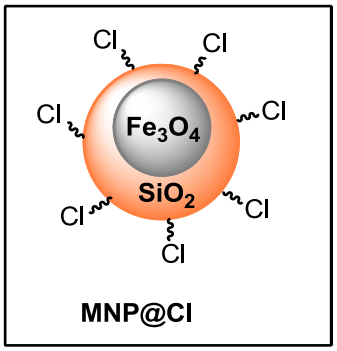

MNP@SiO_2 (1 g) and (3-chloropropyl)triethoxysilane (CPTES) (0.5 mL; 2.07 mmol) were added to dry toluene (40 mL) and kept under stirring at 110 °C, for 12 h. The resulting material was magnetically collected and washed several times with ethyl acetate and acetonitrile. Finally, the solid was dried under vacuum for 24 h. The MNP@Cl were characterized by TG, showing a functionalization corresponding to 0.66 mmol/g of material.

Preparation of CAT4.5

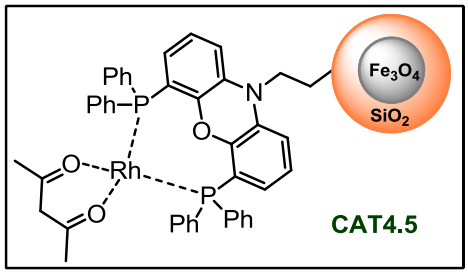

N-xantphos (435 mg, 0.79 mmol) was dissolved with dry DME (80 mL) in a Schlenk tube under inert atmosphere, then, dry sodium hydride (77 mg, 3.2 mmol) was slowly added to the solution and kept for 2 hours at 80 °C under inert atmosphere. After that period, MNP@Cl (900 mg, 0.6 mmol of Cl groups) was added and the mixture was kept stirring for 12 hours under inert atmosphere. After washing with DME (3 x 50 mL) and recovery with magnetic separation under inert atmosphere, $[Rh(CO)_2(acac)]$ (180 mg, 0.7 mmol) and DME (50 mL) was added and the mixture was kept under inert atmosphere for additional 6 hours. After solvent removal, the resulting material was again washed (3 x 50 mL), under inert atmosphere and dried under vacuum. All reactions and manipulations were performed under inert atmosphere. The resulting material was analyzed by TG and ICP-OES and immobilization of *N*-xantphos (0.12 mmol/g) and rhodium (0.061 mmol/g) was obtained.

Preparation of CAT4.6

Tris-2,2,2-(1 -pyrazoyl)ethanol (4.4)

In a 250 mL Schlenk flask, tris(1-pyrazoyl)methane (1.5 g, 7.0 mmol) was dissolved in 2-Me-THF (100 mL) and potassium *tert*-butoxide (2.0 g, 18 mmol) was added slowly, after complete dissolution, paraformaldehyde (0.53 g, 18 mmol) was added to the mixture and stirred at 30 °C. overnight, under inert atmosphere. After that period, water (100 mL) was added and the mixture was extracted with diethyl ether (3 x 100 mL). The organic extracts were combined and dried over sodium sulfate and filtered. The solvent was removed under vacuum resulting and a pale yellow solid was obtained (1.2 g, 80%).

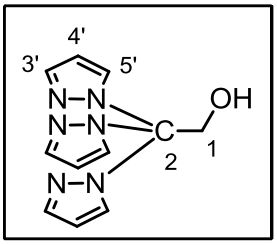

^{1}H NMR (400 MHz, $CDCl_3$) δ(ppm): 7.70 (*d*, J = 1.5 Hz, 3H, $\underline{H_{3'}}$), 7.11 (*d*, J = 2.5 Hz, 3H, $\underline{H_{5'}}$), 6.37 (*dd*, J = 2.5, 1.6 Hz, 3H, $\underline{H_{4'}}$), 5.08 (s, 2H, $\underline{H_1}$)

^{13}C NMR (100 MHz, $CDCl_3$) δ(ppm): 141.5 ($\underline{C_{3'}}$), 129.9 ($\underline{C_{5'}}$), 106.6 ($\underline{C_{4'}}$), 89.2 ($\underline{C_2}$), 67.8 ($\underline{C_1}$).

Tris-2,2,2-(1-pyrazoyl)ethoxyallyl (4.5)

Tris-2,2,2-(1-pyrazoyl)ethanol **4.4** (1.0 g 4.1 mmol) was weighted to a 200 mL Schlenk flask and dissolved in 2-Me-THF (100 mL), potassium *tert*-butoxide (1.0 g, 9.0 mmol) was added slowly, after complete dissolution, allyl bromide (0.5 mL, 6 mmol) was added to the mixture and stirred at r.t. for 24 hours under inert atmosphere. After that period, water (100 mL) was added and the mixture was extracted with diethyl ether (3 x 50 mL). The organic extracts were combined and dried over sodium sulfate and filtered. The solvent was removed under vacuum resulting in a colorless liquid (1.1 g, 98%).

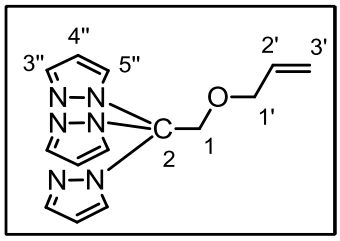

^{1}H NMR (400 MHz, $CDCl_3$) δ(ppm): 7.65 (*d*, J = 1.7 Hz, 3H, $\underline{H_{3''}}$), 7.42 (*d*, J = 2.6 Hz, 3H, $\underline{H_{5''}}$), 6.33 (*dd*, J = 2.5, 1.8 Hz, 3H, $\underline{H_{4''}}$), 5.79 (*ddt*, J = 17.2, 10.4, 5.6 Hz, 2H, $\underline{H_{2'}}$), 5.21 (*dq*, J = 17.2, 1.6 Hz, 1H, $\underline{H_{3'}}$), 5.16 (*dq*, J = 10.4, 1.3 Hz, 1H, $\underline{H_{3'}}$) 5.09 (s, 2H, $\underline{H_1}$), 3.98 (*dt*, J = 5.6, 1.3 Hz, 2H, $\underline{H_{1'}}$)

^{13}C NMR (100 MHz, $CDCl_3$) δ(ppm): 141.3 ($\underline{C_{3''}}$), 133.7 ($\underline{C_{2'}}$), 130.9 ($\underline{C_{5''}}$), 118.0 ($\underline{C_{3'}}$), 106.5 ($\underline{C_{4''}}$), 89.9 ($\underline{C_2}$), 73.2 ($\underline{C_1}$/$\underline{C_{1'}}$), 73.1 ($\underline{C_1}$/$\underline{C_{1'}}$).

HRMS (EI): m/z = calcd for $C_{13}H_{16}N_6NaO^+$ $[M+Na]^+$: 307.1279; found: 307.1278.

Complexation of 4.5 with $FeBr_2$ (4.6)

To a 10 mL ethanolic solution of $FeBr_2$ (1.0 g, 3.5 mmol), an equimolar molar amount of **4.5** (1.0 g, 3.5 mmol) in ethanol (10 mL) was slowly added under inert atmosphere of argon, the formation of precipitate was instantaneous. After stirring for 2 hours, the solid was filtered under inert atmosphere and dried under vacuum. Finally, the obtained orange (95%) powder was washed with cold ethanol and dried under vacuum.

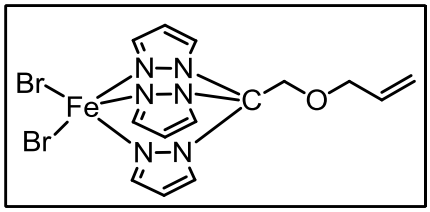

HRMS (EI): m/z = calcd for $C_{14}H_{16}BrFeN_6O^+$ $[M-Br]^+$: 418,9918; found: 418,9911.

Immobilization of iron complex 4.6 onto MNP@NH_2 (CAT4.6)

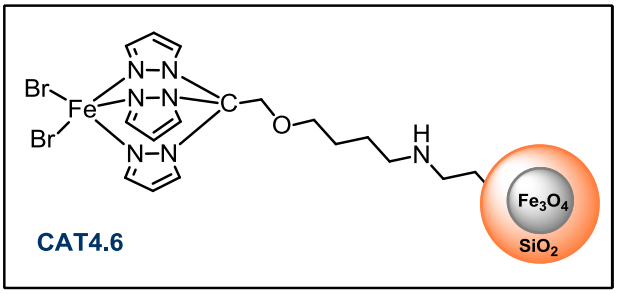

The synthesis of immobilized Iron (II)/C-scorpionate type catalyst onto MNP was performed *via* hydroaminomethylation reaction. Firstly, [$Rh(CO)_2(acac)$] (6 mg, 0.02 mmol) and Xantphos (23.0 mg, 0.04 mmol) were incubated in a high-pressure reactor in anisole (5 mL), with 30 bar (CO/H_2, 1:1), at 80 °C for 1 hour. Then, complex **4.6** (1.0 g, 2.0 mmol), and the aminated nanoparticle, MNP@NH_2 (900 mg, 1.3 mmol of amine groups) were added to the reactor under inert atmosphere. After the addition of freshly dried toluene (10 mL) *via* cannula, the reactor was pressurized with 30 bar (CO/H_2, 1:1) at constant pressure and kept at 65 °C for 48 hours with vigorous magnetic stirring. After this period the reactor was cooled to room temperature, degassed, and finally charged with H_2 (P = 30 bar) at 65 °C for additional 4 hours. The reactor was then cooled to room temperature, depressurized, and opened in a glove box under inert atmosphere. The **CAT4.6** material was isolated from the reaction medium by application of an external magnetic field. After removal of the supernatant, the remaining solid was washed with DME, anisole and acetonitrile (3 x 20 mL) and dried under vacuum at room temperature for 24 hours, the solid was then analyzed by TG and ICP-OES.

5.4.3 General procedures for the hydroformylation/acetalization of olefins

Homogeneous conditions

A 20 mL stainless steel autoclave was charged with [$Rh(CO)_2(acac)$] (5.16 mg, 0.02 mmol), Xantphos (28.9 mg, 0.05 mmol) and [$FeBr_2\{HC(pz)_3$] (22.0 mg, 0.05 mmol). The autoclave was closed, and the air was removed using a vacuum pump. Ethanol (3 mL) was added via cannula and the autoclave was charged with 30 bar ($CO:H_2$) and kept for 2 hours at 80 °C. Then, the alkene (3 mmol) and 3 mL of dry ethanol were added through cannula. After flushing the autoclave with CO/H_2, it was pressurized with 20 bar of the same equimolar mixture of CO/H_2 gas and heated to 80 °C with magnetic stirring. After 24 hours, the autoclave was cooled with icy water and the pressure was released. The crude

reaction mixture was diluted with ethanol and analyzed by gas chromatography using isooctane as an external standard.

Heterogeneous conditions

The desired amount of **CAT4.5** (180 mg, 0.02 mmol Rh) was loaded into a 20 mL high-pressure autoclave, dispersed in ethanol (4 mL) and kept at 30 bar (CO/H_2) pressure for 2 hours, at 80 °C. Then, after substrate addition (3 mmol) and 2 mL of ethanol, the reactor was flushed and pressurized with 20 bar of $CO:H_2$ gas (1:1) and heated to 80 °C under stirring. After 24 hours the catalyst was isolated from the reaction crude through magnetic separation and stored under inert atmosphere. Then the reaction was transferred to another reaction vessel containing **CAT4.6** (300mg, 0.04 mmol Fe) and kept for additional 24 hours at 80 °C, under inert atmosphere, finally **CAT4.6**, was also magnetically separated from the reaction crude and stored under inert atmosphere. An aliquot was taken from both reaction step crudes, diluted with ethanol and analyzed by gas chromatography using isooctane as an external standard. All manipulations were performed under inert atmosphere.

Reutilization Process: The above-described process was repeated for a further three runs and results are shown in Figure 4.19 (Chapter 4). The Rh ICP analysis of **CAT4.5** samples, prior and after the reutilization cycles revealed 0.9% Rh total leaching while Fe ICP analysis of **CAT4.6** showed 1.6% Fe leaching.

5.4.4 Reaction scope

1,1-diethoxynonane (4.10*l*)

According to the general procedure for the hydroformylation/acetalization of olefins, **4.10*l*** was prepared from oct-1-ene and isolated as a colorless liquid in (70%) yield through normal phase silica flash chromatography using ethyl acetate/*n*-hexane as eluent.

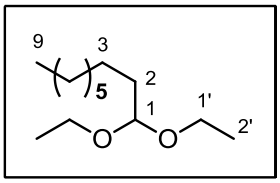

^{1}H NMR (400 MHz, $CDCl_3$) δ(ppm): 4.41 (*t*, J = 5.8 Hz, 1H, $\underline{H_1}$), 3.57 (*dq*, J = 9.4, 7.1, 2H, $\underline{H_{1'}}$), 3.43 (*dq*, J = 9.4, 7.1, 2H, $\underline{H_{1'}}$), 1.52-1.57 (*m*, 2H, $\underline{H_2}$), 1.22 (*bs*, 12H, $\underline{H_3}$-$\underline{H_8}$), 1.14 (*t,* J = 7.1 Hz, 6H, $\underline{H_{2'}}$), 0.82 (*t*, J = 6.9 Hz, 3H, $\underline{H_9}$)

^{13}C NMR (100 MHz, $CDCl_3$) δ(ppm): 103.0 ($\underline{C_1}$), 60.8 ($\underline{C_{1'}}$), 33.6 ($\underline{C_2}$), 31.8, 29.5, 29.2, 24.7, 22.6, 15.3 ($\underline{C_{2'}}$), 14.0 ($\underline{C_9}$).

MS (EI): m/z = 171, 103, 85, 75, 57, 47, 29.

(3,3-diethoxypropyl)benzene (4.11*l*)

According to the general procedure for the hydroformylation/acetalization of olefins, **4.11*l*** was prepared from styrene and isolated as a colorless liquid in (41%) yield through normal phase silica flash chromatography using ethyl acetate/*n*-hexane as eluent.

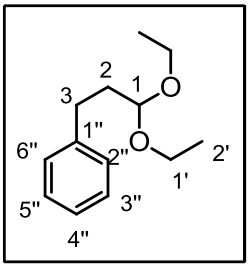

^{1}H NMR (400 MHz, $CDCl_3$) δ(ppm): 7.34-7.31 (*m*, 2H, $\underline{H_{3''}}$, $\underline{H_{5''}}$), 7.26-7.23 (*m*, 3H, $\underline{H_{2''}}$, $\underline{H_{4''}}$, $\underline{H_{6''}}$), 4.54 (*t*, J = 5.7 Hz, 1H, $\underline{H_1}$), 3.70 (*dq*, J = 9.4, 7.1 Hz, 2H, $\underline{H_{1'}}$), 3.56 (*dq*, J = 9.4, 7.1 Hz, 2H, $\underline{H_{1'}}$) 2.75 (*t*, J = 7.8 Hz, 2H, $\underline{H_3}$), 2.02-1.97 (*m*, 2H, $\underline{H_2}$), 1.27 (*t,* J = 7.1 Hz, 6H, $\underline{H_{2'}}$).

MS (EI): m/z = 208 $[M]^+$, 162, 133, 117, 105, 103, 91, 75, 65, 47, 29.

(1,1-diethoxypropan-2-yl)benzene (4.11*b*)

According to the general procedure for the hydroformylation/acetalization of alkenes, **4.11*b*** was prepared from styrene was obtained as a colorless liquid in a 50:50 mixture with **4.11*l*** through normal phase silica flash chromatography using ethyl acetate/*n*-hexane as eluent.

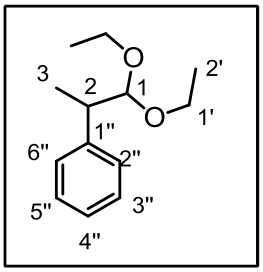

^{1}H NMR (400 MHz, $CDCl_3$) δ(ppm): 7.34-7.31 (*m*, 2H, $\underline{H_{3''}}$, $\underline{H_{5''}}$), 7.26-7.23 (*m*, 3H, $\underline{H_{2''}}$, $\underline{H_{4''}}$, $\underline{H_{6''}}$), 4.52 (*d*, J = 6.5 Hz, 1H, $\underline{H_1}$), 3.62 (*dq*, J = 9.4, 7.1 Hz, 2H, $\underline{H_{1'}}$), 3.38 (*dq*, J = 9.4, 7.1 Hz, 2H, $\underline{H_{1'}}$), 3.08 (*p*, J = 7.0 Hz, 2H, $\underline{H_2}$), 1.39 (*d*, J = 7.1 Hz 3H, $\underline{H_3}$), 1.27 (*t,* J = 7.1 Hz, 3H, $\underline{H_{2'}}$) 1.10 (*t,* J = 7.1 Hz, 3H, $\underline{H_{2'}}$).

MS (EI): m/z = 208 $[M]^+$, 163, 135, 117, 105, 103, 91, 75, 47, 29.

(1*R*,2*S*,5*R*)-2-(-1,1-diethoxybutan-3-yl)-5-methylcyclohexyloxymethylbenzene (4.14*l*)

According to the general procedure for the hydroformylation/acetalization of alkenes, **4.14*l*** was prepared from (-)-isopulegol benzyl ether and isolated as a colorless liquid in

(74%) yield through normal phase silica flash chromatography using ethyl acetate/*n*-hexane as eluent.

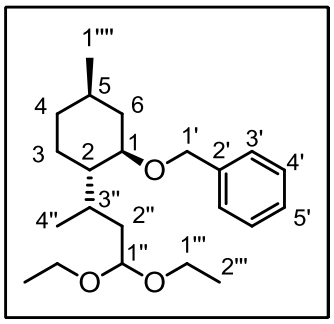

^{1}H NMR (400 MHz, $CDCl_3$) δ(ppm): 7.42-7.25 (*m,* 5H, $H_{3'}$-$H_{7'}$), 4.64 (*d*, J = 11.1 Hz, 1H, $H_{1'}$), 4.56 (*dd*, J = 7.8, 3.9 Hz, 1H, $H_{1''}$), 4.43 (d, J = 11.1 Hz, 1H, $H_{1'}$), 3.63 (*dq*, J = 9.4, 7.1 Hz, 2H, $H_{1'''}$), 3.48 (*dq*, J = 9.3, 7.1 Hz, 2H, $H_{1'''}$) 3.25 (dt, J = 10.6, 4.1 Hz,1H, H_1), 2.34-2.24 (*m*, 1H), 2.22-2.17 (*m*, 1H), 1.78-1.72 (*m*, 1H), 1.69-1.63 (*m*, 2H), 1.39-1.26 (*m*, 3H), 1.20 (*t*, J = 7.1 Hz, 3H, $H_{2'''}$), 1.12 (*t*, J = 7.1 Hz, 3H, $H_{2'''}$), 0.96 (*d*, J = 7.0 Hz 3H), 0.93 (*d*, J = 6.6 Hz 3H), overlap signals 1.12-0.75 (*m*, 3H)

^{13}C NMR (100 MHz, $(CD_3)_2CO$) δ(ppm): 140.8 ($C_{2'}$), 129.0 ($C_{4'}$, $C_{6'}$), 128.5 ($C_{3'}$, $C_{7'}$), 128.0 ($C_{5'}$), 103.1 ($C_{1''}$), 79.2 ($C_{1'}$), 70.9, 61.6, 61.2, 50.0, 41.3, 36.7, 35.7, 32.3, 28.7, 25.9, 22.8, 18.6, 16.0, 15.9.

MS (EI): m/z = 348 $[M]^+$, 319, 211, 194, 179, 165, 150, 103, 99, 91, 71, 55, 47, 28.

(S)-4-(1,1-diethoxybutan-3-yl)-1-methylcyclohex-1-ene (4.16*l*)

According to the general procedure for the hydroformylation/acetalization of olefins, **4.16*l*** was prepared from (+)-limonene and isolated as a colorless liquid in 40% yield through normal phase silica flash chromatography using ethyl acetate/*n*-hexane as eluent.

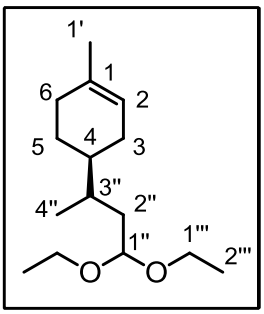

^{1}H NMR (400 MHz, $CDCl_3$) δ(ppm): 5.35 (bs, 1H, H_2), 4.57 (*dd*, J = 7.2 Hz, 4.6 Hz, 1H, $H_{1''}$), 3.67-3.56 (*m*, 2H, $H_{1'''}$), 3.52-3.44 (*m*, 2H, $H_{1'''}$), 1.96-1.88 (*bs*, 3H), 1.77-1.63 (m, 3H), 1.62 (s, 3H, $H_{1'}$), 1.58-1.51 (*m*, 1H), 1.39-1.22 (*m*, 3H), 1.19 (*t,* J = 6.9 Hz, 3H, $H_{2''}$) 1.18 (*t,* J = 7.1 Hz, 3H, $H_{2''}$), 0.87 (*dd*, J = 6.8, 3.7 Hz, 3H, $H_{4''}$)

MS (EI): m/z = 194, 179, 148, 133, 119, 106, 99, 93, 79, 71, 55, 41, 29.

5.5 References

[1] R. M. B. Carrilho, A. R. Abreu, G. Petöcz, J. C. Bayón, M. J. S. M. Moreno, L. Kollár, M. M. Pereira, *Chem. Lett.* "New Binaphthyl-based C_3-symmetric Chiral Hemilabile Monophosphite Ligands: Synthesis and Characterization of Their Platinum Complexes" **2009**, *38*, 844-845.

[2] D. F. Shriver, M. A. Drezdzon, *The Manipulation of Air-Sensitive Compounds*, Wiley and Sons, New York, **1986**.

[3] H. Burrows, M. M. Pereira, *Síntese e Estrutura*, Escolar Editora, Lisboa, **2005**.

[4] W. L. F. Armarego, *Purification of Laboratory Chemicals*, Elsevier, **2017**.

[5] K. K. W. Mak, *J. Chem. Educ.* "Synthesis and Resolution of the Atropisomeric 1,1'-Bi-2-naphthol: An Experiment in Organic Synthesis and 2-D NMR Spectroscopy" **2004**, *81*, 1636-1640.

[6] P. W. N. M. v. Leeuwen, C.F.Roobeek, "Hydroformylation of less reactive olefins with modified rhodium catalysts" **1983**, *258*, 343-350.

[7] C. J. P. Monteiro, S. A. C. Carabineiro, T. Lauterbach, C. Hubbert, A. S. K. Hashmi, J. L. Figueiredo, M. M. Pereira, *ChemNanoMat* "(S)-BINOL Immobilized onto Multiwalled Carbon Nanotubes through Covalent Linkage: A New Approach for Hybrid Nanomaterials Characterization" **2015**, *1*, 178-187.

[8] M. J. Jacinto, P. K. Kiyohara, S. H. Masunaga, R. F. Jardim, L. M. Rossi, *Appl. Catal. A, Gen.* "Recoverable rhodium nanoparticles: Synthesis, characterization and catalytic performance in hydrogenation reactions" **2008**, *338*, 52-57.

[9] L. M. Rossi, L. L. R. Vono, F. P. Silva, P. K. Kiyohara, E. L. Duarte, J. R. Matos, *Appl. Catal. A, Gen.* "A magnetically recoverable scavenger for palladium based on thiol-modified magnetite nanoparticles" **2007**, *330*, 139-144.

[10] D. K. Yi, S. S. Lee, G. C. Papaefthymiou, J. Y. Ying, *Chem. Mater.* "Nanoparticle Architectures Templated by SiO_2/Fe_2O_3 Nanocomposites" **2006**, *18*, 614-619.

[11] O. G. Shakirova, L. G. Lavrenova, N. V. Kurat'eva, D. Y. Naumov, V. A. Daletskii, L. A. Sheludyakova, V. A. Logvinenko, S. F. Vasilevskii, *Russ. J. Coord. Chem.* "Spin crossover in iron(II) complexes with tris(pyrazol-1-yl)methane" **2010**, *36*, 275-283.